UNIVERSIDAD COMPLUTENSE DE MADRID

FACULTAD DE FARMACIA

Departamento de Microbiología II

TESIS DOCTORAL

ESTUDIO DE LA RESPUESTA DE MACRÓFAGOS MURINO Y HUMANOS FRENTE A *Candida albicans* UTILIZANDO DIVERSAS TÉCNICAS PROTEÓMICAS

MEMORIA PARA OPTAR AL GRADO DE DOCTOR

PRESENTADA POR

JOSÉ ANTONIO REALES CALDERÓN

DIRECTORAS

CONCHA GIL GARCÍA
MARÍA GLORIA MOLERO MARTÍN-PORTUGUÉS

Madrid, 2014

UNIVERSIDAD COMPLUTENSE DE MADRID
FACULTAD DE FARMACIA
DEPARTAMENTO DE MICROBIOLOGÍA II

ESTUDIO DE LA RESPUESTA DE MACRÓFAGOS MURINOS Y HUMANOS FRENTE A *Candida albicans* UTILIZANDO DIVERSAS TÉCNICAS PROTEÓMICAS

Memoria presentada para optar al Título de Doctor por la Universidad Complutense de Madrid con Mención Europea

D. JOSE ANTONIO REALES CALDERÓN

Directoras:

Dra. Concha Gil García
Dra. Mª Gloria Molero Martín-Portugués

Madrid, 2013

COMPLUTENSE UNIVERSITY OF MADRID
FACULTY OF PHARMACY
DEPARTMENT OF MICROBIOLOGY II

STUDY OF MURINE AND HUMAN MACROPHAGES RESPONSE TO *Candida albicans* USING DIFFERENT PROTEOMIC TECHNIQUES

DOCTORAL THESIS

D. JOSE ANTONIO REALES CALDERÓN

Directors:

Dra. Concha Gil García
Dra. Mª Gloria Molero Martín-Portugués

Madrid, 2013

Dª. CONCHA GIL GARCÍA, DIRECTORA DEL DEPARTAMENTO DE MICROBIOLOGÍA II DE LA FACULTAD DE FARMACIA DE LA UNIVERSIDAD COMPLUTENSE DE MADRID,

CERTIFICA: Que Don JOSE ANTONIO REALES CALDERÓN ha realizado en el Departamento de Microbiología II de la Facultad de Farmacia de la Universidad Complutense de Madrid bajo la dirección de las Doctoras Concha Gil García y Mª Gloria Molero Martín-Portugués, el trabajo que presenta para optar al grado de Doctor con mención Europea con el título:

ESTUDIO DE LA RESPUESTA DE MACRÓFAGOS MURINOS Y HUMANOS FRENTE A *Candida albicans* UTILIZANDO DIVERSAS TÉCNICAS PROTEÓMICAS

Y para que así conste, firmo la presente certificación en Madrid, 2013

Fdo. Prof. Dra. Dª. Concha Gil García

ESTA TESIS DOCTORAL HA SIDO POSIBLE GRACIAS A LA CONCESIÓN DE DIFERENTES AYUDAS:

- Beca del Programa Nacional de Formación de Profesorado Universitario (FPI) del Ministerio de Educación y Ciencia durante el periodo Julio 2007-2011.
- Ayuda para estancias científicas breves asociada a la Beca FPI en el laboratorio del Dr. Ole N. Jensen en el Protein Research Group, Department of Biochemistry and Molecular Biology en la University of Southern Denmark (Odense, Dinamarca) durante el periodo Mayo a Noviembre de 2010.
- Ayuda para estancias científicas asociada a la Red Española de Investigación en Patología Infecciosa (REIPI) en el laboratorio del Dr. Hidde Ploegh, bajo la supervisión de la Dra. Karin Strijbis en Whitehead Institute en el Massachusetts Institute of Technology (MIT) in Cambridge (Massachusets) durante el periodo Octubre a Diciembre de 2012.
- Ayuda concedida por la "Cátedra de Genómica y Proteómica" de Merck Sharp & Dohme, de la cual es director el Dr. César Nombela Cano.

EL TRABAJO DESCRITO HA ESTADO INCLUIDO EN LOS SIGUIENTES PROYECTOS:

- "Proteómica y Fosfoproteómica de la interacción *Candida albicans*-Macrófago. Caracterización de factores de virulencia y respuesta inmunitaria de valor en Diagnóstico y Protección frente a infecciones". BIO2006-01989 del Ministerio de ciencia e innovación.
- "Interacción *Candida albicans* - Hospedador. Aproximaciones proteómicas globales para el Diagnóstico, Tratamiento e Inmunoprevención de las candidiasis invasivas". BIO2009-07654 del Ministerio de ciencia e innovación.
- Red Española de Investigación en Patología Infecciosa (REIPI). Del Instituto de salud Carlos III.

A mis padres,

A mis hermanas,

A mi abuela,

Y, por supuesto, a Vaquina.

Llegó el momento, el fin de una etapa, ¿difícil?, ¿larga?, ¿complicada?, pues un poco de todo. Pero, como todo, tiene sus más y sus menos y, cuando todo pase, siempre recordaremos lo bueno. ¿Qué es lo bueno? Que por fin acabé la Tesis, es ahora cuando te das cuenta del aporte de aquellas personas que han estado a tu lado durante este trayecto y sin las cuales habría sido imposible terminarla: comienzan los agradecimientos.

En primer lugar quiero agradecer a Concha Gil y Gloria Molero por confiar en mí aquel día en aquella entrevista (junto a Lucía y María Molina) en la que me dejaron impactado, 4 mujeres frente a mí contándome sus proyectos de investigación, una toma de contacto con lo que se hacía en el Departamento. Gracias Concha por permitirme evolucionar como Investigador, por tu apoyo y confianza a la hora de llevar a cabo este proyecto. Y Gloria, gracias porque has sido como mi madre en esta ciudad y, cuando la familia está lejos, siempre es bienvenido ese "apoyo" extra.

También quiero agradecer a César Nombela y a María Molina (directora del "Depar" cuando llegué) por haberme permitido formar parte del Departamento de Microbiología II y por vuestro apoyo a lo largo de estos 6 años.

Gracias a todos los profesores del Departamento;

A Lucía, muchísimas gracias porque para mí has sido como mi tercera directora de Tesis, por escuchar problemas y apoyarme en la investigación y por ese punto de vista ajeno que siempre viene bien.

A Carmen de la Rosa, Carmina, Angelines y Conchita Pintado, las expertas microbiólogas cuyas historias siempre han sido enriquecedoras para mí, tanto personales como de vuestros análisis microbiológicos en los lugares más insospechados. Además, gracias por aquellos momentos que hemos pasado en las prácticas de Micro, he aprendido mucho de vosotras y espero seguir aprendiendo más.

Rosalía, Rosa Cenamor y Rebeca, porque siempre estáis dispuestas a ayudar cuando hay un problema y porque se puede contar con vosotras tanto personal como profesionalmente.

Rafa, Humberto, Víctor, Jesús, Javier, Jose Manuel, Miguel Ángel y Fede, los "varones" del Depar, muchísimas gracias por vuestra alegría, el trato cercano y amable y las ideas que surgen en los seminarios que son muy útiles los que estamos aprendiendo.

A nuestras chicas de secretaría: Mar, Inma, Almu y Ana, que siempre habéis estado solucionando problemas con los pedidos, envíos y todas las demás cosas que no tienen que ver con la labor administrativa.

¿Y qué haríamos sin nuestros técnicos? Jose Alberto, Elena y, sobretodo, Benito, que solucionáis todos los problemas. Benito, vales para todo, eres una joya y siempre me has ayudado con todo lo que te he pedido, aun no sabiendo hacerlo, has buscado la solución. Y también a Mercedes, porque cuando entro cada mañana y no hay casi nadie por los pasillos, tu alegría y cántico matutino siempre me alegra.

Y a mis compis de la Unidad 1, a todos, los que estaban cuando llegué, a los que están actualmente y a nuestros visitantes, porque el día se hace mucho más llevadero con vosotros. Virginia, muchas gracias por enseñarme muchas de las cosas que sé ahora, los macrófagos, que gran descubrimiento, sé que pase lo que pase eres una gran amiga. Vital, el Bioinformático del grupo, con el que he vivido grandes momentos, congresos, viajes y fiestas, eres grande y llegarás lejos, no lo olvides, en breve llegarás a ser un gran Doctor. Claudia, mi Colombiana favorita, gracias por tu apoyo incondicional, porque eres una gran madre y amiga, te has implicado en mi trabajo como si fuera tuyo, me has enseñado mucho y ahora mismo estás donde te mereces, con tu plaza y las pequeñas Mª Antonia y Manuela, gracias. Aída, los piques que tenemos con quién presentará la Tesis antes, creo que al final te he ganado, pero no pasa nada, ya te queda poco, gracias por enseñarnos cosas estadísticas, el diagnóstico y pronóstico y porque siempre se puede contar contigo (excepto los findes que te vas a la sierra). Raquel y Arancha, las Postdoc del grupo cuando llegué, gracias por vuestros consejos y enseñanzas, es una lástima que no estéis por aquí, pero habéis aprovechado muy bien el tiempo (enhorabuena por todo, sobre todo los peques que andan a vuestro lado). Carolina, entraste conmigo y leeremos casi a la vez, me alegro de conocerte y gracias ayudarme a perfeccionar la 2D.

A nuestra última predoctoral por ahora, Ana, que cuando volví de Dinamarca sólo llevaba unos meses y llegué arrasando, te estresé con mi "nerviosismo", pero ya me calaste, eres genial y te quiero muchísimo, gracias por todos y cada uno de los momentos que hemos vivido y los que nos quedan por vivir, en nada voy a visitarte a Los Ángeles. Me da mucha pena que no estés en mi defensa, pero te mantendrán bien informada. Elvi, nueva en el grupo, pero no menos importante, gracias por llegar y traer aire fresco, he aprendido bastante en estos meses y sé que aprenderé más contigo. Karima, que no sabemos si volverás con nosotros, si es así, te esperamos con los brazos abiertos.

También cabe destacar a los visitantes de la U1, esos cameos que han hecho en nuestro laboratorio durante un tiempo, Rafa, Carla, Rosana, Jose Antonio, Freija, Sonia y Emma (inseparables), Leila, Gustavo Godman, Jose Luis, los estudiantes de Máster, Enrique, Jesús, las estudiantes de 5º de colaboración, María, Inés e Irene, y a la loca de la familia, que hasta ha repetido estancia, aunque me perdí la segunda, Noe, esa gran

desconocida, eres genial y personalmente me has aportado mucho, nos trajiste un nuevo aire a la U1 y queremos que vuelvas. Sabes que aquí me tienes para lo que necesites y sé que en Santiago tengo casa y una gran amiga, en nada nos vemos en América, que ganas tengo.

A los "anexos" a la U1, primero fue María Sánchez, y después, Andrea y Nadia, pero luego llegó Victoria y se unió a nosotros y, el último en llegar, Ahmad, no menos importante. Gracias Andrea, por aquellos momentos que hemos compartido tanto en el labo como fuera de él, fiestas, barbacoas, viajes, recetas y demás, eres una gran persona y aún nos quedan muchas cosas por hacer, ahora a por la Tesis y a tu nuevo curro, ¿sabes lo que eso conlleva? Si no lo sabes, te doy una pista, en 9 meses lo sabrás. Victoria, gracias por tus consejos, por tu apoyo, eres genial y, aunque ya no comas con nosotros, te queremos mucho. Gracias Ahmad por tu sencillez, nobleza y porque ahora mismo eres uno de mis grandes apoyos en el labo, sigue así (y trabaja alguna hora más, ¿eh?). El año que viene iremos a visitarte a UK.

Cambiando de tercio, "mis chicas" del depar, esas que cuando llegué me acogieron con los brazos abiertos, Jael, Sonia, Mariajo, Mariaji, Laurita, y, como no a mi primera esposa, Ana, eres muy importante para mí, gracias por todos los años que hemos compartido en el labo y fuera, lástima que os fuerais con Miguel Ángel al CNB, espero verte pronto, te debo una visita, lo sé.

Gracias a la U2, David, Dani, Blanca, Elvira, Inés, Carmen y Verónica, porque sois estupendos, simpáticos, se puede contar con vosotros y creo que estáis poco valorados. Espero que todo os vaya genial.

A la U3, Pablo, Esme, Almu, Isa, Maria O, Maria Ro, Tere y aquellos que habéis pasado por ahí un tiempo corto. Gracias a todos por todos los momentos vividos, aún quedan, ¿eh? Y espero que muchos. Tere, que se acaba esto ya, ánimo y gracias por ser como eres, quizás demasiado buena, pero eso no es malo, sigue así, eres genial.

La U4, los grandes Raúl y Quique, sois geniales, anexos a la U1 los viernes y fiestas de guardar. Gracias por vuestro apoyo, por las fiestas, los viajes, momentos en el parque de atracciones y por los consejos y ayuda que me habéis ofrecido durante estos años, he descubierto a dos grandes amigos. Belén, otra joyita, cuyos palos nunca son mal recibidos, gracias porque eres una gran persona, aunque parezca que eres una borde, desde el principio me has encantado, espero que todo te vaya genial. Sonia, que ya te mencioné antes, pero gracias por todo, ayuda, consejos, y, como no, por los medios de cultivo, aunque son menos necesarios que tú en el Depar. También a Noe por la ayuda,

sobretodo, en este último tramo de la Tesis. Y a aquellos que ya se han ido, Carmen, Laurita, Pedro, Lore y Ali.

A la U5, que poco a poco se va quedando vacía, habrá que pensar como la llenamos. Como ya agradecí a todos me quedan los que ya se han ido, Miguel Relloso, gracias por la ayuda con las cosas que pregunté cuando estaba empezando, a Elvi y Eugenia, porque trabajar en cultivos con vosotros ha sido fácil y ha sido un placer teneros durante estos años a mi lado. Cristina Molero, Kristina y Narcisa, también miembros de la U5, también quiero daros las gracias por los momentos que he pasado en vuestra unidad, sobre todo cuando iba a hablar con Gloria. Y a la U7, que están ahí abajo y los vemos poco, Nacho, Leti y, especialmente, gracias a Clarissa, gran amiga, entramos juntos y ahora ya estás viviendo tu vida de Dra. en Chile, muchísima suerte.

También destacar a los compañeros de la Unidad de Proteómica, anexos a nosotros, Mª Luisa, Lola, Montse, Felipe y David, pero también a los que no están ya; Rasmus, Pilar, Juan, Mar. Muchísimas gracias por todo, tanto profesional como laboralmente, por vuestra ayuda en la planificación de experimentos, las listas y listas de proteínas que nos proporcionáis y, a veces, no hay por dónde cogerlas, gracias por las celebraciones, salidas y demás actividades "extra laborales", sin vosotros nuestro trabajo sería más difícil.

Gracias a nuestros colaboradores, Manuel Fuentes y Ángel Corbí, trabajar con vosotros ha sido un placer, he aprendido mucho con vosotros y me habéis ayudado con todos los problemas que han ido surgiendo.

I would like to thank Ole N. Jensen and Karin Strijbis for the opportunity of going to your labs at University of Southern Denmark and to the Whitehead Institute at MIT, respectively. Thanks for your dedication and thanks for the opportunity to learn with you. Thanks to Jimmy, because you were my support in Odense and you helped me with the analysis of my samples. Pero también a Nerea y Chiara, con las que pasé grandes momentos en aquella pequeña ciudad Danesa. Y, como no, a mis "chicos americanos" Gloria, Víctor, Virginia, Pilar, Joydeep, Estefanía y Juan, gracias por estos tres meses en Boston, no sé qué habría hecho sin vosotros, por las escapadas a ver esos sitios maravillosos, por los viajes a Philly y Whasington, me traje grandes amigos de allí.

A mis nuevos compañeros Pseudomonos, a Jose Luís, Sara, Fernando, Felipe, Blanca, Jorge, Alejandra y Guille, aunque no estoy mucho tiempo allí, una vez termine con esto, seré un Pseudomono más y podréis disfrutar de mi compañía. Comienza la era de las bacterias.

A toda la gente que he ido conociendo en Madrid aunque muchos de ellos ya no siguen estando a mi lado en esta ciudad. Juan, Rodrigo, Rafa, Miguel, Edu, Marta, Javi, gracias por los buenos momentos fuera del laboratorio, por hacerme desconectar cuando salía de trabajar, es muy bonito tener una pequeña familia fuera de tu ciudad. También Marta, David, Alfonso y Araceli, que sois como mi familia en Madrid.

Pero también gracias a todos mis amigos de Orihuela, con los que crecí, aprendí y a los que siempre llevaré allá donde esté. En especial a Sanmartín y Joaquín, gracias por estar ahí cuando os necesito, me encantaría teneros más cerca, pero aunque pase el tiempo y la distancia siempre seguiréis siendo mis mejores amigos, os quiero.

Y, en especial, a toda mi familia, que os quiero con locura. A mis ahijadas, Marta y Gema, porque dais ese toque jovial a mi vida, a mis primos: Benjamín, Abel, Irene, Sandra y Eusebio; con los que paso grandes momentos y a los que quiero un montón. A la tata, mi madrina, gracias por ser mi segunda madre y "consentirme" más que la primera, pero de eso se trata.

Como no, gracias especialmente a mis padres, incondicionales y siempre disponibles para todo, por educarme, por enseñarme vuestros valores y hacerme mejor persona, por apoyarme y confiar en mí, por tener siempre las palabras necesarias para levantarme el ánimo y para hacerme continuar con esto. A mis hermanas, Ana y Patricia, porque siempre están ahí para darme todo, porque, junto a mis padres, me han apoyado en todas mis decisiones y os debo muchísimo, soy muy afortunado de teneros como hermanas y haber crecido con vosotras, os quiero. A mi abuela, aquella que hace casi 7 años, cuando le dije que iba a ser Doctor en unos años se puso muy contenta y me dijo: Hijo, ¿vas a ser médico? Por tu alegría, apoyo y, aunque ahora no estás muy bien, gracias y todo el ánimo del mundo, por ti va esta Tesis. A César, que en estos años te has convertido en parte de mi familia, gracias por aguantarme al salir del trabajo, por haberme apoyado y por sacarme la sonrisa en los peores momentos, por todos los momentos vividos y los que nos quedan, suerte en Barcelona, te lo mereces. Y, por último y no menos importante, a la pequeña vaca, a mi cachorrita, Vaquina, porque siempre estás de buen humor, al salir de trabajar y llegar a casa tras un día de correcciones, un par de lametones y listo, energía recargada. Fiel, incondicional y necesaria como el que más, gracias pequeña.

A todos vosotros van dedicadas todas estas líneas de agradecimientos y de la Tesis, millones de gracias por vuestro apoyo.

“Lo que sabemos es una gota de agua;
lo que ignoramos es el océano”
(Isaac Newton)

Índice

Abreviaturas

2D Two-dimensional/ Bidimensional

2D-DIGE Two-Dimensional Difference In-Gel Electrophoresis

2D-PAGE 2D-polyacrilamide gel electrophoresis/ Electroforesis bidimensional en gel de poliacrilamida

Ab(s) Antibody (ies)/ Anticuerpo(s)

ACN Acetonitrilo

AMPc Cyclic adenosine monophosphate/ Adenosín monofosfato cíclico

APC Antigen presenting cell/ Célula presentadora de antígeno

BSA Bovin seroalbumin/ Seroalbúmina bovina

BVA Biological Variation Analysis/ Análisis de variaciones biológicas

CFUs Colony Forming Units/ Unidades formadoras de colonias

CHAPS 8-[(3-cholamidopropyl)-dimethylammonio]-1-propane sulfonate)/ 3-[(3-colamidopropil) dimetilamonio]-1-propanosulfonato

CO_2 Carbon dioxide/ Dióxido de carbono

Da Daltons

DC Dendritic Cell/ Célula dendrítica

DHR Dihydrorhodamine/ Dihidrorodamina

DIA Differential In gel Analysis/ Análisis diferencial en gel

DTE Dithioerythritol/ Ditioeritrol

DTT Dithiothreitol/ Ditiotreitol

EDTA Ácido etilén diamino tetracético

ELISA Enzyme-Linked Immunosorbent Assay/ Ensayo por inmunoabsorción ligado a enzimas

ER Endoplasmic Reticulum/ Retículo Endoplasmático

ESI Electro Spray Ionization/ Ionización con electro-spray

FBS Fetal Bovine Serum/ Suero de ternera fetal

FDR False Discovery Rate/ Porcentaje de falso positivos

FITC Fluorescein isothiocyanate/ Isocianato de fluoresceína

GM-CSF Granulocyte Macrophage Colony-Stimulating Factor/ Factor estimulador de colonias de granulocitos y macrófagos

h Hour/Hora

H_2O_2 Hydrogen peroxide/ Peróxido de hidrógeno

HCA Hierarchical Clustering Analysis/Análisis jerárquico de grupos

IEC Ion Exchange Chromatography/ Cromatografía de intercambio iónico

IEF Isoelectric focusing/ Isoelectroenfoque

Ig (s) Immunoglobulin(s)/ Inmunoglobulina (s)

IL Interleukin/ Interleuquina

INF-γ Interferón-γ

IP Propidium Iodide/ Ioduro de propidio

IPG Immovilized pH Gradient/ Gradiente de pH inmovilizado

iTRAQ Isotope Tag for Relative and Absolute Quantitation/ Marcaje de isótopos para cuantificación relativa y absoluta

kDa KiloDalton/ KiloDaltons

LC Liquid Chromatography/ Cromatografía líquida

LDS Litium Dodecyl Sulphate/ Dodecil sulfato de lítio

LPS Lipopolysaccharide/ Lipopolisacárido

LTQ Linear Trap Quadrupol/ Trampa iónica lineal

m/z Mass-to-charge ratio/ relación masa-carga

MALDI-TOF Matrix Assisted Laser Desorption Ionization-Time of Flight/ Desorción-ionización asistida por láser sobre matriz. Tiempo de vuelo

MAPK Mitogen-Activated Protein (MAP) kinase/ Kinasa de tipo MAP (proteínas activadas por mitógeno)

M-CSF Macrophage Colony-Stimulating Factor/ Factor estimulador de colonias de macrófagos

MHC/CMH Major Histocompatibility Complex/ Complejo mayor de histocompatibilidad

min Minutes/ Minutos

MR Mannose receptor/ Receptor de manosa

MS Mass Spectrometry/ Espectrometría de masas

NADPH Reduced form of nicotinamide adenine dinucleotide phosphate/ Forma reducida del fosfato dinucleótido nicotinamida adenina

NK Natural Killer

NO Nitric Oxide/ Óxido nítrico

O_2^- Superoxide anion/ Anión superóxido

ºC Celsius degree/ Grados centígrados

PAMPs Pathogen-Associated Molecular Patterns/ Patrones moleculares asociados a patógenos

PBS Phosphate Buffered Saline/ Tampón salino fosfato

PCA Principle Component Analysis/ Análisis de componentes principales

pI Isoelectric point/ Punto isoeléctrico

PMF Peptide Mass Fingerprinting/ Huella peptídica

PMNs Polymorphonuclear cells/ Células polimorfonucleares

PMSF Fenilmetilsulfonilfluorida

PRRs Pattern Recognition Receptors/ Receptores de reconocimiento de patrones

PTM Postranslational modifications/ modificación post-traduccional

RE Retículo Endoplasmático

RNS Reactive Nitrogen Species/ Especies reactivas de nitrógeno

ROS Reactive Oxygen Species/ Especies reactivas de oxígeno

SDS Sodium Dodecyl Sulphate/ Dodecil sulfato sódico

SEM Scanning Electron Microscopy/ Microscopio electrónico de barrido

SILAC Stable Isotope Labeling by Amino acids in Cell culture/ Marcaje isotópico estable con aminoácidos en cultivos celulares

TCA Ácido tricloroacético

T_H T helper cell/ Célula T cooperadora

TLRs Toll-Like Receptor/ Receptor de tipo “Toll”

TNF-α Tumoral Necrosis Factor α/ Factor de necrosis tumoralα.

TOF Time of flight/ Tiempo de vuelo

Treg Regulatory T cells/ Células T reguladoras

TUNEL Terminal deoxynucleotidyl transferase dUTP Nick-End Labeling/ Marcaje del extremo libre por dUTP (desoxi-transferasa terminal)

UV Ultraviolet/ Ultravioleta

WB Western blotting

YPD Yeast extract Peptone Dextrose

µl Microliter/Microlitro

Summary

Introduction:

Candida albicans is one of the most important opportunistic pathogen in humans that can produce different types of infections ranging from superficial to systemic. Invasive candidiasis is an important cause of disease and mortality in immunosuppressed patients and the therapeutic arsenal is reduced, sometimes toxic and can generate resistances. The study of the host response to *Candida* infections can be a very useful tool to discover new therapeutic strategies.

The innate immune system is the first line of defense against *Candida* infection being macrophages crucial elements against systemic candidiasis that display a wide variety of mechanisms to destroy the fungus. Macrophages exhibit a considerable phenotypic diversity and functional plasticity that confer them the ability to efficiently respond to tissue injuries. Upon stimulation, macrophages M1 or classically activated are characterized by a pro-inflammatory cytokine response, generation of reactive oxygen and nitrogen intermediates, promotion of Th1 response, and strong microbicidal and tumoricidal activities; by contrast, macrophage M2 or alternatively activated are primarily immunosuppressive and characterized by the promotion of Treg responses and potent tissue remodeling and tumor promotion activities, and exhibit an overall less efficient microbicidal capacity.

The introduction of proteomics has enabled the simultaneous analysis of changes in many proteins. 2D-Difference Gel Electrophoresis (2D-DIGE) is a powerful analytical tool that allows us the relative quantitation of protein and also for detecting posttranslational modifications of the protein. Stable Isotope Labeling by Amino acids in cell Culture (SILAC) is a powerful and relatively simple method for the accurate quantitation of proteins by mass spectrometry. Phosphoproteomics is the large-scale analysis of protein phosphorylation using mass spectrometry (MS)-based strategies to examine phosphorylation signaling networks. In the present work we report proteomic, sub-proteomic and phosphoproteomic studies on murine (RAW 264.7 cell line) and human M1, M2 macrophages protein response to *C. albicans* interaction. For the first time, a proteomic study has been done on the differential protein expression in human M1 vs. M2 macrophages, as well as their distinctive responses to *C. albicans,* contributing to the dissection of the molecular mechanisms by which differentially polarized macrophages cope with pathogens, and can pave the way for the identification of novel antifungal strategies and to the detection of novel *C. albicans* virulence mechanisms.

Objectives:

The aims of this study are headed for the identification and characterization of the protein and phosphoprotein networks involved in the response of both murine and human macrophages against *C. albicans* infection in order to discover new mechanisms of host defence to *C. albicans* infection.

Results:

The combined use of *in-gel* and *off-gel* proteomic techniques allowed us to identify the protein networks involved in the interaction RAW 264.7 murine macrophages with *C. albicans*, and it has been structured in 3 Chapters:

In the first chapter, the study of the macrophage sub-proteomic fractions (cytosol, membranes/organelles, nucleus and cytoskeleton) using 2D-DIGE technology was boarded. The results obtained permitted the identification of important proteins that are not easily detected in total cell extracts, such us, mitochondrion proteins, a membrane receptor, Galectin-3, and some ER related proteins. The proteins identified are involved in the pro-inflammatory and oxidative responses, the immune response, the unfolded protein response and in apoptosis.

In the second chapter we describe the proteomic and phosphoproteomic study using SILAC to quantify macrophage proteins and phosphoproteins by mass spectrometry, that allowed us the identification and quantitation of 53 most abundant and 15 less abundant macrophage proteins in the presence of *C. albicans* and 126 peptides that showed an increase and 70 a decrease in their phosphorylation level. This phosphoproteomic enrichment contributed to the phosphorylation databases in 327 previously unidentified mouse protein phosphorylation sites.

Most of the macrophage networks affected by the interaction with the fungus were receptors, mitochondrial ribosomal proteins, cytoskeletal proteins, and transcription factor activators involved in inflammatory and oxidative responses. In addition, in previous works and in the present ones, we identified many proteins related to apoptosis, both pro- and anti-apoptotic. The analysis of apoptotic markers revealed that anti-apoptotic signals prevailed during the interaction of the yeast in our experimental conditions that intend to be similar to physiological infection with respect to MOI (Multiplicity Of Infection).

The last chapter of this Thesis is the study of the protein differences between human polarized M1 and M2 macrophages and between their specific responses to *C. albicans* using DIGE technology. This study revealed that the most important differences between both types of macrophages are related to metabolic pathways, specifically glycolysis and gluconeogenesis. The analysis has revealed Fructose 1,6-bisphosphatase (Fbp1), a critical enzyme in gluconeogenesis, more abundant in M1, as a novel protein marker for M1 macrophage polarization. Regarding the response to *C. albicans*, an M1-to-M2 switch in polarization was observed as well as a limitation in Th1 inflammatory responses during the interaction.

Conclusions:

The combination of different proteomic techniques (in gel and off gel, subcellular fractionation and phosphopeptides enrichment) allowed us to obtain a more complete map of the protein networks affected by the interaction of macrophages and *C. albicans*. For this reason, the enrichment in proteins from different sub-cellular fractions and in phosphoproteins is a good choice to study protein less abundant in the whole proteome that could be crucial for the host fight against the pathogen.

The most important pathways involved in the macrophage response to *C. albicans* are the inflammatory response, the increase in the oxidative stress response and the cytoskeleton rearrangement.

The interaction with *C. albicans* seems to inhibit the apoptosis in macrophages. This inhibition might be a host immune mechanism to reinforce defences against the invading pathogen or, on the other hand, a *Candida* virulence factor that favours replication and dissemination inside macrophages.

In the case of human polarized macrophages M1 and M2, Fbp1 appears as a novel protein marker for M1 polarized macrophages. M1 macrophages switch to M2 in response to *C. albicans* interaction. This M1-to-M2 switch might contribute to *Candida* pathogenicity by decreasing the generation of specific immune responses, thus enhancing fungal survival and colonization, or instead, may be part of the host attempt to reduce the inflammation and limit the damage of the infection.

Introducción

1. SISTEMA INMUNITARIO

El sistema inmunitario es un conjunto de células y procesos biológicos que protegen al individuo frente a las enfermedades infecciosas producidas por bacterias, virus, levaduras y hongos, aunque algunas sustancias extrañas como toxinas y componentes de estos organismos, son capaces de activar la respuesta inmune. Está compuesto principalmente por linfocitos (T y B), leucocitos, macrófagos, neutrófilos, anticuerpos y citoquinas, que componen una red elaborada y dinámica que se adapta en el tiempo para reconocer patógenos de forma más específica y así responder más eficientemente. La respuesta inmune frente a microorganismos se clasifica en dos grupos:

Respuesta Innata

También llamada natural o nativa, es la primera línea de defensa del organismo y es la más rápida. Está constituida por mecanismos de defensa celulares y bioquímicos que desencadenan una respuesta rápida frente a las infecciones.

La superficie del cuerpo está protegida por epitelios que constituyen una barrera física entre el medio interno y los agentes patógenos del exterior. Si los patógenos atraviesan esa barrera epitelial se encuentran con los macrófagos y otras células fagocíticas en el tejido subepitelial. Estas células reconocen y fagocitan a los microorganismos y son capaces de activar células colindantes.

Las principales células implicadas en este tipo de respuesta son los macrófagos, los neutrófilos y las células NK (*Natural Killers*).

Respuesta Adaptativa

También conocida como inmunidad adquirida o específica, está estimulada por la exposición a agentes infecciosos o nocivos y aumenta la capacidad de respuesta frente a un patógeno determinado. Las características que definen este tipo de respuesta son la selectividad hacia un tipo de molécula determinado y la capacidad de "recordar" y responder de una manera exacerbada y más eficiente frente a exposiciones repetidas de un mismo microorganismo. Es capaz de distinguir entre patógenos o moléculas muy similares y responder específicamente frente a ellos.

El mayor componente de la respuesta adaptativa son los linfocitos y sus moléculas secretadas (anticuerpos).

1.1. Macrófagos

Los macrófagos son células fagocíticas mononucleares pleiotrópicas implicadas en un gran número de funciones dentro del sistema inmunitario. Son efectores de la respuesta innata y están muy relacionadas, tanto en el inicio, como en las fases posteriores de la respuesta adaptativa. Además, son críticas en el mantenimiento de la homeostasis (eliminación de células apoptóticas, reparación, modelación y angiogénesis de los tejidos, etc.) (Mantovani, *et al.*, 2002).

Están presentes en todos los tejidos del cuerpo y se activan tras un estímulo, produciéndose, entre otras cosas, la síntesis de citoquinas proinflamatorias (Plowden, *et al.*, 2004), a diferencia de otras células del sistema inmunitario. En ausencia de estímulos, los macrófagos mueren por apoptosis, como balance de producción y eliminación de células efectoras (Celada, *et al.*, 1994). La heterogeneidad de los macrófagos refleja una plasticidad y versatilidad de estas células a la hora de responder a la exposición de señales procedentes del medio ambiente.

Origen de los macrófagos

El proceso de formación, desarrollo y maduración de las células sanguíneas a partir de un precursor común (célula madre) es conocido como hematopoyesis (Ogawa, 1993). Estas células madre, conocidas como *stem cells*, poseen capacidad auto-regeneradora y potencial para diferenciarse hacia los distintos tipos celulares de la sangre, gracias a esta característica se consigue un recambio celular adecuado (Compston, 2002).

En la médula ósea se encuentran las células madre en estado de quiescencia hasta que reciben un estímulo procedente de factores de crecimiento específicos, como son las citoquinas y hormonas. Entonces la célula madre experimenta un primer proceso de diferenciación consistente en un cambio por el cual la madre pierde su capacidad autorregeneradora y se diferencia a otra célula un poco más especializada que su predecesora pero que aún mantiene su capacidad de diferenciación. El segundo paso es un proceso de maduración gracias al cual acabará de diferenciarse en un linaje celular específico (línea linfoide, eritroide y megacariocítica y granulocítica) (Figura 1).

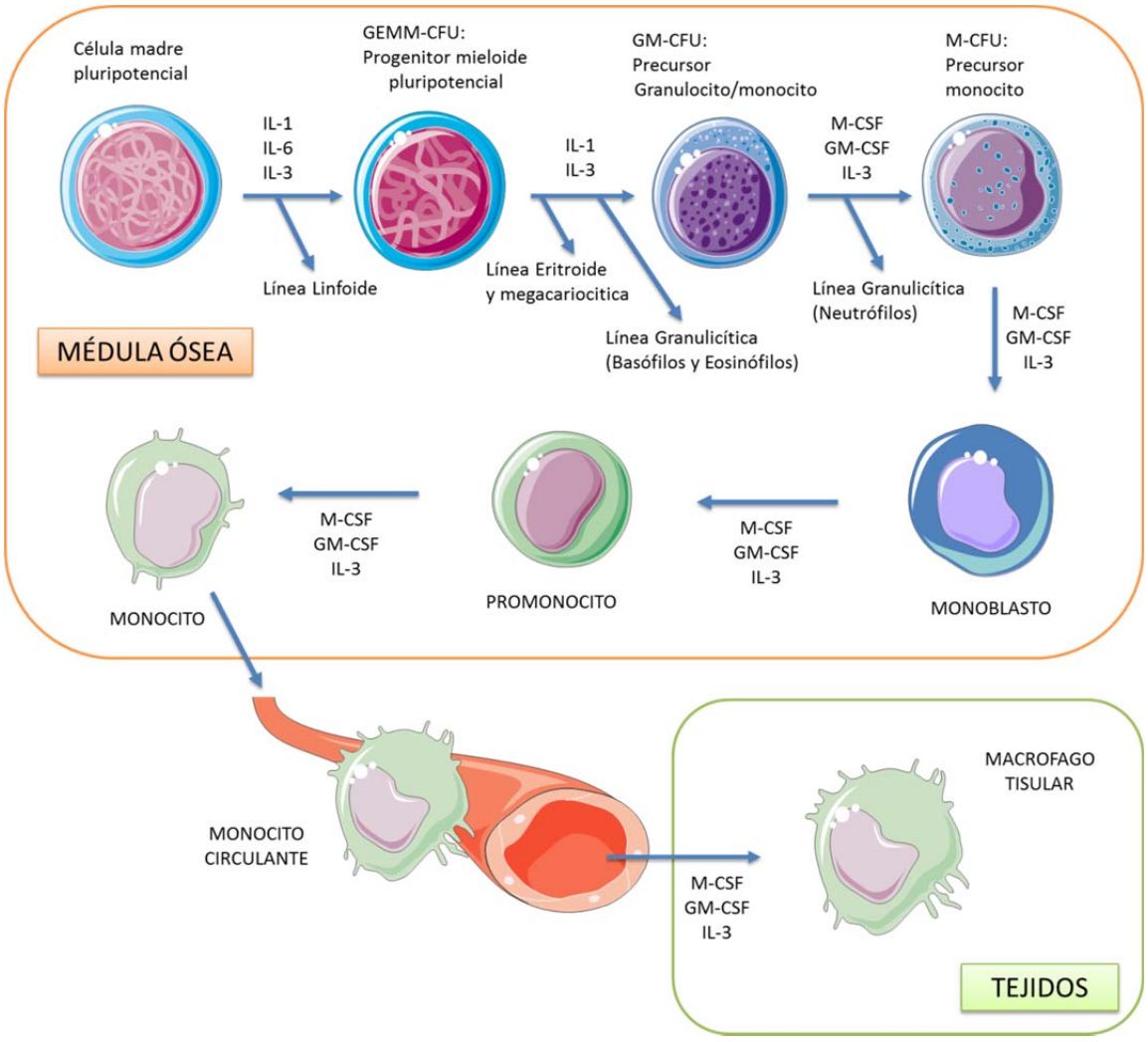

Figura 1: **Proceso de diferenciación del macrófago.** IL, interleuquina; M-CSF, factor estimulador de colonias de macrófagos; GM-CSF, factor estimulador de colonias de granulocitos y macrófagos; GEMM-CFU, unidad formadora de colonias de granulocitos, eritrocitos, megacariocitos y macrófagos; GM-CFU, unidad formadora de colonias de granulocitos y macrófagos; M-CFU, unidad formadora de colonias de macrófagos. Reproducida de Valledor *et al* (Valledor, *et al.*, 1998).

El factor de crecimiento GM-CSF (factor estimulante de colonias de granulocitos y monocitos) y la IL-3, entre otras, inducen la proliferación de la línea celular granulocítica-monocítica. Mientras que, el factor de crecimiento M-CSF (factor estimulante de colonias de monocitos) no sólo induce la proliferación de estas células, sino también su diferenciación hacia precursores propiamente monocíticos denominados M-CFUs (unidad formadora de colonias de monocitos). A partir de este precursor M-CFU pueden derivarse 3 vías distintas de diferenciación: osteoclastos, células dendríticas mieloides o macrófagos (Valledor*, et al.*, 1998).

El monocito es el primer tipo celular que entra en la sangre periférica, cuando estos entran en los tejidos y, tras una serie de estímulos, los monocitos entran en su última etapa de diferenciación mediante la cual adquirirán ya la morfología y la bioquímica propias de un macrófago, tales como un aumento de tamaño, un mayor desarrollo del sistema lisosomal, un incremento de la cantidad de enzimas hidrolíticas y en el número y tamaño de las mitocondrias, así como de su metabolismo energético y de su capacidad fagocítica (Celada*, et al.*, 1992).

Los macrófagos pueden adoptar diferentes formas tras la activación por diferentes estímulos. Dependiendo del tipo de tejido donde resida reciben diferentes nombres: microglía (sistema nervioso central), células de Kupffer (hígado), células espumosas (placa de ateromas), células de Langerhans (piel), histiocito (tejido conjuntivo), osteoclastos (huesos), células mesangiales intraglomerulares (riñón) y macrófagos alveolares (alveolos pulmonares).

Función

Una vez en los tejidos, los macrófagos juegan un papel crítico en el desarrollo de la respuesta inmunológica. La función de los macrófagos y su morfología depende del tejido en el que se encuentren.

Los macrófagos en estado basal se encuentran en disposición de realizar una serie de funciones sin necesidad de ningún tipo de estímulo, aunque muchas de éstas pueden realizarse con mayor eficiencia tras la activación de la célula. Sin embargo, para otras funciones se requiere que la célula haya sido previamente activada para poder llevar a cabo. En general, los macrófagos tienen funciones homeostáticas que incluyen reparación, modelación y angiogénesis de los tejidos y proveen protección al poner en marcha mecanismos inmunes innatos e iniciar el desarrollo de respuestas inmunes específicas a través del procesamiento y presentación de antígenos, la expresión de moléculas co-estimuladoras y la producción de citoquinas.

Fagocitosis

La fagocitosis constituye la primera línea de defensa contra partículas extrañas que han superado la barrera epitelial. El proceso de fagocitosis es muy complejo ya que los macrófagos son capaces de fagocitar macromoléculas, como antígenos, microorganismos e incluso células propias dañadas o muertas, como son las células apoptóticas.

Para discriminar entre agentes infecciosos y propios, los macrófagos han desarrollado un número restringido de receptores fagocíticos, que reconocen motivos conservados en los patógenos (Aderem*, et al.*, 1999a). Janeway propuso llamar a estos receptores “receptores de reconocimiento de

patrones" (PRRs; *Pattern Recognition Receptors*), y a las dianas de estos receptores, "patrones moleculares asociados a patógenos" (PAMPs; *Pathogen-Associated Molecular Patterns*) (Janeway, 1992).

Los macrófagos reconocen estos patógenos a través de sus receptores de superficie, los cuales son capaces de discriminar entre moléculas de superficie mostradas por patógenos o por el propio hospedador. La unión de estos receptores de superficie con patógenos conduce a la fagocitosis del mismo, seguida de su muerte dentro del fagocito.

La fagocitosis es un proceso activo, en el cual el patógeno es rodeado por la membrana celular del fagocito, y después es internalizado en una vesícula conocida como fagosoma o vesícula endocítica. El fagosoma se acidifica posteriormente, matando a la mayoría de los patógenos. Para los microorganismos que resisten esta acidificación, los macrófagos tienen unos gránulos, llamados lisosomas, que contienen enzimas, proteínas, y péptidos que son capaces de mediar una respuesta intracelular antimicrobiana. A través de una serie de eventos de fusión y fisión, la membrana vacuolar y su contenido maduran, fusionándose con endosomas tardíos y finalmente con lisosomas para formar el fagolisosoma, en el que el contenido lisosomal es liberado para destruir al patógeno (Janeway, *et al.*, 2005).

Además de fagocitar, los macrófagos también producen una gran variedad de productos tóxicos que ayudan a matar al microorganismo fagocitado. Las más importantes son óxido nítrico (NO), el anión superóxido (O_2^-), y el peróxido de hidrógeno (H_2O_2), que son tóxicos directamente para las bacterias y otros microorganismos. El óxido nítrico es producido principalmente por la forma inducible de la NO sintasa (iNOS), el anión superóxido es generado por una oxidasa NADPH asociada a membrana celular, en un proceso conocido como "estallido respiratorio" (*oxidative burst*) porque va acompañado de un incremento transitorio del consumo de oxígeno y es convertido por la superóxido dismutasa en H_2O_2. Además, otras reacciones químicas y enzimáticas producen otros compuestos tóxicos a partir del peróxido de hidrógeno, como son, el radical hidroxilo (OH^-) y los iones hipoclorito (OCl^-) e hipobromito (OBr^-) (Janeway, *et al.*, 2005).

Liberación de citoquinas

La interacción entre patógenos y macrófagos tisulares tiene otro efecto importante, la activación de los macrófagos para liberar citoquinas, quimioquinas (citoquinas quimoatrayentes), y otros mediadores que establecen un estado de inflamación en el tejido y que atraen neutrófilos y proteínas plasmáticas al sitio de la infección. Los patógenos inducen la secreción de citoquinas y quimioquinas a través de señales comunicadas por los mismos receptores a los que se unen para ser fagocitados, o por otros receptores diferentes.

Los macrófagos secretan un amplio rango de citoquinas, quimioquinas, factores de crecimiento y enzimas, en respuesta a patógenos y "señales de peligro". Más de 100 factores diferentes son secretados por macrófagos (Nathan, 1987). Éstos incluyen citoquinas (IL-1, IL-6, IL-10, IL-12, IL-15, IL-18, TNF-α, IFN-α y β, TGF-β, GM-CSF, M-CSF, y factores de angiogénesis como VEGF), quimioquinas CXC (IL-8, GROα, β y γ, IP-10, MIP-1, MCP-1, ENA-78), factores de coagulación, PGE_2, leucotrienos, especies reactivas de oxígeno (ROS) y de nitrógeno (RNS), componentes del complemento, y numerosas proteasas y enzimas.

La secreción de estos factores depende del tipo de estímulo, del tipo de macrófago y de la localización. El resultado de esta capacidad de los macrófagos es que pueden crear y modular el entorno iniciador de la respuesta inmunitaria adaptativa (Plowden*, et al.*, 2004).

La liberación de unas citoquinas u otras dirige el siguiente paso de la defensa del hospedador. Por ejemplo, IL-12 es una inductora del desarrollo de las células T cooperadores (*helper*) tipo 1 (Th-1), además estimula la producción de INF-γ por parte de los linfocitos y células NK, incrementando así la respuesta inflamatoria y la actividad citotóxica de los LT citotóxicos (LTc) y NK. La IL-10 es un inhibidor de los macrófagos y células dendríticas activadas y está implicado en el control de las reacciones inmunes innatas y en la inmunidad mediada por células. Sin embargo la IL-4 estimula una producción de IgE y favorece el desarrollo de células Th-2.

Presentación de antígenos

Los macrófagos que han fagocitado a los microorganismos, contribuyen a la respuesta inmunitaria adaptativa actuando como células presentadoras de antígenos (APC).

Para ello es necesario que el macrófago exprese moléculas del complejo mayor de histocompatibilidad tipo II (MHC II) y moléculas B7 en su superficie, lo que es inducido por el reconocimiento e ingestión de microorganismos. Es decir, los receptores fagocíticos, de los que hemos hablado anteriormente, que reconocen y unen microorganismos a la superficie celular del macrófago. Esos microorganismos son ingeridos y degradados en endosomas y lisosomas, generando péptidos que pueden ser presentados por moléculas MHC tipo II. Estas moléculas activan a los linfocitos T $CD4^+$ (Ramachandra*, et al.*, 1999) y transmiten señales que conducen a la expresión de moléculas MHC tipo II y moléculas B7 (Bynoe*, et al.*, 2005). Los antígenos fagocitados también pueden ser presentados por el MHC tipo I y activar a los linfocitos T $CD8^+$ en un proceso llamado presentación cruzada ("*cross-presentation*") (Lehner*, et al.*, 2004).

Activación y Polarización de macrófagos

Los monocitos circulantes constituyen un 5-10% del número total de leucocitos en sangre periférica en humanos. Dan lugar a una gran variedad de macrófagos residentes en tejidos, pero también a células dendríticas y a osteoclastos. La morfología de monocitos maduros circulantes es muy heterogénea ya que poseen diferentes tamaños, grados de granularidad y morfología nuclear. En los tejidos, los monocitos se diferencian a macrófagos residentes con un fenotipo determinado que depende del microambiente tisular, matriz extracelular y moléculas de superficie de las células adyacentes y de sus productos de secreción. Esta cualidad de expresar rangos de fenotipos morfológicos y funcionales muy amplios contribuye a la gran heterogeneidad de los mismos (Gordon, 2003, Gordon*, et al.*, 2005).

La activación de los macrófagos comprende de alteraciones morfológicas, bioquímicas y funcionales que confieren al macrófago activado la capacidad de realizar alguna función que no puede realizar el monocito en reposo, como matar microorganismos, lisar células tumorales secretar mediadores inflamatorios, actuar como células presentadoras de antígenos más eficaces, etc. En general, la activación del macrófago es el resultado de una nueva transcripción génica o de un aumento de la misma (Mantovani*, et al.*, 2007,

Puig-Kroger, *et al.*, 2009). Los agentes más potentes en la activación de los macrófagos son el lipopolisacárido (LPS) y la citoquina INF-γ, aunque también hay otros agentes como el GM-CSF, M-CSF, IL-1, IL-2, IL-4 y el TNF-α que pueden inducir algunos cambios en la activación (Celada y Nathan, 1994).

La activación de los macrófagos, tanto clásica como alternativa, es un proceso regulado y complejo de modificaciones morfológicas y bioquímicas que provocan en la célula un aumento de su capacidad para ejercer funciones.

Activación Clásica

La activación clásica de los macrófagos (CAMs) es inducida por citoquinas proinflamatorias tipo I (IFN-γ, TNF-α), por el M-CSF, o tras el reconocimiento de los PAMPs (LPS, lipoproteínas, dsRNA, ácido lipoteicoico,...) y señales de peligro endógenas. Juega un papel muy importante en la protección frente a patógenos intracelulares, lisis de células tumorales. Los macrófagos así activados (CaMΦ o M1) poseen un fenotipo IL-12^{alto}, IL-23^{alto}, IL-10^{bajo} (Verreck, *et al.*, 2004) y son, consecuentemente, promotores de la respuesta inmune de tipo Th1. Además, estas células ejercen funciones anti-proliferativas y citotóxicas, secretando especies reactivas del oxígeno y del nitrógeno (NO, peroxinitrito, peróxido de Hidrógeno, superóxido), citoquinas proinflamatorias (TNF-α, IL-1, IL-6) (Bonnotte, *et al.*, 2001, Mytar, *et al.*, 1999, Stuehr, *et al.*, 1989) cambios fagolisosomales y aumento de la expresión del MHC II y de CD86, potenciando así su capacidad presentadora de antígenos asociada con células Th1 (Goerdt, *et al.*, 1999, Katakura, *et al.*, 2004, Mantovani, *et al.*, 2004, Mantovani, *et al.*, 2002).

Activación Alternativa

La activación alternativa del macrófago (AAMs) es inducida por citoquinas tipo Th2 como son la IL-4 o la IL-13, citoquinas desactivantes (como IL-10 y TGF-β), el GM-CSF, hormonas, la vitamina D3 y células apoptóticas (Goerdt, *et al.*, 1999, Gough, *et al.*, 2001). En general, los macrófagos alternativos (AaMΦ o M2) poseen un fenotipo IL-12^{bajo}, IL-23^{bajo}, IL-10^{alto}. No son capaces de producir NO a partir de L-Arg ni de controlar el desarrollo de patógenos intracelulares. Poseen tienen aumentada la capacidad endocítica y fagocítica, hay un aumento en la expresión del receptor de manosa (MR) y varios receptores basurero o "scavengers" y quimioquinas. Todas estas características le ofrecen una capacidad reparadora/autorregeneradora de tejidos.

La heterogeneidad de estos macrófagos anti-inflamatorios los lleva a tener una nomenclatura diferente. Gordon y colaboradores propusieron la restricción de la activación alternativa a los macrófagos activados por IL-4 y/o IL-13 (Gordon, 2003). Posteriormente, Mantovani y colaboradores utilizaron la producción elevada de IL-10 y la baja producción de IL-12 para unificar la nomenclatura de M2 (Mantovani, *et al.*, 2004). Posteriormente, se sugirió una subdivisión del grupo entre M2a, M2b y M2c, representando los estimulados por IL-4/IL-13 (activados alternativamente en sentido estricto), estimulados por complejos inmunes + ligandos de los TLR, y los macrófagos estimulados por IL-10 (desactivados), respectivamente. De este modo, M2 ejerce funciones inmunosupresoras selectivas e inhibe la proliferación de células T (Brys, *et al.*, 2005).

1.2. Línea celular de macrófagos murinos RAW 264.7

Esta línea celular deriva de la línea celular monocito/macrófago RAW 264.7 obtenida por el Dr. Peter Ralph (Ralph, *et al.*, 1977), y se diferencia de esta última en que necesita la presencia de lipopolisacárido (LPS) para producir óxido nítrico (NO), ya que el mero tratamiento con IFN-γ no es suficiente. Esta propiedad hace que su comportamiento sea más parecido a macrófagos normales procedentes de diferentes cepas de ratón como por ejemplo C3H/HeN.

Las células RAW 264.7 producen una cantidad de nitritos (metabolito estable de la reacción del NO con el oxígeno (Moncada, *et al.*, 1991). Por otro lado, su actividad candidacida es menor que la de macrófagos peritoneales de ratones C.B-17 (un 20% frente a un 80%), pero superior a la de otras líneas celulares de macrófagos como J774, WEHI-3, ANA-1, y GG2EE (Vázquez-Torres, *et al.*, 1995).

El modelo murino de candidiasis invasiva es el más utilizado debido a que la infección sistémica en ratones es muy similar a la infección sistémica en humanos, tanto en órganos afectados como en gravedad y curso de la infección (Cole, *et al.*, 1989, Louria, 1985, Odds, 1988a, Papadimitriou, *et al.*, 1986).

Todas estas características hacen de RAW 264.7 sea una línea celular muy adecuada para el estudio de la interacción macrófago-*C. albicans*.

2. *Candida albicans*

Desde un punto de vista taxonómico *C. albicans* está dentro del Phylum Ascomycota, Clase Hemiascomycetes, Orden Saccharomycetales, Familia Candidaceae y Género *Candida* (Barnett, *et al.*, 2000).

C. albicans es un organismo diploide que se reproduce asexualmente por gemación, (Odds, 1988a). Hasta hace poco tiempo, se creía que no tenía ciclo sexual, sin embargo existen evidencias recientes de que el cambio fenotípico blanco-opaco regula el programa sexual, siendo las células opacas las únicas competentes para el apareamiento (*mating*) (Miller, *et al.*, 2002). Hay una diferencia en expresión de unos 1300 genes entre células blancas y opacas, incluyéndo genes directamente implicados en la señalización del apareamiento (Lan, *et al.*, 2002).

C. albicans es un hongo polimórfico, ya que presenta distintas morfologías bajo diferentes condiciones ambientales (Figura 2):

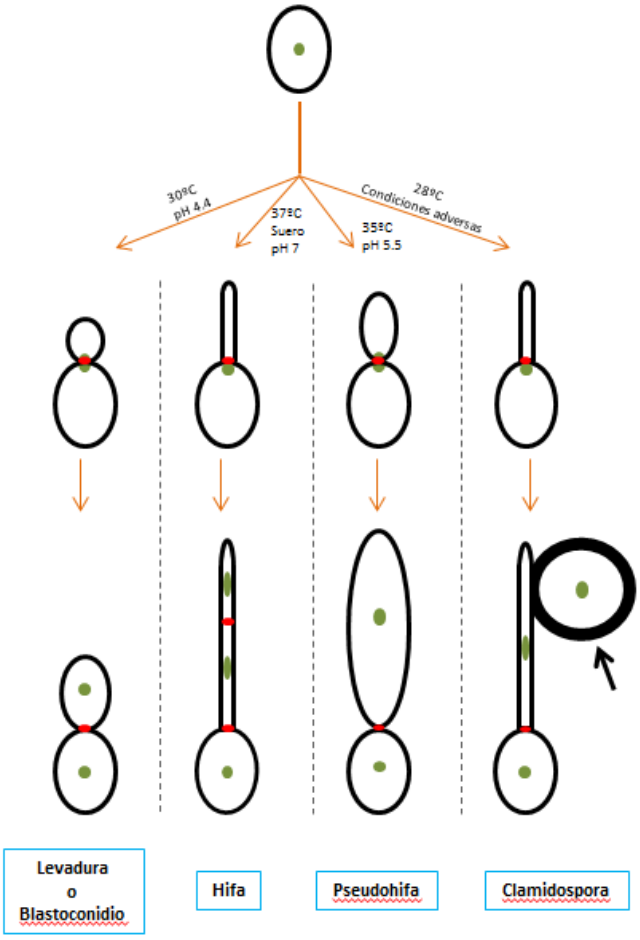

Figura 2: **Polimorfismo de *C. albicans*:** Levadura, Hifa, Pseudohifa y Clamidospora.

La **levadura o blastoconidio** es la forma unicelular del hongo. Célula ovoide germinativa. La formación de una yema ocurre en la región polar de la célula.

Las **hifas** son células filamentosas encadenadas separadas por septos o tabiques. La transición de levadura a hifa se ve favorecida por temperaturas que rondan los 37ºC, alto CO_2 y un pH neutro, además de factores nutricionales como suero, sales de hierro o zinc, biotina, N-acetil-glucosamina, etc. (Odds, 1988a).

Las **pseudohifas** son células alargadas y estrechas. Se forman por gemación a partir de una levadura sin producirse la separación por septos entre la célula madre y la hija. Parecen células filamentosas en cadenas. La formación de pseudohifas se ve favorecida por crecimientos a pH 5.5 o temperaturas de 35ºC.

Por último, las **clamidosporas** podrían ser formas de resistencia que se originan en condiciones ambientales adversas in vitro, son células de pared gruesa, más grandes, redondeadas y refráctiles que las formas levaduriformes.

2.1. *C. albicans* como agente patógeno oportunista

Las infecciones fúngicas más frecuentes son las causadas por la levadura *C. albicans* y por varias especies de hongos filamentosos del género *Aspergillus*. Otros hongos patógenos han emergido en los últimos años, incluyendo especies de levaduras como *C. glabrata*, *C. tropicalis*, *C. krusei*, especies de *Cryptococcus* y *Trichosporon* y hongos filamentosos como *Fusarium*, *Rhizopus* y *Rhizomucor* (Richardson, 2005).

C. albicans es comensal de humanos en tracto gastrointestinal, oral y en la vagina de hasta el 60% de la población (Odds, 1988a). Normalmente no ocasiona problemas, pero al ser un patógeno oportunista puede producir distintos tipos de infecciones denominadas genéricamente candidiasis. El término candidiasis se refiere a cualquier infección causada por especies del género *Candida*, y aunque la especie *C. albicans* sigue siendo la más frecuentemente aislada en las infecciones nosocomiales, en los últimos años ha aumentado el aislamiento de otras especies como *C. tropicalis*, *C. glabrata, C. parapsilosis, C. dubliniensis, C. guilliermondii, C. krusei, C. rugosa*, etc. (Gutierrez*, et al.*, 2002, Moran*, et al.*, 2002, Pfaller*, et al.*, 2006).

C. albicans es responsable de la mayoría de las infecciones fúngicas en pacientes inmunosuprimidos. En individuos sanos se mantiene un equilibrio entre la capacidad de invasión e infección de *C. albicans* y las defensas del hospedador. Sin embargo, cuando existe algún tipo de inmunosupresión (enfermos de cáncer, SIDA o trasplantados), este equilibrio se rompe y se pueden producir desde candidiasis superficiales (en piel o mucosas) hasta candidiasis invasivas. La infección mucosa afecta a las superficies mucosas y la piel, incluyendo cavidad oral, faringe, esófago, intestinos, tracto urinario y vagina. Este tipo de candidiasis es la más común, en ocasiones puede presentan un carácter crónico, aunque en la mayoría de los casos, suele resolverse tras un tratamiento antifúngico.

La resolución de las candidiasis invasivas se dificulta por los importantes efectos secundarios derivados de los antifúngicos disponibles, la aparición de resistencias y la falta de un procedimiento de diagnóstico rápido y preciso (Kontoyiannis*, et al.*, 2002), siendo una de las causas más importantes de morbilidad y mortalidad entre la población

inmunocomprometida (Enoch, *et al.*, 2006, Kullberg, *et al.*, 2002, Pitarch, *et al.*, 2006a, b).

En España la incidencia de las candidiasis sistémicas ha aumentado notablemente en las últimas décadas debido a la concurrencia de una serie de factores, como la terapia masiva con antibióticos antibacterianos de amplio espectro, la utilización de pautas inmunosupresoras intensivas en pacientes neoplásicos y trasplantados, la nutrición parenteral, el empleo de prácticas quirúrgicas y técnicas terapéuticas y diagnósticas agresivas, etc. (Dixon, *et al.*, 1996, Peman, *et al.*, 2005, Pfaller, *et al.*, 2007, Tortorano, *et al.*, 2004). Cabe destacar el importante incremento de mortalidad por *Candida* spp. en las unidades de cuidados intensivos de neonatos (Rodriguez, *et al.*, 2006).

2.2. Factores de virulencia

Los factores de virulencia son definidos de varias formas; se definen como "todo rasgo requerido para establecer enfermedad" (Furman, *et al.*, 1983) "factores que interactúan directamente con las células hospedadoras de mamífero" (Odds, *et al.*, 2001) y "el componente del patógeno que causa daño en el hospedador" (Casadevall, *et al.*, 2001). En este sentido, *C. albicans* debe entrar en contacto con la célula hospedadora, evadir el sistema inmune, sobrevivir y proliferar en el medio ambiente del hospedador y diseminarse a nuevos tejidos para comenzar el proceso infeccioso. La patogenicidad de *C. albicans* es un proceso multifactorial regulado por más de un determinante de virulencia: capacidad de adhesión, capacidad de inducir su propia endocitosis, transición morfológica, *switching* fenotípico y producción de hidrolasas extracelulares. Aunque el factor más determinante en las infecciones por *C. albicans* es la condición inmunológica del hospedador (Calderone, *et al.*, 2001, Mayer, *et al.*, 2013).

Adhesión

El contacto y la adherencia de *C. albicans* a las células hospedadoras son los principales pasos durante la infección, siendo el determinante asociado a la virulencia más importante, crítico en el inicio de la colonización e infección (San Millan, *et al.*, 1996). *C. albicans* presenta diferentes adhesinas en la superficie celular, sobretodo, manoproteínas (como la adhesina superficial específica de hifas, Hwp1p) ((Staab, *et al.*, 1999, Sundstrom, 1999, 2002), quitina (Soares, *et al.*, 2000), glicoproteínas de la familia Als (secuencia similar a aglutinina) Als1p y Als5p (Hoyer, 2001) y diversos receptores (como la integrina INT1p) capaces de unirse a una gran variedad de ligandos del hospedador (fibronectina, fibrinógeno, laminina y colágeno tipo I y IV) (Pendrak, *et al.*, 1995).

Transición morfológica

La transición morfológica es la conversión de células levaduriformes unicelulares a la forma filamentosa (hifa o pseudohifa). *C. albicans* tiene esta capacidad reversible de convertirse de levadura a hifa aumentando así su invasividad. Las señales que promueven estos cambios morfológicos son variados: estrés celular (Brown, 1999), cambios en la temperatura de crecimiento de 30ºC a 37ºC y pH neutro en el medio de cultivo (Lee, *et al.*, 1975, Saporito-Irwin, *et al.*, 1995, Shepherd, *et al.*, 1980), o crecimiento en suero hasta ayuno metabólico. Los mutantes que no son capaces de realizar esta transición son menos

virulentos a la hora de causar patología (Braun, *et al.*, 1997, Diez-Orejas, *et al.*, 1999, Lo, *et al.*, 1997, Rocha, *et al.*, 2001). Aunque se han encontrado lesiones en tejidos infectados que solo contenían formas levaduriformes (Odds, 1988b) y mutantes hiperfilamentosos cuya capacidad infectiva está bastante disminuida (Alonso-Monge, *et al.*, 1999, Laprade, *et al.*, 2002), lo que significa que tanto la forma levaduriforme como la de hifa contribuyen al establecimiento y al progreso de la enfermedad (Odds, 1994).

Secreción de enzimas

La producción de hidrolasas juega un papel primordial en la patogenicidad de *C. albicans*. Las hidrolasas extracelulares facilitan la adhesión y la invasión, también crean daños en las células y en las moléculas del sistema de defensa del hospedador (Cunningham, *et al.*, 2004). Las tres enzimas hidrolíticas más importantes secretadas por *C. albicans* son: aspartil-proteinasas (SAP), fosfolipasas (PL) y lipasas, aunque también se han identificado glucanasas y quitinasas que no parecen estar relacionadas con virulencia (Hube, 2002).

Switching fenotípico

Pomés y colaboradores, demostraron que bajas dosis de luz ultravioleta daban lugar a unas colonias rugosas de *C. albicans* con una frecuencia muy alta ($3x10^{-3}$), y que la reversión de este fenotipo al de una colonia normal ocurría con una frecuencia mucho mayor ($9x10^{-4}$) (Pomes, *et al.*, 1985). A esta capacidad de cambiar fenotípicamente para adaptarse rápidamente a los cambios ambientales se le conoce como plasticidad o *switching* fenotípico. Afecta a la morfología colonial y al tamaño y forma de las blastoconidias. Implica cambios en la expresión de antígenos de superficie, afecta a la transición levadura-hifa, a la adhesión a las células del epitelio humano, a la susceptibilidad de células a neutrófilos y oxidantes, a la secreción de proteinasas y a la susceptibilidad a fármacos (Soll, 2002). Esta plasticidad confiere a *C. albicans* la capacidad para vivir como agente comensal y patógeno al igual que la capacidad para evadir la respuesta inmune y la terapia antifúngica (Anderson, *et al.*, 1990, Anderson, *et al.*, 1987).

De todos los fenotipos de cambio el más estudiado es el sistema "*white-opaque*" en la cepa WO-1 de *C. albicans* (Slutsky, *et al.*, 1985). Se ha visto que las levaduras en fase opaca no filamentan a 37ºC, pH 6,7 y son más virulentas en infecciones cutáneas, mientras que las células en fase blanca son más virulentas en las infecciones sistémicas (Kvaal, *et al.*, 1999).

Formación de biofilms

Los *biofilms* o biopelículas son comunidades microbiológicas estructuradas en las que las células se unen a una superficie y quedan incrustadas en una matriz de polímeros extracelulares tridimensional (Ramage, *et al.*, 2005). Los biofilms de *C. albicans* están formados por una mezcla de células de levadura, pseudohifas y de hifas (Nett, *et al.*, 2006). La matriz extracelular está compuesta por proteínas y carbohidratos (Douglas, 2003) cuya función es mantener la estructura de la matriz.

C. albicans puede formar biofilms en casi todos los instrumentos médicos. Los más comúnmente infectados son las lentes de contacto y las dentaduras, aunque también los catéteres urinarios y vasculares, prótesis, válvulas cardíacas, marcapasos, etc. (Nett y Andes, 2006).

La formación de biofilms dota a las células características conformacionales y propiedades

fenotípicas que son diferentes de sus compañeras planctónicas. La diferencia más notable es la elevada resistencia al sistema inmunitario del hospedador y a la terapia convencional (Kuhn*, et al.*, 2004).

2.3. Tratamiento de las candidiasis

Como *C. albicans* es un organismo eucariota y comparte componentes y procesos biológicos con los humanos, las diferencias entre los dos tipos celulares se ha utilizado para desarrollar medicamentos antifúngicos con toxicidad selectiva para las células de *C. albicans*. Los tratamientos más utilizados actualmente tienen como diana componentes de la envoltura celular (pared celular y membrana plasmática), también se utilizan otras dianas como son, la síntesis de ergosterol en el RE, el ensamblaje de los microtúbulos y la síntesis de DNA, RNA y proteínas (Odds*, et al.*, 2003).

Debido a la importancia clínica de las candidiasis, hay una constante búsqueda de nuevas dianas de acción de los fármacos y de mejora del diagnóstico para proporcionar alternativas terapéuticas, así como nuevas propuestas como son la combinación de quimioterapia e inmunoterapia para mejorar el estado inmunológico de los pacientes (Vonk*, et al.*, 2006).

Existen distintos tipos de antifúngicos para el tratamiento de las infecciones por *Candida*, con mecanismos de acción y dianas diferentes, como son los azoles (actúan en la vía de síntesis del ergosterol), polienos (rotura de la membrana plasmática), alilaminas (síntesis de ergosterol) y equinocandinas (alteración de la síntesis del β-1,3-glucano), entre otros.

3. INTERACCIÓN PATÓGENO-HOSPEDADOR

En las últimas décadas las enfermedades infecciosas se han convertido en un importante campo en la investigación. Las infecciones fúngicas presentan un grave problema en la salud de los países industrializados, por esta razón el estudio de la interacción patógeno hospedador nos ayuda a comprender el mecanismo de acción de los patógenos y las forma de responder del hospedador frente a la infección.

3.1. Interacción *C. albicans*-Macrófago

Los diferentes factores de virulencia de la levadura no son los únicos determinantes para que provoquen la infección en el hospedador. Como se ha mencionado anteriormente, la patogenicidad de *C. albicans* va a depender del equilibrio entre los factores de virulencia del hongo y el estado inmunológico del hospedador, estableciéndose relaciones complejas entre el sistema inmunitario del hospedador y *C. albicans* que van a determinar el desarrollo o no de la infección.

Tanto la respuesta innata como la adquirida están implicadas en la resistencia de *C. albicans*, siendo necesaria, en primer lugar, la intervención de la respuesta innata para que posteriormente se produzca la respuesta específica frente a *C. albicans* (Calderone*, et al.*, 2002, Romani, 2011).

3.2. Respuesta inmunitaria frente a candidiasis sistémica

Tanto la respuesta innata como la adquirida regulan el control y la resistencia frente a las candidiasis, siendo esencial la coordinación entre ambos tipos de inmunidad.

Respuesta innata

En el hospedador existe una primera línea de defensa frente a la invasión microbiana, constituida por barreras físicas, bioquímicas y microbiológicas. La superficie del cuerpo está protegida por epitelios que constituyen una barrera física entre el medio interno y los agentes patógenos del exterior. En la epidermis se han descrito diferentes tipos de esfingosinas activas frente a *C. albicans*, y se han aislado varias proteínas con acción antifúngica, que pueden tener un papel importante en la defensa frente a infecciones fúngicas cutáneas (Calderone y Gow, 2002). Además, las mucosas epiteliales secretan un fluido viscoso (mucus) que contiene glucoproteínas denominadas mucinas. Los microorganismos envueltos por el mucus no pueden adherirse al epitelio, y así pueden ser expulsados con el flujo de mucus conducido por el movimiento de los cilios (Janeway*, et al.*, 2005). En el tracto intestinal las células de Paneth sintetizan péptidos bactericidas y fungicidas denominados criptidinas o α-defensinas. En los epitelios producen péptidos antimicrobianos denominadas β-defensinas que, en general, son capaces de suprimir el crecimiento de bacterias y de hongos a través de distintos mecanismos (Janeway*, et al.*, 2005, Schneider*, et al.*, 2005). Se ha descrito que *C. albicans* es capaz de inducir la expresión de β-defensinas, tanto en epitelios humanos (Meyer*, et al.*, 2004) como en tejidos de ratón (Schofield*, et al.*, 2004). Además, se ha descrito que las β-defensinas tienen un efecto fungicida directo sobre *C. albicans* (Vylkova*, et al.*, 2007).

Por último, es importante destacar que la mayoría de las superficies epiteliales están asociadas a una microbiota normal de microorganismos no patógenos con los que el microorganismo patógeno debe competir por los nutrientes y los sitios de unión a las células. La microbiota normal puede producir sustancias antimicrobianas que previenen la colonización por otros microorganismos patógenos (Janeway*, et al.*, 2005). Está demostrado que la colonización por *C. albicans* y por otros hongos es mayor en animales a los que se les ha alterado la microbiota normal con antibióticos y en humanos tratados con antibióticos de amplio espectro (Calderone y Gow, 2002, Peman*, et al.*, 2005, Tortorano*, et al.*, 2004).
Cuando la levadura ha pasado las barreras físicas, se encuentra con una serie de mecanismos de defensa innatos, incluidas las membranas celulares, receptores celulares y factores humorales.

Inmunidad innata mediada por células

La inmunidad innata frente a *C. albicans* está mediada por diferentes tipos celulares como neutrófilos, macrófagos y células NK que fagocitan células fúngicas opsonizadas o no a través de varios receptores (receptores de manosa, del complemento y de fragmentos Fc de las inmunoglobulinas) (Figura 3).
La destrucción de formas levaduriformes e hifas de *C. albicans* por macrófagos y neutrófilos incluye mecanismos oxidativos, como la producción de óxido nítrico (NO) (Romani*, et al.*, 2001), como se ha comentado en apartados anteriores. El estallido respiratorio produce modificaciones en las proteínas del hongo y rompe ácidos nucleicos, entre otros efectos (Mansour*, et al.*, 2002). Además de los mecanismos oxidativos, podemos encontrar otros mecanismos no oxidativos que implican la acción de diversas enzimas para matar a los microorganismos patógenos (Reeves*, et al.*,

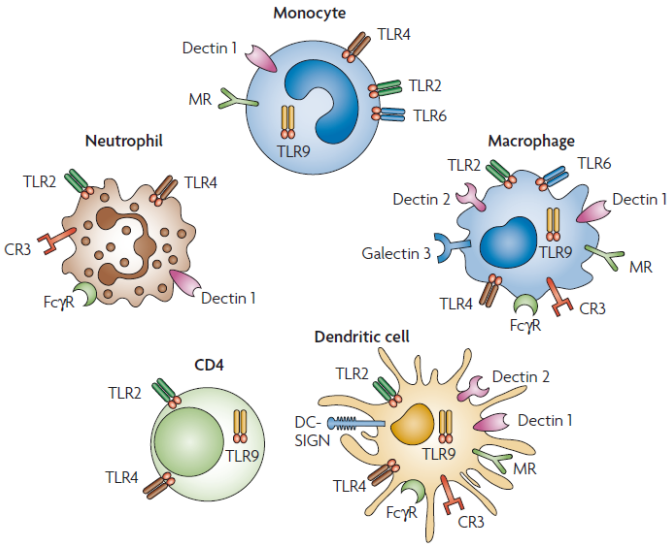

Figura 3: Receptores de las poblaciones celulares implicadas en el reconocimiento de *C. albicans.* Figura tomada de Netea *et al.* (Netea, *et al.*, 2008).

2002). Algunas de estas enzimas son la catepsina G, la lisozima y la lactoferrina. A diferencia de la activación de los neutrófilos, la de los macrófagos por diferentes citoquinas (IFN-γ, M-CSF y GM-CSF, IL-1) es necesaria para su actividad anti-*Candida*. De estas citoquinas, el IFN-γ es considerado un excelente estimulador de la capacidad de los macrófagos para destruir a C. *albicans* (Vázquez-Torres, *et al.*, 1997).

Las células dendríticas (DCs) son capaces de fagocitar células de *C. albicans* (Romani, 2004), aunque su función principal es la de inducir una respuesta inmunitaria específica, no tienen la función de eliminar al patógeno. Las DCs actúan como células presentadoras de antígenos (APCs). Estas células destruyen a las células de *C. albicans* fagocitadas mediante mecanismos no oxidativos similares a los utilizados por macrófagos y neutrófilos, aunque la formación ROS y RNS no es muy importante en el interior del fagolisosoma (Mansour y Levitz, 2002).

Moléculas solubles:

Existe un gran número de proteínas plasmáticas que reaccionan entre sí para opsonizar agentes patógenos produciendo así una serie de respuestas inflamatorias que facilitan la lucha contra la infección. Estas proteínas forman el sistema del complemento, que produce una respuesta rápida frente a un estímulo, esta fenómeno se ve amplificado por una reacción en cascada (Janeway, et al., 2005).

Además de estas opsoninas, existen otras moléculas que median la inmunidad innata como son, proteínas de unión a manosa, colectinas y defensinas (Romani, *et al.*, 1998).

Respuesta adaptativa

En mamíferos, la respuesta inmunitaria innata generada en los tejidos periféricos suele ser insuficiente para destruir por completo al agente infeccioso, por lo que es necesaria la activación de la respuesta específica en los tejidos linfoides.

Inmunidad adaptativa mediada por células

Las células T desempeñan un papel central en la regulación de la respuesta inmunitaria frente *C. albicans* mediante la secreción de citoquinas que controlan el desarrollo y la actividad de los efectores inmunitarios.

De las poblaciones de linfocitos T descritos, los T $CD8^+$ tienen actividad citotóxica y los T $CD4^+$, secretora de citoquinas, son un arma muy importante en la defensa frente a las infecciones fúngicas, ejerciendo los T $CD4^+$ un papel muy importante en la resolución de las infecciones por *C. albicans*.

Está descrito que en la respuesta inmunitaria frente a diferentes hongos una respuesta Th1, caracterizada por la producción de IL-12, IFN-γ,

TNF-α, está relacionada con la resistencia a la infección, la IL-12 favorece la inmunidad mediada por células, mientras que una respuesta Th2, caracterizada por la producción de IL-4, IL-5, IL-13 e IL-10, se relaciona con una mayor susceptibilidad a las infecciones fúngicas, una disminución de la capacidad fungicida y alergia (Huffnagle*, et al.*, 2003). Las citoquinas producidas por las células Th1 activan a las células fagocíticas favoreciendo la eliminación de *C. albicans*, mientras que las citoquinas que provienen de células Th2 inhiben el desarrollo de una respuesta Th1 y por lo tanto desactivan las células encargadas de la fagocitosis (Romani, 2011).

Además de una adecuada respuesta Th1/Th2 es necesaria la aparición de células T $CD4^+$ $CD25^+$ reguladoras (Treg), las cuales en respuesta a la presencia de IL-10 producen más IL-10 y TGF-β, que básicamente conducen a una disminución de expresión de moléculas del CMH de tipo II, y respuesta de inhibición de la proliferación de linfocitos respectivamente, modulando de una manera negativa la respuesta inmunitaria Th1, para evitar una exacerbada respuesta inmune. Este tipo de respuesta se ha relacionado con la limitación de la patología, así como la capacidad de la permanencia del microorganismo en el hospedador. La inducción de las células Treg durante la candidiasis requiere la secreción de IL-10 por células dendríticas en respuesta a micelios del hongo, e implica la participación de los TLRs y de la molécula B7 (Montagnoli*, et al.*, 2002, Netea*, et al.*, 2004, Romani*, et al.*, 2006).

Finalmente, se ha descrito un perfil Th17 el cual responde al influjo de IL-23 produciéndose IL-17, relacionándose con una patología inflamatoria crónica además de con la disminución en la eliminación del hongo. El linaje Th17 que secreta IL-17, está adquiriendo importancia (Palm*, et al.*, 2007, Romani*, et al.*, 2007). El desarrollo de las células Th17 ocurre en presencia de TGF-β e IL-6, es inhibido por citoquinas Th1 y se mantiene en presencia de IL-23, citoquina producida por las células dendríticas en respuesta a una elevada carga fúngica. La IL-17 induce la producción de quimioquinas en los sitios de infección y provoca el reclutamiento de neutrófilos. Se ha comprobado que ratones deficientes en el receptor de la IL-17 son más susceptibles que los ratones control a la candidiasis sistémica, lo que puede atribuirse a una menor llegada de neutrófilos a los órganos infectados (Huang*, et al.*, 2004). Recientemente, se ha descrito que la vía Th17 se desarrolla en respuesta a *C. albicans* (Acosta-Rodriguez*, et al.*, 2007, LeibundGut-Landmann*, et al.*, 2007) y que la IL-23 y la vía Th17 actúan como reguladores negativos de la resistencia inmunitaria Th1 frente a *C. albicans* (Zelante*, et al.*, 2007).

La forma en que en el tiempo se desarrollan y participan cada una de estas subpoblaciones de linfocitos Th (Th1, Th2, Treg, o Th17) define la capacidad fungicida de la respuesta, y el predominio de una u otra respuesta está directamente relacionado con el desarrollo y gravedad de la infección. En modelos de ratones experimentales de candidiasis invasivas, la protección se relaciona con la aparición de una respuesta inicial y predominante tipo Th1 (Puccetti*, et al.*, 1994, Romani*, et al.*, 1992a, Romani*, et al.*, 1993, Romani*, et al.*, 1992b) , mientras que una respuesta Th2 inicial está asociada con exacerbación de la enfermedad (Romani*, et al.*, 1992a, Romani*, et al.*, 1994, Spaccapelo*, et al.*, 1995). Sin embargo, el papel de células Th17 es controvertido, la vía Th17 puede promover la inflamación y alterar la inmunidad antifúngica,

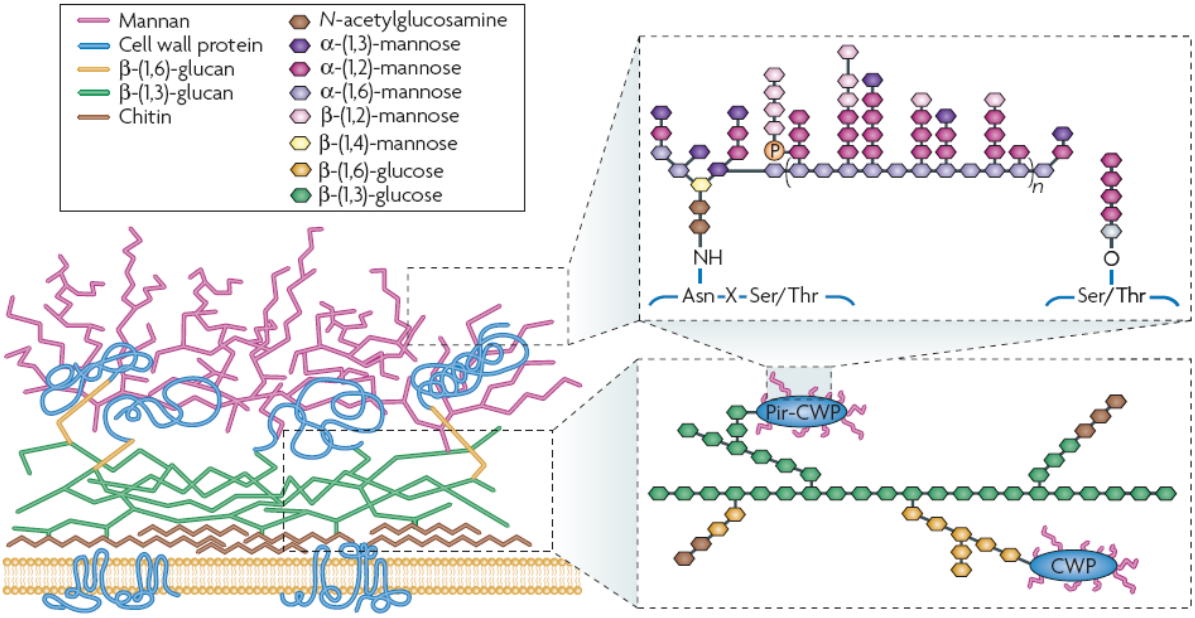

Figura 4: Estructura de la pared celular de *C. albicans*. El esquema muestra los principales componentes de la pared celular y su distribución: manano, glucano, quitina y proteínas. Figura tomada de Netea *et al* (Netea, *et al.*, 2008).

actuando como regulador negativo de la respuesta Th1 frente a *C. albicans*. Además, la vía Th17 puede ser la responsable de respuestas inflamatorias previamente atribuidas a respuestas Th1 exacerbadas (Romani y Puccetti, 2007, Zelante, *et al.*, 2007).

Inmunidad mediada por anticuerpos

Desde hace unos años se ha relacionado la respuesta humoral a las candidiasis invasivas, con diferentes mecanismos: actividad candidacida directa (Polonelli, *et al.*, 1994), inhibición de la adhesión (Han, *et al.*, 1995, Scheld, *et al.*, 1983, Umazume, *et al.*, 1995, Vudhichamnong, *et al.*, 1982), favoreciendo la fagocitosis mediante opsonización (Chilgren, *et al.*, 1968), unión a polisacáridos inmunomoduladores (Fischer, *et al.*, 1978), neutralización de proteasas extracelulares (Cassone, *et al.*, 1995) e, incluso, inhibición de la transición dimórfica (Casanova, *et al.*, 1990).

3.3. Reconocimiento de *C. albicans* por los macrófagos

El primer punto de contacto de la levadura con las células del sistema inmune es la pared celular, por eso es muy importante conocer cuál es la composición de la misma para entender cómo *C. albicans* es reconocida por el sistema inmune del hospedador y como dirige la respuesta del mismo (Netea, *et al.*, 2008). Básicamente, la estructura de la pared celular de *C. albicans* está compuesta por un esqueleto de fibras de polisacárido compuesto por β-1,3-glucano (40%) covalentemente unido a β-1,6-glucano (20%) y quitina (1-10%), también manoproteínas (30-40%) como se esquematiza en la Figura 4. Esta estructura está diseñada para funcionar como un exoesqueleto robusto.

3.4. Receptores implicados en el reconocimiento de *C. albicans* por el macrófago

Cuando la célula hospedadora se encuentra con hongos patógenos vivos, la respuesta inicial del sistema inmunitario innato está determinada por el reconocimiento de los componentes de la pared celular. A primera vista, parece que la unión de los distintos receptores de las células del sistema inmune a los PAMPs de *C. albicans*, conducen a un conjunto de rutas estandarizadas y posiblemente redundantes, que estimulan la producción de citoquinas, la fagocitosis y la muerte del hongo. Sin embargo, este modelo de respuesta ha sido perfeccionado en los últimos años. Varios PRRs permiten al sistema inmune innato, no sólo reconocer PAMPs específicos, sino modular específicamente la respuesta que se va a desencadenar (Figura 5) (Netea*, et al.*, 2008).

Existen 2 tipos fundamentales de receptores en las células del hospedador:

a) Receptores del tipo C-Lectinas (CLR)

Son una amplia familiar de proteínas que tienen la habilidad de unirse a carbohidratos dependiente de Ca^{+2} (Weis*, et al.*, 1998). Esta superfamilia está compuesta por receptores solubles y receptores unidos a membrana, compartiendo entre ellos un dominio de reconocimiento de carbohidratos (CDR), requerido para la unión específica a

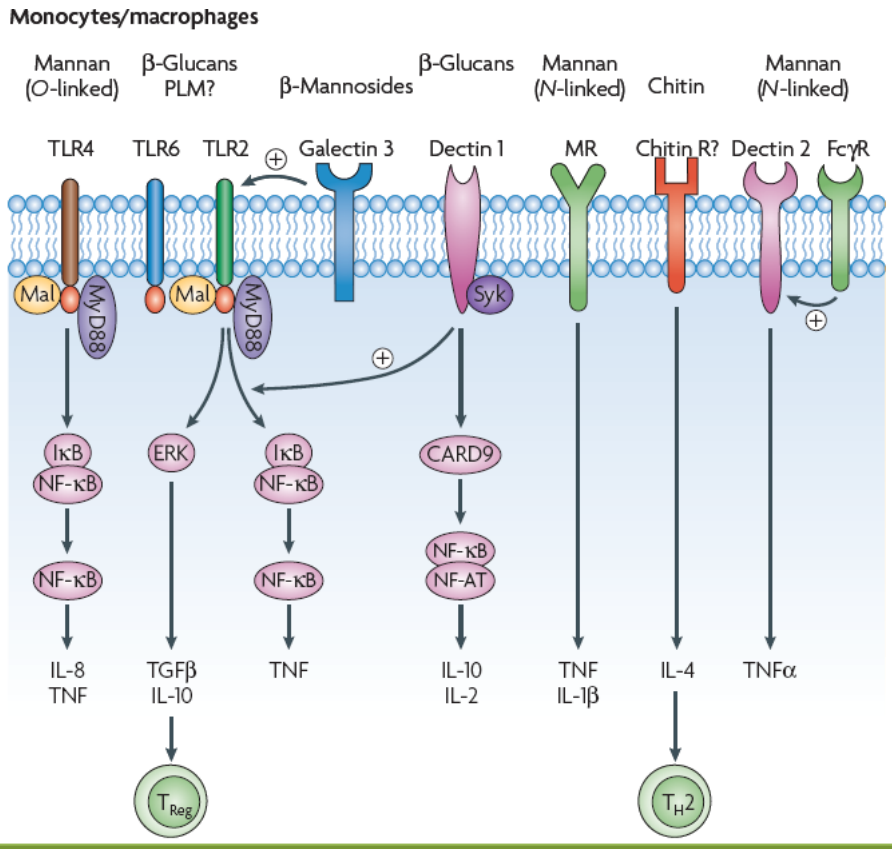

Figura 5: Reconocimiento de *C. albicans* a nivel de la membrana del macrófago. Este reconocimiento es mediado por TLRs y LRs. (CARD9, proteína caspasa 9 con dominio implicado en reclutamiento; ERK, proteína kinasa regulada por señales extracelulares; FcγR, receptor Fcγ; IL, interleuquina; IL-1Ra, receptor antagonista de la interleuquina-1; LR, receptor de lectina; MR, receptor de manosa; MyD88, gen 88 de respuesta primaria a diferenciación mieloide; NF-κB, factor nuclear κB; PLM, fosfolipomanano; Syk, tirosina kinasa de bazo; TGFβ, factor de crecimiento; TH, T cooperadoras; TLR, receptor de tipo Toll; TNF, factor de necrosis tumoral; TReg, células T reguladoras). Figura tomada de Netea *et al* (Netea, *et al.*, 2008).

carbohidratos procedentes de microorganismos o ligandos endógenos (Iobst*, et al.*, 1994). Estos receptores son los principales para el reconocimiento de los hongos y la inducción de la respuesta inmune innata contra los mismos, los más relevantes en la respuesta contra *C. albicans* son:

Receptor de Manosa (MR):

El manano de la pared celular es el principal antígeno de *Candida* responsable de la especificidad de las diferentes reacciones serológicas.

C. albicans tiene también la habilidad de sintetizar residuos de manosa unidos a través de un enlace poco común, β-1,2 manosa, que confiere una estereoespecificidad única y que se ha detectado únicamente en fosfolipomanano (PLM) (Nitz*, et al.*, 2002).

El receptor de manosa se expresa en la superficie de macrófagos, células dendríticas (DC) y otras células. Este receptor es capaz de unirse a manosa, fucosa, N-acetilglucosamina y glucosa, pudiendo reconocer *C. albicans, Cryptococcus. neoformans, Pneumocystis carini*, y otros patógenos incluidos virus. Tras el reconocimiento de la levadura, el receptor media la internalización del patógeno mediante fagocitosis, ayudando a la muerte intracelular. Su actividad hacia *C. albicans* es dependiente de IL-13 a través de una ruta intracelular endocítica dependiente de PPARγ (*peroxisome proliferator-activated receptor*) (Coste*, et al.*, 2003), en modelos murinos la unión del MR con *Candida* induce la formación de citoquinas proinflamatorias (IL-1β, IL-6 y GM-CSF) (Eyerich*, et al.*, 2008).

DC-SIGN *(dendritic cell-specific ICAM [intercellular adhesion molecule]-grabbing nonintegrin)*

Es un receptor específico de células dendríticas y macrófagos. Tiene gran afinidad por manosas ramificadas presentes en moléculas complejas (receptor de partículas opsonizadas) (Koppel*, et al.*, 2005). Este receptor reconoce *C. albicans* de manera calcio dependiente y lleva a la captura y fagocitosis de la levadura (Graham*, et al.*, 2009). Este receptor produce una señalización intracelular vía Raf-kinasa, ERK1 y ERK2, modulando las respuestas mediadas por los TLR e incrementando la expresión de IL-10.

Dectina-1

Es el principal receptor de β-1,3-glucano (Herre*, et al.*, 2004), y media el reconocimiento del zimosán no opsonizado. También contribuye al reconocimiento de partículas opsonizadas que contienen β-glucano. Dectina-1 está involucrada en la fagocitosis y en la inducción de citoquinas proinflamatorias por macrófagos murinos.

Además puede mediar la fagocitosis de la forma levaduriforme de *C. albicans*, y la inducción de citoquinas proinflamatorias, la fosforilación de proteínas citosólicas determinadas e iniciar el "estallido respiratorio", mientras que las hifas de *C. albicans* fallan a la hora de unirse o iniciar estas respuestas a través de dectina-1. Por otro lado, reconoce mejor las células de la levadura inactivadas por calor que las células vivas, indicando que el β-glucano se expone de manera diferente en las diferentes morfologías de *C. albicans* (Heinsbroek*, et al.*, 2005).

Dectina-2

A diferencia de Dectina-1, es un receptor que es incapaz de inducir rutas de señalización por sí

mismo. Se expresa en macrófagos y células dendríticas y es capaz de unir a hifas de *C. albicans*, al igual que moléculas de zimosán, mediante el reconocimiento de estructuras complejas de manosa (McGreal*, et al.*, 2006). También ha sido definido su papel como PRR fúngico debido a su capacidad para inducir una respuesta inmunitaria innata mediante la señalización a través del FcɣR (Receptor de fragmentos Fcɣ) induciendo TNF en respuesta a las hifas de *C. albicans* (Sato*, et al.*, 2006). Recientemente se ha mostrado que dectina-2 tiene una importante actividad inducida por Th17 durante la infección por *Candida* (Robinson, M.J. et al. (2009).

Receptor Mincle *(macrophage-inducible C-type lectin)*

Se expresa fundamentalmente en macrófagos, donde ejerce una función importante en las respuestas inmunitarias innatas frente a *C. albicans* (Matsumoto*, et al.*, 1999). En ausencia de este receptor, la producción de TNF-α por macrófagos se reduce, tanto in vivo como in vitro, y además ratones deficientes en Mincle presentan una mayor susceptibilidad a la candidiasis sistémica. Sin embargo Mincle parece no ser esencial para la fagocitosis del hongo (Wells*, et al.*, 2008) y su unión con el ligando no está caracterizada todavía.

Galectina-3

Principalmente expresada en macrófagos, fibroblastos y células epiteliales, es esencial para la fagocitosis (Sano*, et al.*, 2003) y está implicado en la unión de levaduras a través de los β-1,2-oligomanósidos, relacionados con el manano y el fosfolipomanano, presentes en la pared celular de *C. albicans*, pero ausente en *S. cerevisiae* (Fradin, *et al.*, 2000a). Este tipo de glucano está implicado en la unión con la membrana del macrófago, que lleva a la activación de NF-κβ dependiente de TLR2 y a la producción de TNF-α (Fradin*, et al.*, 1996). Recientemente se ha descrito que la unión de galectina-3 con β-1,2-oligomananos (no con α-manosa) de *C. albicans* tiene un papel microbicida contra la levadura (Kohatsu*, et al.*, 2006).

b) Otros receptores

Receptor del complemento 3: CR3 (CD11b/CD18)

Es una β-integrina ampliamente expresado en neutrófilos, monocitos y células NK y poco presente en macrófagos que reconoce β-glucano y también media el reconocimiento del zimosán no opsonizado. Es un receptor "promiscuo" lo que le convierte en pieza fundamental de la fagocitosis. La unión de CR3 no media la respuesta protectora del hospedador, pero puede ser utilizada para suprimir las señales proinflamatorias, como las del TNF.

Lectina de unión a manosa (MBL)

Es una proteína sérica capaz de opsonizar levaduras mediante la activación del complemento. Se une a manosa y a grupos N-acetilglucosamina presentes en glicolípidos y glicoproteínas de bacterias Gram negativas, Gram positivas y hongos. Es un miembro de la familia de las lectinas dependientes de calcio, o colectinas.

MBP, aislada de suero de conejo, inhibe la fagocitosis de *C. albicans* por macrófagos murinos, lo que sugiere que la MBP soluble puede interferir en la interacción macrófago-*Candida*. MBP soluble puede también interferir en la adherencia de *C. albicans* a los tejidos del hospedador, debido a que la adherencia a tejido parece que depende parcialmente de las interacciones entre mananos y receptor de manosa (Vazquez-Torres*, et al.*, 1997).

TLRs (“*Toll-like receptors*”)

Los TLRs son una familia de proteínas transmembrana muy conservadas que se caracterizan por presentar un dominio extracelular rico en residuos de leucina (LRR; “Leucine Rich Repeat domain”), responsable del reconocimiento de estructuras fúngicas, bacterianas o víricas, además de factores endógenos producidos durante el daño celular (Weindl*, et al.*, 2007), y una región intracitoplasmática denominada TIR (*Toll-Interleukin-1 Receptor*), homóloga a la región intracitoplasmática del receptor de la IL-1 y de la IL-18, responsable de la transducción de señales intracelulares (Akira, 2006, Takeda*, et al.*, 2004). En mamíferos, se han identificado 30 TLRs de los cuales 10 tienen importancia funcional en humanos. TLR1, TLR2, TLR4, TLR5 y TLR6 están asociados a la membrana celular, mientras que TLR3, TLR7, TLR8 y TLR9 están localizados en el compartimento endosomal o lisosomal.

En cuanto a la implicación de los TLRs en la fagocitosis, se sabe que este proceso viene acompañado de una respuesta inflamatoria originada por el reconocimiento de ligandos de los microorganismos por los TLRs y/o por otros receptores tipo lectina. De hecho, se ha demostrado que algunos TLRs son reclutados al fagosoma, donde detectan el contenido de este e inician la respuesta inflamatoria. Los datos actuales muestran que los TLRs no funcionan directamente como receptores fagocíticos, pero que sí pueden afectar a la maduración del fagosoma y regular la expresión de genes cuyos productos participan directamente en la fagocitosis (Underhill*, et al.*, 2004).

La activación de las rutas de señalización de los TLRs lleva a la activación del factor diferenciación mieloide 88 (MyD88), a nivel citoplásmico, que lleva a la estimulación de citoquinas proinflamatorias y, en el caso de TLR4 y TLR3, de la activación de una ruta que induce a los interferones de tipo I (Akira, 2006). Se ha descrito que la activación de MyD88 es necesaria para la fagocitosis y muerte de *C. albicans* (Marr*, et al.*, 2003).

Varios TLRs están implicados en la respuesta inflamatoria inducida por *C. albicans*, de ellos TLR2, TLR4 son los más importantes. Estos dos receptores son expresados por muchas células del sistema inmunitario innato, incluidos monocitos, macrófagos, células dendríticas, neutrófilos, células T $CD4^+$ y células epiteliales (Bellocchio*, et al.*, 2004, Netea*, et al.*, 2006, Weindl*, et al.*, 2007). La activación del TLR2 por componentes de la pared celular de *C. albicans*, como el fosfolipomanano, lleva a la producción de citoquinas como TNF, IL-1β e IL-10 (Jouault*, et al.*, 2003), mientras que la IL-12 y el INF-γ no son inducidos, resultando en un balance favorable a la respuesta celular Th2 (Weis*, et al.*, 1998). TLR4 reconoce mananos de *S. cerevisiae* y *C. albicans* pero necesita a CD14 (Tada*, et al.*, 2002) induciendo la producción de numerosos mediadores proinflamatorios como las citoquinas TNF-α, IL-1 y IL-6, pero su función en la defensa frente a las candidiasis sistémicas todavía continúa en debate.

Actualmente se sabe que el zimosán induce la señalización a través del heterodímero TLR2/TLR6. Aunque no se ha caracterizado el componente del zimosán responsable de la interacción con el receptor, parece ser que dicha interacción no está mediada por el glucano, ya que al eliminar del zimosán los demás componentes mediante hidrólisis alcalina, pierde la capacidad de activar por TLR2 (Underhill, 2003).

3.5. Activación del macrófago por los PRRs

Una vez que varios receptores se han ligado con los PAMPs de *C. albicans*, se activan una serie rutas de señalización que estimulan la producción de citoquinas, la fagocitosis y la muerte del hongo. Además, mediante la inducción de determinados perfiles de citoquinas, los PRRs llevan hasta cierto punto de especificidad de la respuesta inmune innata.

Ingestión de C. albicans

Tras el reconocimiento de *C. albicans*, el macrófago envuelve a la levadura para dar lugar al fagosoma, que proporciona un ambiente hostil a la levadura, expuesta a un gran número de compuestos microbicidas, especies reactivas de oxígeno y nitrógeno, bajo pH y un gran número de hidrolasas lisosomales, todas ellas contribuyendo a la muerte y digestión del patógeno. Esta digestión facilita la presentación de antígeno a las células T, activando así la respuesta inmune adaptativa (Aderem*, et al.*, 1999b, Houde*, et al.*, 2003).

Inducción de citoquinas

La interacción entre patógenos y macrófagos tiene un efecto importante, la activación de los macrófagos libera citoquinas, quimioquinas, y otros mediadores que establecen un estado de inflamación en el tejido y que atraen neutrófilos y proteínas plasmáticas al sitio de la infección.

Se sabe que por lo menos cuatro TLRs (TLR2, TLR4, TLR6 y TLR9) están implicados en la inducción de la producción de citoquinas por *C. albicans*.

Después del reconocimiento de la levadura, los TLRs activan NFκB (Factor Nuclear kappa B), o bien la ruta de MAP kinasas, lo que conduce a la estimulación de la producción de citoquinas proinflamatorias (Akira*, et al.*, 2003). El balance entre las señales inducidas por TLR2 y TLR4 parece tener un papel importante en la regulación de la respuesta inmunitaria.

TLR4 puede estimular la producción de citoquinas proinflamatorias vía MyD88 o mediante el factor 3 regulador del interferón (IRF3), que induce la producción de citoquinas tipo Th1 como INF-ɣ (Van Der Graaf*, et al.*, 2005). La unión de TLR2 también puede inducir la producción de citoquinas proinflamatorias, pero es un efecto menor que el de TLR4, sin embargo, TLR2 no induce la producción de IL-12 y INF-ɣ tipo Th1, favoreciendo la respuesta Th2 o tipo Treg (linfocitos T reguladores) (Re*, et al.*, 2001). Mientras que el papel de TLR6 y TLR9 en la producción de citoquinas frente a *C. albicans* es menos importante.

Mecanismos de escape basados en los PRRs

A pesar de la evidencia del papel de los PRRs en el reconocimiento de *C. albicans* y la inducción de la respuesta inmunitaria posterior, existen datos que muestran que ciertos hongos patógenos han desarrollado estrategias para reducir este reconocimiento por los PRRs, o para usar el reconocimiento como una ventaja para evadir la respuesta inmunitaria.

Además de inducir directamente efectos antinflamatorios, *C. albicans* ha desarrollado estrategias para bloquear o evitar el reconocimiento por los PRRs, por ejemplo, la transición morfológica levadura- hifa tras la adhesión de la levadura al endotelio intravascular y la invasión de los tejidos circundantes puede resultar un mecanismo mediante el cual la levadura puede evitar el reconocimiento del β-

glucano por el sistema inmunitario (d'Ostiani*, et al.*, 2000).

Modelo integrado de reconocimiento, captura y muerte de la levadura

Aunque hay mucho que aprender todavía sobre el reconocimiento de los hongos por el sistema inmunitario, hay algunos principios que caracterizan el reconocimiento de *C. albicans* por el sistema inmune innato y su activación durante la candidiasis:

a) El reconocimiento depende distintos PAMPs en la pared del hongo. Para este reconocimiento se han desarrollado sistemas de receptores específicos, como el MR y DC-SIGN para el reconocimiento de cadenas ramificadas de mananos unidas por un enlace *N*-glicosídico, TLR4 para cadenas lineales de mananos unidas por un enlace *O*-glicosídico , galectina-3 para los β-manósidos, dectina-1 y TLR2 para los β-glucanos y fosfolipomanano (PLM) y CR3 para el β-(1,6)-glucano.

b) A pesar de la superposición y, a veces, redundancia de funciones, cada sistema ligando-receptor activa rutas específicas de señalización intracelulares, y esto tiene distintas consecuencias para la activación de distintos componentes de la respuesta inmunitaria del hospedador.

c) La expresión diferencial de los distintos PRRs es un mecanismo importante para la respuesta específica de tipo celular a patógenos fúngicos.

d) Por último, la respuesta integrada a un patógeno específico depende del mosaico de PRRs. La co-estimulación debida a múltiples interacciones PAMP-PRR puede aumentar la sensibilidad y especificidad del proceso de reconocimiento del sistema inmune (Netea*, et al.*, 2008).

4. TECNOLOGÍA PROTEÓMICA

En los últimos años, el gran avance tecnológico ha impulsado el desarrollo de estrategias que permiten analizar los problemas biológicos desde un punto de vista más global e integrado, como la Genómica, Proteómica o Metabolómica. Así, el desarrollo de la genómica ha permitido hasta el momento la secuenciación de 6868 genomas completos y hay más de 20000 están en proyecto (www.genomesonline.org). Sin embargo aún se desconoce la función biológica de muchas proteínas codificadas por los genes detectados. La proteómica es uno de los campos que puede ayudar a establecer una conexión entre las secuencias genómicas y su comportamiento biológico, constituyendo una herramienta importante en el análisis funcional de genes de función desconocida.

En los años 70 se desarrolló la electroforesis bidimensional (O'Farrell, 1975). En los años 90, la espectrometría de masas emergió como una herramienta muy potente para el estudio de las proteínas. Además, los genomas de muchos organismos, incluido el del ser humano, fueron publicados, comenzando una nueva era para la proteómica. El término “proteoma” se utilizó por primera vez en 1995 y se define como la dotación completa de proteínas expresadas por un individuo, tejido, cultivo celular, etc., en un momento determinado y bajo condiciones específicas (Wilkins, 1995). A diferencia del genoma, el proteoma es dinámico, ya que una misma información genética puede dar lugar a distintos proteomas según las condiciones de crecimiento o los procesos de diferenciación llevados a cabo por las células.

Además, cada gen puede dar lugar a varias especies proteicas, según el procesamiento del mRNA y/o las modificaciones post-traduccionales que haya sufrido. Por lo tanto el número de posibles proteínas de un proteoma es mucho mayor que el número de genes que contiene (Figura 6). Por esta razón, el estudio del proteoma es, probablemente, el sistema experimental más adecuado para analizar células y tejidos, puesto que examina directamente el producto final del genoma.

La proteómica es el estudio del proteoma y abarca una gran cantidad de áreas, se puede clasificar en diferentes: la proteómica de expresión (identificación de los componentes del proteoma que sufren alteraciones en sus niveles de expresión a consecuencia de alteraciones fisiopatológicas o inducidas por agentes externos), la proteómica celular o estructural (estudio de la localización subcelular de las proteínas y de las interacciones proteína-proteína) y proteómica analítica o funcional (diversas aproximaciones proteómicas que permiten el estudio y caracterización de un grupo de proteínas determinado proporcionando información importante sobre señalización, mecanismos de la enfermedad o interacciones proteína-fármaco, modificaciones post-traduccionales) (Figura 7).

Uno de los principales obstáculos a los que se ha enfrentado la investigación proteómica en los últimos tiempos es la dificultad que supone la identificación de todas las proteínas presentes dentro de una muestra biológica compleja. Esta dificultad se ve agravada por el limitado rango dinámico de concentraciones que las técnicas actuales son capaces de resolver. Otros problemas están asociados a la evaluación de la enorme cantidad de información que genera esta tecnología, que complica la selección e interpretación de los datos potencialmente útiles de entre todos los obtenidos.

Los estudios proteómicos a gran escala se basan

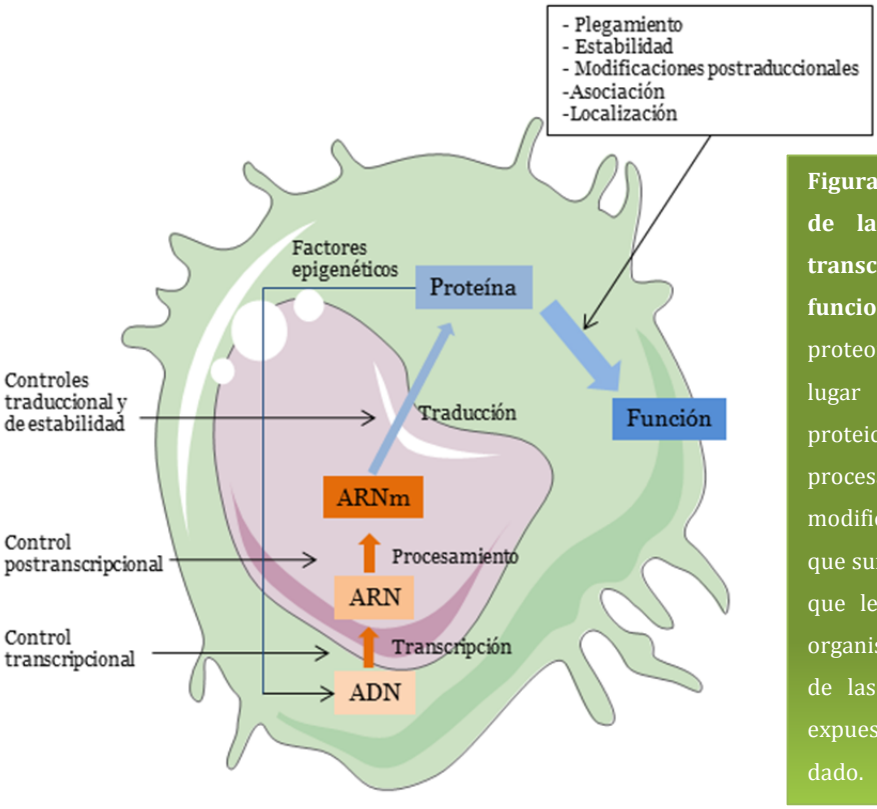

Figura 6: Esquema representativo de la relación entre genoma, transcriptoma, proteoma y funciones celulares. Dinamismo del proteoma. Un solo gen puede dar lugar a numerosas especies proteicas debido, por ejemplo, al procesamiento alternativo o a las modificaciones post-traduccionales que sufre la proteína. Por eso se dice que le proteoma de una célula u organismo es algo dinámico y reflejo de las condiciones a las que son expuestas las células en un momento dado.

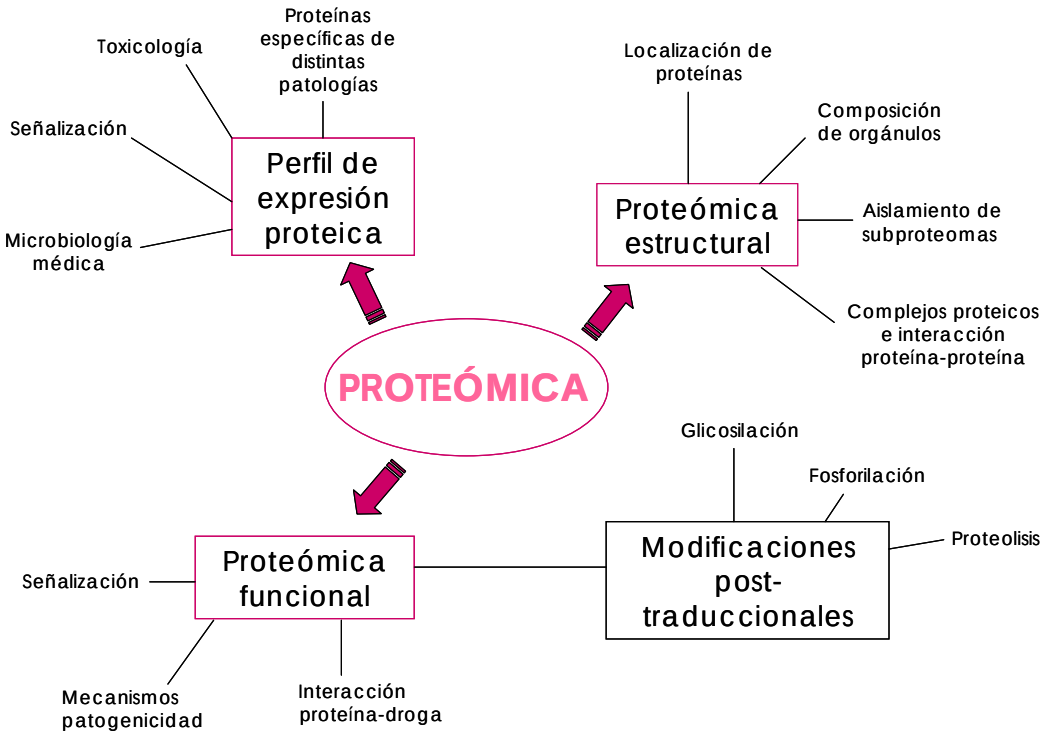

Figura 7: Clasificación de la proteómica y sus aplicaciones. Figura tomada de la Tesis de Virginia Cabezón.

fundamentalmente en dos tipos de técnicas: técnicas de separación y técnicas de identificación y caracterización de proteínas mediante espectrometría de masas (Aebersold y Mann, 2003). Dichas técnicas, junto con la bioinformática, en la que se apoya toda esta tecnología tanto para su desarrollo, como para el análisis, interpretación e integración de la enorme cantidad de datos obtenidos, son los pilares básicos de los estudios proteómicos.

4.1. Métodos de separación de proteínas

Debido a la enorme complejidad del proteoma (varios miles de proteínas) de la mayor parte de los organismos, los estudios proteómicos requieren la separación de proteínas para facilitar el análisis posterior. Dentro de las técnicas de separación de proteínas, las dos más utilizadas y con mayor poder de resolución son la electroforesis (monodimensional (SDS-PAGE) y bidimensional en geles de poliacrilamida (2D-PAGE)) y la cromatografía líquida (sobre todo la cromatografía líquida de alta resolución o HPLC).

Electroforesis bidimensional

La electroforesis bidimensional separa las proteínas basándose en dos parámetros: su punto isoeléctrico, en la primera dimensión, y su peso molecular en la segunda. Es una técnica de separación de gran capacidad resolutiva.

La separación de la primera dimensión se realiza mediante isoelectroenfoque (IEF), donde las proteínas son separadas en un gradiente continuo de pH hasta alcanzar una posición en la que su carga neta (punto isoeléctrico, pI) es cero. En la segunda dimensión las proteínas son separadas en función de su peso molecular mediante electroforesis en presencia de SDS (Laemmli,

1970). La dirección del movimiento de las proteínas en esta segunda etapa electroforética es perpendicular a la primera, de manera que se obtiene un mapa de "manchas proteicas" que se distribuye en dos dimensiones. La innovación clave para la 2D-PAGE fue el desarrollo de geles con un gradientes de pH inmovilizado (IPG) (Bjellqvist, *et al.*, 1993) que mejoran, entre otras cosas, la reproducibilidad de los geles bidimensionales.

Una vez separadas, las proteínas se visualizan mediante diferentes métodos de tinción como el Azul de Coomassie, la tinción con plata o la tinción con compuestos fluorescentes (Sypro Rubi, CyDye, etc.). A pesar de que esta técnica fue introducida hace más de 30 años (O'Farrell, 1975), su verdadera aplicación a la proteómica ha sido posible gracias al desarrollo de la espectrometría de masas para la identificación de proteínas a gran escala.

Entre las ventajas de la electroforesis bidimensional destacan la posibilidad de establecer mapas de referencia de los distintos proteomas, su elevada capacidad de carga y su gran capacidad de resolución. Por otro lado, las limitaciones más relevantes de esta técnica se relacionan con la dificultad de resolución de proteínas de elevado peso molecular, muy hidrofóbicas, muy ácidas o muy básicas, además de ser una técnica laboriosa y difícil de automatizar.

Cromatografía líquida

Para solventar los problemas de la electroforesis 2D, se han desarrollado técnicas que no necesitan geles para la separación de proteínas, sino que emplean la cromatografía líquida acoplada a espectrometría de masas (LC-MS).

La cromatografía líquida (LC) es una técnica de fraccionamiento que puede aplicarse para separar proteínas o péptidos según diferencias en sus propiedades físicas y/o químicas (hidrofobicidad, tamaño, carga eléctrica), utilizando para ello diversos tipos de soporte cromatográfico (fase reversa, intercambio iónico, exclusión molecular, afinidad, etc.). Permite además el acoplamiento directo de la columna con el espectrómetro de masas mediante la ionización con ESI (Smith, *et al.*, 1990), lo que posibilita la automatización de este proceso (Issaq, *et al.*, 2001, Lesley, 2001). Este hecho hace que las técnicas basadas en la separación cromatográfica conectada a espectrometría de masas en tándem, como la tecnología multidimensional de identificación de proteínas (MudPIT), superen a las técnicas basadas en gel, en rapidez, sensibilidad, reproducibilidad y aplicabilidad a diferentes muestras y condiciones (Griffin, *et al.*, 2001).

4.2. Análisis de proteínas mediante espectrometría de masas

Las proteínas pueden ser identificadas por diversos procedimientos, entre los que se incluyen la secuenciación del extremo *N*-terminal, la detección con anticuerpos específicos, la composición de aminoácidos, la co-migración con proteínas conocidas, y las sobre-expresión y deleción de genes (Garrels, *et al.*, 1994, Humphery-Smith, *et al.*, 1997, Sagliocco, *et al.*, 1996, Wilkins, *et al.*, 1997). Todos estos métodos generalmente son lentos, laboriosos o caros, y por tanto no resultan apropiados para su utilización como estrategias a gran escala.

Debido a su rapidez y a su elevada sensibilidad, la espectrometría de masas (MS) se ha convertido en el método más utilizado para la identificación de proteínas a gran escala (Patterson, 1998). También

permite la caracterización de modificaciones post-traduccionales que presentan relevancia fisiológica, tales como glicosilación, fosforilación, ubiquitinación, etc.

La espectrometría de masas es una técnica analítica clásica que permite analizar la composición de elementos químicos e isótopos atómicos, separando los iones del analito en fase gaseosa por su relación masa/carga (m/z), permitiendo conocer la masa molecular de un analito de una forma muy precisa. El desarrollo a finales de los años 80 de las técnicas de ionización suave, que permiten generar iones a partir de analitos grandes y no volátiles, ampliando la aplicabilidad de la espectrometría de masas a las biomoléculas (incluyendo las proteínas) e inició una rápida evolución de esta tecnología que continúa hoy en día.

Los espectrómetros de masas están compuestos principalmente por tres elementos: una fuente de ionización, un analizador de masas y un detector (Figura 8).

Las muestras a analizar son introducidas en la fuente de iones (en forma líquida o seca) donde los componentes de la muestra son convertidos en iones en la fase gaseosa. Estos iones son transferidos al analizador de masas donde se analizan y separan según su relación m/z utilizando diferentes principios físicos según el tipo de analizador. Los datos registrados por el detector son procesados mediante programas de ordenador específicos, que habitualmente generan gráficos de abundancia relativa de iones frente a m/z conocidos como espectros de masas.

Fuentes de ionización

Existe una gran variedad de métodos de ionización que se pueden dividir en suaves y fuertes, según la cantidad de energía que transfieren a las moléculas analizadas. Los métodos suaves generan iones en fase gaseosa con poca energía residual después de la ionización, mientras que los métodos fuertes depositan un exceso de energía sobre la muestra que origina la producción de múltiples fragmentos iónicos a partir de las moléculas originales.

La aparición de métodos de ionización suave por ESI y la ionización por MALDI permite la generación de iones a partir de analitos no volátiles y de elevado peso molecular, sin una fragmentación significativa y son, debido a su eficiencia, las dos técnicas preferidas para el análisis de péptidos (Fenn*, et al.*, 1989).

MALDI: Ionización/Desorción por láser asistida por matriz (*Matrix-Assisted Laser-Desorption Ionization*).

El MALDI utiliza pulsos de luz láser en la frecuencia del UV o del IR para ionizar la muestra previamente cristalizada junto a una matriz (Karas*, et al.*, 1988). La matriz tiene la función de incorporar y dispersar las moléculas del analito y absorber la energía de radiación para producir iones del analito a través de reacciones fotoquímicas. Las matrices más utilizadas son los ácidos sinapínico, para analizar péptidos y proteínas grandes, el α-ciano-4-hidroxicinámico, para péptidos y el DHB, para moléculas grandes.

El acoplamiento de esta fuente de ionización con analizadores de tiempo de vuelo (MALDI-TOF) es

Figura 8: Esquema de los componentes básicos de un espectrómetro de masas.

un método estándar para el análisis de péptidos y proteínas, caracterizado por su robustez, su sencillez de manejo y su capacidad de automatización, así como por su alta sensibilidad y su relativa tolerancia a sales y otras interferencias.
En un espectrómetro MALDI-TOF los iones formados en la fuente se aceleran mediante la aplicación de un campo eléctrico. Estos iones adquieren la misma energía cinética durante la aceleración por lo que iones con distinta masa presentan "velocidades de vuelo" diferentes, de forma que los iones más pequeños atraviesan más rápidamente el analizador (tubo de vuelo). El tiempo que tarda cada ion en incidir sobre el detector a la salida del tubo de vuelo depende de su relación m/z y de su energía cinética, haciendo posible, de una manera muy precisa, determinar la masa de cada uno de estos iones.

ESI: Electroespray o electronebulización (*Electro Spray Ionization*).

Desarrollado por Fenn y colaboradores en 1989 (Fenn*, et al.*, 1989). ESI es una técnica de ionización a presión atmosférica en la que una solución de la muestra es nebulizada a la salida de un tubo capilar por la acción de un fuerte campo eléctrico (Whitehouse*, et al.*, 1985). Las sustancias en solución son introducidas en la fuente a través de un tubo capilar a cuya salida se produce la nebulización gracias a un fuerte campo eléctrico. El ESI forma gotas muy pequeñas que se evaporan muy rápidamente y generan iones policargados del analito en fase gaseosa (Whitehouse*, et al.*, 1985).
Este tipo de ionización es extremadamente suave, permitiendo producir no sólo iones de la molécula intacta, con enlaces débiles, sino también complejos formados a través de interacciones no covalentes (Farmer*, et al.*, 1998). Normalmente produce iones multicargados. El grado de carga de un determinado ion depende de su estructura (presencia de grupos ácidos o básicos) y del disolvente utilizado (Qian*, et al.*, 2006).
Existe además otra variante del ESI que se diferencia en el flujo de solvente que soporta, el nanoelectrospray (nESI), el cual trabaja con flujos por debajo del microlitro por minuto, permitiendo analizar poco volumen de muestra o analitos que se encuentran en baja concentración en una muestra (Liu*, et al.*, 2009).

Analizadores de masa

Los analizadores se clasifican en cuatro grupos: de sectores (eléctricos o magnéticos), de campos eléctricos cuadrupolo ("quadrupole", Q), de tiempo de vuelo ("time-of-flight", TOF) y de eyección selectiva de los iones (analizadores de resonancia citrónica (ICR) y trampas iónicas (IT)) (Kicman*, et al.*, 2007).
El **cuadrupolo** trabaja como un filtro de masas, donde sólo una relación m/z atraviesa el sistema al mismo tiempo. La selectividad de la masa es creada utilizando unos campos eléctricos oscilantes, que estabilizan o desestabilizan el recorrido de los iones (Paul*, et al.*, 2003).
Los analizadores de **tiempo de vuelo** miden el tiempo que lleva a los iones viajar a través del tubo de vuelo. La velocidad de los iones es proporcional a la masa, por lo que las moléculas más pequeñas viajan más rápido. Se utiliza un campo eléctrico para acelerar a los iones dentro de la zona de vuelo en el tubo de vuelo.
En la **trampa iónica** la relación m/z de los iones se determina en función del movimiento de los mismos en un campo cuadrupolar tridimensional.
Los analizadores de **resonancia citrónica de iones con Transformador de Fourier** miden la masa por

detección de la corriente producida por iones ciclotrónicos en un campo magnético. Los iones afectados por el campo magnético se mueven hasta alcanzar la frecuencia ciclotrónica dependiente de su m/z, la cual es medida. Utilizando la transformante de Fourier la frecuencia es convertida en valor masa/carga.

El análisis por MS provee de información molecular sobre los péptidos o proteínas analizadas, si bien la información sobre su secuencia es muy limitada, debiendo recurrir a la MS/MS.

Hay un tipo de espectrómetros en tándem que utilizan dos analizadores dispuestos en serie. El ion precursor se selecciona en el primer analizador y se fragmenta mediante procesos de colisión en una cámara situada entre ambos analizadores. Los iones del fragmento se detectan el segundo analizador. El instrumento más utilizado para esta aplicación es el espectrómetro de masas de triple cuadrupolo (LTQ) formado por tres cuadrupolos colocados consecutivamente (Q1 y Q3 son analizadores y Q2 es la cámara de colisión). También se pueden utilizar otros instrumentos como son el q-TOF y el TOF-TOF (Pinzi, *et al.*, 2009) (Figura 9).

Para la separación en el tiempo se utiliza un único analizador donde tiene lugar la selección de los iones precursores, su fragmentación y el análisis de los fragmentos, pero que lleva a cabo estos procesos en momentos diferentes. Las trampas iónicas y los ICR funcionan de esta manera. Este método es muy efectivo para la secuenciación de péptidos.

4.3. Identificación de proteínas

La espectrometría de masas proporciona medidas muy precisas de la masa molecular y de la carga de proteínas o péptidos en una muestra. Las medidas de masas de las proteínas intactas pueden proporcionar información rápida y valiosa sobre el

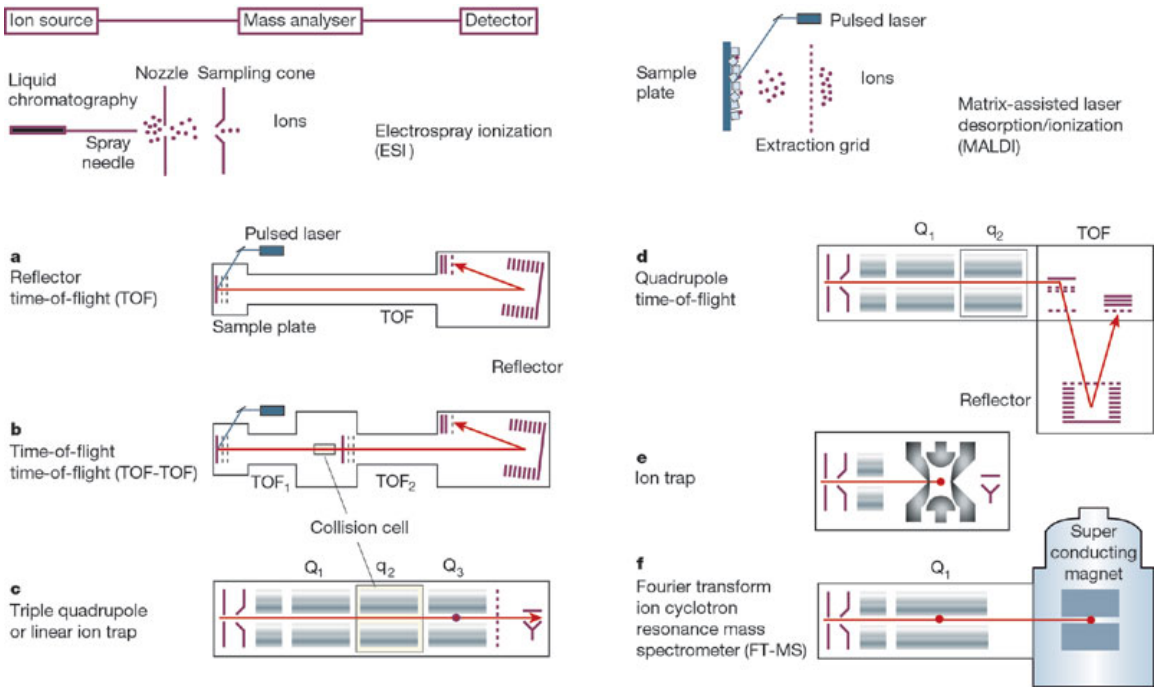

Figura 9: Espectrómetros de masas utilizados en proteómica. Los esquemas de la línea superior corresponden a los dos tipos de fuentes de ionización más utilizadas (ESI y MALDI). Los esquemas de la a-f corresponden a los distintos analizadores junto con la fuente a la que suelen ir acoplada. Imagen tomada de Aebersold y Mann (Aebersold, *et al.*, 2003).

perfil proteico de una muestra, aunque a la hora de identificar una proteína no es práctico basarse únicamente en su relación m/z, ya que existen múltiples factores (procesamientos pre o postraduccionales) que pueden variar la masa molecular real de una proteína respecto a la masa teórica de la base de datos. Además, cuanto mayor es la masa de una proteína, menor es la exactitud de la medida. Por ello se han desarrollado estrategias complementarias para la identificación de proteínas que podemos dividir en dos categorías generales:

Análisis de las masas de los péptidos o "**huella peptídica"** (PMF, *Peptide Mass Fingerprinting*). Esta técnica se basa en las medidas de las masas de los péptidos obtenidos tras la digestión enzimática de una proteína. La tripsina es la proteasa más comúnmente utilizada, ya que su corte altamente reproducible en el extremo C-terminal de los residuos de lisina y arginina permite identificar la proteína mediante la comparación de los valores de masa peptídica medidos (reales) con los valores calculados (teóricos) en la digestión virtual de todas las proteínas en la base de datos. La identificación se produce por comparación de la masa peptídica obtenida con la masa calculada teóricamente a partir de la secuencia de aminoácidos de péptidos o proteínas conocidos. Cuantos más péptidos experimentales coincidan con los teóricos, mayor probabilidad existe de que la proteína identificada sea la correcta. Es el método de elección en aquellos casos en los que se trabaja con genomas secuenciados y anotados en bases de datos. Para la identificación por *huella peptídica* es muy usual la utilización del espectrómetro tipo MALDI-TOF (Patterson*, et al.*, 1995).

A veces, es necesario el uso de dos analizadores de masas consecutivos, en los cuales se hace análisis de las masas resultantes de la **fragmentación de los péptidos** obteniendo la secuencia total o parcial de los aminoácidos (etiqueta de secuencia). Se selecciona un ion por la masa en un primer espectrómetro y se fragmenta por colisión con un gas, generando los iones a, b, c (por el extremo N-terminal de los péptidos) y los iones x, y, z (por el extremo C-terminal de los péptidos), analizándose estos iones en un segundo espectrómetro (Roepstorff*, et al.*, 1984). La fragmentación de los iones precursores se lleva a cabo utilizando CID (disociación inducida por colisión) o ETD (disociación de la transferencia del electrón), la Orbitrap es el espectrómetro de masas más utilizado para estas técnicas.

La interpretación de los espectros de fragmentación nos permitirá la identificación de partes de la secuencia de las proteínas por comparación con espectros teóricos de las proteínas de las bases de datos, o por secuenciación *de novo* u obtención de la secuencia mediante interpretación directa del espectro. Esta estrategia es la única viable en caso de no conocerse la secuencia del organismo a estudiar o de algún organismo muy homólogo (Patterson y Aebersold, 1995).

Tras la adquisición de los datos, éstos son enfrentados a las bases de datos de secuencia de modo automático (Shevchenko*, et al.*, 1996), o interpretados manualmente (Clauser*, et al.*, 1995).

4.4. Cuantificación de proteínas

Una de las aplicaciones más importante de la proteómica es el estudio del perfil de expresión proteica de las muestras (células, tejidos,

organismos, orgánulos…) y comparar este perfil proteico entre dos estados celulares distintos. El conocimiento de las proteínas que varían entre dos muestras distintas (aparecen o desaparecen, aumenta o disminuye su síntesis) es clave para conocer las diferencias fisiológicas entre ambas. La proteómica de expresión estudia los cambios en la cantidad relativa de cada proteína en distintas condiciones de crecimiento (Aebersold y Mann, 2003, Blackstock*, et al.*, 1999).

Estas aproximaciones pueden basarse en la comparación entre geles bidimensionales (análisis clásico y 2D-DIGE) o bien comparación sin gel, basada en el marcaje a nivel de proteína o a nivel de péptido.

Proteómica en gel

Los extractos proteicos obtenidos de células en las distintas condiciones de estudio se separan en geles bidimensionales distintos. En estos geles las proteínas se detectan por distintos métodos (tinción de Coomassie, tinción de plata, Sypro Rubi,…). En estas imágenes, el tamaño y la intensidad de la mancha proteica están directamente relacionados con la cantidad de proteína. Estos datos deben ser analizados informáticamente para detectar aquellas manchas con cambios entre ambos geles o condiciones de estudio.

Es una técnica limitada, pero en los últimos años se ha desarrollado la técnica 2D-DIGE (*Two-Dimensional Difference in-Gel Electrophoresis*) (Tonge*, et al.*, 2001), en la que antes de la separación de las proteínas, cada una de las muestras se marca con un fluorocromo distinto, Cy3 o Cy5, y el estándar interno (creado a partir de una mezcla de todas las muestras proteicas que se van a analizar) se marca con Cy2. Los extractos proteicos marcados se mezclan y se separan en el mismo gel bidimensional, que se excita con distintas longitudes de onda para obtener la imagen correspondiente a cada una de las muestras. El marcaje fluorescente es cuantitativo y tiene un rango dinámico lineal entre cuatro o cinco órdenes de magnitud en comparación con otros métodos de tinción.

El hecho de que las muestras se separen en el mismo gel y el uso de un estándar interno disminuye la variabilidad experimental gel a gel y facilita el uso de un programa de análisis de imagen (DeCyder) para la cuantificación automática y precisa de las manchas proteicas, el emparejamiento gel a gel y el análisis estadístico (Monteoliva*, et al.*, 2004).

Proteómica "sin gel"

Las técnicas de cuantificación relativa en estrategias proteómicas "sin gel" se basan en la incorporación en las proteínas o péptidos, que provienen de cada una de las muestras a comparar, de una versión distinta (ligera o pesada) de un reactivo con varios átomos de distintos isótopos estables no radiactivos (12C/13C; 14N/15N; 1H/2H; 16O/18O). Esto permite la cuantificación relativa por comparación de la intensidad de los picos del espectro. Aunque también se puede hacer una cuantificación de las proteínas sin marcar en una carrera de MS, determinando la cantidad de proteína relativa mediante la suma de los espectros de MS/MS para un determinado péptido a partir de múltiples muestras, lo que está directamente correlacionado con la abundancia de la proteína (Liu*, et al.*, 2004).

Debido a la enorme cantidad de péptidos en una muestra biológica, sólo una pequeña cantidad de todos los péptidos de la muestra pueden ser

analizados en una carrera de MS, lo cual limita mucho el número de proteínas que pueden ser identificadas en la muestra. El rango dinámico de cuantificación suele limitarse a 10 o 20, dependiendo de la sensibilidad del instrumento y de la complejidad de la muestra (Figura 10).

Existen diferentes estrategias de marcaje que incorporan los isótopos en distintos momentos de la obtención de la muestra: durante el cultivo celular (SILAC, *Stable Isotope labeling with Amino acids in Cell culture*) (Ong, *et al.*, 2002), después de la extracción de proteínas (ICAT, *Isotope-Coded Affinity Tag*) (Gygi, *et al.*, 2000), durante la digestión enzimática (digestión con agua pesada) (Aebersold y Mann, 2003), o incluso marcan los péptidos después de la digestión enzimática (iTRAQ, *Isotope Tag for Relative and Absolute Quantitation*) (Ross, *et al.*, 2004). Estos sistemas se están revelando como muy útiles para detectar diferencias de expresión proteica a gran escala (Figura 11).

Marcaje Metabólico

Hay varios métodos de marcaje de proteínas *in vivo*. El marcaje metabólico descrito por Oda (Oda, *et al.*, 1999) y, posteriormente desarrollado para el uso en líneas celulares por Mann y colaboradores (Ong, *et al.*, 2002) quienes lo denominaron **SILAC** (marcaje con isotopos estables en cultivo celular). En vez de marcar todos los aminoácidos con ^{15}N, como hizo Oda con *S. cerevisiae*, las células son cultivadas en un medio de cultivo que contiene $^{13}C_6$-Lisina y/o $^{13}C_6$-Arginina, elegidos porque es donde corta la tripsina en digestión y asegura que en el extremo C-terminal haya, al menos, un aminoácido marcado (excepto el extremo C-terminal de la proteína).

Uno de los beneficios de este marcaje es que las células inmortalizadas pueden incorporar el isótopo en más de un 90% de las proteínas tras 5-8 pases (generaciones). Tras la incorporación, las muestras ligera y pesada se mezclan y se preparan para el análisis por MS, resultando el error de cuantificación muy bajo. Este marcaje es muy útil para detectar cambios muy pequeños en niveles de proteína y modificaciones postraduccionales

Marcaje Isotópico

Las muestras que no pueden ser marcadas metabólicamente (muestras clínicas como tejidos, fluidos biológicos,…) o, cuando el tiempo es limitante, están disponibles métodos de marcajes

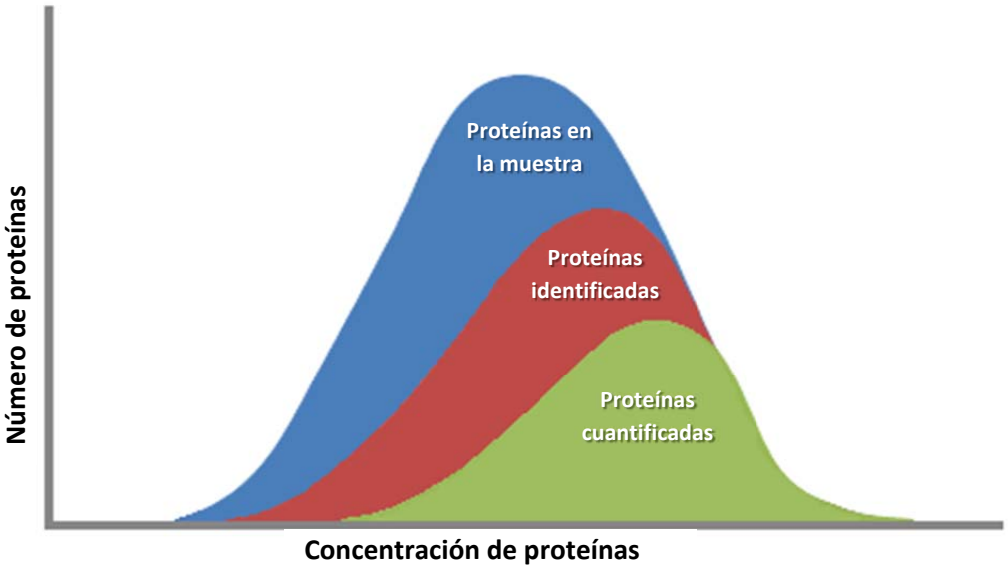

Figura 10: Limitación de la disponibilidad de las proteínas para proteómica cuantitativa.

isotópicos químicos o enzimáticos para el análisis cuantitativo. Estas técnicas de se basan en la unión de átomos o etiquetas a los péptidos o proteínas.

Podemos marcar enzimáticamente con **^{18}O** durante la digestión, basándose en el mecanismo que tiene la tripsina en incorporar dos átomos de oxígeno del $H_2{}^{18}O$ en el extremo C-terminal de los péptidos trípticos (Mirgorodskaya, *et al.*, 2000). Otra estrategia de marcaje enzimático es la tecnología estándar interna global (**GIST**) que usa agentes acetilantes deuterados (^{2}H) como N-acetoxysuccinamida (NAS) para marcar los grupos amino primarios en los péptidos digeridos (Mirgorodskaya, *et al.*, 2000). El **ICAT** (*Isotope-Coded Affinity Tag*) se basa en el marcaje con unas etiquetas homólogas a iodoacetamida que

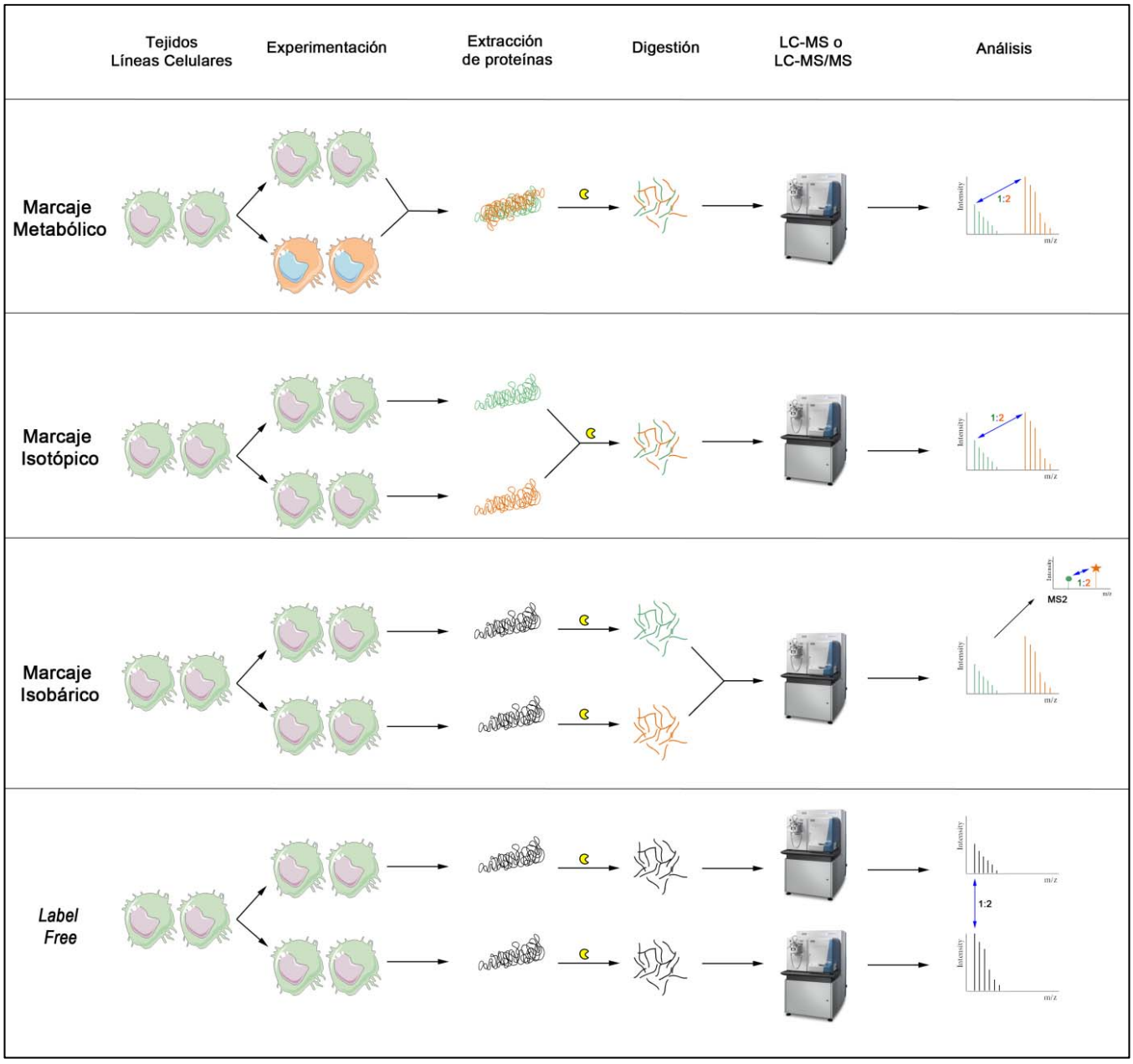

Figura 11: Resumen de flujo de trabajo de las distintas aproximaciones en proteómica cuantitativa: Este gráfico muestra el flujo de trabajo cuando las muestras son marcadas isotópicamente (indicado con el color verde para el ligero y naranja para el pesado) para análisis por espectrometría de masas. Como excepción está la cuantificación sin marcaje (label free) cuyo análisis se realiza individualmente a cada muestra y, se comparan los datos utilizando múltiples aproximaciones (conteo de espectros y la intensidad de los picos).

reaccionan con el grupo funcional tiol de a las cisteínas, estas etiquetas están marcadas con biotina que contiene ^{13}C o ^{12}C, otorgando una diferencia de masa entre el ligero y pesado de 9 Da. Los péptidos marcados se purifican en una columna de afinidad con avidina y así se simplifica la mezcla peptídica. Esta aproximación tiene como desventaja que no todos los péptidos tienen cisteína, por lo que disminuye considerablemente número de péptidos que se identifican de la proteína, disminuyendo su cobertura. Estos problemas mejoraron con el desarrollo del **ICPL** (*Isotope-Coded Protein Labeling*), en el que se marcan isotópicamente los extremos amino terminal de las proteínas y a los residuos de lisina con etiquetas de ácido nicotínico deuterado. Esta técnica permite la utilización de 4 etiquetas, por lo que podríamos comparar 4 muestras diferentes.

Marcaje Isobárico

La tecnología **iTRAQ** (*Isobaric Tags for Relative and Absolute Quantitation*) un tipo de marcaje isobárico estable. Fue diseñado para conservar la información relacionada con las modificaciones post-traduccionales y poder comparar hasta 8 muestras simultáneamente.

El sistema se caracteriza porque la cuantificación se produce en la fragmentación de los péptidos (MS/MS). El reactivo está constituido por un grupo "*reporter*" cargado (que permite la cuantificación en el espectro de fragmentación del péptido), un grupo peptídico reactivo y un grupo neutro que compensa la masa del reactivo para que sume 145. Cada muestra se digiere por separado y después se lleva a cabo el marcaje. El reactivo iTRAQ se une a aminas primarias (N-terminal y cadena lateral de lisinas) a través de un grupo NHS reactivo. As, distintos digeridos trípticos se pueden combinar y analizar en un único experimento LC-MS/MS. La existencia de 8 iones *reporter* permite comparar simultáneamente hasta 8 condiciones. Los iones precursores (MS) son exactamente iguales y los iones fragmentados (MS/MS) sólo difieren en lo que respecta a los iones *reporter*. Cuando se fragmenta el reactivo iTRAQ lo hace dando lugar a los marcadores de 113, 114, 115, 116, 117, 118, 119 y 121 Da, respectivamente. El área bajo la curva de estos picos es proporcional a la abundancia relativa de cada uno de ellos. Para una cuantificación absoluta, una de las cuatro muestras debe contener una concentración conocida de los péptidos a cuantificar.

Label free o libre de marcaje

La tecnología proteómica ha desarrollado un método de cuantificación libre de marcaje cuyo objetivo es determinar la cantidad relativa de proteínas en dos o más réplicas biológicas. La cuantificación de proteínas está basada principalmente en dos categorías de mediciones. En la primera son medidas tanto las cargas de intensidad de los iones como las áreas de los picos de los péptidos en la cromatografía. La segunda está basada en el conteo de espectros de las proteínas identificadas tras el análisis de espectrometría de masas. Ambas son medidas para cada carrera y los cambios en la abundancia de proteínas son calculados comparando diferentes análisis independientes (Zhu*, et al.*, 2010).

La utilización de las técnicas proteómicas en el estudio de la interacción entre patógeno y hospedador abre nuevos caminos en la comprensión de los mecanismos de virulencia de los patógenos y cómo actúa el sistema inmunitario para combatir la infección. Al utilizar diversas técnicas, tanto basadas en gel como de proteómica sin gel, podría proporcionarnos gran información para el estudio de este tema.

Objetivos

El objetivo general de este trabajo es profundizar en el estudio de los procesos implicados en la respuesta de los macrófagos frente a *C. albicans* mediante el uso de técnicas proteómicas de expresión diferencial.

Los objetivos concretos de esta Tesis se exponen a continuación, señalando el capítulo en el que se desarrollan:

Capítulo I:

- Estudio de proteínas minoritarias de macrófagos murinos implicados en la respuesta frente a *C. albicans* por 2D-DIGE utilizando fracciones subcelulares enriquecidas en proteínas de Citosol, Membranas/Organelas, Núcleo y Citoesqueleto.

Capítulo II:

- Identificación de nuevas rutas de señalización implicadas en la respuesta de los macrófagos frente a *C. albicans* mediante el estudio global proteómico y fosfoproteómico utilizando el marcaje metabólico SILAC.

Capítulo III:

- Estudio de la respuesta de macrófagos humanos M1 (proinflamatorios) y M2 (antiinflamatorios) frente a *C. albi*cans. Medida de la respuesta fagocítica, de la actividad candidacida y la producción de citoquinas. Estudio mediante 2D-DIGE, tanto las diferencias entre los dos tipos de macrófagos M1 y M2, como su respuesta frente a la levadura patógena.

The overall objective of this Thesis is to deepen the study of the processes involved in the macrophages response against *C. albicans* using diverse differential proteomics techniques.

The specific objectives of this thesis are presented below, indicating the chapter in which they are developed:

Chapter I:

- Study of murine macrophage less abundant proteins involved in the response to *C. albicans* by 2D-DIGE using cytosolic, membrane/organelles, nucleus and cytoskeletal subcellular enriched fractions.

Chapter II:

- Identification of new signaling pathways involved in the macrophage response to *C. albicans* by global proteomic and phosphoproteomic studies using the metabolic labeling SILAC.

Chapter III:

- Study on the response of human macrophages M1 (pro-inflammatory) and M2 (antiinflammatory) against C. albicans. Measurement of their phagocytic response, candidacidal activity and cytokine production. 2D-DIGE study of both the differences between the two types of macrophages M1 and M2 and between their responses to the pathogenic yeast.

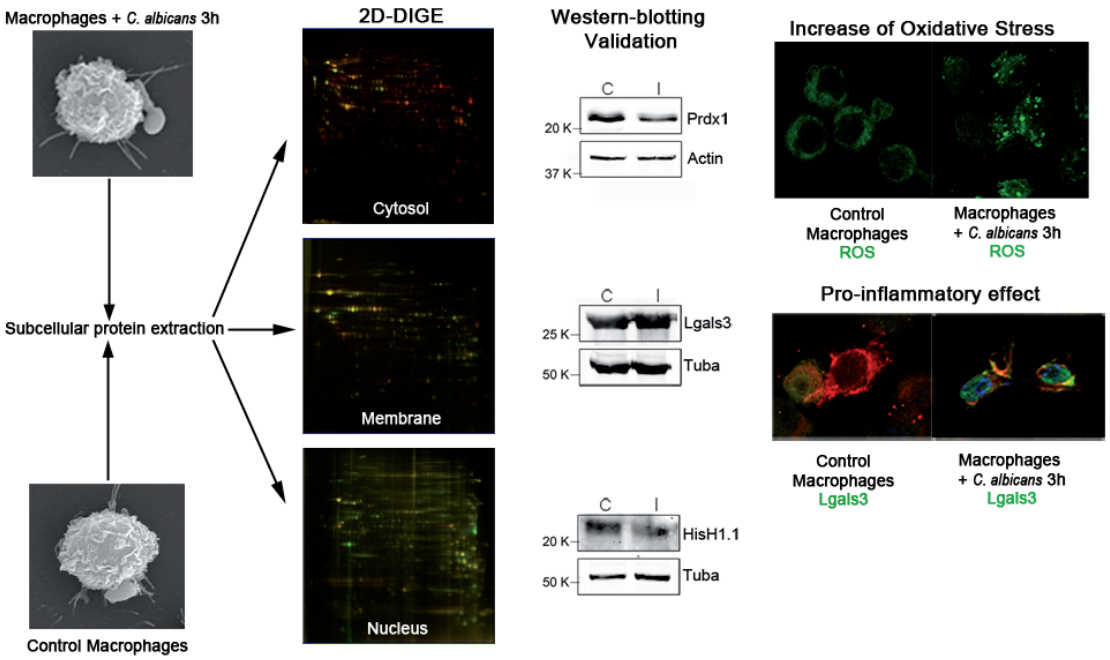

Capítulo I

*** Este capítulo contiene material suplementario que se encuentra disponible después del capítulo**

Available online at www.sciencedirect.com

SciVerse ScienceDirect

www.elsevier.com/locate/jprot

Sub-proteomic study on macrophage response to *Candida albicans* unravels new proteins involved in the host defense against the fungus☆

Jose Antonio Reales-Calderón[a], *Laura Martínez-Solano*[a], *Montserrat Martínez-Gomariz*[b], *César Nombela*[a], *Gloria Molero*[a,*], *Concha Gil*[a,b]

[a]*Departamento de Microbiología II, Facultad de Farmacia, Universidad Complutense de Madrid, Spain*
[b]*Unidad de Proteómica, Parque Científico de Madrid-UCM, Spain*

ARTICLE INFO

Available online 9 February 2012

Keywords:
Candida albicans
Macrophages
Subcellular
Inflammation
Oxidative stress
Galectin-3

ABSTRACT

In previous proteomic studies on the response of murine macrophages against *Candida albicans*, many differentially expressed proteins involved in processes like inflammation, cytoskeletal rearrangement, stress response and metabolism were identified. In order to look for proteins important for the macrophage response, but in a lower concentration in the cell, 3 sub-cellular extracts were analyzed: cytosol, organelle/membrane and nucleus enriched fractions from RAW 264.7 macrophages exposed or not to *C. albicans* SC5314 for 3 h. The samples were studied using DIGE technology, and 17 new differentially expressed proteins were identified. This sub-cellular fractionation permitted the identification of 2 mitochondrion proteins, a membrane receptor, Galectin-3, and some ER related proteins, that are not easily detected in total cell extracts. Besides, the study of different fractions allowed us to detect, not only total increase in Galectin-3 protein amount, but its distinct allocation along the interaction. The identified proteins are involved in the pro-inflammatory and oxidative responses, immune response, unfolded protein response and apoptosis. Some of these processes increase the host response and others could be the effect of *C. albicans* resistance to phagocytosis. Thus, the sub-proteomic approach has been a very useful tool to identify new proteins involved in macrophage–fungus interaction. This article is part of a Special Issue entitled: Translational Proteomics.

1. Introduction

Candida albicans is an important human opportunistic pathogen that can produce different types of infections ranging from superficial to systemic. Invasive candidiasis is an important cause of disease and mortality in immunosuppressed patients [1,2], and the therapeutic arsenal is reduced and sometimes toxic [2–4]. Thus, the study of host response to *Candida* infections can be a very useful tool to discover new therapeutic strategies. Macrophages are crucial elements of the innate and adaptive immunity to systemic candidiasis [5,6]. *C. albicans* is recognized by dedicated pattern recognition receptors (PRRs), including *Toll*-like receptors (TLRs) and lectins through its *Candida*-specific pathogen-associated molecular patterns (PAMPs) mainly mannan and β-glucan, present on its cell wall. Mannan and beta-glucan receptors, mannoside-binding lectins (such as Galectin-

☆ This article is part of a Special Issue entitled: Translational Proteomics.

* Corresponding author at: Departamento de Microbiología II, Facultad de Farmacia, Plaza de Ramón y Cajal s/n, 28040, Universidad Complutense de Madrid, Spain. Tel.: +34 913941744; fax: +34 913941745.
E-mail address: gloros@farm.ucm.es (G. Molero).

1874-3919/$ – see front matter © 2012 Elsevier B.V. All rights reserved.
doi:10.1016/j.jprot.2012.01.037

3), and Toll-like receptors 2, 4 and 6 recognize *C. albicans* cells and trigger the activation of macrophages (see recent reviews by Jouault et al. [7], Netea et al. [8] and Bourgeois et al. [9]). The recognition of *C. albicans* by macrophages causes phagocytosis and activation of cellular proinflammatory pathways (production of inflammatory mediators, toxic compounds like reactive oxygen (ROS) and reactive nitrogen (RNS) species). Macrophages also capture and process foreign antigens for their presentation to T cells, enabling host defense and immunological memory [10]. While macrophages display a wide variety of mechanisms to destroy the fungus, *C. albicans* attempts to survive the action of phagocytes by inhibiting the production of toxic compounds like NO [11,12] by preventing phagolysosome fusion [13–15]; or modulating the pH of this compartment [15].

Macrophage murine cell line RAW 264.7 was used in this study, due to its ability to employ both oxidative and non-oxidative mechanisms to kill the fungus [16]. Macrophages activated by gamma-interferon (IFN-γ), tumor necrosis factor alpha (TNF-α), or lipopolysaccharide (LPS) produce two kinds of reactive products characterized by their cytotoxic activity: reactive oxygen intermediates (ROI) and reactive nitrogen intermediates (RNI).

The introduction of proteomics has enabled the simultaneous analysis of changes in many proteins. Using a proteomic approach, we described the differential protein profile of control and murine macrophages interacting with live and heat-inactivated *C. albicans* cells and a pro- and anti-inflammatory effect was showed, respectively [17,18]. 2D-Difference Gel Electrophoresis (2D-DIGE) [19] is a powerful analytical tool within the field of proteomics, allowing not only the relative quantitation of protein spot intensity across carefully matched gels, but also for detecting posttranslational modifications of the protein [20]. Because gel-based techniques have a bias toward abundant proteins, proteins in lower quantity are not often detected in the 2-DE analysis of total cellular proteins due to the complexity of these samples. The use of pre-fractionation methods by subcellular isolation or selective enrichment of a specific group of proteins provides an effective approach to eliminate this drawback. Thus in this work, we have combined cellular fractionation with 2D-DIGE technology to study cytosol, membrane, nucleus and cytoskeletal enriched protein fractions and analyze the differential protein profile of murine macrophages after 3 h of interaction with *C. albicans*.

2. Materials and methods

2.1. *C. albicans* strains

The *C. albicans* strain used in this study was SC5314, from a clinical isolate [21]. This strain was maintained on solid YED medium (1% D-glucose, 1% Difco Yeast Extract and 2% agar) and incubated at 30 °C for at least 2 days.

2.2. *Macrophage cell culture*

2.2.1. *Culture medium and reagents*

RPMI 1640 medium, fetal bovine serum (FBS), L-glutamine, and antibiotics (penicillin–streptomycin) were obtained from GIBCO BRL (Grand Island, N.Y.). Macrophages were resuspended in RPMI supplemented with glutamine (2 mM), antibiotics (penicillin 100 U/ml–streptomycin 100 μg/ml), and 10% heat-inactivated fetal bovine serum (complete medium).

2.2.2. *Macrophage cell line*

The RAW 264.7 gamma NO (–) cell line was obtained from the American Type Culture Collection (Rockville, Md.). Cells were grown in complete medium in a 5% CO_2 incubator at 37 °C and maintained at low densities (75% confluence) and passaged until reaching the confluent state, usually every 3–4 days on sterile culture plates.

2.3. *Protein extraction*

Subcellular fractionation was performed using the ProteoExtract™, Subcellular Proteome Extraction Kit from Calbiochem (Nottingham), according to the manufacturer's protocol. Briefly, control RAW 264.7 cells after 3 h of interaction with *C. albicans* cells (ratio 1:1), were treated with the buffers supplied by the manufacturer to obtain 4 different extracts: cytosolic, organelle/membrane, nuclear, and cytoskeletal enriched fractions. The samples were stored at −80 °C. To clean up the samples, proteins were precipitated using the 2-D-Clean Up Kit (GE Healthcare) and resuspended in 30 mM Tris–HCl, 7 M urea, 2 M thiourea, and 4% CHAPS. Protein concentration was determined using the Bradford assay (Bio-Rad).

2.4. *Sample labeling*

Four biological replicates of the subproteomic fractions (cytosol, organelle/membrane, nucleus and cytoskeleton) both from control and treated samples were fluorescently labeled for DIGE analysis following the protocol of the manufacturer. Briefly, 400 pmol of Cy Dye (N-hydroxysuccinamide esters of cyanine fluorescent dyes from GE Healthcare) in 1 μl of anhydrous N,N-dimethylformamide (DMF, Sigma) was used per 50 μg of protein. After 30 min of incubation on ice in the dark, the reaction was quenched with 10 mM L-Lysine for 10 min under the same conditions, except for the cytoskeletal fractions, where 25 μg of protein and 200 pmol of Cy Dye were used.

2.5. *Two-dimensional differential in-gel electrophoresis (2D-DIGE)*

For each fraction, labeled samples were combined according to the experimental design and four 2-DE gels were performed. Each gel contained a pair of Cy3 and Cy5 labeled samples (50 μg of protein of each sample), corresponding to the control and treated samples from the corresponding subproteome (dye-swaps were performed), and a 50 μg aliquot of a Cy2 labeled pooled standard made by mixing equal amounts of all the samples used for each DIGE experiment. The experimental design is detailed in Supplementary Fig. S.1. The mixtures (150 μg) were diluted 1:1 with the loading buffer [7 M urea, 2 M thiourea, 4% (w/v) CHAPS, 2% DTT and 4% Pharmalytes, pH 3–11]. First dimension (IEF) of the 2-DE was performed with 18 cm Immobiline IPG-strips (GE Healthcare) providing a non-linear pH 3–11 gradient. They were passively rehydrated with 350 μl of rehydration buffer [7 M urea, 2 M thiourea, 4% (w/v) CHAPS, 100 mM DeStreak and 2% Pharmalytes,

pH 3–11] during 12 h. The mixtures were then applied by cup loading. The IEF was performed at 20 °C using the following sequential steps: 120 V for 1 h; 500 V for 1 h; 500–2000 V gradient for 1 h; 2000–8000 V gradient for 30 min; 8000 V for 6.5 h. After the IEF, strips were equilibrated for 12 min in reducing solution [100 mM Tris–HCl (pH 8.0), 6 M urea, 30% (v/v) glycerol, 2% (w/v) SDS, 2% (w/v) DTT], and then for 5 min in alkylating solution [100 mM Tris–HCl (pH 6.8), 6 M urea, 30% (v/v) glycerol, 2% (w/v) SDS, and 2.5% (w/v) Iodoacetamide and 0.002% Bromophenol blue]. The equilibrated strips were transferred onto 12% homogeneous polyacrilamide gels (2.6%C) casted in low fluorescent glass plate using an Ettan-DALT six system (GE Healthcare). Electrophoresis was carried out at 2 W/gel for about 18 h at 18 °C.

2.6. Image visualization and DIGE data analysis

After electrophoresis, the differentially labeled co-resolved proteins within each gel were imaged using a Typhoon 9400 laser scanner (GE Healthcare). For the Cy3, Cy5 and Cy2 image acquisition, the 532-nm/580-nm, 633-nm/670-nm and 488-nm/520-nm excitation/emission wavelengths were used respectively, adjusting the pixel size resolution to 100 μm. The gel images obtained were cropped in the ImageQuant v5.1 software (GE Healthcare). For spot detection, determination of quantity, inter-gel matching and statistics gel images were analyzed using DeCyder v6.5 software (GE Healthcare).

The differential in-gel analysis (DIA) module was used to assign spot boundaries and to calculate parameters such as normalized spot volumes. The intergel variability was corrected by matching and normalizing it with the internal standard spot maps in the biological variation analysis (BVA) module. A control versus treated comparison was carried out. The average ratio and unpaired Student's *t* test were also calculated. To reduce the false positives in the *p*-value calculation, the false discovery rate (FDR) was applied. We considered statistical significance to be at the 95% confidence level when standardized average spot volume ratios exceeded ±1.5 in at least three of the four analyzed gels [22]. Unsupervised principal component analysis (PCA), hierarchical cluster (HC) and *k*-means clustering analyses were performed using the DeCyder Extended Data Analysis (EDA) module on the group of spots identified as significantly changed. These multivariate analyses clustered the individual Cy3- and Cy5-labeled samples based on collective comparison of expression patterns from the set of proteins.

2.7. Protein identification by MALDI-TOF MS

After fluorescence scanning, the total protein profile was detected by staining the DIGE gels with Colloidal Coomassie Blue (CCB). The changes observed by 2D-DIGE analysis were aligned with CCB profiling, and spots of interest were manually excised from the gels and transferred to microcentrifuge tubes. Samples selected for analysis were in-gel reduced, alkylated and digested with trypsin according to Sechi and Chait [23]. Protein identification was done at the Proteomics Facility of Universidad Complutense de Madrid-Parque Científico de Madrid, Spain (UCM-PCM), a member of ProteoRed Network. Briefly, spots were washed twice with double-distilled water, dehydrated with 75% Acetonitrile (ACN) and dried in a Savant SpeedVac. They were reduced with 10 mM DTT and alkylated with 55 mM iodoacetamide. Finally, samples were digested with 12.5 ng/μl sequencing-grade trypsin (Roche Molecular Biochemicals, IN, USA) in 25 mM ammonium bicarbonate (pH 8.5) overnight at 37 °C. After digestion, the supernatants were collected and 1 μl was spotted onto a matrix assisted laser desorption ionization (MALDI) target plate and allowed to air-dry at room temperature. Then, 0.5 μl of a 3 mg/ml of α-cyano-4-hydroxy-trans-cinnamic acid matrix in 0.1% TFA–50% ACN was added to the dried peptide digest spots and again allowed to air-dry again.

MS analyses were performed in a MALDI-TOF/TOF spectrometer 4700 Proteomics Analyzer (PerSeptives Biosystems, Framingham, MA). The instrument was operated in reflector positive ion mode, with an accelerating voltage of 20,000 V. All mass spectra were internally calibrated using autodigested trypsin peptides. MALDI-TOF spectra with a signal-to-noise 20 were collated and represented as a list of monoisotopic molecular weights. Proteins for which peptide mass fingerprints provided an ambiguous identification were subjected to MS/MS sequencing analyses.

MALDI TOF/TOF fragmentation spectra with a signal-to-noise 10 were collected by selecting the suitable precursor ions of each MALDI-TOF peptide mass map. Fragmentation was carried out using the acquisition method 1 kV ion reflector mode CID on and precursor mass window ±10 Da.

2.8. Database search

The monoisotopic peptide mass fingerprinting data obtained from MS and the amino acid sequence obtained from each peptide fragmentation in MS/MS analyses were used to search for protein candidates using Mascot version 1.9 from Matrix Science (http://www.matrixscience.com).

The searches for peptide mass fingerprints and tandem MS spectra were performed in the Swiss-Prot release 53.0 (http://www.expasy.ch/sprot) and TrEMBL release 37.0 (http://www.ebi.ac.uk/trembl) databases without taxonomy restriction, containing 269,293 and 4,672,908 sequence entries respectively for each software version and database release. The Mascot search parameters were (1) species, all; (2) allowed number of missed cleavages, 1; (3) fixed modification, carbamidomethyl cystein; (4) variable modifications, methionine oxidation; (5) peptide tolerance, ±50 (PMF)–100 (combined search) ppm; (6) MS/MS tolerance, ±0.3 Da; and (7) peptide charge, +1. In all identified proteins, the probability score was greater than the one fixed by Mascot as being significant, that is, a p value <0.05. The parameters for the combined search (peptide mass fingerprint and MS/MS spectra) were the same as described above.

The identified proteins have been included into the Proteopathogen Database (http://proteopathogen.dacya.ucm.es/) [24].

2.9. Western-blotting detection

50 μg of protein per well were separated onto 10% SDS-polyacrylamide minigels and transferred to Hybond-ECL Nitrocellulose membranes (Amersham Biosciences). The western-blotting was performed with Odyssey system

(Infrared Imaging System (LI-COR Biosciences, Nebraska, USA)), which allows the measurement of the relative levels of fluorescence of the different bands and simultaneous labeling with two different antibodies. After 1 h of incubation with primary antibodies: 1/2000 monoclonal anti-Peroxiredoxin-1 (Sigma-Aldrich), 1/2000 Rat anti-Galectin-3 (Santa Cruz Biotechnology), 1/1000 Rabbit polyclonal anti-Histone H1.1 (Abcam), and 1/2000 Rat anti-Tubulin alpha (AbD serotec), the membranes were washed 4 times in PBS with 0.1% Tween-20. After this, the membranes were incubated with fluorescently labeled secondary antibodies: 1/4000 IRDye 800CW conjugated Goat (polyclonal) anti-Rabbit IgG, 1/2000 highly cross absorbed (LI-COR Biosciences) and 1/4000 IRDye 680 conjugated Goat (polyclonal) anti-Mouse IgG, highly cross absorbed (LI-COR Biosciences) or IRDye 680 Goat anti-Rat IgG, highly cross absorbed (LI-COR Biosciences) for 30–60 min at room temperature and protected from light. The membranes were washed again and scanned for fluorescence detection with Odyssey system (LI-COR Biosciences, Nebraska, USA). In our case, Peroxiredoxin-1 (Prdx1) and actin in the cytosolic fraction and Galectin-3 (Lgals3) and Tubulin in the membrane fraction were detected and measured in the same membrane.

For nuclear fraction, traditional western blotting was performed using 1/1000 Rabbit polyclonal anti-Histone H1.1 (Abcam), and 1/2000 Rat anti-Tubulin alpha as primary antibodies and 1/4000 anti-Rabbit IgG HRP (GE Healthcare) and 1/4000 anti-Rat IgG HRP (GE Healthcare) as secondary antibodies in the same membrane after stripping the membrane.

Actin was used as loading control for cytosol enriched fraction and Tubulin for membrane and nuclear enriched fractions. Data were expressed as mean ± SD. The unpaired Student's *t*-test was used to compare differences between groups and $p < 0.05$ was considered significant.

2.10. *Immunofluorescence assay*

2×10^5 RAW 264.7 macrophages were plated onto 18-mm coverslips placed in 24-well multiwell plates for 24 h at 37 °C in a 5% CO_2 atmosphere, washed twice with culture medium without serum, and treated with 5×10^5 blastospores for 3 h. The coverslips were incubated with PKH26 (2× PKH Dye Solution, 4×10^{-6} M in diluent C) (Sigma) for 5 min at 25 °C. The reaction was quenched with 1% BSA. The coverslips were washed twice with PBS and cells were fixed with 3.7% formaldehyde in PBS for 30 min at 4 °C. The coverslips were washed twice with PBS and cell membranes were permeabilized for 15 min with PBS containing 0.2% Tween 20 at room temperature. After two washes with PBS, the macrophage Fc receptors were blocked with IgG from mouse serum (Sigma-Aldrich) overnight (1:500) in RPMI containing 10% BSA and 0.2% Saponin. After this, the coverslips were washed twice for 10 min in gentle sacking, and overlaid with Rat anti-Galectin-3 antibody, diluted 1:1000, incubated for 1 h, washed with PBS three times and overlaid with anti-Rat FITC antibody (Sigma-Aldrich, diluted 1:1000), incubated for 1 h, washed with PBS three times in the dark and mounted with anti-fading solution with DAPI. Digital images were captured using a confocal fluorescence microscopy Leica TCS SP2.

2.11. *Flow cytometric analysis*

Dihydrorhodamine 123 (DHR123) 0.02 mM was added to the culture medium 40 min before the end of the incubation with/without *C. albicans*. DHR123 was purchased from SIGMA, dissolved in DMSO in the dark at a concentration of 2 mM, and stored at −80 °C until use. After the incubation, cells were trypsinized at 37 °C for 10 min, the reaction was quenched with complete medium and cells were spun down for 10 min at 1000 rpm. Pellet was washed twice with PBS and, before analysis, cells were resuspended in PBS at a concentration of 1×10^6 cells/ml.

Flow cytometry analyses were done using a FACScan equipped with an ion laser with an excitation at 488 nm. The fluorescence of 10,000 cells was collected on a linear scale through right angle scatter (side scatter) was collected at 530 nm (FL1). Data were expressed as mean ± S.D. Statistical analyses were performed using the Student's *t* test. Differences were considered significant at p-value < 0.05.

2.12. *In vitro candidacidal assay*

The candidacidal activity was carried out in vitro by a growth inhibition assay and a CFU assay as previously reported [25]. In brief, a total of 10^6 *C. albicans* cells were grown into a p24 plate with 1 ml of the macrophages supernatant or with 1 ml

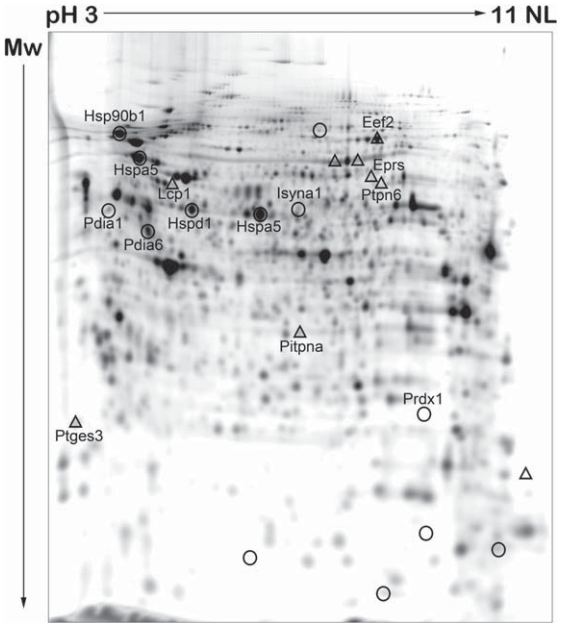

Fig. 1 – Representative 2-DE of RAW 264.7 cells cytosol enriched fraction after the interaction with *C. albicans*. Proteins were resolved in the 3–11 (non linear) pH range on the first dimension, and on 10% polyacrylamide gels on the second dimension. Proteins that exhibited a significant alteration in expression in macrophages after interaction with *C. albicans* were identified by MALDI-TOF/TOF mass spectrometry, and are listed in Table 1 by the same name as that in the figure. Circled spots matched with down-expressed proteins after the interaction with the yeast and spots included into triangles matched with over-expressed proteins.

of the supernatant and 10^6 macrophages or 1 ml of RPMI, which was used as a control. The cell suspensions were incubated at 37 °C and 5% CO_2. After 3 h of interaction, the fungal cells were diluted 1:200 and 1:2000 and the solutions were dispensed and streaked on the surface of YED plates (three dishes for each condition) which were then incubated at 30 °C 24–48 h, and CFUs were enumerated. For statistical analysis, the results were expressed as mean ± standard deviations. Differences in the numbers of CFU were evaluated by using the Student *t* test. The experiment was carried out 4 times.

3. Results

3.1. *Differential protein expression of macrophages upon C. albicans interaction: analysis of subcellular fractions by 2D-DIGE*

Control RAW 264.7 macrophages and after 3 h of interaction with *C. albicans* SC5314 cells at a 1:1 ratio, were treated as described in Materials and methods to obtain 4 subproteomic samples: cytosol, organelle/membrane, nucleus and cytoskeleton enriched fractions. These samples were analyzed separately using 2D-DIGE methodology. Four 2D-DIGE gels per subfraction, corresponding to Cy3-, Cy5- and pooled internal standard Cy2-labeled sample images, were analyzed using DeCyder software (v6.5). DIA module analysis allowed the detection of an average of 1730, 1634, 1405 and 1688 protein spots in cytosol, organelle/membrane, nucleus and cytoskeleton fractions, respectively. Then, inter-image spot matching was carried out by BVA module. In this step, an average of 1188, 1295, 1105 and 1052 spots were matched on the cytosol, organelle/membrane, nucleus and cytoskeleton gels, respectively. Also in this module, an average of standardized volume ratio and unpaired Student's *t* test, were calculated.

Protein spots with 1.5-fold as a threshold in the average ratio with $p<0.05$ between control macrophages and macrophages upon interaction for each fraction were considered. The analysis resulted in 10 spots increased and 10 spots decreased in the cytosolic fraction (Fig. 1), 11 spots increased in the membrane/organelle fraction (Fig. 2), 4 spots increased and 6 decreased in the nuclear fraction (Fig. 2) and 70 spots increased and 7 decreased in the cytoskeleton fraction (Supplementary Fig. S.2) of macrophages after 3 h of interaction with the yeast.

3.2. *Identification of differentially expressed proteins*

For protein identification, spots were selected, digested in-gel and analyzed by MALDI-TOF-MS. Mascot database search using the peptide mass fingerprint spectra allowed the identification of the proteins in 25 of the 44 spots obtained from the gels from cytosol, organelle/membrane and nucleus fraction. Proteins identified as altered in macrophages are listed in Table 1, with detailed information comprising accession number, pI, MW and identification parameters. The corresponding spots are depicted on DIGE gel images in Figs. 1 and 2.

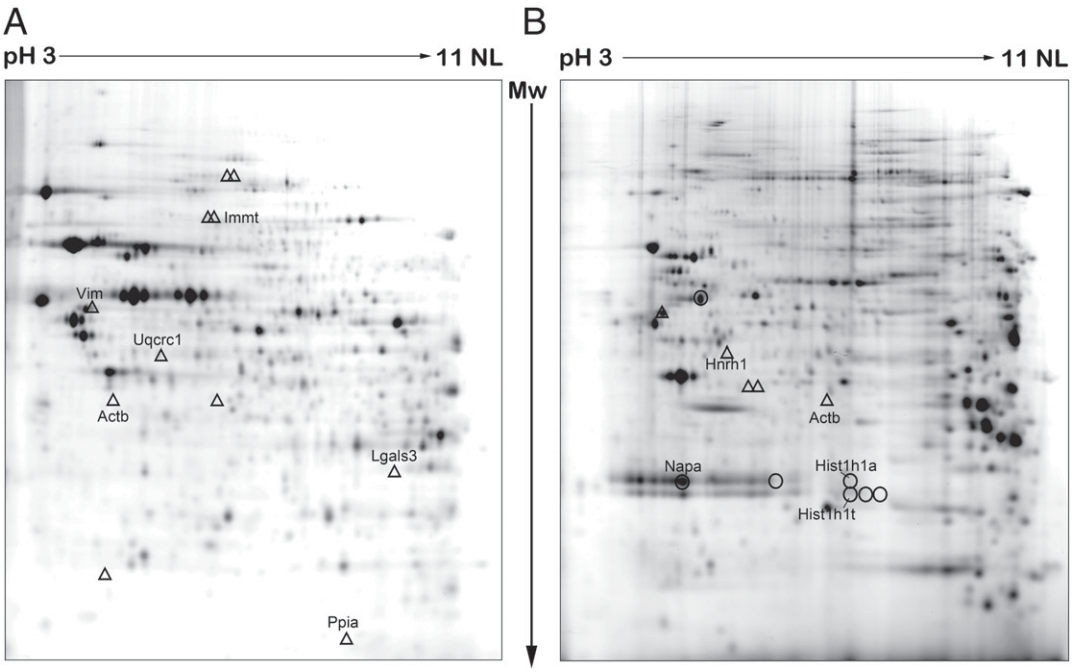

Fig. 2 – Representative 2-DE of organelle/membrane (A) and nuclear (B) enriched fractions of RAW 264.7 cells after interaction with *C. albicans*. Proteins were resolved in the 3–11 (non linear) pH range on the first dimension, and on 10% polyacrylamide gels on the second dimension. Proteins that exhibited a significant alteration in expression in macrophages after the interaction with *C. albicans* were identified by MALDI-TOF/TOF mass spectrometry, and are listed in Table 1 by the same name as that in the figure. Circled spots matched with down-expressed proteins after interaction with the yeast and spots included into triangles matched with over-expressed proteins.

Table 1 – Functional classification of macrophages' differentially abundant proteins of cytosolic, membrane and nuclear enriched fractions identified from 2D-DIGE broad range pH gels (pH 3–11 NL IPG strips).

Protein ID [a]	Swiss Prot [a]	Protein name	Av, ratio [c]	t-test [c]	Loc [d]	M_r [b]	pI [b]	Score [b]	No of pept [b]	% Cov [d]
Nucleic acid processing										
Hnrph1	O35737	Heterogeneous nuclear ribonucleoprotein H1	3.67	0.0012	Nucleus	49.19	5.67	490	6/6	18
Hist1h1a	P43275	Histone cluster 1, H1a K.SLAAAGYDVEKNNSR.I (47)	−1.91	0.02	Nucleus	21.78	10.93	47	1	7
Hist1h1t	Q07133	Histone cluster 1, H1t K.ALAAAGYDVEKNNSR.I (69)	−2.04	0.16	Nucleus	21.54	11.71	69	1	7
Translation										
Eef2	P58252	Eukaryotic translation elongation factor 2	1.56	0.34	Cytosol	96.22	6.51	159	27/65	30
Eprs	Q8CGC7	Bifunctional aminoacyl-tRNA synthetase	1.63	0.0039	Cytosol	170	7.62	311	35/65	21
Stress response and protein fate										
Pdia3, GRP58	P27773	Protein disulfide isomerase associated 3	−2.12	0.35	Cytosol	56.67	5.81	185	24/65	38
Hspa5, GRP78	P20029	Heat shock protein 5	−2.27	0.26	Cytosol	72.49	5.01	328	36/65	51
Hsp90b1, GRP94	P08113	Tumor rejection antigen gp96	−1.96	0.25	Cytosol	92.71	4.74	229	34/65	33
Hspd1	P63038	Heat shock protein 1 (chaperonin)	−2.82	0.25	Cytosol	60.95	5.36	96	14/49	33
Napa	Q9DB05	N-ethylmaleimide sensitive fusion protein attachment protein alpha	−2.43	0.031	Nucleus	33.19	5.25	84	6/12	22
Ppia	P17742	Peptidylprolyl isomerase A	2.04	0.008	Membrane	17.97	7.88	95	8/34	31
Signal transduction										
Lgals3	P16110	Galectin 3, Lectin galactoside-binding soluble 3	1.85	0.032	Membrane	27.51	8.5	88	7/17	23
Pdia6	Q922R8	Protein disulfide isomerase associated 6	−1.68	0.12	Cytosol	48.46	5	110	10/69	19
Ptpn6	P29315	Protein tyrosine phosphatase, non-receptor type 6	1.79	0.041	Cytosol	67.55	7.66	135	17/57	33
Ptges3	Q9R0Q7	Prostaglandin E synthase 3	2.21	0.0034	Cytosol	18.72	4.36	87	7/29	35
Lipid metabolism and transport										
Isyna1	Q9JHU9	Inositol-3-phosphate synthase 1/Myo-inositol-1-phosphate synthase	−2.21	0.017	Cytosol	60.93	5.99	135	16/65	40
Pitpna	P53810	Phosphatidylinositol transfer protein, alpha	1.5	0.4	Cytosol	31.97	5.98	109	8/20	39
Oxidoreductase activity										
Pdia1	P09103	Protein disulfide-isomerase precursor	−2.56	0.043	Cytosol	57.14	4.91	138	18/64	33
Prdx1	P35700	Peroxiredoxin 1	−2.58	0.005	Cytosol	22.18	8.73	204	13/45	54
Mitochondrion structure and function										
Immt	Q8CAQ8	Inner membrane protein, mitochondrial	2.88	0.0004	Membrane	84.24	6.18	96	18/65	28
Uqcrc1	Q9CZ13	Ubiquinol-cytochrome c reductase core protein 1	3.82	1E-05	Membrane	53.42	5.75	201	23/65	46
Cytoskeletal structural constituents and actin binding proteins										
Actb	P60710	Actin, beta	1.78	0.04	Membrane	41.73	5.29	155	6/18	15
Actb	P60710	Actin, beta	1.69	0.0062	Nucleus	41.73	5.29	155	6/18	15
Lcp1	Q61233	Plastin-2 (L-plastin)	1.66	0.21	Cytosol	70.73	5.2	222	26/52	41
Vim	P20152	Vimentin	2.37	0.4	Membrane	51.59	4.96	150	17/48	46

[a] Protein name and accession number according to Human PSD and GPCR-PD human, mouse and rat database (Mouse Protein Report with PSD Interactions) of Proteome Bioknowledge Library (https://www.proteome.com/control/tools/proteome). These protein spots are labeled with the same Protein ID in Figs. 1 and 2.
[b] Experimental molecular mass, pI, matched peaks/unmatched peaks' peptides and protein score are derived from Mascot result page.
[c] Average ratio and Student's *t*-test *p*-values were calculated using Decyder software v6.
[d] The protein coverage corresponds to a percentage in proteins identified by peptide mass fingerprinting. For proteins identified by PMF combined with fragmentation analysis of some peptides, the protein coverage and the protein score data are derived from the Mascot results page of the combined search. The sequences of the peptides that were identified by TOF/TOF analysis are shown in the protein name column and the individual ion score of the fragmented peptides are shown in brackets.

A database search (BLK Proteome (Biobase), PubMed and MGI) was carried out to analyze the protein function to assign them into different functional groups. As it can be observed in Table 1, proteins identified in the cytosol enriched fraction are involved in stress response and protein fate, oxidoreductase activity, signal transduction, translation and lipid metabolism and transport. Most of the proteins identified in organelle enriched fraction are related to

mitochondrion and cytoskeleton. In addition a membrane receptor, Galectin-3, was identified. And the proteins identified in the nuclear fraction are mostly related to nucleic acid processing. The abundance of proteins involved in signal transduction and stress response was somehow predictable because the interaction with the yeast is a stress for macrophage.

With respect to the already described sub-cellular location of the proteins in the databases, 90% of the proteins were isolated and identified in a fraction consistent with previously published works.

3.3. *Validation of differentially expressed proteins*

To confirm proteomic results, Western blotting experiments were performed using antibodies against one protein per fraction. The proteins selected were: Peroxiredoxin-1 for the cytosol fraction, Galectin-3 for the membrane/organelle fraction and Histone H1.1 for the nuclear extract. In addition, some biological processes related to the identified proteins were assayed.

3.3.1. *Peroxiredoxin-1 decrease and ROS increase in the macrophages upon C. albicans interaction*

As it can be observed in Fig. 3, Peroxiredoxin-1 decreases in the cytosolic fraction after the interaction, in agreement with the DIGE data (Fig. 1, Table 1). This decrease could be accompanied by an increase in the oxidative stress inside macrophages. To check this question, we measured the generation of free radical species of oxygen inside the macrophage after the incubation with/without *C. albicans* by flow cytometry using DHR123 as a reporter of ROS production. As shown in Fig. 4, intracellular ROS production in macrophages increases in 45% (45 min) and 39% (3 h) with respect to control cells ($p=0.01$).

3.3.2. *Histone H1.1 decrease*

The Histone H1.1 decrease in the nuclear enriched fraction (Table 1) was validated by western blotting (Fig. 2). Histones are proteins directly related to the DNA function, thus, its presence in the nuclear fraction was expected. Only two isoforms (H1a and H1t) were detected as decreased. As Lin and co-worker showed, the deletion of these two genes in mice is partially compensated by the other H1 isoform genes thus although the expression of some genes is affected, the mice showed no phenotypic abnormalities [26].

3.3.3. *Galectin-3 allocation and secretion in macrophages after the interaction with C. albicans. Candidacidal effect of macrophage supernatants*

DIGE revealed an increase in the expression levels of Galectin-3 after the interaction in the organelle/membrane fraction (Fig. 2, Table 1), and this was confirmed by western blotting (Fig. 3). Galectin-3 is found in the phagocytic cups and phagosomes [27] and it is also secreted [28,29]. This distribution was observed by immunofluorescent staining, in which the lipophilic dye PKH26 (red) was used to stain cell membranes, Galectin-3 appeared in green, while nuclei were stained with DAPI (blue), and by western blotting. Confocal images showed considerable overlap between Galectin-3 and PKH26 (yellow area) in phagocytic cups of macrophages after the interaction with respect to control macrophages (Fig. 5). The protein level in cytoplasm and membrane/organelle enriched fractions was also checked by 2D-western blotting in the same samples (Fig. 6A), showing an overall increase in the protein species of Galectin-3 in the organelle/membrane enriched fraction during the interaction and a decrease in the cytosolic ones. The secretion of Galectin-3 was also measured by 1D-western-blotting (Fig. 6B), showing that it is independent of the presence of *C. albicans*, although it is increased along the interaction. Direct candidacidal action of Galectin-3 has already been shown by other authors [30].

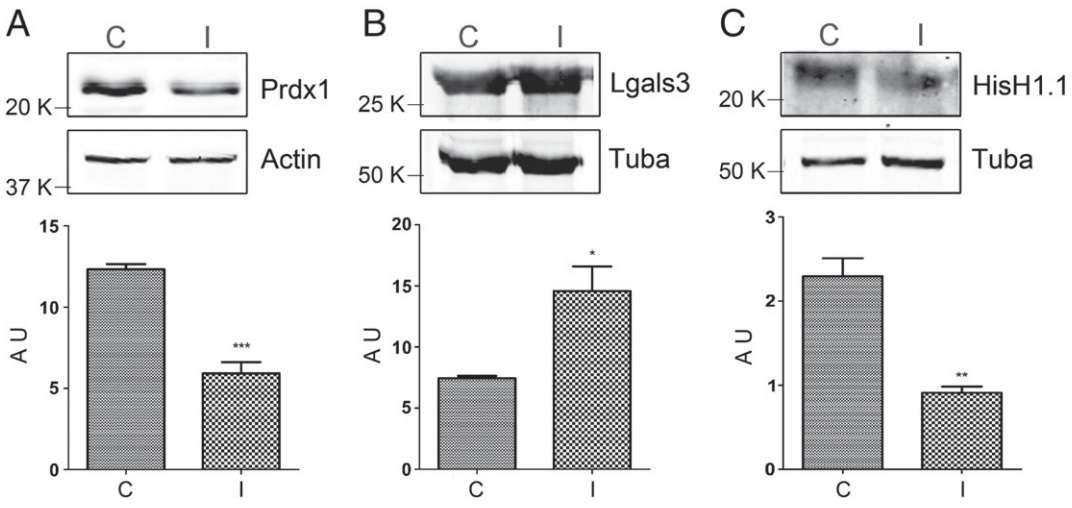

Fig. 3 – Confirmation of differential expression of Peroxiredoxin 1, Galectin-3 and Histone H1.1 in cytosol, organelle/membrane and nucleus fraction of RAW 264.7 macrophage. Fractions were separated on 10% 1D-SDS-PAGE gels and transferred onto nitrocellulose membranes. Western blotting for Peroxiredoxin 1, Galectin-3 and Histone H1.1 in cytosol, membrane and nucleus fraction, respectively, was performed. Decrease of Prdx1 and HisH1.1 and increase of Gal3 can be observed in the relative densitometry. Data are expressed as the means ± SD for each group. Significant differences from control are indicated (*, $p<0.05$; **, $p<0.01$; ***, $p<0.001$).

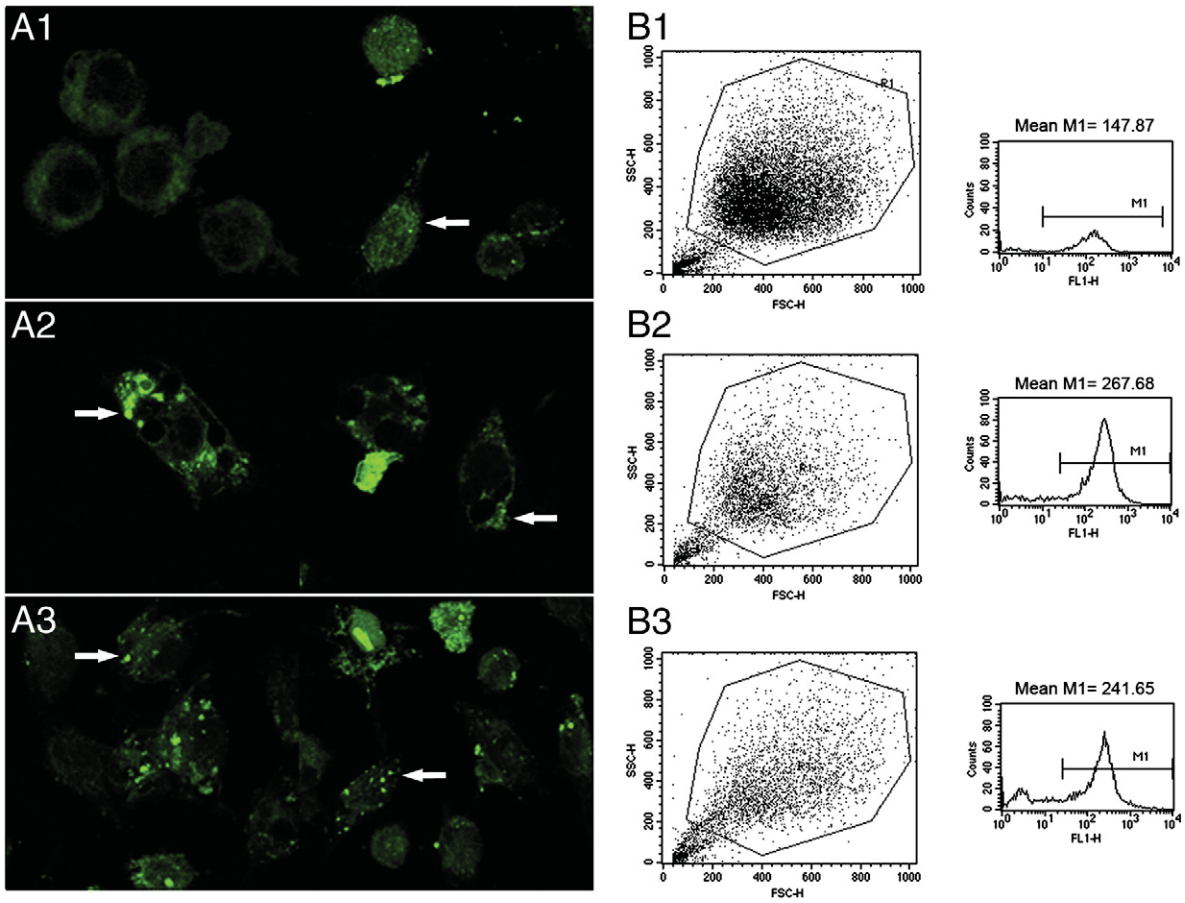

Fig. 4 – Oxidative stress measurement in RAW 264.7 cells after interaction with *C. albicans* with dihydrorhodamine-123. (A) Microscopic images of RAW 264.7 control (A.1) and after 45 min (A.2) and 3 h (A.3) of interaction with *C. albicans*. Green fluorescence shows intracellular oxidative species levels. (B) Representative scatter dot plot (FSC = forward scatter, SSC = side scatter, FL-1 = dihydrorhodamine123) of control macrophages (B.1) and after 45 min (B.2) and 3 h (B.3) of interaction. The values show the mean of the fluorescence positive population.

Thus, candidacidal activity of the macrophage supernatant was measured, and it resulted in 50% of the total macrophage candidacidal activity after 3 h of incubation at a 1:1 ratio of *Candida*: macrophages (Fig. 6C).

4. Discussion

Macrophages are important cells for the eradication of pathogens from the tissues. Our group has boarded the study of its interaction with *C. albicans* trying to find both new virulence traits of this opportunistic pathogen and new mechanisms responsible for its destruction. In previous works [17,18], we have studied the differential protein expression of RAW264.7 after 45 min of interaction with *C. albicans*. These studies allowed us to conclude that many processes were affected: cytoskeleton organization, signal transduction, metabolism, protein biosynthesis, stress response and protein fate. We observed a pro-inflammatory response that was very important at 3 h of incubation with the yeast. However, many of the protein spots that showed variation could not be identified, most of them, probably, because they were lower in abundance with respect to major proteins (metabolic proteins, for example). Thus, we decided to get different subcellular extracts: cytosol, organelle/membrane and nucleus and cytoskeleton enriched fractions. The analysis of the fractions by DIGE technology allowed the comparison of different biological replicates of the two studied conditions using less number of gels than in other classical approaches and with a pooled internal standard that makes easier the correct location of the spots. In this work, three fractions were analyzed in more detail: cytosol, organelle/membrane and nucleus, and some proteins were validated. The cytoskeleton fraction unraveled many differences between control and interacting macrophages but the amount of protein was insufficient for protein identification. This fraction is being extracted by more selective methods and analyzed by other proteomic techniques (Reales-Calderón et al., unpublished results).

4.1. *Differential protein expression*

Proteins that were identified are grouped regarding to their molecular function in Table 1. In this section, the hypothetical role of its variation during the interaction will be discussed.

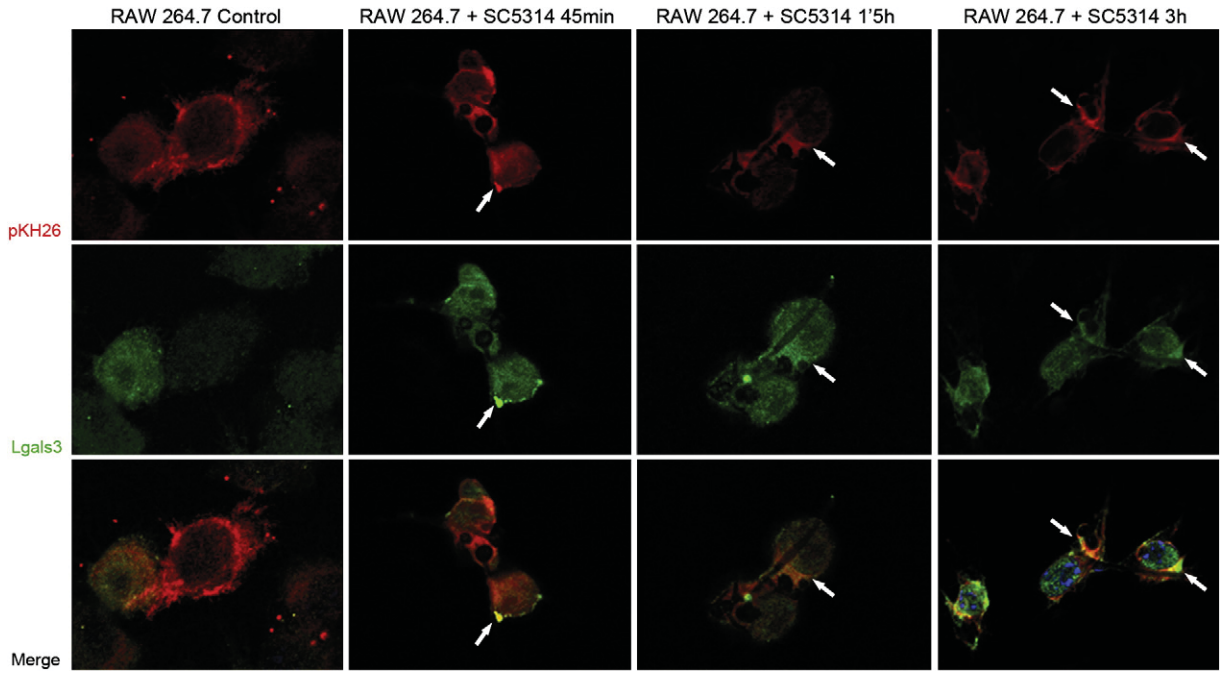

Fig. 5 – Co-localization of Galectin-3 with membranes of murine macrophages after interaction with *C. albicans*. Representative sections of control RAW 264.7 and after co-culture with the yeast at a 1:1 ratio. Membranes were stained using pKH26 dye (red) and Galectin-3 with anti-galectin-3 mAb (green) respectively. Blue color (DAPI) shows macrophage *nuclei*. Arrows point out to the co-localization of Galectin-3 with pKH26 (yellow).

4.1.1. *Increase in oxidative and pro-inflammatory responses*

As can be observed in Table 1, proteins related to oxidoreductase activity are decreased (Prdx1 and Pdia1), and this decrease can be responsible for increasing the oxidative level inside macrophages (Fig. 4). The cytosolic Peroxiredoxin 1 is the most abundant and ubiquitously distributed member of the mammalian Prdxs [31]. It is up-regulated by various oxidative stress stimuli [32–34] to protect against oxidative injury, thus its knock-down increases the ROS levels [35].

Another contribution to the oxidative stress inside macrophages, can be the increase in Uqcrc1p, a protein involved in the cellular red ox milieu, that increases as well in human lung carcinoma cells infected with *Mycoplasma pneumoniae* [36].

With respect to the effect on the inflammatory response, the decrease in Prdx1and Pdia1 can have a pro-inflammatory effect on RAW 264.7 macrophages, as it has been described that both proteins can suppress the NF-κB pathway and the consequent inflammatory response [37–40]. Also important are the decrease in Pdia6 [41] and Hspd1 [42] and the increase in Galectin-3 and Vimentin. Galectin-3 has been described as an important contributor to the development of a pro-inflammatory response to *C. albicans* [43] and to the increase in the oxidative response of macrophages [44]. The Vimentin increase in membranes contributes in a similar way to that of Galectin-3, as it has been described as surface exposed and secreted by activated human macrophages, and it has been involved in microorganism killing and in oxidative metabolite production [45].

On the other hand, there are anti-inflammatory signals, like the increase in Ptpn6 (SHP-1), a protein tyrosine phosphatase that acts as a negative regulator of both innate and acquired immune cytokine signaling [46], the decrease in Hspa5 [18,47], or the increase in Ptges3 levels [48].

As it has already been described for our model of interaction, pro-inflammatory signals are successful during the interaction [18].

4.1.2. *Pro and anti-apoptotic signals*

Apoptosis is a very important process for immune cells. For J774 macrophages, the induction of apoptosis by *C. albicans* phospholipomannan has been described [49], however in our model of interaction, RAW 264.7 macrophages display both pro and anti-apoptotic signals.

As anti-apoptotic signals, we can point out to the increase in Eef2p, Galectin-3 [50], Hnrph1, Pitpna and Vimentin. Vimentin is a substrate for caspases [51,52], however, when Jurkat cells are transformed with a caspase resistant Vimentin, these cells are more resistant to apoptosis [51,53]. The Pitpna overexpression significantly increased mouse fibroblast resistance to apoptosis [54]; Eef2p is required to maintain expression of the anti-apoptotic protein Mcl-1 [55], and Hnrph1 is necessary to block MST-2 apoptotic route in cancer cells [56]. All these results suggest an important anti-apoptotic tendency.

But, on the other hand, the variation of other proteins can be pointing out to an induction of the apoptotic routes. As it can be observed in Table 1, the proteins related to oxidoreductase activity (Prdx1 and Pdia1) and the ones related to stress response, above all the ER response ones (Napa and GRP78), are decreased. This fact is critical for the susceptibility of the

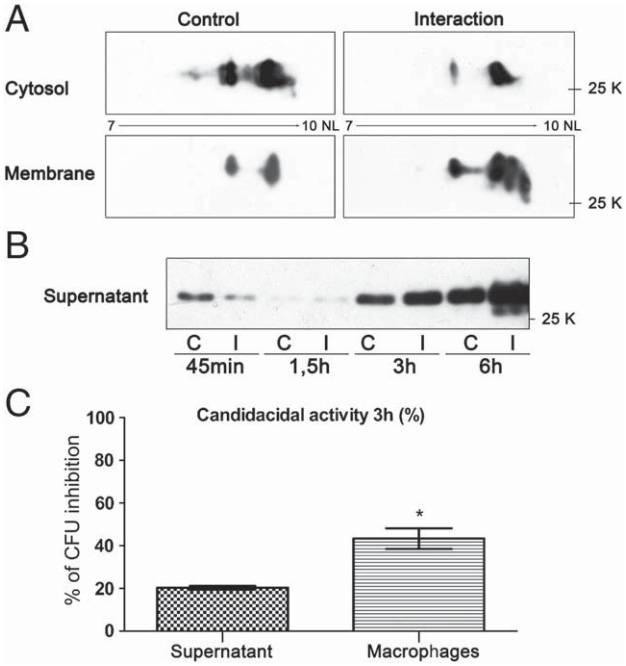

Fig. 6 – A) Galectin-3 expression in RAW 264.7 macrophages after the interaction with *C. albicans* in cytosol and organelle/membrane enriched fractions. Comparative 2D-PAGE western-blotting of Galectin-3 levels in cytosol and membrane enriched fractions. The image shows the section corresponding to Galectin-3 MW and pI. B) Galectin-3 secretion. Western-blotting analysis of Galectin-3 secretion in culture supernatant from control macrophages (C) and macrophages + *C. albicans* (I) at different times of interaction. C) Candidacidal activity of RAW 264.7 supernatants. The values in the y axis represent the percentage of *C. albicans* SC5314 CFU inhibition after 3 h of treatment with RAW 264.7 supernatant or after 3 h of interaction with RAW 264.7 macrophages with respect to untreated cells. The values are the mean ± S.D. of three independent experiments.

cells to apoptosis as it has been shown in several works: the decrease in Prdx1 and Pdia1 is increasing the susceptibility to ROS induced cell death [35] and the silencing of Napa contributes to apoptosis [57]. With respect to GRP78 (BiP, Hspa5), this protein is a member of the unfolded protein response pathway (UPR) and a marker for apoptotic cells [58,59].

Other protein variations that might be indicating apoptosis are the decrease in Isyna1, a protein required to suppress cell death in *Arabidopsis thaliana* [60]; the increase in Ptpn6 (SHP-1), that acts on inhibitors of JNK, thus positively regulating apoptosis [61] and the decrease in α-SNAP, whose knock-down sensitizes cells to apoptosis-inducing agents [62].

To reveal which signals take over during the interaction, experiments with antibody arrays (Panorama Cell Signalling Antibody Arrays, SIGMA) at different times of interaction (1, 3 and 6 h) have been done. Preliminary results show no increase in the caspases 3 and 9 activation at these times of interaction (data not shown). However, validation tests and further experiments with other apoptotic markers have to be done before reaching a conclusion.

4.1.3. *Effect on immune response*

A virulence trait of many pathogens is the inhibition of the immune response of the host cells. Our proteomic approach allowed us the detection of immunological processes that are the target for pathogen virulence factors. In our model of interaction, we have detected a decrease in Hsp90b1 (GP96), Pdia3, α-SNAP, GRP78 and Pdia1 (PDI), all of them necessary for the development of a correct immune response, and an increase in Ptpn6 (SHP-1), a negative controller of both innate and acquired immune cytokine signaling [46]. Hsp90b1 (GP96) acts as chaperone for TLR receptors in macrophages thus being necessary for the development of antimicrobial response [63], it has been described as a target for an intracellular bacteria, *Orientia tsutsugamushi* [64], thus, the same can be happening for *C. albicans*. Mutant mice lacking Pdia3 have defects in the MHC class I peptide-loading complex assembly [65], and GRP78 and Pdia1 seem to be necessary for antibody folding [66]. With respect to phagocytosis, the decrease in α-SNAP can be impairing the efficient fusion of phagosomes with the early endosomes [67].

On the other hand, many other proteins might be intensifying the immune response of macrophages: the increase in L-plastin (Lcp1) is crucial for the formation of lamellipodia, enabling T cell activation [68] and the increase in Galectin-3 levels, also involved in immune reactions (revised in [69]). Besides, as previously discussed, the pro-inflammatory and the oxidative stress responses are increased to destroy the pathogen.

4.1.4. *Increase in Galectin-3*

Galectin-3 is a lectin with important effects on immune cells: it is involved in inflammation, apoptosis, phagocytosis and adhesion to different molecules (revised in [69]). With respect to the interaction with *C. albicans*, Galectin-3 has already been described as a beta 1,2-linked oligomannosides adhesine [70], able to discriminate between *C. albicans* and *Saccharomyces cerevisiae*. It is overexpressed in macrophages in response to *C. albicans* [71] and it is necessary for the specific recognition of *C. albicans* both by mouse [72] and by human macrophages [73], contributing in the development of a pro-inflammatory response to *C. albicans* [43].

Our DIGE results showed an over-expression of Galectin-3 in cytoplasmic membrane, and, as the 2D-western blotting proved, there is a different distribution of the protein in response to *C. albicans* (Fig. 6A). Its secretion, although produced in control macrophages, is stimulated by the interaction with the yeast (Fig. 6B).

Also, the specific direct binding of Galectin-3 to *Candida* beta-1,2-linked oligomannosides has a candidacidal effect [30], thus, its secretion might be contributing to the total candidacidal activity of macrophages. In our experimental model, the supernatant itself has the 50% of the total candidacidal activity of RAW 264.7 macrophages (Fig. 6C), not only attributable to Galectin-3, but to the wide variety of substances with antimicrobial effect that macrophages secrete as well, as NO [11,12] or Vimentin [45].

5. Conclusions

This sub-proteomic approach has allowed us to identify 17 new proteins involved in the interaction of macrophages with *C. albicans* that were not detected in our previous studies.

First of all, few metabolic proteins have been identified among the differentially expressed, supporting the importance of analyzing sub-cellular fractions to detect variations in proteins that are less abundant than the metabolic ones. As already described, there is a significant decrease in proteins involved in ER stress response, thus affecting Unfolded Protein Response and protein transport; this effect could be a fungal virulence trait. It was not surprising to find a pro-inflammatory effect of many of the protein variations, an increase in the oxidative stress and in the cytoskeleton related proteins, as they are part of the phagocytic response. The effect of the protein variation on apoptosis will be studied in future works, as we found pro and anti-apoptotic signals. Mitochondrion is a very important structure that will deserve more studies. With the current approach, 2 mitochondrial proteins have been identified that could not be observed in total extracts. Besides, the study of different fractions allowed us to detect, not only the increase, but the distinct distribution of Galectin-3 along the interaction. To summarize, the subproteomic approach has been a very useful tool to identify new proteins involved in host defense against *C. albicans*.

Acknowledgments

Protein identification was carried out in the Proteomics Unit UCM-Parque Científico, a member of the National Institute for Proteomics, ProteoRed, funded by Genoma España. This work was supported by BIO 2009-07654 from the Comisión Interministerial de Ciencia y Tecnología (CYCIT, Spain), DEREMICROBIANA-CM and PROMT (S2010/BMD-2414) from the Comunidad Autónoma de Madrid, and REIPI, Spanish Network for the Research in Infectious Diseases, RD06/0008/1027, from the Instituto de Salud Carlos III and the Banco Santander Central Hispano-Universidad Complutense Research Group (UCM-920685). Dr. C. Nombela is the director of the Merck, Sharp & Dohme (MSD) Special Chair in Genomics and Proteomics.

Appendix A. Supplementary data

Supplementary data to this article can be found online at doi:10.1016/j.jprot.2012.01.037.

REFERENCES

[1] Pfaller MA, Yu WL. Antifungal susceptibility testing. New technology and clinical applications. Infect Dis Clin North Am 2001;15:1227–61.
[2] Pfaller MA, Diekema DJ. Epidemiology of invasive candidiasis: a persistent public health problem. Clin Microbiol Rev 2007;20:133–63.
[3] Vermes A, Guchelaar HJ, Dankert J. Flucytosine: a review of its pharmacology, clinical indications, pharmacokinetics, toxicity and drug interactions. J Antimicrob Chemother 2000;46:171–9.
[4] Bates DW, Su L, Yu DT, Chertow GM, Seger DL, Gomes DR, et al. Mortality and costs of acute renal failure associated with amphotericin B therapy. Clin Infect Dis 2001;32:686–93.
[5] Bistoni F, Vecchiarelli A, Cenci E, Puccetti P, Marconi P, Cassone A. Evidence for macrophage-mediated protection against lethal *Candida albicans* infection. Infect Immun 1986;51:668–74.
[6] Qian Q, Jutila MA, van Rooijen N, Cutler JE. Elimination of mouse splenic macrophages correlates with increased susceptibility to experimental disseminated candidiasis. J Immunol 1994;152:5000–8.
[7] Jouault T, Sarazin A, Martinez-Esparza M, Fradin C, Sendid B, Poulain D. Host responses to a versatile commensal: PAMPs and PRRs interplay leading to tolerance or infection by *Candida albicans*. Cell Microbiol 2009;11:1007–15.
[8] Netea MG, Marodi L. Innate immune mechanisms for recognition and uptake of *Candida* species. Trends Immunol 2010;31:346–53.
[9] Bourgeois C, Majer O, Frohner IE, Tierney L, Kuchler K. Fungal attacks on mammalian hosts: pathogen elimination requires sensing and tasting. Curr Opin Microbiol 2010;13:401–8.
[10] McGreal EP, Miller JL, Gordon S. Ligand recognition by antigen-presenting cell C-type lectin receptors. Curr Opin Immunol 2005;17:18–24.
[11] Chinen T, Qureshi MH, Koguchi Y, Kawakami K. *Candida albicans* suppresses nitric oxide (NO) production by interferon-gamma (IFN-gamma) and lipopolysaccharide (LPS)-stimulated murine peritoneal macrophages. Clin Exp Immunol 1999;115:491–7.
[12] Schroppel K, Kryk M, Herrmann M, Leberer E, Rollinghoff M, Bogdan C. Suppression of type 2 NO-synthase activity in macrophages by *Candida albicans*. Int J Med Microbiol 2001;290:659–68.
[13] Marodi L, Korchak HM, Johnston Jr RB. Mechanisms of host defense against *Candida* species. I. Phagocytosis by monocytes and monocyte-derived macrophages. J Immunol 1991;146:2783–9.
[14] Marodi L, Forehand JR, Johnston Jr RB. Mechanisms of host defense against *Candida* species. II. Biochemical basis for the killing of *Candida* by mononuclear phagocytes. J Immunol 1991;146:2790–4.
[15] Newman SL, Bhugra B, Holly A, Morris RE. Enhanced killing of *Candida albicans* by human macrophages adherent to type 1 collagen matrices via induction of phagolysosomal fusion. Infect Immun 2005;73:770–7.
[16] Vázquez-Torres A, Jones-Carson J, Balish E. Nitric oxide production does not directly increase macrophage candidacidal activity. Infect Immun 1995;63:1142–4.
[17] Martínez-Solano L, Nombela C, Molero G, Gil C. Differential protein expression of murine macrophages upon interaction with *Candida albicans*. Proteomics 2006;6(Suppl 1):S133–44.
[18] Martínez-Solano L, Reales-Calderón JA, Nombela C, Molero G, Gil C. Proteomics of RAW 264.7 macrophages upon interaction with heat-inactivated *Candida albicans* cells unravel an anti-inflammatory response. Proteomics 2009;9:2995–3010.
[19] Unlu M, Morgan ME, Minden JS. Difference gel electrophoresis: a single gel method for detecting changes in protein extracts. Electrophoresis 1997;18:2071–7.
[20] Kolkman A, Slijper M, Heck AJ. Development and application of proteomics technologies in *Saccharomyces cerevisiae*. Trends Biotechnol 2005;23:598–604.
[21] Gillum AM, Tsay EY, Kirsch DR. Isolation of the *Candida albicans* gene for orotidine-5′-phosphate decarboxylase by complementation of *S. cerevisiae ura3* and *E. coli pyrF* mutations. Mol Gen Genet 1984;198:179–82.
[22] Karp NA, McCormick PS, Russell MR, Lilley KS. Experimental and statistical considerations to avoid false conclusions in proteomics studies using differential in-gel electrophoresis. Mol Cell Proteomics 2007;6:1354–64.
[23] Sechi S, Chait BT. Modification of cysteine residues by alkylation. A tool in peptide mapping and protein identification. Anal Chem Dec 15 1998;70(24):5150–8.
[24] Vialás V, Nogales-Cadenas R, Nombela C, Pascual-Montano A, Gil C. Proteopathogen, a protein database for studying *Candida albicans*–host interaction. Proteomics 2009;9:4664–8.

[25] Diez-Orejas R, Molero G, Moro MA, Gil C, Nombela C, Sánchez-Pérez M. Two different NO-dependent mechanisms account for the low virulence of a non-mycelial morphological mutant of *Candida albicans*. Med Microbiol Immunol (Berl) 2001;189:153–60.
[26] Lin Q, Inselman A, Han X, Xu H, Zhang W, Handel MA, et al. Reductions in linker histone levels are tolerated in developing spermatocytes but cause changes in specific gene expression. J Biol Chem 2004;279:23525–35.
[27] Sano H, Hsu DK, Apgar JR, Yu L, Sharma BB, Kuwabara I, et al. Critical role of galectin-3 in phagocytosis by macrophages. J Clin Invest 2003;112:389–97.
[28] Hughes RC. Secretion of the galectin family of mammalian carbohydrate-binding proteins. Biochim Biophys Acta 1999;1473:172–85.
[29] Gong HC, Honjo Y, Nangia-Makker P, Hogan V, Mazurak N, Bresalier RS, et al. The NH2 terminus of galectin-3 governs cellular compartmentalization and functions in cancer cells. Cancer Res 1999;59:6239–45.
[30] Kohatsu L, Hsu DK, Jegalian AG, Liu FT, Baum LG. Galectin-3 induces death of *Candida* species expressing specific beta-1,2-linked mannans. J Immunol 2006;177:4718–26.
[31] Immenschuh S, Baumgart-Vogt E. Peroxiredoxins, oxidative stress, and cell proliferation. Antioxid Redox Signal 2005;7: 768–77.
[32] Bast A, Fischer K, Erttmann SF, Walther R. Induction of peroxiredoxin I gene expression by LPS involves the Src/PI3K/JNK signalling pathway. Biochim Biophys Acta 2010;1799:402–10.
[33] Ishii T, Yamada M, Sato H, Matsue M, Taketani S, Nakayama K, et al. Cloning and characterization of a 23-kDa stress-induced mouse peritoneal macrophage protein. J Biol Chem 1993;268: 18633–6.
[34] Sato H, Ishii T, Sugita Y, Tateishi N, Bannai S. Induction of a 23 kDa stress protein by oxidative and sulfhydryl-reactive agents in mouse peritoneal macrophages. Biochim Biophys Acta 1993;1148:127–32.
[35] Shan SW, Tang MK, Cai DQ, Chui YL, Chow PH, Grotewold L, et al. Comparative proteomic analysis identifies protein disulfide isomerase and peroxiredoxin 1 as new players involved in embryonic interdigital cell death. Dev Dyn 2005;233:266–81.
[36] Sun G, Xu X, Wang Y, Shen X, Chen Z, Yang J. *Mycoplasma pneumoniae* infection induces reactive oxygen species and DNA damage in A549 human lung carcinoma cells. Infect Immun 2008;76:4405–13.
[37] Rhee SG, Kang SW, Jeong W, Chang TS, Yang KS, Woo HA. Intracellular messenger function of hydrogen peroxide and its regulation by peroxiredoxins. Curr Opin Cell Biol 2005;17: 183–9.
[38] Kisucka J, Chauhan AK, Patten IS, Yesilaltay A, Neumann C, Van Etten RA, et al. Peroxiredoxin1 prevents excessive endothelial activation and early atherosclerosis. Circ Res 2008;103: 598–605.
[39] Higuchi T, Watanabe Y, Waga I. Protein disulfide isomerase suppresses the transcriptional activity of NF-kappaB. Biochem Biophys Res Commun 2004;318:46–52.
[40] Hansen JM, Moriarty-Craige S, Jones DP. Nuclear and cytoplasmic peroxiredoxin-1 differentially regulate NF-kappaB activities. Free Radic Biol Med 2007;43:282–8.
[41] Gumireddy K, Sun F, Klein-Szanto AJ, Gibbins JM, Gimotty PA, Saunders AJ, et al. In vivo selection for metastasis promoting genes in the mouse. Proc Natl Acad Sci U S A 2007;104: 6696–701.
[42] Hsieh SY, Shih TC, Yeh CY, Lin CJ, Chou YY, Lee YS. Comparative proteomic studies on the pathogenesis of human ulcerative colitis. Proteomics 2006;6:5322–31.
[43] Jawhara S, Thuru X, Standaert-Vitse A, Jouault T, Mordon S, Sendid B, et al. Colonization of mice by *Candida albicans* is promoted by chemically induced colitis and augments inflammatory responses through galectin-3. J Infect Dis 2008;197:972–80.
[44] Liu FT, Hsu DK, Zuberi RI, Kuwabara I, Chi EY, Henderson Jr WR. Expression and function of galectin-3, a beta-galactoside-binding lectin, in human monocytes and macrophages. Am J Pathol 1995;147:1016–28.
[45] Mor-Vaknin N, Punturieri A, Sitwala K, Markovitz DM. Vimentin is secreted by activated macrophages. Nat Cell Biol 2003;5:59–63.
[46] Christophi GP, Hudson CA, Panos M, Gruber RC, Massa PT. Modulation of macrophage infiltration and inflammatory activity by the phosphatase SHP-1 in virus-induced demyelinating disease. J Virol 2009;83:522–39.
[47] Niu J, Azfer A, Rogers LM, Wang X, Kolattukudy PE. Cardioprotective effects of cerium oxide nanoparticles in a transgenic murine model of cardiomyopathy. Cardiovasc Res 2007;73: 549–59.
[48] Nakatani Y, Hokonohara Y, Tajima Y, Kudo I, Hara S. Involvement of the constitutive prostaglandin E synthase cPGES/p23 in expression of an initial prostaglandin E2 inactivating enzyme, 15-PGDH. Prostaglandins Other Lipid Mediat 2011;94:112–7.
[49] Ibata-Ombetta S, Idziorek T, Trinel PA, Poulain D, Jouault T. *Candida albicans* phospholipomannan promotes survival of phagocytosed yeasts through modulation of bad phosphorylation and macrophage apoptosis. J Biol Chem 2003;278:13086–93.
[50] Hsu DK, Yang RY, Pan Z, Yu L, Salomon DR, Fung-Leung WP, et al. Targeted disruption of the galectin-3 gene results in attenuated peritoneal inflammatory responses. Am J Pathol 2000;156:1073–83.
[51] Morishima N. Changes in nuclear morphology during apoptosis correlate with vimentin cleavage by different caspases located either upstream or downstream of Bcl-2 action. Genes Cells 1999;4:401–14.
[52] Nakanishi K, Maruyama M, Shibata T, Morishima N. Identification of a caspase-9 substrate and detection of its cleavage in programmed cell death during mouse development. J Biol Chem 2001;276:41237–44.
[53] Belichenko I, Morishima N, Separovic D. Caspase-resistant vimentin suppresses apoptosis after photodynamic treatment with a silicon phthalocyanine in Jurkat cells. Arch Biochem Biophys 2001;390:57–63.
[54] Schenning M, van Tiel CM, Van Manen D, Stam JC, Gadella BM, Wirtz KW, et al. Phosphatidylinositol transfer protein alpha regulates growth and apoptosis of NIH3T3 cells: involvement of a cannabinoid 1-like receptor. J Lipid Res 2004;45:1555–64.
[55] Bewley MA, Pham TK, Marriott HM, Noirel J, Chu HP, Ow SY, et al. Proteomic evaluation and validation of cathepsin D regulated proteins in macrophages exposed to *Streptococcus pneumoniae*. Mol Cell Proteomics 2011;10 M111.008193.
[56] Veraldi KL, Arhin GK, Martincic K, Chung-Ganster LH, Wilusz J, Milcarek C. hnRNP F influences binding of a 64-kilodalton subunit of cleavage stimulation factor to mRNA precursors in mouse B cells. Mol Cell Biol 2001;21:1228–38.
[57] Wu ZZ, Chao CC. Knockdown of NAPA using short-hairpin RNA sensitizes cancer cells to cisplatin: implications to overcome chemoresistance. Biochem Pharmacol 2010;80: 827–37.
[58] Misra UK, Pizzo SV. Up-regulation of GRP78 and antiapoptotic signaling in murine peritoneal macrophages exposed to insulin. J Leukoc Biol 2005;78:187–94.
[59] Miyake H, Hara I, Arakawa S, Kamidono S. Stress protein GRP78 prevents apoptosis induced by calcium ionophore, ionomycin, but not by glycosylation inhibitor, tunicamycin, in human prostate cancer cells. J Cell Biochem 2000;77: 396–408.
[60] Donahue JL, Alford SR, Torabinejad J, Kerwin RE, Nourbakhsh A, Ray WK, et al. The *Arabidopsis thaliana* Myo-inositol 1-phosphate synthase1 gene is required for Myo-inositol

synthesis and suppression of cell death. Plant Cell 2010;22: 888–903.
[61] Mizuno K, Tagawa Y, Mitomo K, Watanabe N, Katagiri T, Ogimoto M, et al. Src homology region 2 domain-containing phosphatase 1 positively regulates B cell receptor-induced apoptosis by modulating association of B cell linker protein with Nck and activation of c-Jun NH2-terminal kinase. J Immunol 2002;169:778–86.
[62] Wu ZZ, Chao CC. Knockdown of NAPA using short-hairpin RNA sensitizes cancer cells to cisplatin: implications to overcome chemoresistance. Biochem Pharmacol 2010;80(6):827–37.
[63] Yang Y, Liu B, Dai J, Srivastava PK, Zammit DJ, Lefrancois L, et al. Heat shock protein gp96 is a master chaperone for toll-like receptors and is important in the innate function of macrophages. Immunity 2007;26:215–26.
[64] Cho NH, Choi CY, Seong SY. Down-regulation of gp96 by *Orientia tsutsugamushi*. Microbiol Immunol 2004;48:297–305.
[65] Garbi N, Hammerling G, Tanaka S. Interaction of ERp57 and tapasin in the generation of MHC class I-peptide complexes. Curr Opin Immunol 2007;19:99–105.
[66] Mayer M, Kies U, Kammermeier R, Buchner J. BiP and PDI cooperate in the oxidative folding of antibodies in vitro. J Biol Chem 2000;275:29421–5.
[67] Mukherjee K, Siddiqi SA, Hashim S, Raje M, Basu SK, Mukhopadhyay A. Live *Salmonella* recruits N-ethylmaleimide-sensitive fusion protein on phagosomal membrane and promotes fusion with early endosome. J Cell Biol 2000;148:741–53.
[68] Wang C, Morley SC, Donermeyer D, Peng I, Lee WP, Devoss J, et al. Actin-bundling protein L-plastin regulates T cell activation. J Immunol 2010;185:7487–97.
[69] Dumic J, Dabelic S, Flogel M. Galectin-3: an open-ended story. Biochim Biophys Acta 2006;1760:616–35.
[70] Fradin C, Poulain D, Jouault T. Beta-1,2-linked oligomannosides from *Candida albicans* bind to a 32-kilodalton macrophage membrane protein homologous to the mammalian lectin galectin-3. Infect Immun 2000;68:4391–8.
[71] Shin YK, Lee HJ, Lee JS, Paik YK. Proteomic analysis of mammalian basic proteins by liquid-based two-dimensional column chromatography. Proteomics 2006;6:1143–50.
[72] Jouault T, El Abed-El Behi M, Martinez-Esparza M, Breuilh L, Trinel PA, Chamaillard M, et al. Specific recognition of *Candida albicans* by macrophages requires galectin-3 to discriminate *Saccharomyces cerevisiae* and needs association with TLR2 for signaling. J Immunol 2006;177:4679–87.
[73] Esteban A, Popp MW, Vyas VK, Strijbis K, Ploegh HL, Fink GR. Fungal recognition is mediated by the association of dectin-1 and galectin-3 in macrophages. Proc Natl Acad Sci U S A 2011;108:14270–5.

SUPPLEMENTAL MATERIAL

Supplemental Figure S1:

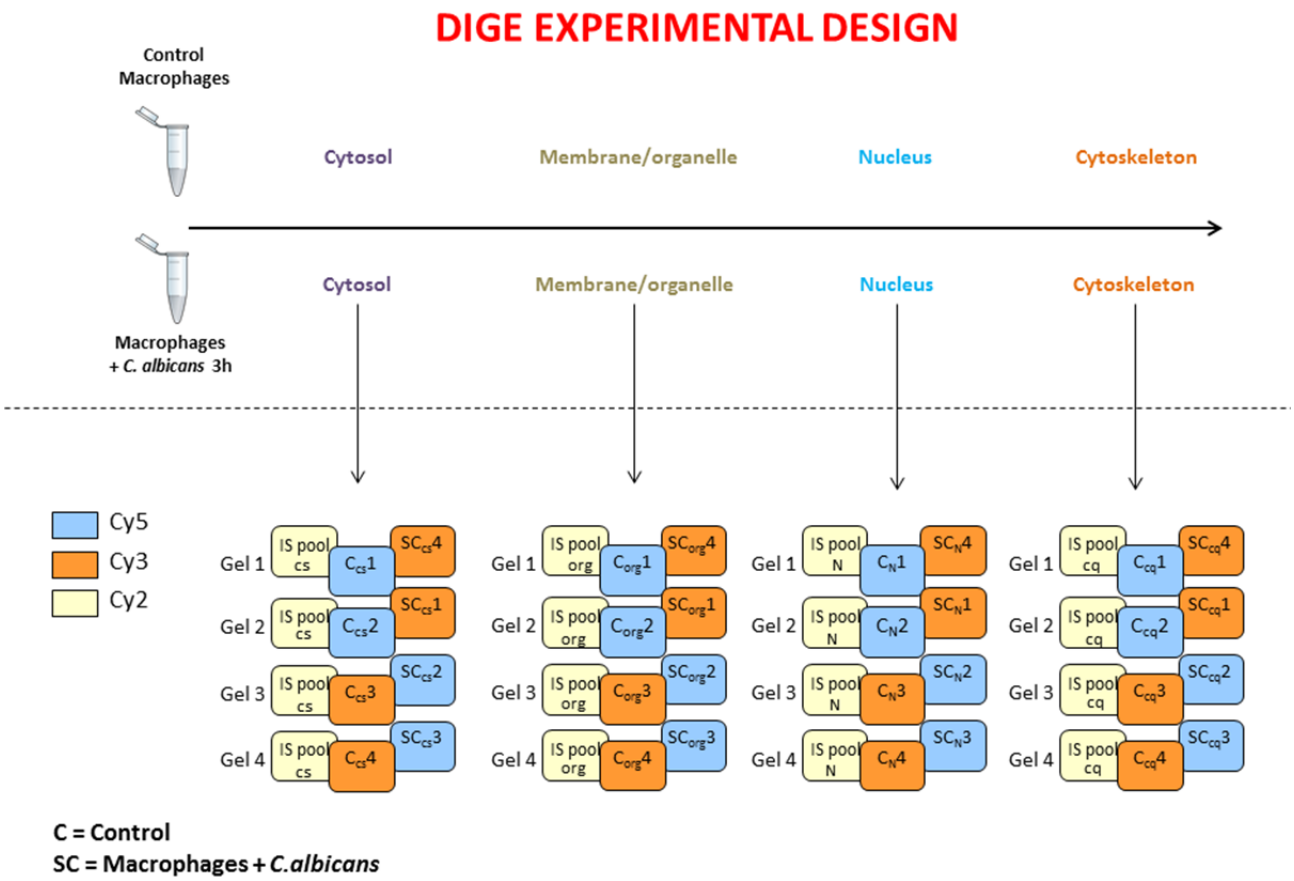

Fig. S.1. **Experimental design for the DIGE experiments.**

Supplemental Figure S2:

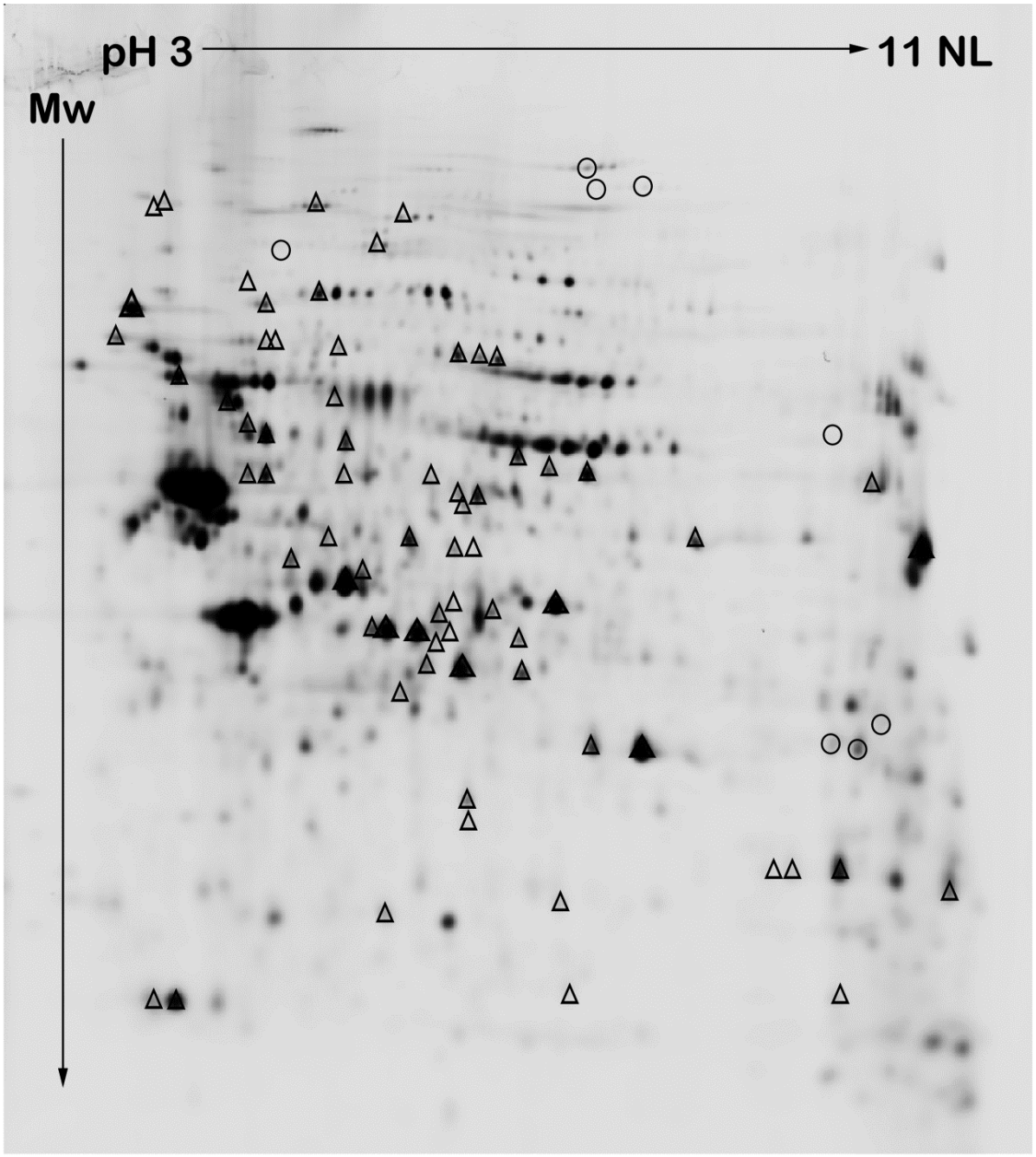

Fig. S.2. Representative 2-DE of cytoskeleton enriched fraction of RAW 264.7 cells after interaction with *C. albicans*. Proteins were resolved in the 3–11 (non linear) pH range on the first dimension, and on 10% polyacrylamide gels on the second dimension. Circled spots matched with down-expressed proteins after the interaction with the fungus and spots included into triangles matched with overexpressed proteins.

Addendum

CYTOSKELETAL CHANGES IN MACROPHAGES IN RESPONSE TO *C. albicans*

INTRODUCTION

The recognition of *Candida albicans* and it's phagocytosis by macrophages causes the activation of different proinflammatory pathways and a variety of morphological changes to catch and contain *C. albicans*. Phagocytosis comprises multiple events: particle binding, actin assembly, membrane remodelling, and pseudopod extension and phagosomes closure.

Previous studies in our group using murine macrophage cell line RAW 264.7 have described a wide variety of changes in the cytoskeletal proteins of macrophages after 45 min and 3h of interaction with the yeast [1-3]. However, although more than 70 spots with differential expresión between control and interacting macrophages where shown in the cytoskeletal enriched fraction [1], proteins couldn't be identified because of the low amount of protein obtained by this technique.

The cytoskeleton is a cellular "skeleton" and its dynamic structure maintains cell shape, enables cellular motion, intracellular transport, cellular division, phagocytosis, and membrane organization. Eukaryotic cells contain three main types of cytoskeletal filaments: microfilaments, intermediate filaments, and microtubules, composed mainly of actin, vimentin, and tubulin, respectively.

The objective of the present study was to improve the cytoskeleton extraction to identify the constituents of the macrophage cytoskeleton by proteomic profiling and their changes upon interaction with *C. albicans*.

Several subproteomic methods have been described as useful to isolate cytoskeletal proteins, using specifics kits and buffers, however most of them had a slight enrichment in the proteins of interest. For the present study, we chose a technique described by Funchal *et al* [4] that uses two buffers (Low-salt (LS) and High-salt (HS)) to isolate different cytoskeletal fractions. The Low Salt Buffer allows the isolation of proteins from intermediate filaments, tubulins, actin and cytoskeletal associated proteins, while with the treatment with High Salt Buffer produces enrichment in intermediate filaments and associated proteins. The fractions obtained showed an important increase in the percentage of cytoskeletal and cytoskeletal-related proteins, allowing us the quantitative analysis of macrophage cytoskeleton response to *C. albicans* infection.

EXPERIMENTAL PROCEDURES

Candida albicans strains

C. albicans SC5314 was the strain used in this study, from a clinical isolate [5]. This strain was maintained on solid YED medium (1% D-glucose, 1% Difco Yeast Extract and 2% agar) and incubated at 30ºC for at least 2 days. Blue Fluorescent Protein-expressing *C. albicans* (*Candida*-BFP) used for confocal microscopy studies was described by Strijbis *et a*l [6].

Culture medium and reagents

RPMI 1640 medium, fetal bovine serum (FBS), L-glutamine, and antibiotics (penicillin-streptomycin) were obtained from GIBCO BRL (Grand Island,

N.Y.). Cell-line macrophages were resuspended in RPMI supplemented with glutamine (2mM), antibiotics (penicillin 100U/ml-streptomycin 100 µg/ml), and 10% heat-inactivated fetal bovine serum (complete medium).

Macrophage cell line

The RAW 264.7 gamma NO (-) cell line was obtained from the American Type Culture Collection (Rockville, Md.). Cells were grown in complete medium in a 5% CO_2 incubator at 37ºC and maintained at low densities (75% confluence) and passaged until reaching the confluent state, usually every 3-4 days on sterile culture plates.

Preparation cytoskeletal samples

3 replicas of control RAW 264.7 macrophages and after 3h of interaction with *C. albicans* SC5314 (ratio 1:1) were obtained with two different buffers: High-Salt and Low-Salt buffers.

- ***High-Salt Buffer***

After the interaction, $25x10^7$ control and stimulated macrophages were washed with PBS and then, lysed in 1 ml of ice-cold HS buffer (5 mM KH_2PO_4, 600 mM KCl, 10 mM $MgCl_2$, 2 mM EGTA and 1 mM EDTA (pH 7.4), 1% Triton X-100 and 1:1000 protease inhibitor cocktail). The pH was adjusted to 7.1 with 1 M Na_2HPO_4) and used for the cytoskeletal fraction extraction. After 10 min at 4ºC, lysates were centrifuged at 15000g for 10 min at 4ºC. The insoluble material was resuspended in 500 µl of ice-cold HS buffer, extracted and centrifuged as above.

The pellet obtained was a cytoskeletal fraction enriched in intermediate filaments and associated proteins.

- ***Low-Salt Buffer***

$25x10^7$ macrophages control and after the interaction with *C. albicans*, were washed with PBS and then lysed in 1 ml of ice-cold LS buffer A (50 mM Tris-HCl (pH 7.4), 5 mM EGTA, 1% Triton X-100 and 1:1000 protease inhibitors cocktail) during 10 min at 4ºC. Then, samples were centrifuged at 15000g for 10 min at 4ºC. The insoluble material was resuspended in 500 µl of ice-cold LS buffer B (50 mM Tris-HCl (pH 7.4), 5 mM EGTA, 1% Triton X-100, 0.85 M sucrose and 1:1000 protease inhibitors cocktail). After 10 min in ice, the pellet was separated by centrifugation at 15000g for 10 min at 4ºC.

The pellet obtained was a cytoskeletal fraction containing intermediate filament proteins, tubulins, actin and cytoskeletal associated proteins.

- ***Cytoskeletal proteins solubilization***

Pellets from both buffers were dissolved in 200 µl of MES buffer (50 mM MES ([N-morpholino] ethanesulfonic acid), 10 mM $MgCl_2$ and 1:1000 protease inhibitors cocktail, pH 6.5).

The protein concentrations of the cell lysates were determined by using RC-DC assay (BioRad).

Protein digestion

250 µg of each sample were reduced by adding 25 mM DTT for 30 min at 60ºC. Then, samples were loaded into an Amicon (Nanosep 10K Omega; Pall Corporation) and centrifuged for 45 min at 12000*g*. Samples were washed twice with DB2 (20mM TEAB, 0.5% Sodium Deoxycolate) and alkylated with 50 mM Iodoacetamide during 20 min in the dark. After two washes with DB2, digestion was started by adding Trypsin (Promega) 1:100. After 4h in the dark at RT in wet atmosphere, peptides were collected into a clean collection tube and the amicon was washed with DB2 and collected the flow-through. Samples were acidified with 0,5% TFA final, and SCD-precipitates forms were separated by centrifugation 5 min at 16000*g*.

Mass Spectrometric Analysis Using a Linear Ion Trap (LTQ)

Protein identification was done at the Proteomics Facility of Universidad Complutense de Madrid-Parque Científico de Madrid, Spain (UCM-PCM), a member of ProteoRed Network.

Digested peptides were analyzed by LC-MS/MS using a Surveyor LC system coupled to a linear ion trap mass spectrometer (model LTQ, Thermo Electron, San Jose, CA). Peptides were concentrated and desalted onto an RP trap column (PepMap C18 µ-precolumn, 300 mm id × 1 mm; Dionex, Amsterdam, The Netherlands) for 5 min and eluted online onto an RP analytical column (Biobasic C18, 0.18 id × 150 mm, Thermo Electron) operating at 2 µL/min and using the following gradient: 5% B for 3 min, 5-70% B for 60 min and 95% B for 5 min (solvent A: 0.1% formic acid, 2% acetonitrile; solvent B: 0.1% formic acid, 80% acetonitrile). The LTQ was operated in data-dependent MS experiments: full-scan MS (400-1600 m/z) plus top five peaks Zoom/MS/ MS (isolation width 2 m/z), normalized collision energy 35%.

The scanning was performed using a dynamic exclusion list (60 s exclusion list size of 50 and exclusion width of 2.5 m/z).

Database search

Bioworks 3.2 software (Thermo Electron) was used Swiss-Prot release 53.0 (http://www.expasy.ch/sprot) and TrEMBL release 37.0 (http://www.ebi.ac.uk/trembl) databases without taxonomy restriction, containing 269293 and 4672908 sequence entries respectively for each software version and database release. The following database search parameters were used: peptide tolerance, 2 Da; fragment ion tolerance, 1 Da; missed cleavage sites, 1.0; fixed modification, carbamidomethyl cysteine and variable modifications, methionine oxidation. A peptide probability of 10-3 and the crossing correlation score (Xcorr) of 2.0 (+2), 2.5 (+3) were used as cutoff filters. To estimate the false positive rate (FDR) a search in the decoy database was performed.

Confocal Microscopy

$2x10^5$ RAW 264.7 macrophages were grown on glass coverslips onto a p12 plate and treated with *C. albicans* for 3h. The coverslips were fixed with 4% formaldehyde in PBS for 20 min at RT, washed twice with PBS and cell membranes were permeabilized for 15 min with PBS containing 0.2% Tween-20 at room temperature. After two washes with PBS, the coverslips were incubated with Binding Buffer (0.1% Saponin, 0.2% BSA in PBS) for 30 min and overlaid with Anti-Vimentin or Anti-Moesin antibody (Sigma-Aldrich, diluted 1:1000), incubated for 1h, washed with Binding Buffer three times and incubated for 1h with Alexa Fluor 568 anti-rabbit and with 1/2000 Phalloidin FITC (Sigma-Aldrich), washed with Binding Buffer three times and prepared for microscopy by mounting them on slides in 50% glycerol.

Confocal images were collected in the W. M. Keck Facility for Biological Imagining using a PerkinElmer Live Cell imaging spinning disk confocal system mounted on a Zeiss Axiovert 200M with a 63x and 100x 1.4NA oil immersion objectives. Excitation light was generated by gas and solid state laser (Argon laser for 488 nm, Krypton laser for 568nm, solid state laser for 405 nm and 647 nm) and passed through an AOFT for wavelength selection and laser power control. A quadrupole bandpass filter separated the excitation and emission light inside the CSU-22 confocal scanhead (Yokogawa) and a filter wheel (Prior Scientific) provided selection of emission Filters (TagBFP & RFP: dual band 445/60 and 615/70 nm; GFP: 527/55 nm).

Volocity image acquisition software was used to capture images from a Hamamatsu Orca-ER cooled-CCD camera and to control the equipment.

RESULTS AND DISCUSSION

Cytoskeleton constitutes a dynamic compound in macrophages during infection. Cytoskeletal and cytoskeletal-associated proteins are implicated in the polymerization/depolymerization of the cytoskeletal constituents, crucial for cell function.

In this study we chose the best procedures to study the changes in macrophage cytoskeleton during *C. albicans* infection. Two different Triton insoluble fractions, HS (containing intermediate filament subunits and vimentin) and LS (tubulins, actins and intermediate filaments), were extracted and analysed by MS/MS to obtain the whole map of cytoskeletal and cytoskeletal-related proteins.

RAW 264.7 macrophages cytoskeleton enrichment

Control RAW 264.7 macrophages and after 3h of interaction with *C. albicans* SC5314 cells at a 1:1 ratio, were treated as described in Materials and Methods to obtain 2 different and complementary enriched cytoskeletal samples: high-salt and low-salt. These samples were analysed separately by MS/MS to identify cytoskeletal proteins.

- **Identification of cytoskeletal proteins**

For protein identification, samples were digested in-solution and analysed by MALDI-TOF-MS. Mascot database search using the peptide mass fingerprint spectra allowed the identification of the proteins in 137 proteins in high-salt and low-salt control samples and 125 proteins in high-salt and low-salt treated samples.

A database search was carried out to analyse their relation with the cytoskeleton. As it can be observed in Tables 1-4, HS buffer had a higher number of cytoskeletal related proteins than LS buffer, and after interaction there was an increase in the number and percentage of cytoskeletal proteins, such as it was already observed in our previous work [1].

Analysis of cytoskeletal fractions from RAW 264.7 control and after *C. albicans* interaction

As it has already been stated, with this extraction procedure more than the 30% of the proteins identified was cytoskeleton related.

Along these extractions, we had differences with respect to the quantity of protein yield. While when using LS buffer the same number of control and interacting macrophages rendered the same protein amount, when the extraction was done with HS buffer, the interacting macrophages rendered almost 50% more protein amount than the control macrophages. This fact might be due to the presence of *C. albicans* proteins associated to cytoskeletal macrophage proteins, although the viability of the yeast cells after the interaction and present in the pellet extraction was checked by CFU counting and it was more than 99% of viability. When searching for *Candida* proteins in the HS fraction, only around 10% of the total proteins were from the yeast. Thus, the increases in the amount of cytoskeletal proteins in our extract after the interaction were mainly due to macrophage proteins, not to the yeast ones.

In LS samples, increases in proteins related to Actin polymerization, such as Capza1, Capza2, Capzb and Cofilin, were detected, all these proteins playing an important role during cytoskeleton assembly.

The same happened in the HS samples, where Cof1, Cof2 and Capza were identified only in the samples with *Candida*.

Table I: Macrophage cytoskeletal proteins identified in Low-Salt control sample.

Protein ID	Swiss Prot	Protein Name	Score	% Cov	Nº Pept
		CYTOSKELETON			
Acta1	P68134	Actin, alpha skeletal muscle	100.27	29.20	46
Actb	Q8BFZ3	Actin, cytoplasmic 1	124.38	36.30	31
Actbl2	Q8BFZ3	Beta-actin-like protein 2	8.21	4.80	3
Actg1	Q9QZ83	Gamma actin-like protein	30.33	5.60	4
Actl6a	Q9Z2N8	Actin-like protein 6A	20.33	10.00	2
Actr2	P61161	Actin-related protein 2	10.28	4.30	2
Actr3	Q99JY9	Actin-related protein 3	20.25	6.50	2
Capzb	P47757	Isoform 2 of F-actin-capping protein subunit beta	10.20	7.40	1
Des	P31001	Desmin	10.23	2.60	1
Krt1	P04104	Keratin, type II cytoskeletal 1	10.17	1.90	1
Krt8	P11679	Keratin, type II cytoskeletal 8	8.16	2.40	1
Lamb1-1	P02469	laminin B1 subunit 1	10.20	0.80	1
Lbr	Q3U9G9	Lamin-B receptor	10.26	2.40	1
Lmna	P48678-3	Isoform C2 of Lamin-A/C	40.29	14.70	5
Lmnb1	P14733	Lamin-B1	10.29	4.10	1
Mybbp1a	Q7TPV4	Myb-binding protein 1A	50.34	6.20	1
Myh9	Q8VDD5	Myosin-9	10.27	1.00	1
Npm1	Q61937	Nucleophosmin	30.32	14.00	3
Plec1	Q9QXS1-16	Isoform PLEC-1I of Plectin-1	20.31	0.90	1
Prph	P15331-1	Isoform 5g of Peripherin	10.19	2.10	1
Tubb2b	Q9CWF2	Tubulin beta-2B chain	10.37	5.80	1
Vim	P20152	Vimentin	130.25	24.00	22
		RELATED TO CYTOSKELETON			
Eef1a1	P10126	Elongation factor 1-alpha 1	30.24	13.90	3
Eef1a2	P62631	Elongation factor 1-alpha 2	30.38	11.20	3
Hspa8	P63017	Heat shock cognate 71 kDa protein	20.25	5.70	1

Table II: Macrophage cytoskeletal proteins identified in Low-Salt sample (after the interaction).

Protein ID	Swiss Prot	Protein Name	Score	% Cov	Nº Pept
		CYTOSKELETON			
Acta1	P68134	Actin, alpha skeletal muscle	110.33	31.80	47
Actb	Q8BFZ3	Actin, cytoplasmic 1	48.34	27.20	21
Actbl2	Q8BFZ3	Beta-actin-like protein 2	18.27	9.00	6
Actg1	Q9QZ83	Gamma actin-like protein	10.29	5.30	2
Actl6a	Q9Z2N8	Actin-like protein 6A	20.25	7.20	4
Arpc3	Q9JM76	Actin-related protein 2/3 complex subunit 3	10.17	7.30	1
Capza1	P47753	F-actin-capping protein subunit alpha-1	20.17	12.20	2
Capza2	P47754	F-actin-capping protein subunit alpha-2	10.25	5.90	2
Capzb	P47757-2	Isoform 2 of F-actin-capping protein subunit beta	60.28	26.10	9
Cfl1	Q9CX22	Cofilin 1	10.16	4.80	1
Dstn	Q9R0P5	Destrin	10.22	9.70	1
Dync2h1	Q45VK7-1	Isoform 1 of Cytoplasmic dynein 2 heavy chain 1	8.15	0.40	1
EG620772	IPI00409405.2	Similar to Cofilin-1 isoform 1	10.20	8.40	5
Krt1	P04104	Keratin, type II cytoskeletal 1	50.32	12.90	6
Krt10	P02535-3	keratin complex 1, acidic, gene 10	20.23	4.50	4
Krt13	P08730-1	Isoform 1 of Keratin, type I cytoskeletal 13	10.18	2.50	2
Krt14	Q61781	Keratin, type I cytoskeletal 14	10.22	2.50	1
Krt16	Q3ZAW8	Keratin intermediate filament 16a	10.23	2.30	1
Krt42	Q6IFX2	Keratin, type I cytoskeletal 42	10.23	2.70	2
Krt5	Q922U2	Keratin, type II cytoskeletal 5	10.20	2.10	1
Krt6a	P50446	Keratin, type II cytoskeletal 6A	10.14	2.00	1
Krt73	Q6NXH9	Keratin, type II cytoskeletal 73	10.23	2.20	4
Krt78	A1L0X5	keratin Kb40	10.19	1.10	8
Krt79	Q8VED5	Keratin, type II cytoskeletal 79	10.23	2.30	4
Krt8	P11679	Keratin, type II cytoskeletal 8	8.21	2.40	11
Msn	P26041	Moesin	10.12	1.60	1
Plec1	Q9QXS1-16	Isoform PLEC-1I of Plectin-1	10.14	0.30	1
Rpgrip1	Q9EPQ2-5	Isoform 5 of X-linked retinitis pigmentosa GTPase regulator-interacting protein 1	10.12	4.70	1
Ssx2ip	Q8VC66	Afadin- and alpha-actinin-binding protein	10.17	2.30	1
Twf1	Q91YR1	Twinfilin-1	20.22	6.30	3
Twf2	Q9Z0P5-1	Isoform 1 of Twinfilin-2	20.26	7.20	2
Vasp	P70460	Vasodilator-stimulated phosphoprotein	10.23	6.70	1
		RELATED TO CYTOSKELETON			
Adamts9	Q69ZM2	Disintegrin-like and metalloprotease with thrombospondin type 1 motif, 9	10.14	1.00	1
Arhgap12	Q8C0D4	Rho GTPase-activating protein 12	2.13	2.30	1
Ccdc79	IPI00881545.1	38 kDa protein	10.13	5.60	1
Hspa1l	P16627	Heat shock 70 kDa protein 1L	20.26	4.50	13
Hspa5	P20029	78 kDa glucose-regulated protein precursor	100.26	20.30	30
Hspa8	P63017	Heat shock cognate 71 kDa protein	168.26	23.70	39
Hspa9	P38647	Stress-70 protein, mitochondrial precursor	10.20	1.80	1
Sdccag10	Q3TKY6	Peptidyl-prolyl cis-trans isomerase SDCCAG10	10.18	5.10	1
Slc25a4	P48962	ADP/ATP translocase 1	10.19	4.00	2
Tns3	Q5SSZ5-1	Isoform 1 of Tensin-3	4.15	1.20	1
Trim25	Q61510	Tripartite motif-containing protein 25	8.22	3.00	1

Table III: Macrophage cytoskeletal proteins identified in High-Salt control sample.

Protein ID	Swiss Prot	Protein Name	Score	% Cov	Nº Pept
		CYTOSKELETON			
Acta1	P68134	Actin, alpha skeletal muscle	20.24	7.2	7
Actb	Q8BFZ3	Actin, cytoplasmic 1	68.35	26.9	13
Actbl2	Q8BFZ3	Beta-actin-like protein 2	8.20	4.8	2
Ctsd	P18242	Cathepsin D precursor	10.29	4.4	2
Krt1	P04104	Keratin, type II cytoskeletal 1	10.21	2.1	1
Krt10	P02535-3	keratin complex 1, acidic, gene 10	20.21	4.5	10
Krt13	P08730-1	Isoform 1 of Keratin, type I cytoskeletal 13	10.16	2.5	1
Krt16	Q3ZAW8	Keratin intermediate filament 16a	10.22		1
Krt42	Q6IFX2	Keratin, type I cytoskeletal 42	10.21	2.7	1
Krt6b	Q9Z331	Keratin, type II cytoskeletal 6B	10.21	2.1	1
Krt73	Q6NXH9	Keratin, type II cytoskeletal 73	10.23	2.2	3
Krt78	A1L0X5	keratin Kb40	10.23	1.1	3
Krt79	Q8VED5	Keratin, type II cytoskeletal 79	10.23	2.3	1
Krt8	P11679	Keratin, type II cytoskeletal 8	8.23	2.4	3
Mybbp1a	Q7TPV4	Myb-binding protein 1A	20.17	1.9	2
Nexn	Q7TPW1	Nexilin	10.14	2.5	1
Npm1	Q61937	Nucleophosmin	10.24	7.2	1
Tuba1a	P68369	Tubulin alpha-1A chain	10.18	2.3	2
Tubb2b	Q9CWF2	Tubulin beta-2B chain	30.24	8.3	4
Tubb4	Q9D6F9	Tubulin beta-4 chain	10.20	2.7	1
Tubb5	P99024	Tubulin beta-5 chain	10.26	3.8	1
Vdac2	Q60930	Voltage-dependent anion-selective channel protein 2	10.14	1.3	1
Vim	P20152	Vimentin	30.25	9.2	3
		RELATED TO CYTOSKELETON			
Eef1a2	P62631	Elongation factor 1-alpha 2	10.37	6.3	2
Eef1g	Q9D8N0	Elongation factor 1-gamma	10.23	3	1
Eef2	P58252	Elongation factor 2	8.15	2.2	1
Hsp90aa1	P07901	Heat shock protein HSP 90-alpha	10.19	1.8	1
Hsp90ab1	Q71LX8	Heat shock protein 84b	30.25	5.7	4
Hsp90b1	P08113	Endoplasmin precursor	20.20	1.7	2
Hspa1l	P16627	Heat shock 70 kDa protein 1L	10.24		1
Hspa5	P20029	78 kDa glucose-regulated protein precursor	10.30		1
Hspa8	P63017	Heat shock cognate 71 kDa protein	30.36		3

Table IV: Macrophage cytoskeletal proteins identified in High-Salt sample (after the interaction).

Protein ID[a]	Swiss Prot[a]	Protein Name	Score[b]	% Cov[d]	Nº Pept[b]
		CYTOSKELETON			
Acta1	P68134	Actin, alpha skeletal muscle	130.25	34.00	79
Actb	Q8BFZ3	Actin, cytoplasmic 1	94.42	38.40	49
Actbl2	Q8BFZ3	Beta-actin-like protein 2	26.20	10.90	14
Actg1	Q9QZ83	Gamma actin-like protein	20.30	5.60	8
Actl6a	Q9Z2N8	Actin-like protein 6A	10.22	3.00	2
Actrt2	Q9D9L5	Actin-related protein T2	10.16	6.10	1
Aif1	O70200	Allograft inflammatory factor 1	10.31	11.60	1
C230094A16Rik	Q8C4R3	16 days embryo head cDNA, clone:C130015N21	10.14	2.90	1
Capza2	P47754	F-actin-capping protein subunit alpha-2	10.18	3.50	1
Cfl1	Q9CX22	Cofilin-1	10.30	8.40	1
Cfl2	P45591	Cofilin-2	18.21	18.70	11
Coro1a	O89053	Coronin-1A	30.16	8.70	4
Coro7	Q9D2V7	Coronin-7	10.18	1.70	1
Dstn	Q9R0P5	Destrin	10.29	9.70	4
Fgd1	P52734	RhoGEF and PH domain-containing protein 1	10.13	1.90	2
Flna	Q8BTM8-1	Isoform 1 of Filamin-A	10.14	0.60	1
Krt1	P04104	Keratin, type II cytoskeletal 1	20.22	3.60	7
Krt10	P02535-3	keratin complex 1, acidic, gene 10	20.23	4.50	7
Krt13	P08730-1	Isoform 1 of Keratin, type I cytoskeletal 13	10.17	2.50	1
Krt2	Q61764	Keratin (Fragment)	10.16	3.30	2
Krt42	Q6IFX2	Keratin, type I cytoskeletal 42	20.19	4.90	2
Krt6b	Q9Z331	Keratin, type II cytoskeletal 6B	10.23	2.10	4
Krt73	Q6NXH9	Keratin, type II cytoskeletal 73	10.24	2.20	3
Krt78	A1L0X5	keratin Kb40	10.21	1.10	14
Krt79	Q8VED5	Keratin, type II cytoskeletal 79	20.22	4.00	2
Krt8	P11679	Keratin, type II cytoskeletal 8	8.21	2.40	14
Lmna	P48678-3	Isoform C2 of Lamin-A/C	10.17	1.90	1
Msn	P26041	Moesin	10.12	1.60	1
Rpgrip1	Q9EPQ2-5	Isoform 5 of X-linked retinitis pigmentosa GTPase regulator-interacting protein 1	8.10	4.70	1
Ssx2ip	Q8VC66	Afadin- and alpha-actinin-binding protein	8.16	2.30	1
Tmpo	Q61820	Isoform Alpha of Lamina-associated polypeptide 2 isoforms alpha/zeta	10.18	5.10	1
Tpm3	P21107-2	Isoform 2 of Tropomyosin alpha-3 chain	10.29	6.00	1
Twf1	Q91YR1	Twinfilin-1	10.25	3.70	1
Vim	P20152	Vimentin	20.21	5.40	2
Wdr1	O88342	WD repeat-containing protein 1	40.27	10.70	12
		RELATED TO CYTOSKELETON			
Arhgap21	A2AUE8	Rho GTPase activating protein 21	4.16	0.80	1
Eef1a2	P62631	Elongation factor 1-alpha 2	10.15	2.40	2
Eef1b2	O70251	Elongation factor 1-beta	20.29	12.40	3
Eef1g	Q9D8N0	Elongation factor 1-gamma	10.17	3.20	1
Hspa1l	P16627	Heat shock 70 kDa protein 1L	30.27	6.20	21
Hspa5	P20029	78 kDa glucose-regulated protein precursor	130.31	29.20	23
Hspa8	P63017	Heat shock cognate 71 kDa protein	140.27	25.50	20
Hspa9	P38647	Stress-70 protein, mitochondrial precursor	10.21	1.80	1
Slc25a4	P48962	ADP/ATP translocase 1	10.17	4.00	1

Microscopy analysis of cytoskeletal proteins in control and after *C. albicans* interaction conditions

To visualize the subcellular localization of Actin, Moesin and Vimentin during *C. albicans* phagocytosis, we did confocal immunofluorescence studies. Vimentin is a cytoskeletal protein that is part of intermediate filaments which has also been implicated in inflammation and bactericidal effects of macrophages [7-9]. Moesin is a member of the ERM protein family that includes Ezrin and Radixin. ERM proteins appear to function as cross-linkers between plasma membranes and actin-based cytoskeletons [10].

Moesin location in macrophages in response to *C. albicans*

To simplify imagining of *C. albicans*-macrophage interaction, microscopy experiments were done using a *Candida*-GFP strain. The distribution of Moesin was investigated after the incubation with *Candida*-BFP for 30, 90 and 180 min. Phalloidin staining to detect F-actin polymerization showed no recruitment of Moesin to the phagocytic cup of *C. albicans*-BFP yeast and hyphae at 30, 90 and 180 min (Figure 1).

Vimentin location in macrophages in response to *C. albicans*

Vimentin showed a perinuclear location in macrophages along the interaction (Figure 2), but displayed no co-localization with F-actin formation after 30, 90 and 180 min of *C. albicans*-BFP phagocytosis (Figure 2).

CONCLUDING REMARKS

Cytoskeleton studies allow us to understand the cell dynamics and the constituents of the macrophage cytoskeleton by proteomic profiling and their changes upon interaction with *C. albicans*. With this new approach we have improved the cytoskeleton enrichment in more than 25%. This enrichment warrants the protein amount necessary to label and quantify the differentially expressed proteins in macrophages after 3h of interaction with the yeast.

More experiments will be performed to obtain representative and significant results.

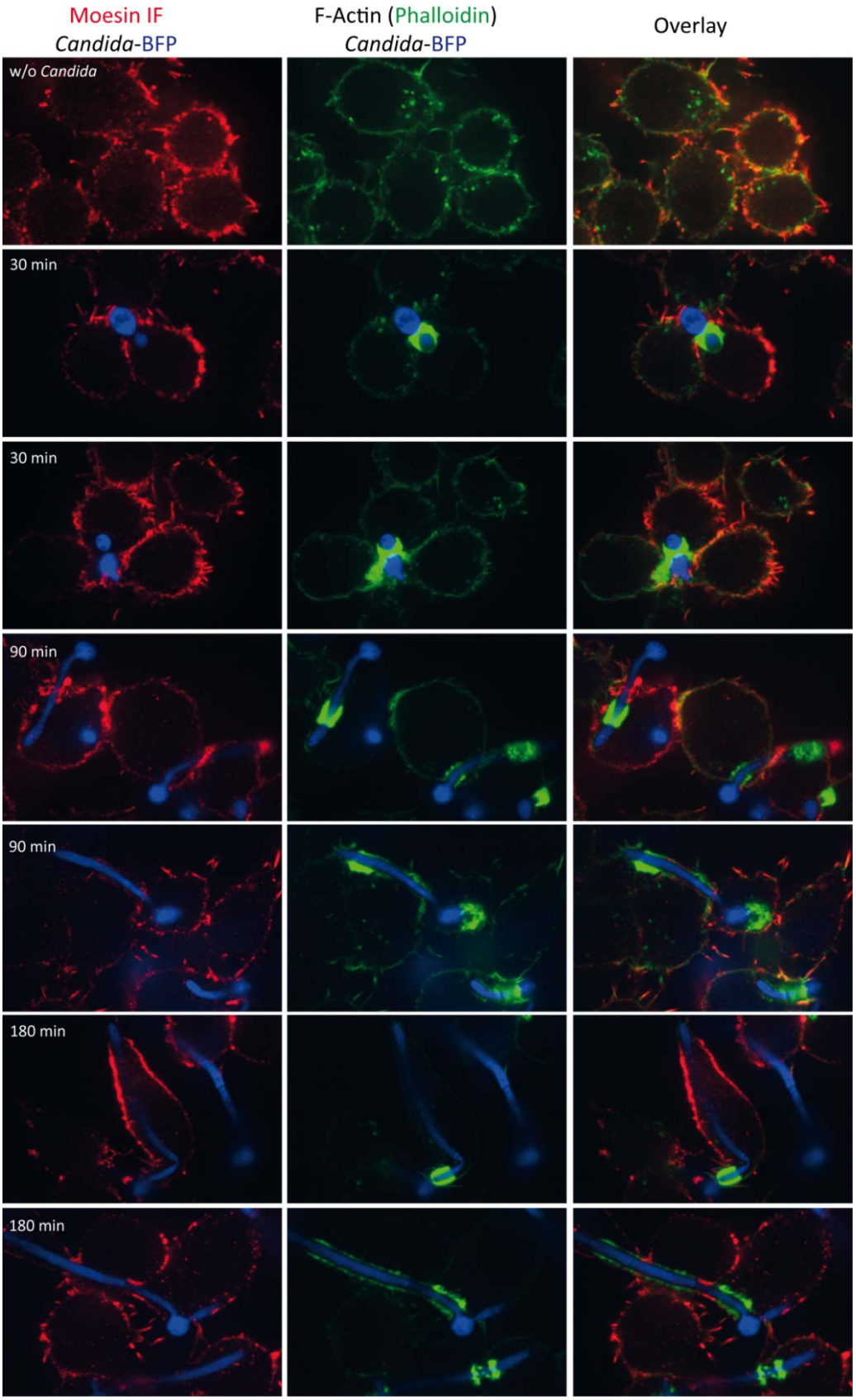

Fig. 1 – Moesin distribution in macrophages after *C. albicans* interaction. Confocal images show Moesin localization in RAW 264.7 macrophages incubated with *C. albicans*-BFP. Images were taken without or after 30, 90 and 180m of co-incubation with *C. albicans*.

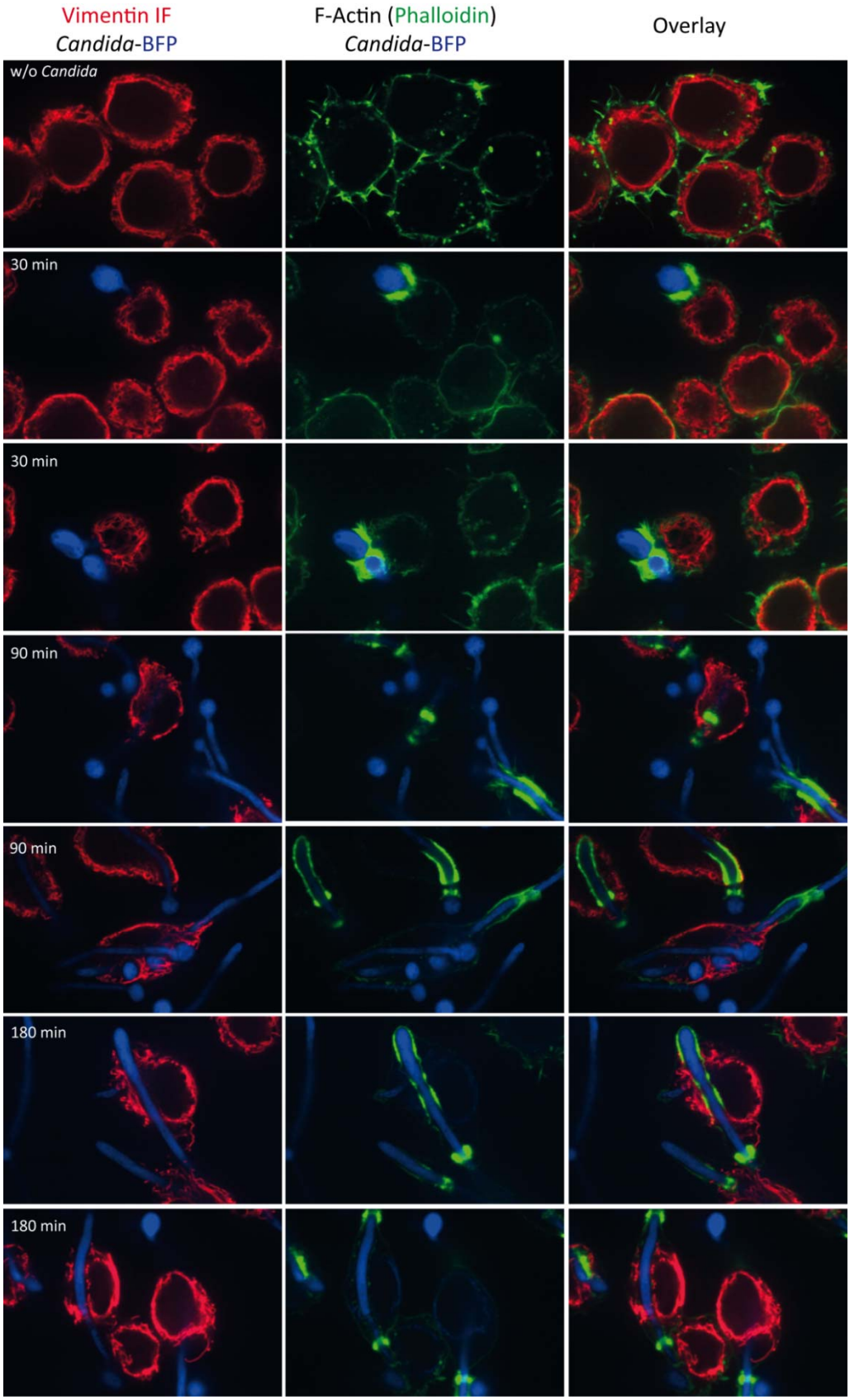

Fig. 2 – Vimentin distribution in macrophages after *C. albicans* interaction. Confocal images showing Vimentin localization in RAW 264.7 macrophages incubated with *C. albicans*-BFP. Images were taken without or after 30, 90 and 180m of co-incubation with *C. albicans*.

BIBLIOGRAPHY

[1] Reales-Calderon JA, Martinez-Solano L, Martinez-Gomariz M, Nombela C, Molero G, Gil C. Sub-proteomic study on macrophage response to *Candida albicans* unravels new proteins involved in the host defense against the fungus. J Proteomics. 2012;75:4734-46.

[2] Martínez-Solano L, Reales-Calderón JA, Nombela C, Molero G, Gil C. Proteomics of RAW 264.7 macrophages upon interaction with heat-inactivated *Candida albicans* cells unravel an anti-inflammatory response. Proteomics. 2009;9:2995-3010.

[3] Martínez-Solano L, Nombela C, Molero G, Gil C. Differential protein expression of murine macrophages upon interaction with *Candida albicans* Proteomics. 2006;6 Suppl 1:S133-44.:S133-S44.

[4] Funchal C, de Almeida LM, Oliveira Loureiro S, Vivian L, de Lima Pelaez P, Dall Bello Pessutto F, et al. In vitro phosphorylation of cytoskeletal proteins from cerebral cortex of rats. Brain research Brain research protocols. 2003;11:111-8.

[5] Gillum AM, Tsay EY, Kirsch DR. Isolation of the *Candida albicans* gene for orotidine-5'-phosphate decarboxylase by complementation of *S. cerevisiae* ura3 and *E. coli* pyrF mutations. Mol Gen Genet. 1984;198:179-82.

[6] Strijbis K, Fairn GD, Witte MD, Tafesse FG, Dougan SK, Watson N, et al. Identification of Bruton's Tyrosine Kinase (BTK) and Vav1 as contributors to Dectin1-dependent phagocytosis of *Candida albicans* in macrophages. Submitted manuscript.

[7] Benes P, Maceckova V, Zdrahal Z, Konecna H, Zahradnickova E, Muzik J, et al. Role of vimentin in regulation of monocyte/macrophage differentiation. Differentiation. 2006;74:265-76.

[8] Mor-Vaknin N, Punturieri A, Sitwala K, Markovitz DM. Vimentin is secreted by activated macrophages. Nature cell biology. 2003;5:59-63.

[9] Perlson E, Michaelevski I, Kowalsman N, Ben-Yaakov K, Shaked M, Seger R, et al. Vimentin binding to phosphorylated Erk sterically hinders enzymatic dephosphorylation of the kinase. J Mol Biol. 2006;364:938-44.

[10] Defacque H, Egeberg M, Habermann A, Diakonova M, Roy C, Mangeat P, et al. Involvement of ezrin/moesin in de novo actin assembly on phagosomal membranes. EMBO Journal. 2000;19:199-212.

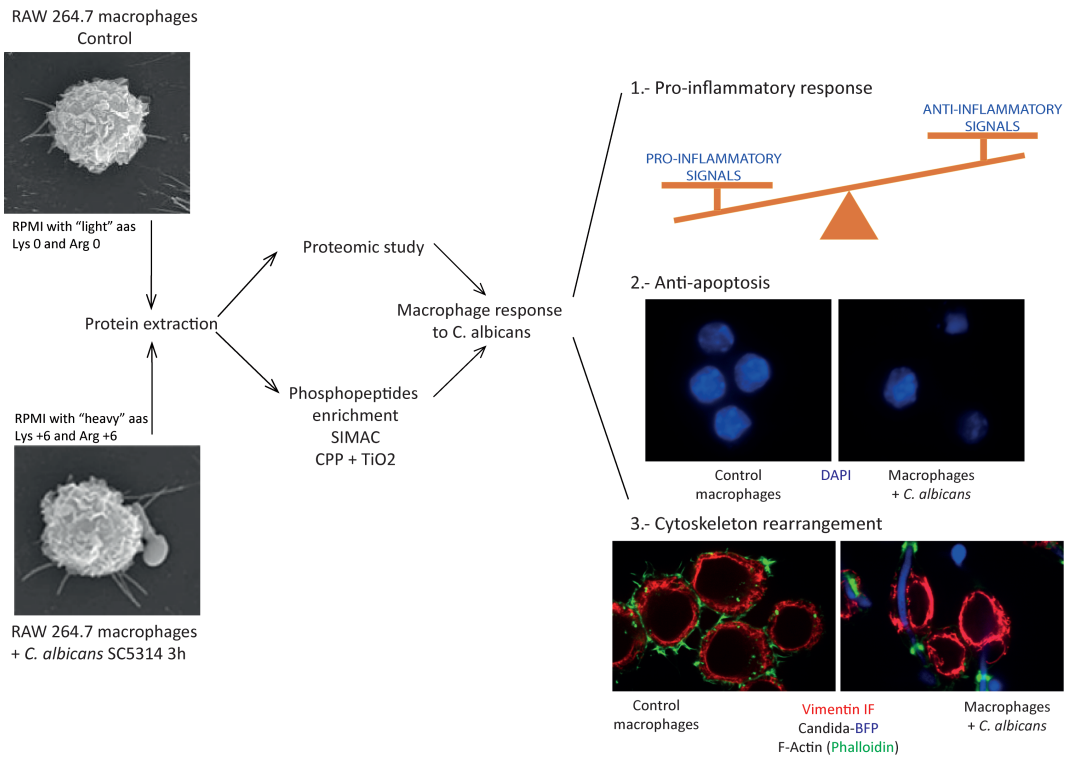

Capítulo II

*** Este capítulo contiene material suplementario que se encuentra disponible después del capítulo y tablas suplementarias accesibles en el CD adjunto**

JOURNAL OF PROTEOMICS 91 (2013) 106–135

Available online at www.sciencedirect.com

SciVerse ScienceDirect

www.elsevier.com/locate/jprot

Candida albicans induces pro-inflammatory and anti-apoptotic signals in macrophages as revealed by quantitative proteomics and phosphoproteomics

Jose Antonio Reales-Calderón[a,b], *Marc Sylvester*[c], *Karin Strijbis*[d], *Ole N. Jensen*[c], *César Nombela*[a,b], *Gloria Molero*[a,b,*], *Concha Gil*[a,b]

[a]*Departamento de Microbiología II, Facultad de Farmacia, Universidad Complutense de Madrid, Madrid, Spain*
[b]*Instituto Ramón y Cajal de Investigaciones Sanitarias (IRYCIS), Madrid, Spain*
[c]*Department of Biochemistry and Molecular Biology, University of Southern Denmark, Campusvej 55, DK-5230 Odense M, Denmark*
[d]*Whitehead Institute for Biomedical Research, 9 Cambridge Center, Cambridge, MA 02142, USA*

ARTICLE INFO

Article history:
Received 13 June 2013
Accepted 16 June 2013
Available online 5 July 2013

Keywords:
Candida albicans
Macrophage
SILAC
Phosphoproteomic
Inflammation
Apoptosis

ABSTRACT

Macrophages play a pivotal role in the prevention of *Candida albicans* infections. Yeast recognition and phagocytosis by macrophages is mediated by Pattern Recognition Receptors (PRRs) that initiate downstream signal transduction cascades by protein phosphorylation and dephosphorylation. We exposed RAW 264.7 macrophages to *C. albicans* for 3 h and used SILAC to quantify macrophage proteins and phosphoproteins by mass spectrometry to study the effects of infection. We identified 53 macrophage up-regulated proteins and 15 less abundant in the presence of *C. albicans* out of a total of 2071 identified proteins. 922 unique protein phosphorylation sites were identified by phosphopeptide enrichment and mass spectrometry, including 327 previously unidentified mouse protein phosphorylation sites. 126 peptides showed an increase and 70 a decrease in their phosphorylation level. The majority of the differentially expressed and phosphorylated proteins are receptors, mitochondrial ribosomal proteins, cytoskeletal proteins, and transcription factor activators involved in inflammatory and oxidative responses. In addition, we identified 22 proteins and phosphoproteins related to apoptosis. The analysis of apoptotic markers revealed that anti-apoptotic signals prevailed during the interaction of the yeast. Our proteomics study suggests that besides inflammation, apoptosis is a central pathway in the immune defense against *C. albicans* infection.

Biological significance
This work uses SILAC and SIMAC methodology combined with CPP (+ TiO_2) to study protein and phosphopeptide changes in RAW 264.7 macrophages in response to coincubation with *Candida albicans* for 3 h. We show that the presence of *C. albicans* induces inflammatory

Abbreviations: PRRs, Pattern Recognition Receptors; PAMPs, Pathogen-Associated Molecular Patterns; IMAC, Immobilized Metal Affinity Chromatography; TiO_2, Titanium Dioxide; SIMAC, Sequential Elution from IMAC; CPP, Calcium Phosphate Precipitation; SILAC, Stable Isotope Labeling by Amino acids in cell Culture; IL, Interleukin; TUNEL, Terminal deoxynucleotidyl transferase (TdT)-mediated dUTP nick end labeling; YPD, Yeast Extract Peptone Dextrose; MAPK, Mitogen-Activated Protein Kinases.

* *Corresponding author at:* Departamento de Microbiología II, Facultad de Farmacia, Universidad Complutense de Madrid, Plaza de Ramón y Cajal s/n, 28040 Madrid, Spain. Tel.: +34 913941755; fax: +34 3941745.
E-mail address: gloros@farm.ucm.es (G. Molero).

http://dx.doi.org/10.1016/j.jprot.2013.06.026

responses and inhibits apoptosis in the macrophages. Our phosphoproteomic analysis identified 327 new mouse protein phosphorylation sites.

1. Introduction

The polymorphic fungus *Candida albicans* is an important opportunistic pathogen [1–3]. The innate immune system is the first line of defense against a *Candida* infection and innate immune defects predispose individuals to invasive candidiasis [4,5].

Macrophages are crucial in innate and adaptive immune responses against systemic candidiasis [6,7]. Pathogen recognition of fungal species by macrophages is mediated by Pattern Recognition Receptors (PRRs) that recognize specific Pathogen-Associated Molecular Patterns (PAMPs). PRRs involved in anti-*Candida* immune responses are, among others, the β-glucan receptor Dectin-1, the mannose receptor (MR), the complement system, Toll like receptors 2 and 4, Mincle and DC-SIGN [8,9]. Activation of individual receptors or receptor complexes leads to effector responses that involve inflammatory mediators, toxic compounds, cytokine production and secretion and antigen presentation for T cells [10]. Many of these signals are controlled by kinases, including Syk [11], Bruton's Tyrosine Kinase [12,13] and MAPKs (Mitogen-Activated Protein Kinases), that regulate phosphorylation cascades [14–16]. Reversible phosphorylation at serine, threonine and tyrosine residues regulated by kinases and phosphatases allows tailoring of immune responses to commensal and pathogenic fungi.

The analysis of phosphorylation events in macrophages would therefore be instrumental in understanding the complex signaling events initiated after *Candida* recognition and their response against systemic candidiasis. To study the macrophage–*C. albicans* interaction our group has previously applied proteomic technologies to identify the important fungal and mammalian pathways during macrophage–yeast encounters. On the yeast side, the prominently up-regulated pathways can be divided into metabolism and energy, protein fate, cellular transport, cell rescue, defense and virulence, biogenesis of the cell wall, fungal cell type differentiation and metal homeostasis [16]. Macrophages on the other hand showed changes in pro-inflammatory pathways, cytoskeleton and metabolism and pro- and anti-apoptotic signals after exposure to *Candida* [17–19].

Phosphoproteomics is the large-scale analysis of protein phosphorylation using mass spectrometry (MS)-based strategies to examine phosphorylation signaling networks [20]. Recently, several phosphoproteomic techniques have been developed for specific enrichment in phosphorylated peptides and proteins, such as immunoprecipitation, Immobilized Metal Affinity Chromatography (IMAC) [21], titanium dioxide (TiO_2) [22] and Calcium Phosphate Precipitation (CPP) [23] or a combination of two techniques, such as Sequential Elution from IMAC (SIMAC) [24].

Quantitative proteomics is the method of choice for large-scale analysis of regulatory events in cells, tissues and whole organisms. Stable Isotope Labeling by Amino acids in cell Culture (SILAC) is a powerful and relatively simple method for the accurate quantitation of proteins by mass spectrometry [25]. Stable isotope-labeled amino acids are incorporated into cellular proteins through endogenous protein synthesis pathways, allowing accurate quantification of all native proteins without any subsequent chemical modification [25,26]. The combination of SILAC and SIMAC is a powerful technique to assess macrophage signaling events during the interaction with *C. albicans*.

The aim of the present study is the quantitative identification and characterization of the (phospho)-protein networks involved in the response of macrophages to *C. albicans* infection. We used quantitative proteomics and phosphoproteomics by SILAC to study RAW 264.7 macrophages after 3 h of interaction with wild type *C. albicans* SC5314. We identified macrophage proteins that are affected by the interaction with the yeast, including proteins involved in inflammation, stress response and apoptosis. 327 new protein phosphorylation sites were identified in the RAW 264.7 mouse-derived macrophages.

2. Material and methods

2.1. *Candida albicans* strains

The *C. albicans* strain used in this study was SC5314, from a clinical isolate [27]. This strain was maintained on solid YPD medium (1% D-glucose, 1% Difco yeast extract and 2% agar) and incubated at 30 °C. Blue Fluorescent Protein-expressing *C. albicans* (*Candida*-BFP) used for confocal microscopy studies was described by Strijbis et al. [13].

2.2. *Macrophage cell line*

The RAW 264.7 gamma NO (–) cell line was obtained from the American Type Culture Collection (Rockville, Md.). Cells were grown in complete medium in a 5% CO_2 incubator at 37 °C and maintained at low densities (75% confluence) and passaged until reaching the confluent state, usually every 3–4 days on sterile culture plates.

2.3. *Culture medium and reagents*

RPMI 1640 medium, fetal bovine serum (FBS), L-glutamine, and antibiotics (penicillin–streptomycin) were obtained from GIBCO BRL (Grand Island, NY). Cell-line macrophages were resuspended in RPMI supplemented with glutamine (2 mM), antibiotics (penicillin 100 U/ml–streptomycin 100 μg/ml), and 10% heat-inactivated fetal bovine serum (complete medium).

For SILAC labeling, arginine and lysine were added in either "light SILAC medium" (Arg0 and Lys0) or "heavy SILAC medium" (Arg6, Cambridge Isotope Laboratories CLM-2247-0.1, Lys6, Cambridge Isotope Laboratories CLM-2265-0.1) from a concentration of 100 mg/l for arginine and 50 mg/l for lysine (Arg0/Lys0: arginine and lysine with normal "light" carbons (12C); Arg6/Lys6: arginine and lysine derivatives with "heavy" carbons (13C). After five cell doublings on culture dishes, protein

extractions of both different macrophages were tested in a LTQ linear ion trap (Thermo Scientific) for full incorporation of the label after five passages. Then, cells with heavy amino acids were treated with *C. albicans* (ratio 1:1) for 3 h and cells with light amino acids were used as control.

2.4. *Preparation of proteomics samples*

For each labeling condition, RAW 264.7 macrophages were grown in 5 large dishes (15 cm diameter) to a final cell number of about 4×10^7 per dish. After 3 h of interaction, the light (control) and heavy (stimulated) macrophages were washed 3 times with ice-cold PBS and then scraped and collected by centrifugation at 1000 *g*.

The cell pellets were resuspended in RIPA Buffer modified for SILAC (with 1% protease inhibitor cocktail (Roche), 5 mM sodium fluoride, 1 mM sodium orthovanadate, 5 mM beta-glycerol phosphate and 5 mM sodium pyrophosphate) for 20 min with occasional vortexing. Cell lysates were centrifuged at 12,000 *g* at 4 °C for 10 min, and the resulting supernatants were collected. The protein concentrations of the cell lysates were determined by using RC-DC assay (BioRad).

2.4.1. *1-D SDS-PAGE separation and in-gel trypsin digestion*

The light (control) and heavy (stimulated) cell lysates were combined at 1:1 ratio (w/w), 100 μg of each, denatured by heating in Laemmli loading buffer for 10 min at 70 °C. The protein samples were separated by one-dimensional SDS-PAGE using NuPage 4–12% Bis–Tris Gels and NuPage MOPS running buffer (Invitrogen) according to the manufacturer's instructions. The gel was stained with Coomassie blue; after destaining, the gel was cut into 10 bands. Gel slices were cut into 1 mm^3 cubes, washed twice with water, dehydrated with 100% ACN, and incubated with 10 mM DTT in 50 mM ammonium bicarbonate for 30 min at 56 °C for protein reduction. The resulting solution was subsequently alkylated by incubation with 55 mM iodoacetamide in 50 mM ammonium bicarbonate for 20 min at room temperature in the dark. The gel pieces were washed with 50% ACN and then with 10 mM ammonium bicarbonate, dehydrated with 100% ACN, and dried in a vacuum concentrator. The gel pieces were rehydrated with 12.5 ng/μl of trypsin (Promega) in 50 mM ammonium bicarbonate and incubated overnight at room temperature in the dark for protein digestion. Supernatants were transferred to clean tubes, and gel pieces were incubated in 50 mM NH_4HCO_3 at 50 °C during 1 h, the supernatant were collected, the remaining peptides were extracted by incubation with 5% formic acid during 15 min and with 100% ACN during 15 min more. The extracts were combined, and the organic solvent was removed in a vacuum concentrator. Desalting and concentration were carried out in a pipette tip with R2 Poros C18 resin on top of a C18 plug [28] and the eluted peptides were dried in a vacuum concentrator and subjected to LC–MS.

2.4.2. *In-solution digestion of proteins*

The light (control) and heavy (stimulated) cell lysates were combined at 1:1 ratio (w/w), 250 μg of each for SIMAC and 100 μg of each for CPP. Samples were reduced by adding 25 mM DTT for 30 min at 60 °C. Then, samples were loaded into an Amicon (Nanosep 10 K Omega; Pall Corporation) and centrifuged 45 min at 12,000 *g*. Samples were washed twice with DB2 buffer (20 mM TEAB, 0.5% sodium deoxycolate) and alkylated with 50 mM iodoacetamide during 20 min in the dark. After twice washes with DB2, digestion was started by adding Trypsin (Promega) 1:100. After 4 h in the dark at RT in wet atmosphere, peptides were collected into a clean collection tube and the amicon was washed with DB2 and collected the flow-through. Samples were acidified with 0.5% TFA final, and sodium deoxycolate precipitates forms were separated by centrifugation 5 min at 16,000 *g*. Peptide concentration was estimated with Qubit (Invitrogen) to further enrichment of phosphopeptides.

2.5. *Phosphopeptides enrichment*

2.5.1. *SIMAC (Sequential Elution from IMAC)*

2.5.1.1. IMAC. For each 100 μg peptides, 40 μl of iron-coated PHOS-select™ metal chelate beads (Sigma) were used. The beads were washed twice in loading buffer (0.1% TFA, 50% ACN) as previously described [29] and then, incubated with loading buffer and 500 μg of peptide mixture for 30 min at RT in vibrating shaker. After the incubation, the beads were packed in the constricted end of a 200 μl GELoader tip by application of air pressure forming an IMAC microcolumn. The IMAC flow-through was collected in an Eppendorf tube for further analysis by TiO_2 chromatography. The IMAC column was washed using 50 μl of loading buffer, which was pooled with the IMAC flow-through. The monophosphorylated peptides and the contaminating non-phosphorylated peptides were eluted from the IMAC column using elution solution acidic (1% TFA, 20% ACN) and the multiply phosphorylated peptides were subsequently eluted using elution solution basic (0.5% of ammonia). The IMAC flow-through and the IMAC eluents were dried in a vacuum concentrator.

2.5.1.2. Titanium dioxide (TiO_2) chromatography. After lyophilization, the pooled flow-through and the eluted acidic fraction from the IMAC were enriched in phosphopeptides using TiO_2 chromatography. A TiO_2 microcolumn was prepared by stamping out a small plug of C18 material from a C18 extraction disk and placing the plug in the constricted end of a 200 μl GELoader tip [22,30]. The TiO_2 beads suspended in loading solution (1 M glycolic acid in 5% TFA, 80% ACN) were mixed with the sample previously diluted five times in loading solution. The mix was incubated for 15 min in a vibrating shaker. The sample and the beads were sedimented and 90% of the supernatant was removed to minimize the volume in the column. The sample was applied to the tip and the TiO_2 microcolumn was packed by the application of air pressure. The TiO_2 microcolumn was washed with loading buffer and subsequently with washing buffer (80% ACN, 5% TFA). The phosphopeptides that bound to the TiO_2 microcolumns were eluted using 30 μl of 0.5% ammonia followed by elution using 1 μl of 30% ACN to elute phosphopeptides that bound to the C18 disk. The eluent was acidified by adding 5 μl of 100% formic acid and was dried in the vacuum concentrator.

2.5.2. CPP (Calcium Phosphate Precipitation)

The peptide solution was adjusted to 50 μl and pH was adjusted to 9–10 using ammonia water. 2 μl of 0.5 M Na_2HPO_4 and 2 μl of 2 M ammonia water were added and mixed followed by the addition of 2 μl of 2 M $CaCl_2$. The solution was vortexed and centrifuged at 20,000 *g* for 10 min at room temperature. Subsequently the supernatant was removed, and the pellet was resuspended in 60 μl of 80 mM $CaCl_2$ and washed. After centrifugation as described above, the washing solution was removed, and the resulting pellet was dissolved in 20 μl of 5% formic acid. Desalting and concentration were carried out in a pipette tip with R3 microcolumn C18 [28] and the eluted peptides were dried in a vacuum concentrator.

2.5.3. Titanium dioxide (TiO_2) chromatography

Desalting peptide solution was enriched in phosphopeptides with a TiO_2 microcolumn (as described above).

2.6. Peptide sequencing by tandem mass spectrometry

Peptide mixtures were analyzed by LC–MS/MS using an Easy-nLC system (Thermo Scientific Proxeon) interfaced to a LTQ-Orbitrap XL instrument (ThermoFisher Scientific, Bremen, Germany). The nanoliter flow LC was operated in one column set-up with an 18 cm analytical column (100 μm inner diameter, 350 μm outer diameter) packed with C18 resin. Solvent A was 0.1% formic acid in ddH_2O and solvent B was 90% acetonitrile (Fisher Scientific) with 0.1% formic acid. Samples were injected in an aqueous 1% TFA solution at a flow rate of 550 nl/min. Peptides were separated with a gradient of 0–34% solvent B 113 min with a flow rate of 250 nl/min. MS measurements were performed on an LTQ-Orbitrap XL instrument set to resolution 60,000 at 400 *m/z* for the precursor scan (330–1800 *m/z* range, automatic gain control set to 1,000,000, 500 ms maximum injection time). Each of the eight most intense multiply charged ions was fragmented by collision induced dissociation (CID) with automatic gain control set to 20,000, isolation width 2.5 *m/z*, 30 ms activation time and a normalized collision energy of 35. A dynamic exclusion of 45 s was used. For phosphopeptide enriched samples CID detection was performed as a multistage activation (MSA) experiment if a phosphate neutral loss was detected.

2.7. Protein/peptides identification and quantitation

The raw data from LTQ-Orbitrap was converted to a .mgf file using Proteome Discoverer 1.2 software (ThermoFisher Scientific). Top 10 of fragment ions per 100 Da were extracted for a protein database search using the Mascot search engine (version 2.2.2, Matrix Science) against the concatenated Swiss-Prot release 53.0 (http://www.expasy.ch/sprot) and TrEMBL release 37.0 (http://www.ebi.ac.uk/trembl) databases without taxonomy restriction, containing 269,293 and 4,672,908 sequence entries respectively for each software version and database release. The search parameters were set as follows: Carbamidomethylation (C) was chosen as the fixed modification. As variable modifications, Oxidation (M), N-acetylation (protein), Phosphorylation (STY) and SILAC labels: 13C (6) (K) and 13C (6) (R) were chosen, 8 ppm for MS tolerance, 0.6 Da for MS/MS tolerance, and 2 for missing cleavage. CID data was searched with instrument setting 'ESI-trap'. Mascot search results were exported and low-confidence identifications were filtered using Microsoft Office Excel 2007 with the following criteria: Peptides with low score (cut-off score value = 20) and with many putative PTMs (≥5 PTMs/peptide) were removed. Redundant peptides were filtered by selecting the peptide with the highest mascot score among peptides with the same ID. We accepted the peptide and protein identifications with FDR less than 1%. For protein quantification, the proteins with at least two ratio peptide counts were considered. The median value of the SILAC ratios was calculated as protein abundance (H/L ratio) to minimize the effect of outlier values.

2.8. Western blotting

50 μg of protein per well was separated onto 10% SDS-polyacrylamide minigels and transferred to Hybond-ECL Nitrocellulose membranes (Amersham Biosciences). The western-blotting was performed with Odyssey system (Infrared Imaging System (LI-COR Biosciences, Nebraska, USA), which allows the measurement of the relative levels of fluorescence of the different bands and simultaneous labeling with two different antibodies.

After 1 h of incubation with primary antibodies: 1/2000 monoclonal, Anti-Vimentin (SIGMA), anti-Mcl1, anti-Eef2 and anti-Phospho Eef2 (Thr^{57} + Thr^{59}) (Abcam), anti-Tubulin alpha (Serotec), anti-c-Jun and anti-Phospho c-Jun (Ser^{63}) (Cell Signalling), the membranes were washed 4 times in PBS with 0.1% Tween-20. After this, the membranes were incubated with fluorescently labeled secondary antibodies: 1/4000 IRDye 800CW conjugated Goat (polyclonal) anti-Rabbit IgG, 1/2000 highly cross absorbed (LI-COR Biosciences) and 1/4000 IRDye 680 conjugated Goat (polyclonal) anti-Mouse IgG, highly cross absorbed (LI-COR Biosciences) or IRDye 680 Goat anti-Rat IgG, highly cross absorbed (LI-COR Biosciences) for 30–60 min at room temperature and protected from the light. The membranes were washed again and scanned for fluorescence detection with Odyssey system (LI-COR Biosciences, Nebraska, USA).

Anti-Cleaved Caspase-3 (Asp175) Rabbit mAb (Cell Signalling) 1/1000 was used as primary antibody to assess the apoptotic status of the macrophages during the interaction with *C. albicans* along the time. Western blottings were performed as described above using Odyssey system and using fluorescently labeled secondary antibodies: 1/4000 IRDye 800CW anti-Rabbit IgG (LI-COR Biosciences).

Tubulin was used as loading control for the proteomic validation, and the non-phosphorylated protein for the phosphoproteins validation. Data were expressed as mean ± SD. The unpaired Student's *t*-test was used to compare differences between groups and $p < 0.05$ was considered significant.

2.9. Confocal microscopy

Cells were grown on glass coverslips onto a p12 plate and treated with *C. albicans* for 3 h. The coverslips were fixed with 4% formaldehyde in PBS for 20 min at RT, washed twice with PBS and cell membranes were permeabilized for 15 min with PBS containing 0.2% Tween-20 at room temperature. After two

washes with PBS, the coverslips were incubated with Binding Buffer (0.1% Saponin, 0.2% BSA in PBS) for 30 min and overlaid with Anti-Vimentin antibody (Sigma-Aldrich, diluted 1:1000), incubated for 1 h, washed with Binding Buffer three times and incubated for 1 h with Alexa Fluor 568 anti-rabbit, washed with Binding Buffer three times and prepared for microscopy by mounting them on slides in 50% glycerol.

Confocal images were collected in the W. M. Keck Facility for Biological Imagining using a PerkinElmer Live Cell imaging spinning disk confocal system mounted on a Zeiss Axiovert 200M with a 63× and 100× 1.4NA oil immersion objectives. Excitation light was generated by gas and solid state laser (argon laser for 488 nm, krypton laser for 568 nm, solid state laser for 405 nm and 647 nm) and passed through an AOFT for wavelength selection and laser power control. A quadrupole bandpass filter separated the excitation and emission light inside the CSU-22 confocal scanhead (Yokogawa) and a filter wheel (Prior Scientific) provided selection of emission filters (TagBFP & RFP: dual band 445/60 and 615/70 nm; GFP: 527/55 nm). Volocity image acquisition software was used to capture images from a Hamamatsu Orca-ER cooled-CCD camera and to control the equipment.

The intensity of red fluorescence (Vimentin) was measured by quantitative image analysis with Volocity software (Perkin Elmer). Data are mean ± SD of values from 3 fields from two experiments (n = 5 each).

2.10. *Determination of chromatin condensation and fragmentation*

Chromatin DNA condensation and fragmentation in adherent and detached cells were assessed by examination of nuclear morphology using DAPI. Cells were grown onto 18-mm coverslips placed in 24-well multiwell plates. After one day, macrophages were incubated with *C. albicans* (ratio 1:1) or 5 mM Staurosporine during 45 min, 1.5, 3, 6, 8, 12 and 24 h at 37 °C in a 5% CO_2. After the interaction, coverslips were fixed 5 min in cold paraformaldehyde, washed in PBS and permeabilized using 0.1% Triton and 0.1% sodium citrate in PBS. After this, the coverslips were washed twice and incubated

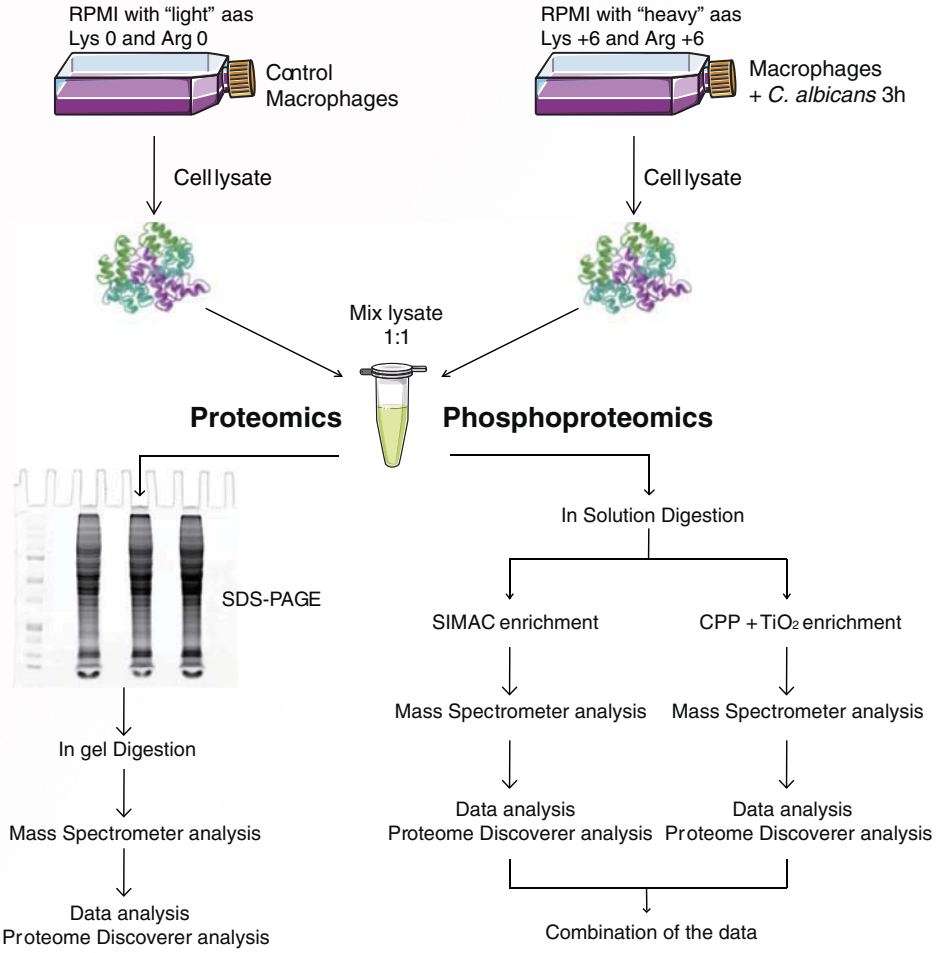

Fig. 1 – Flow chart for analysis of macrophage proteome and phosphoproteome in response to *C. albicans*. Workflow of the quantitative phosphoproteomics approach by SILAC. Three replicates of RAW 264.7 macrophages were labeled with light and heavy stable isotope-substituted arginine and lysine, creating proteins and peptides distinguishable by mass. After the labeling, "heavy" macrophages were incubated with *C. albicans* for 3 h. Protein extracts were loaded onto SDS-PAGE gels, and 10 fractions of each were trypsin-digested and analyzed by LC–MS/MS. Phosphopeptides were enriched by either SIMAC or CPP affinity purification. LC–MS/MS analysis of the eluted fractions was performed to identify phosphopeptides and the light/heavy ratio was calculated for quantification.

with DAPI during 5 min. Then, the coverslips were washed with PBS three times in the dark and mounted with anti-fading solution.

The cells were examined by fluorescence microscopy and the number of cells exhibiting condensed or fragmented nuclei as well as the total number of cells was determined, more than 300 macrophages were examined for each sample and images of the condensation states of the chromatin were taken with a charge-coupled device camera.

Cells with condensed and fragmented nuclei were scored as apoptotic.

DNA strand breaks were assessed with a TUNEL (terminal deoxynucleotidyl transferase-mediated dUTP-biotin end labeling of fragmented DNA) staining procedure (Roche Applied Science, Indianapolis, IN). In brief, macrophages were grown in 100 mm culture dish. After one day, macrophages were incubated with *C. albicans* (ratio 1:1) during 45 min, 1.5, 3 and 6 h at 37 °C in a 5% CO_2. After the incubation, cells were trypsinized at 37 °C for 10 min, the reaction was quenched with complete medium and cells were centrifuged for 10 min at 1000 rpm. Cells were fixed in cold paraformaldehyde overnight, washed in PBS and permeabilized using 0.1% Triton and 0.1% sodium citrate in PBS. The pellet was resuspended in 50 μl TUNEL reaction mixture (45 μl labeling solution and 5 μl enzyme solution), incubated for 1 h at 37 °C in a humidified atmosphere in the dark and washed twice with PBS. Cells were resuspended in PBS at a concentration of 1×10^6 cells/ml.

The percentage of $TUNEL^+$ cells was assessed by flow cytometry using a FACScan equipped with an ion laser and an excitation at 488 nm. A minimum of 10,000 macrophage-gated events were collected.

2.11. Statistics

All quantitative data were presented as mean ± standard deviation (S.D.). For Western blotting, comparisons between two groups were performed by Student's *t* test. Statistical significance was defined as $^*p < 0.05$, $^{**}p < 0.01$ and $^{***}p < 0.001$.

3. Results

3.1. Proteomic analysis of the macrophage response to C. albicans

A stable isotope labeling approach (SILAC) was used to study changes in protein expression from murine macrophages in response to 3 h of interaction with *C. albicans* (1:1 ratio) (Fig. 1). After 3 h of coincubation, *Candida* has formed extensive hyphae that are thought to enable escape from the macrophage. Our study was designed to study the macrophage response at this critical time. Proteins were identified by Gel-LC–MS (1D SDS-PAGE, trypsin digestion and analysis by EASY-nLC LTQ Orbitrap XL Mass Spectrometer). Protein quantitation and identification was carried out with Proteome Discoverer v1.2 software. The relative abundance of a protein was measured by averaging the intensities of all peptides identified for the protein at each sample. Three independent biological replicates and two technical replicates of each were performed.

Proteins with at least 2 peptides with high confidence were identified and quantified, and the variation among these peptides ratios was <20%. Changes were considered significant within at least CV < 0.25 (Coefficient of Variation), and standardized $\log_2$ Heavy/Light ratios exceeding ±0.5. Consequently, protein abundance values with CVs higher than 0.25 but with averaged ratios that varied significantly between both samples (average $\log_2$ Heavy/Light ratios ± SD above or below zero) were kept and standardized $\log_2$ Heavy/Light ratios exceeding ± 0.5; the remaining proteins (protein abundance values without good reproducibility between biological replicates) were discarded. Combining the 3 biological and 2 technical replicates, 3178 non-redundant proteins were initially identified of which 2071 proteins that made our statistical cut off. The protein IDs and expression ratios are listed in Suppl. Table S1.

A total of 53 proteins were found to be more abundant (ratio < 0.5) and 15 less abundant (ratio > 0.5), after 3 h of interaction with *C. albicans*. These proteins are listed and functionally classified in Table 1. A database search was carried out to analyze their function and to assign them to different functional groups. As can be observed in Table 1 and Supplemental Fig. S1, proteins with differential expression are involved in stress response and oxidoreductase activity, apoptosis, immune response, cytoskeleton rearrangement, metabolism, and some of them are structural components of the mitochondrial ribosome.

3.2. Phosphoproteomic analysis of the macrophage response to C. albicans

3.2.1. Phosphosite analysis

Two different and complementary phosphopeptide enrichment approaches were performed. Equal amounts of SILAC samples from control macrophages (grown in "light medium" $^{12}C_6$-arginine and $^{12}C_6$-lysine) and macrophages after 3 h of coincubation with *C. albicans* (grown in "heavy medium" $^{13}C_6$-arginine and $^{13}C_6$-lysine) were mixed and digested prior to phosphopeptide enrichment by ion metal affinity chromatography (IMAC) combined with TiO_2 enrichment (SIMAC) [29] or by Calcium Phosphate Precipitation (CPP) combined with TiO_2 [22,30] (Fig. 1). Three biological and 2 technical replicates were performed for each enrichment. All the SIMAC and CPP samples were analyzed by EASY-nLC LTQ Orbitrap XL Mass Spectrometer. Raw data files were processed with the Proteome Discoverer v1.2 software for peptide and protein identification and the quantification of phosphorylation changes. Finally, phosphorylation site ratios measured in the technical replicates were averaged prior to further data analysis.

To determine the correct identification of the phosphorylation site of each peptide, the Ascore (ambiguity score) algorithm was used [31]. Ascore is a probabilistic algorithm that predicts the likelihood of matching site-determining ions to specific phosphorylation sites. An Ascore value of ≥19 corresponds to sites that have been localized with high certainty (>99%, $p \leq 0.01$), phosphopeptides with Ascores between 15 and 19 are localized with moderate certainty (>90%, $p < 0.05$), and phosphopeptides with Ascores from 3 to 15 had the lowest statistical certainty (80%, $p < 0.1$). The distribution of scores for all phosphopeptides in the individual experiments is shown in Suppl. Table S2.

Table 1 – Functional classification of macrophages differentially abundant proteins during *C. albicans* interaction.

Protein ID	Swiss Prot [a]	Protein name	Ratio (log_2 H/L)	CV (%)	Mascot score [b]	Coverage [c] (%)	No. of peptides
Stress response/oxidoreductase activity							
Glut1	P17809	Glucose transporter type 1, erythrocyte/brain	0.61	0.06	628.14	9.76	4
Sels	Q9BCZ4	Selenoprotein S (Seps1) (H47)	0.51	0.22	281.68	27.89	3
Retsat	Q64FW2	All-trans-retinol 13,14-reductase	0.82	0.11	178.04	15.27	6
Coq9	Q8K1Z0	Ubiquinone biosynthesis protein COQ9, mitochondrial	0.54	0.10	115.38	15.65	3
Pex11b	Q9Z210	Peroxisomal membrane protein 11B	0.50	0.00	104.64	19.31	4
Tmx3	Q8BXZ1	Protein disulfide-isomerase TMX3	0.67	0.35	158.67	15.35	3
Immune response/cell recognition							
Fabp4	P04117	Fatty acid-binding protein, adipocyte (Ap2)	−0.58	0.03	156.16	27.27	3
Cd36	Q08857	Platelet glycoprotein 4	0.56	0.13	654.94	29.87	9
Rtn4	Q99P72	Reticulon-4 (Nogo-A)	0.51	0.09	1091.48	11.79	9
Lilrb4	Q64281	Leukocyte immunoglobulin-like receptor subfamily B member 4 (ILT3)	0.71	0.14	40.70	8.96	2
Cd14	P10810	Monocyte differentiation antigen CD14	0.59	0.12	327.37	16.67	5
Tyrobp	O54885	TYRO protein tyrosine kinase-binding protein (Dap12)	0.51	0.08	186.38	25.44	2
Csf1r	P09581	Macrophage colony-stimulating factor 1 receptor	−0.80	0.38	294.34	10.54	7
Mcl1	P97287	Induced myeloid leukemia cell differentiation protein Mcl-1 homolog	0.60	0.08	95.94	22.36	5
Cytoskeletal components and actin binding proteins							
Ckap5	A2AGT5	Cytoskeleton-associated protein 5	−0.51	0.07	234.57	2.85	6
Vim	P20152	Vimentin	2.08	0.51	822.59	46.35	18
Tor1aip1	Q921T2	Torsin-1A-interacting protein 1	0.66	0.10	374.27	11.15	4
Krt76	Q3UV17	Keratin, type II cytoskeletal 2 oral	−3.67	0.71	264.58	8.42	8
Nup37	Q9CWU9	Nucleoporin Nup37	−0.59	0.07	165.61	13.50	3
Metabolism							
Pycr1	Q922W5	Pyrroline-5-carboxylate reductase 1, mitochondrial	0.50	0.05	459.67	20.06	4
Pycr2	Q922Q4	Pyrroline-5-carboxylate reductase 2	0.51	0.08	1017.33	45.31	11
Fdx1	P46656	Adrenodoxin, mitochondrial (Ferredoxin-1)	0.52	0.03	76.94	16.49	3
Acadm	P45952	Medium-chain specific acyl-CoA dehydrogenase, mitochondrial	0.51	0.11	244.43	17.10	6
Acadvl	P50544	Very long-chain specific acyl-CoA dehydrogenase, mitochondrial	0.53	0.27	153.31	10.82	4
Hmgcr	Q01237	3-Hydroxy-3-methylglutaryl-coenzyme A reductase	1.14	0.36	315.69	5.98	4
Dhrsx	Q8VBZ0	Dehydrogenase/reductase SDR family member on chromosome X homolog	0.64	0.12	64.50	14.03	2
Cpox	P36552	Coproporphyrinogen-III oxidase, mitochondrial	0.52	0.11	86.06	11.51	4
Acaa2	Q8BWT1	3-Ketoacyl-CoA thiolase, mitochondrial	0.54	0.11	429.91	21.91	6
Hint2	Q9D0S9	Histidine triad nucleotide-binding protein 2, mitochondrial	0.58	0.17	269.77	39.88	4
Car2	P00920	Carbonic anhydrase 2	−0.50	0.07	1249.33	54.62	10
Smpd4	Q6ZPR5	Sphingomyelin phosphodiesterase 4	0.66	0.09	91.36	4.86	3
Bphl	Q8R164	Biphenyl hydrolase-like protein	0.52	0.17	148.63	18.56	4
Nucleic acid processing							
Ssrp1	Q08943	Structure specific recognition protein 1 (T160)	−0.58	0.35	80.17	7.06	3
Son	Q9QX47	Protein SON (Nrebp) Negative regulatory element-binding protein	0.78	0.10	157.23	2.66	4
Top2b	Q64511	DNA topoisomerase 2-beta	−0.52	0.04	197.28	5.77	8
Nono	Q99K48	Non-POU domain-containing octamer-binding protein (p54nrb)	0.50	0.11	1446.09	51.80	22
Banf1	O54962	Barrier-to-autointegration factor (Baf)	0.52	0.11	470.77	53.93	4
Structural component of the ribosome/ribosome synthesis							
Mrps21	P58059	28S ribosomal protein S21, mitochondrial	0.53	0.09	948.75	48.28	4
Mrpl21	Q9D1N9	39S ribosomal protein L21, mitochondrial	0.50	0.15	355.82	41.15	6
Mrpl22	Q8BU88	39S ribosomal protein L22, mitochondrial	0.79	0.33	157.98	30.10	5
Mrpl23	O35972	39S ribosomal protein L23, mitochondrial	0.55	0.12	304.49	51.37	5
Mrpl32	Q9DCI9	39S ribosomal protein L32, mitochondrial	0.56	0.09	301.34	25.67	4
Mrpl4	Q9DCU6	39S ribosomal protein L4, mitochondrial	0.55	0.14	102.86	30.61	5
Mrpl44	Q9CY73	39S ribosomal protein L44, mitochondrial	0.59	0.18	116.29	12.01	2
Mrpl51	Q9CPY1	39S ribosomal protein L51, mitochondrial	0.60	0.20	155.06	22.66	3
Rpf2	Q9JJ80	Ribosome production factor 2 homolog	0.62	0.27	100.04	20.26	5
Las1l	A2BE28	Protein LAS1 homolog	0.52	0.18	153.44	6.31	4
Transport							
Abcc3	B2RX12	Canalicular multispecific organic anion transporter 2	0.76	0.12	154.77	4.33	3
Praf2	Q9JIG8	PRA1 family protein 2	0.53	0.04	163.52	22.47	3
Sec31b	Q3TZ89	Protein transport protein Sec31B	−4.78	0.05	64.17	2.16	3

Table 1 (*continued*)

Protein ID	Swiss Prot[a]	Protein name	Ratio (log_2 H/L)	CV (%)	Mascot score[b]	Coverage[c] (%)	No. of peptides
Transport							
Timm23	Q9WTQ8	Mitochondrial import inner membrane translocase subunit Tim23	0.56	0.10	321.45	22.49	3
Nemf	Q8CCP0	Nuclear export mediator factor Nemf	−0.61	0.14	61.42	3.76	3
Golga2	Q921M4	Golgin subfamily A member 2	0.56	0.11	392.59	7.61	5
Protein fate							
Pmpcb	Q9CXT8	Mitochondrial-processing peptidase subunit beta	0.55	0.12	232.15	27.20	7
Ubxn1	Q922Y1	UBX domain-containing protein 1	−0.64	0.04	121.70	26.26	3
Uba5	Q8VE47	Ubiquitin-like modifier-activating enzyme 5	−0.60	0.11	130.55	13.90	3
Vcpip1	Q8CDG3	Deubiquitinating protein VCIP135	−0.53	0.05	138.52	4.84	4
Unknown function							
Ccdc127	Q3TC33	Coiled-coil domain-containing protein 127	0.53	0.19	122.61	16.54	3
Ccdc167	Q9D162	Coiled-coil domain-containing protein 167	0.51	0.17	202.97	36.08	3
Mpeg1	A1L314	Macrophage-expressed gene 1 protein	0.82	0.16	139.33	8.84	5
Ociad1	Q9CRD0	OCIA domain-containing protein 1	0.50	0.22	316.95	32.79	4
UPF0466	Q9DB10	UPF0466 protein C22orf32 homolog, mitochondrial	0.57	0.12	30.33	35.51	3
Cdv3	Q4VAA2	Carnitine deficiency-associated gene expressed in ventricle 3 (41)	−0.50	0.08	173.22	33.81	4
Coa5	Q99M07	Cytochrome c oxidase assembly factor 5	0.77	0.06	281.75	58.11	3
Erlin2	Q8BFZ9	Erlin-2 (SPFH2)	0.51	0.06	318.66	17.35	3
Hdhd3	Q9CYW4	Haloacid dehalogenase-like hydrolase domain-containing protein 3	0.51	0.11	42.20	17.53	3
Pdap1	Q3UHX2	28 kDa heat- and acid-stable phosphoprotein (HASPP28)	−0.56	0.22	88.70	13.26	2
Tmem33	Q9CR67	Transmembrane protein 33	0.50	0.09	676.16	19.43	5

[a] Protein name and accession number according to UniProt-SwissProt database (https://www.proteome.com/control/tools/proteome).
[b] Protein score are derived from Mascot result page.
[c] The protein coverage corresponds to a percentage in proteins identified by peptide mass fingerprinting.

A total of 25,860 phosphopeptides were identified, of which 959 unique phosphopeptides were present in two or more biological replicates. 840 phosphopeptides showed a CV across the 3 replicates <0.25. LC–MS/MS analysis using a combination of MS2-only and MSA allowed the identification of 922 distinct phosphosites from 517 phosphoproteins. Based on the Ascore distribution of the 922 phosphorylation sites, 57% of the dataset (527 sites) achieved the highest certainty ($p \leq 0.01$) with regard to phosphorylation site identification, and 7% (67 sites) had an Ascore 13–19 ($p < 0.05$), also indicating high certainty. An additional 23% (209 sites) could be localized with >90% confidence. 131 ambiguous phosphopeptides (Ascore value <3) (14% of the total psites) were also predicted.

A database of all phosphopeptide identifications including quantitative data for both phosphopeptides and the corresponding protein level abundances is available online (Proteopathogen: http://proteopathogen.dacya.ucm.es/). The spectra and data from the LC–MS/MS analysis are available at the PRIDE repository of the European Bioinformatics Institute (www.ebi.ac.uk/pride/) [32], accession number 2324.

The majority of phosphopeptides (90% of the total) were mono-phosphorylated and phosphoserine (pSer) residues were the most commonly modified amino acid (89% of the total), and phosphothreonine (pThr) and phosphotyrosine (pTyr) were less represented, 10% and 1%, respectively.

3.2.2. *Differential phosphorylation of macrophage proteins upon interaction with C. albicans*

Of the phosphopeptides that were present in at least 2 biological replicates, 196 displayed significantly altered phosphorylation levels in the macrophages after incubation with *Candida*. The phosphorylation level of 70 phosphopeptides was decreased (corresponding to 57 proteins) and phosphorylation levels of 126 phosphopeptides were increased (89 proteins) in the presence of *Candida*. Phosphopeptides that increased or decreased are listed in Table 2. This table includes numerous trafficking proteins and protein kinases, proteins related to immune responses and to cytoskeleton rearrangement and transcription factors, the most relevant differentially phosphorylated proteins are depicted in Suppl. Fig. S2.

3.2.3. *Newly identified phosphorylation sites*

We compared our phosphoproteome data to published phosphoprotein repositories that contained human, mouse, and rat databases (www.phosphosite.org, www.phosida.com and www.uniprot.org). 154 phosphorylation sites (17.2%) from our study have not previously been described identified as phosphorylation sites in human, mouse, or rat homologues proteins and 173 phosphorylation sites (18.3%) are phosphorylation sites described by similarity (Table 3).

3.3. *Protein and phosphoprotein validation*

To confirm the quantitative MS data, Western blot analyses were performed for selected proteins and phosphoproteins (using regular and phosphorylation-site-specific antibodies). For phosphoproteins validated by Western-blotting, total protein expression levels were determined to differentiate the changes arising from protein expression or from phosphorylation stoichiometry.

Table 2 – Macrophage phosphopeptides that significantly increased in abundance in response to *C. albicans*.

Protein ID	Swiss accession	Protein name	Peptide(s) sequence(s) [a]	Ratio (log_2 H/L)	CV	Mod site	Max Ascore [b]
Stress response/oxidoreductasa activity							
Cyba	Q61462	Cytochrome b-245 light chain	KKPpSEGEEEAASAGGPQVNPMPVTDEVV	1.31	0.33	168	11.92
Tmx1	Q8VBT0	Thioredoxin-related transmembrane protein 1	VEEEQEADEEDVpSEEEAEDREGASK	0.60	0.20	245	39.79
			KVEEEQEADEEDVpSEEEAEDREGASK	0.61	0.30	245	31.33
Immune response/cell recognition							
Atp6v0a2	P15920	Immune suppressor factor J6B7	KDpSEEEVSLLGNQDIEEGNSR	0.73	0.18	695	15.95
Cd44	P15379	CD44 antigen	KPpSELNGEASK	0.50	0.18	733	34.33
Fcgr1	P26151	High affinity immunoglobulin gamma Fc receptor I	KANpSFQQVR	1.31	0.16	347	Infinity
			ANpSFQQVR	1.36	0.19	347	Infinity
Hmha1	Q3TBD2	Minor histocompatibility protein HA-1	KGpSFNPGDASGPEAAGSPPEEGGTSEAAPNK	−0.67	0.08	577	30.16
Msr1	P30204	Macrophage scavenger receptor types I and II (CD204)	LCPHEREDADCSpSESVKFDAR	0.96	0.05	23	13.27
			pSMTASLPHSTK	1.13	0.15	32	9.82
			pSMTApSLPHSTK	1.34	0.10	32,36	15.87
Nfatc2	Q60591	Nuclear factor of activated T-cells, cytoplasmic 2	DAGLpSPEQPALALAGVAASPR	−0.93	0.02	136	116.16
Inpp5d	Q9ES52	Phosphatidylinositol-3,4,5-trisphosphate 5-phosphatase 1	GEGPPTPPSQPPLpSPK	−0.75	0.16	972	33.91
			DSSLGPGRGEGPPTPPSQPPLpSPK	−0.65	0.19	972	49.21
			STLpSPDQQLTAWSYDQLPK	1.25	0.02	935	12.22
Spp1	P10923	Osteopontin	LVLDPKpSKEDDR	0.60	0.33	271	Infinity
			FRIpSHELESSpSSEVN	1.80	0.02	283, 290	49.62
Lcp1	Q61233	Plastin-2	GSVpSDEEMMELR	0.98	0.14	7	24.75
Ebag9	Q9D0V7	Estrogen receptor-binding fragment-associated gene 9 protein	KLpSGDQITLPTTVDYSSVPK	0.69	0.15	36	92.87
Rtn4	Q99P72	Reticulon-4	RRGSGpSVDETLFALPAASEPVIPSSAEK	0.55	0.14	167	8.91
Sash3	Q8K352	SAM and SH3 domain-containing protein 3	RKPpSNASDKEPTQK	−1.22	0.11	7	
Ufl1	Q8CCJ3	E3 UFM1-protein ligase 1	KDEDpSDDESQSSHGGK	0.63	0.12	458	57.39
			GRKDEDpSDDESQSSHGGK	0.63	0.09	458	82.44
Cytoskeletal components and actin binding proteins							
Apbb1ip	Q8R5A3	Amyloid beta A4 precursor protein-binding family B member 1-interacting protein	RSpSDTCGpSPALPSK	−0.71	0.09	532, 537	27.56
			RSpSDTCGSPALPSK	−0.64	0.21	532	17.90
Agfg1	Q8K2K6	Arf-GAP domain and FG repeats-containing protein 1	GTPpSQSPVVGR	−0.58	0.16	179	
Cd2ap	Q9JLQ0	CD2-associated protein	pSVDLDAFVAR	0.51	0.12	458	Infinity
Clasp1	Q80TV8	CLIP-associating protein 1	SRpSDIDVNAAASAK	−0.50	0.10	600	9.82
Dock2	Q8C3J5	Dedicator of cytokinesis protein 2	VEEEPIpSPGSTLPEVK	1.03	0.10	1683	11.56
Epb41l2	O70318	Protein 4.1G	AKEVENEQTPVSEPEEEKGpSQPGPPVER	0.64	0.13	38	8.05
Fmnl2	A2APV2	Formin-like protein 2	pSIEDLHR	0.50	0.11	171	
Tubgcp2	Q921G8	Gamma-tubulin complex component 2	VLAIEpTK	0.66	0.34	594	
Kif22	Q3V300	Kinesin-like protein KIF22	QVEpSFLK	−0.52	0.31	642	
Lima1	Q9ERG0	LIM domain and actin-binding protein 1	RLpSENNCSLDDWEIGAGHLSSSAFNSEK	1.08	0.27	225	34.46
			SDNEETLGRPAQPPNAGESPHpSPGVEDAPIAK	1.38	0.26	488	19.55
Lmna	P48678	Prelamin-A/C	ASSHSSQSQGGGpSVTK	0.73	0.15	414	21.30
			KLEpSSESR	0.78	0.35	423	
			ASSHpSpSQSQGGGSVTK	0.81	0.17	406, 407	17.01
Lnp	Q7TQ95	Protein lunapark	ADpSVPNLEPSEESLVTK	0.77	0.36	411	58.26
Myo5a	Q99104	Myosin-Va	TSpSIADEGTYTLDSILR	0.86	0.22	1650	16.20

Myo9b	Q9QY06	Myosin-IXb	AQDKPESPSGpSTQIQR	0.59	0.03	1268	7.38
Fam82a2	Q3UJU9	Regulator of microtubule dynamics protein3	SHpSLPNSLDYAQASER	0.60	0.15	46	8.58
Stmn1	P54227	Stathmin	RApSGQAFELILSPR	0.66	0.02	16	97.62
			ASGQAFELILpSPR	1.21	0.36	25	87.22
Tns3	Q5SSZ5	Tensin-3	KLpSIGQYDNDAASQVTFSK	−0.52	0.35	769	9.53
Twf2	Q9Z0P5	Twinfilin-2	LIRGPGENGEDpS	−0.56	0.13	349	
Vasp	P70460	Vasodilator-stimulated phosphoprotein	NSTpTLPR	−0.74	0.35	311	13.24
			KVpSKQEEASGGPLAPK	−0.50	0.08	235	42.90
Signal transduction							
Arhgef2	Q60875	Rho guanine nucleotide exchange factor 2	ANpSRDGEAGR	1.08	0.07	781	Infinity
			LEpSFESLR	1.40	0.08	646	49.62
Arhgef6	Q8K4I3	Rho guanine nucleotide exchange factor 6	KApSEEEYVIR	−0.60	0.21	639	20.12
			KDpSVPQVLLPEEEK	−0.59	0.12	679	Infinity
Arhgef7	Q9ES28	Rho guanine nucleotide exchange factor 7	KEpSAPQVLLPEEEKIIVEETK	−0.52	0.20	776	76.11
Ccny	Q8BGU5	Cyclin-Y	SApSADNLILPR	0.50	0.17	326	10.28
Cdk4	P30285	Cyclin-dependent kinase 4	ALQHSYLHKEEpSDAE	−0.51	0.11	300	35.16
Dock7	Q8R1A4	Dedicator of cytokinesis protein 7	SLSNpSNPDISGTPTSPDDEVR	−1.27	0.55	900	24.21
Dok1	P97465	Docking protein 1 (p62)	VGQAQDILRTDpSHDGETEGK	0.61	0.08	269	
Jun	P05627	Proto-oncogene c-Jun	LApSPELER	2.33	0.12	73	Infinity
Mef2c	Q8CFN5	Myocyte-specific enhancer factor 2C	NpSPGLLVSPGNLNK	−1.56	0.65	222	52.41
Map4k6	Q9JM52	MAPK/ERK kinase kinase kinase 6	LDSpSPVLSPGNK	−0.60	0.19	746	10.28
Marcksl1	P28667	Macrophage myristoylated alanine-rich C kinase substrate	GDVTAEEAAGApSPAK	0.52	0.15	22	79.33
			GEVAPKEpTPK	1.01	0.33	85	Infinity
			AAApTPESQEPQAK	1.97	0.45	148	46.24
Nucks1	Q80XU3	Nuclear ubiquitous casein and cyclin-dependent kinases substrate	LKATVTPpSPVKGK	−1.03	0.08	181	29.98
			SGKNSQEDpSEDpSEEKDVK	−0.85	0.10	58,61	40.34
Pkn1	P70268	Serine/threonine-protein kinase N1	TDVSNFDEEFTGEAPTLpSPPR	−0.52	0.20	920	30.70
Pgrmc1	O55022	Membrane-associated progesterone receptor component 1	LLKEGEEPTVYpSDDEEPKDETAR	0.58	0.16	181	18.99
Psen1	P49769	Presenilin-1	AAVQELSGSILpTSEDPEER	0.82	0.22	370	19.16
Ptpn6	P29351	Tyrosine-protein phosphatase non-receptor type 6	DLpSGPDAETLLK	−0.51	0.21	10	60.94
Tbc1d10b	Q8BHL3	TBC1 domain family member 10B	RApSAGPVPGAVVIAEGLHPSLPSPTGNSTPLGTSK	−0.69	0.11	673	66.92
Tbc1d15	Q9CXF4	TBC1 domain family member 15 (GTPase-activating protein RAB7)	SLSQpSFENLLDEPAYGLIQK	0.91	0.13	205	
Brf1	Q8CFK2	Transcription factor IIIB 90 kDa subunit	GGGpSPPRDDSQPPER	−0.50	0.03	552	
Mbp	P04370	Myelin basic protein	pSVGKLSQTASEDSDVFGEADAIQNNGTSAEDTAVTDSK	−0.51	0.05	31	16.18
Metabolism							
Nop56	Q9D6Z1	Nucleolar protein 56	KFpSEEPEVAANFTK	1.10	0.16	554	54.79
Plcb3	P51432	1-Phosphatidylinositol-4,5-bisphosphate phosphodiesterase beta-3	NNpSISEAK	−0.50	0.17	1105	
Ampd2	Q9DBT5	AMP deaminase 2	QIpSQDVKLEPDILLR	0.55	0.14	87	Infinity
Bckdk	O55028	[3-methyl-2-oxobutanoate dehydrogenase [lipoamide]] kinase, mitochondrial	STSApTDTHHVELAR	0.58	0.21	35	9.62
Galnt7	Q80VA0	N-acetylgalactosaminyltransferase 7	HAGGDpSQRDVMQR	0.88	0.06	103	
Phka2	Q8BWJ3	Phosphorylase b kinase regulatory subunit alpha, liver isoform	pSLNLVDSPQPLLK	−0.77	0.17	729	88.57
Nudt5	Q9JKX6	ADP-sugar pyrophosphatase	ESTESpSPGKHLVTSEELISEGK	−0.50	0.02	10	
Nvl	Q9DBY8	Nuclear valosin-containing protein-like	ESLPLDLpSDDQSNSK	−0.64	0.49	190	15.62
Trim65	Q8BFW4	Tripartite motif-containing protein 65	RDpSATSHSAR	−0.59	0.30	89	28.35

(continued on next page)

Table 2 (*continued*)

Protein ID	Swiss accession	Protein name	Peptide(s) sequence(s) [a]	Ratio (log_2 H/L)	CV	Mod site	Max Ascore [b]
Nucleic acid processing							
Npm1	Q61937	Nucleophosmin	DLKPpSTPR	0.77	0.12	216	7.38
Ccdc88b	Q4QRL3	Coiled-coil domain-containing protein 88B	LGADGAGpSTESLGGPLETELPEGR	−1.07	0.39	1350	16.22
			AQVLKQEpSPK	−0.95	0.59	649	Infinity
Bclaf1	Q8K019	Bcl-2-associated transcription factor 1	SIFREEpSPLR	0.58	0.30	529	43.29
			EVQpSPEQVK	0.58	0.20	494	Infinity
			DNHNQADHpSPLTTAAPFSR	0.61	0.06	658	13.15
			KAEGEPQEEpSPLK	0.62	0.23	177	Infinity
			KEVQpSPEQVK	0.77	0.27	494	Infinity
			IDIpSPSALR	0.80	0.33	656	22.01
			KAEGEPQEESPLKpSK	0.80	0.29	181	22.24
			NTPSQHSHSIQHpSPER	0.90	0.27	267	16.76
			ADGDWDDQEVLDYFpSDKESAK	0.91	0.42	383	14.89
			GRADGDWDDQEVLDYFpSDKESAK	1.37	0.07	383	4.08
Cbx8	Q9QXV1	Chromobox protein homolog 8	VDDKPSpSPGDSSK	−0.70	0.17	164	
Csda	Q9JKB3	DNA-binding protein A (Cold shock domain-containing protein A)	pSRPLNAVSQDGK	−0.59	0.27	328	80.89
Ddx21	Q9JIK5	Nucleolar RNA helicase 2	EIITEEPpSEEEADMPKPK	0.62	0.11	118	26.42
Ddx24	Q9ESV0	ATP-dependent RNA helicase DDX24	AQAVpSEEEEEEEGQSSSPK	−0.68	0.22	80	63.31
			FGATAHLGpSPCKDR	−0.63	0.47	288	11.89
Eef2	P58252	Elongation factor 2	FpTDTRKDEQER	−0.82	0.21	57	
Eif3b	Q8JZQ9	Eukaryotic translation initiation factor 3 subunit B	GHPSAGAEEEGGpSDGSAAEAEPR	0.55	0.22	120	64.46
Fip1l1	Q9D824	Pre-mRNA 3′-end-processing factor FIP1	RHEpSEEGDSHR	0.54	0.21	541	79.50
Hist1h1c	P15864	Histone H1.2	KApTGAATPKK	−0.50	0.00	142	23.64
Hist1h1d	P43277	Histone H1.3					
Hmgn1	P18608	Non-histone chromosomal protein HMG-14	KVpSADGAAK	3.09	0.08	7	Infinity
Hnrnph1	O35737	Heterogeneous nuclear ribonucleoprotein H	HTGPNpSPDTANDGFVR	0.71	0.31	104	14.89
Eif4g1	Q6NZJ6	Eukaryotic translation initiation factor 4 gamma 1	TASTPpTPPQTGGSLEPQPNGESPQVAVIIRPDDR	−1.10	0.37	214	18.99
			TQpTPPLGQTPQLGLK	−0.68	0.16	507	10.28
Tmpo	Q61029	Lamina-associated polypeptide 2, isoforms beta/delta/epsilon/gamma	AKpTPVTLK	0.57	0.17	207	34.46
			QNGSNDSDRYpSDNDEDSKIELK	0.62	0.06	183	12.20
Larp4b	Q6A0A2	La-related protein 4B	RApSPPAAGK	−0.70	0.27	721	Infinity
			SPpSPVHLPEDPKVAEK	−0.52	0.26	603	12.32
Larp1	Q6ZQ58	La-related protein 1	DGAERESPRPPAAAEAPAGpSDGEDGGRR	−1.01	0.31	81	17.86
			ETESAPGpSPR	−0.83	0.45	498	23.64
			AVpTPVPTKTEEVSNLK	−0.59	0.42	503	31.51
			ESPRPPAAAEAPAGpSDGEDGGRR	−0.52	0.20	81	33.72
			SLPTTVPEpSPNYR	−0.50	0.26	751	26.21
Lrrfip1	Q3UZ39	Leucine-rich repeat flightless-interacting protein 1	AENQRPAEDSALpSPGPLAGAK	1.24	0.47	302	107.89
Lsm14a	Q8K2F8	Protein LSM14 homolog A	RpSPVPARPLPPTSQK	−0.72	0.16	216	
Lemd3	Q9WU40	Inner nuclear membrane protein Man1	VLLGFSSDEpSDVEASPR	0.69	0.07	140	13.38
Mybbp1a	Q7TPV4	Myb-binding protein 1A	DIPSDpTQSPVSTK	0.58	0.24	1162	10.33
			DIPSDTQpSPVSTK	0.61	0.22	1164	13.15
			LSQVNGATPVpSPIEPESK	0.77	0.20	1280	13.38
Med24	Q99K74	Mediator of RNA polymerase II transcription subunit 24	LLSpSSDDDANILSSPTDR	0.50	0.16	861	24.44

Ncbp1	Q3UYV9	Nuclear cap-binding protein subunit 1	KTpSDANETEDHLESLICK	0.58	0.09	22	4.97
			RKpTSDANETEDHLESLICK	0.65	0.06	21	5.29
			RHSpYENDGGQPHKR	0.92	0.19	8	9.25
Ncoa3	O09000	Nuclear receptor coactivator 3	AVpSLDSPVSVGSGPPVK	−1.04	0.40	847	55.25
Ncl	P09405	Nucleolin	VEGpSEPTTPFNLFIGNLNPNK	−0.97	0.53	303	8.08
Serbp1	Q9CY58	Plasminogen activator inhibitor 1 RNA-binding protein	TDKSpSASAPDVDDPEAFPALA	0.93	0.04	391	13.27
			pSKSEEAHAEDSVMDHHFR	1.86	0.15	327	31.51
Pbxip1	Q3TVI8	Pre-B-cell leukemia transcription factor-interacting protein 1	GREPpSSSQPVVPVDVEDQAK	−0.51	0.07	164	11.51
Raly	Q64012	RNA-binding protein Raly	LPAPQEDTApSEAGTPQGEVQTR	0.51	0.27	270	22.01
Rbl1	Q64701	Retinoblastoma-like protein 1	VIAISGDADpSPAKR	−0.90	0.06	1036	39.33
Rbm14	Q8C2Q3	RNA-binding protein 14	TRLpSPPR	−0.79	0.60	582	
Rfc1	P35601	Replication factor C subunit 1	KDpSEEGEESFSSVQDDLSK	0.58	0.04	244	63.34
Sfrs9	Q9D0B0	Serine/arginine-rich splicing factor 9	GpSPHYFSPFRPY	0.62	0.04	212	26.79
Slirp	Q9D8T7	SRA stem-loop-interacting RNA-binding protein, mitochondrial	ALHGAQTpSDEER	0.72	0.27	105	10.28
Srrm2	Q8BTI8	Serine/arginine repetitive matrix protein 2	RQPpSPQPpSPR	0.60	0.14	2656, 2660	Infinity
Top2b	Q64511	DNA topoisomerase 2-beta	KTSFDQDpSDVDIFPSDFTSEPPALPR	−1.07	0.00	1568	25.73
Thrap3	Q569Z6	Thyroid hormone receptor-associated protein 3	ERpSPALK	0.60	0.26	248	Infinity
			NKKpSPEIHR	0.73	0.24	669	Infinity
			ASVSDLpSPR	0.73	0.25	243	46.24
			IDISPpSTFR	0.82	0.23	681	11.95
			RIDIpSPSTFR	0.93	0.26	679	11.36
			ERpSPALKpSPLQSVVVR	0.96	0.01	248, 253	50.82
Trex2	Q9R1A9	Three prime repair exonuclease 2	pSSLENPER	−3.53	0.09	38	
Np95	Q8VDF2	Nuclear protein 95	RPLIApSPSQPPPALR	−1.09	0.31	289	12.16
Ybx1	P62960	Nuclease-sensitive element-binding protein/Y-box-binding protein 1	NEGSEpSAPEGQAQQR	−1.30	0.45	174	12.20
Zfp106	O88466	Zinc finger protein 106	ATHVPENpSDTEQDVFTAKPAR	−0.59	0.00	1381	24.15
Zfr	O88532	Zinc finger RNA-binding protein	RRDpSDGVDGFEAEGK	1.04	0.14	1054	Infinity
Transport							
Golga5	Q9QYE6	Golgin subfamily A member 5	KKpSEPDDELLFDFLNSSQK	0.60	0.28	116	53.43
Slc43a2	Q8CGA3	Large neutral amino acids transporter small subunit 4	LCLpSTVDLEVK	0.63	0.22	297	24.44
Aaat	P51912	Neutral amino acid transporter B	NEVpSLNPLPLATEEGNPLLK	0.74	0.24	518	94.00
Slc35c2	Q8VCX2	Solute carrier family 35 member C2	SLGpSSADLELLLR	0.52	0.19	335	10.28
Slc1a5	P51912	Solute carrier family 1 member 5	MPSpSEPELIQVK	0.82	0.21	506	
			MPpSSEPELIQVK	1.18	0.46	505	
Slc16a1	P53986	Solute carrier family 16 member 1	LKpSKEpSLQEAGK	0.74	0.15	210, 213	Infinity
Mcoln1	Q99J21	Mucolipin-1	RApSETER	0.51	0.28	10	24.84
Nucb1	Q02819	Nucleobindin-1	KVPEQPPELPQLDpSQHL	0.65	0.14	456	Infinity
			AQRLpSQETEALGR	0.89	0.29	368	21.99
Prpf4b	Q61136	Serine/threonine-protein kinase PRP4 homolog	LCDFGSASHVADNDITPpYLVSR	0.51	0.09	849	28.76
Rab7a	P51150	Ras-related protein Rab-7a	FQpSLGVAFYR	2.47	0.02	72	68.95
Ranbp2	Q9ERU9	E3 SUMO-protein ligase RanBP2	SHETDGGpSAHGDEEDDGPHFEPVVPLPDKIEVK	−0.59	0.17	1154	13.59
Sap30	O88574	Histone deacetylase complex subunit SAP30	KGpSDDDGGDSPVQDIDTPEVDLYQLQVNTLR	0.62	0.19	131	19.32
Scamp3	O35609	Secretory carrier-associated membrane protein 3	KLpSPTEPR	1.01	0.27	78	13.27
Scn10a	Q6QIY3	Sodium channel protein type 10 subunit alpha	WQREEpSPR	−0.61	0.31	1071	
Sgpp1	Q9JI99	Sphingosine-1-phosphate phosphatase 1	RNpSLTGEEGELVK	0.57	0.19	101	18.88
Snap23	O09044	Synaptosomal-associated protein 23	ATWGDGGDNpSPSNVVSK	0.52	0.17	110	13.15
Stx4	P70452	Syntaxin-4	QGDNIpSDDEDEVR	0.54	0.13	15	Infinity

(continued on next page)

Table 2 (*continued*)

Protein ID	Swiss accession	Protein name	Peptide(s) sequence(s) [a]	Ratio (log_2 H/L)	CV	Mod site	Max Ascore [b]
Nucleic acid processing							
Stt3b	Q3TDQ1	Source of immunodominant MHC-associated peptides	ENPPVEDpSpSDEDDKRNPGNLYDK	0.56	0.32	495, 496	52.58
Tcof1	O08784	Treacle protein	AASAPAKEpSPK	0.51	0.23	794	30.85
			KLpSGDLEAGAPK	0.72	0.12	1191	Infinity
Tram1	Q91V04	Translocating chain-associated membrane protein 1	GTENGVNGTVTSNGADpSPR	0.53	0.27	365	42.07
Vamp4	O70480	Vesicle-associated membrane protein 4	NLLEDDpSDEEEDFFLR	0.54	0.20	30	Infinity
Ap3d1	O54774	AP-3 complex subunit delta-1	HSSLPTEpSDEDIAPAQR	−0.71	0.26	760	22.01
Protein fate							
Copa	Q8CIE6	Coatomer subunit alpha	NLpSPGAVESDVR	0.58	0.22	173	52.62
Dnajc5	P60904	DnaJ homolog subfamily C member 5	pSLSTSGESLYHVLGLDK	0.55	0.28	8	6.97
Psmf1	Q8BHL8	Proteasome inhibitor PI31 subunit	ANpSPPREFPPATAR	−0.63	0.26	153	90.46
Ptpra	P18052	Receptor-type tyrosine-protein phosphatase alpha	TEDVEPQSVPLLARpSPSTNR	0.81	0.24	202	24.15
Bat2d	Q3TLH4	BAT2 domain-containing protein 1	ATSTpSPNSQSSK	−0.71	0.42	2628	15.06
Ssr1	Q9CY50	Signal sequence receptor subunit alpha	VEMGTSSQNDVDMSWIPQETLNQINKApSPR	0.75	0.34	268	17.11
			AQKRpSVGSDE	1.30	0.00	281	37.91
Ssr3	Q9DCF9	Signal sequence receptor subunit gamma	KLpSEADNR	0.80	0.06	105	Infinity
Tomm70a	Q9CZW5	Mitochondrial import receptor subunit TOM70	NSERKpTPEGR	0.53	0.28	88	
Usp10	P52479	Ubiquitin carboxyl-terminal hydrolase 10	TCDpSPQNPVDFISGPVPDSPFPR	−0.58	0.23	208	
Unknown function							
Atxn2l	Q7TQH0	Ataxin-2-like protein	STSTPTpSPGPR	−0.78	0.12	687	
HCFT1	Q99M08	Uncharacterized protein C4orf3 homolog	RGpSFEAGR	0.55	0.16	19	Infinity
Ct030	Q8CIB6	UPF0414 transmembrane protein C20orf30 homolog	LApSTDDGYIDLQFK	1.18	0.24	24	18.42
Ehbp1l1	Q99MS7	EH domain-binding protein 1-like protein 1	VApSRDTDLSCSSK	−0.50	0.07	1383	30.66
Evi2b	Q8VD58	Ecotropic viral integration site 2b (CD361)	LFEpSSEHINDTSNLK	0.56	0.25	295	20.35
Hn1	P97825	Hematological and neurological expressed 1 protein	SNpSSEASSGDFLDLK	1.04	0.27	87	21.51
Plekho2	Q8K124	Pleckstrin homology domain-containing family O member 2	ALpTPDSASSGANPESQEDAETPAKEDSDVK	0.51	0.12	233	27.14
Rsrc2	A2RTL5	Arginine/serine-rich coiled-coil protein 2	LNpSSENGEDR	0.53	0.07	45	32.40
Fam83h	Q148V8	Protein FAM83H	KGpSPTPAYPER	−0.54	0.23	893	30.70
Pphln1	Q8K2H1	Periphilin-1	DAPFFREpSPVGR	0.58	0.05	147	

[a] The preceding p indicates phosphorylated amino acid.
[b] Sites with Ascores > 13 have a p-value <0.05 and >95% certainty for correct phosphorylation site localization. Sites with Ascores > 19 have a p-value <0.01 and >99% certainty for correct phosphorylation site localization.

Vimentin and Mcl1 protein levels were determined (Fig. 2A, B). Phosphorylation levels of the transcription factor c-Jun at Ser^{63} and the elongation factor Eef2 at Thr^{57} + Thr^{59} were also measured (Fig. 2C, D) and compared to the non-phosphorylated protein (total protein expression levels were determined to differentiate the changes arising from protein expression or from phosphorylation stoichiometry). Increase in Vimentin and Mcl1 expression, the increase in c-Jun phosphorylation levels and the decrease in Eef2 phosphorylation corroborated the MS results.

Vimentin is a cytoskeletal protein that is part of intermediate filaments which has also been implicated in inflammation and bactericidal effects of macrophages [33–35]. We previously detected overexpression of Vimentin in macrophages incubated with *C. albicans* [17] while expression was decreased during the interaction with heat inactivated-*C. albicans* [18]. To visualize the subcellular localization of Vimentin during phagocytosis of *C. albicans*, we performed confocal immunofluorescence studies. Macrophages were incubated with *C. albicans* expressing blue-fluorescent protein (BFP) for 3 h followed by immunofluorescent staining using a Vimentin antibody. The observed Vimentin localization resembles intermediate filaments and did not change after 3 h of coincubation with *C. albicans* (Fig. 3A), suggesting that Vimentin does not play a direct role in formation of the phagocytic cup. Quantification of fluorescence intensity showed that levels of Vimentin are increased after 3 h of coincubation with *C. albicans*, which is in line with our proteomics data (Fig. 3B).

3.4. *Measurement of the apoptotic status of macrophages following interaction with C. albicans*

As many of the differentially expressed proteins and phosphoproteins founded in this study were related to apoptosis (Suppl. Figs. S1 and S2), the apoptotic status of RAW 264.7 macrophages after different time points of interaction with the yeast was analyzed. Macrophages were incubated with *C. albicans* or with 5 mM Staurosporine for 45 min, 1.5, 3, 6, 8, 12 and 24 h followed by chromatin condensation assays. While Staurosporine-incubated macrophages displayed an increase in positive chromatin condensation over time up to 100% after 24 h, incubation with *C. albicans* did not lead to a significant increase in positive macrophages over time (<15%) (Fig. 4A, B).

In addition, we performed terminal deoxynucleotidyl transferase dUTP nick end labeling (TUNEL) assays to investigate macrophage apoptosis in the presence of *Candida*. No DNA condensation and degradation characteristic of apoptotic cells was detected at any of the incubation periods tested (Suppl. Fig. S3B, C).

Caspase-3 activation by cleavage is a hallmark of apoptosis. To determine whether Caspase-3 was activated in RAW 264.7 cells during interaction with *Candida*, macrophages were treated with 5 mM Staurosporine or exposed to *C. albicans* at different interaction times. Activated Caspase-3 was assayed by Western blotting using cell free lysates prepared from these cultures. Activated (cleaved) Caspase-3 was detectable in Staurosporine-treated cells but only minimal levels of activated Caspase-3 were detectable in macrophages incubated with *Candida* (Suppl. Fig. S3A). Fragmentation of Vimentin is also associated with apoptosis in macrophages [36,37], Western-blotting studies were carried out to investigate Vimentin fragmentation at different time points (45 min, 1.5, 3, 6 and 8 h) but no fragmentation was detectable (data not shown). In conclusion, while apoptotic proteins were identified as differentially expressed in our (phospho)proteomics studies, chromatin condensation assays, TUNEL assays and Caspase-3 and Vimentin cleavage studies indicate that apoptosis is not increased in macrophages incubated with *C. albicans*.

4. Discussion

Macrophages are the first line of defense against *Candida* infections and prevent spreading of the fungus after colonization. Efforts within our group have focused on studying the interaction between macrophages and *C. albicans* to identify yeast virulence factors and host factors important for anti-fungal responses [17–19]. PRR recognition of *C. albicans* by macrophages leads to activation of downstream kinases that controls metabolism, signal transduction, stress response and protein fate. In this study we therefore took a quantitative (phospho)-proteomics SILAC approach to identify differentially expressed and phosphorylated macrophage proteins after 3 h of interaction with *C. albicans*. 53 macrophage proteins were significantly more abundant after incubation with *Candida*, while the expression of 15 proteins was decreased in the samples with the yeast. Phosphopeptide enrichment allowed us to identify 922 non-redundant phosphorylation sites, of which 126 peptides showed an increased and 70 a decreased phosphorylation. Differentially expressed proteins and phosphoproteins have been grouped according to their biological role in macrophages in Tables 1 and 2. Their possible roles in the inflammatory response, the apoptotic status and in cytoskeletal rearrangement are discussed below.

4.1. *C. albicans induces pro-inflammatory and stress responses*

One of the major macrophage responses against *C. albicans* is the up-regulation of pro-inflammatory pathways and the production of reactive oxygen species [17]. As can be observed in Tables 1 and 2, our study identified 29 differentially expressed proteins related to oxidative stress and to the inflammatory response. A schematic model illustrating the differentially expressed oxidative and inflammatory (phospho)-proteins is depicted in Fig. 5.

Upon interaction with *C. albicans*, the generation of the oxidative burst is initiated by the NADPH oxidase enzyme complex [38]. This complex is composed of several membrane subunits, including the cytochrome b-light chain subunit (Cyba, also known as p22-phox) [39] that is up-regulated in our studies. Cyba produces large amounts of antimicrobial ROS such as the superoxide anion (O_2^-), hydrogen peroxide (H_2O_2), and nitric oxide (NO^-). Additionally, the elevated expression of Pex11b, the glucose transporter Glut1 and CD36, together with the decrease in Fabp4, may also relate to the production of O_2^-, H_2O_2 and NO^-. Selenoprotein S (SelS), Ubiquinone biosynthesis protein (Coq9) and Pyrroline-5-carboxylate reductase 1 (Pycr) are other up-regulated proteins

Table 3 – New phosphorylation sites in RAW 264.7 macrophages.

Protein ID	Swiss accession	Protein name	Peptide sequence [a]	Ratio (log2 H/L)	CV	By similarity [b]	Novel p-site [c]	Max Ascore [d]
Cul4b	A2A432	Cullin-4B	DpSASPSTSSFCLGVPVATSSHVPIQK	−0.12	0.15		147	
Kiaa1429	A2AIV2	Protein virilizer homolog	SFLSEPpSSPGR	0.17	0.19		1577	10.28
Fmnl2	A2APV2	Formin-like protein 2	pSIEDLHR	0.50	0.11	171		
Ppig	A2AR02	Peptidyl-prolyl cis-trans isomerase G	pSPPKADDKER	−0.26	0.20	288		Infinity
Ppig	A2AR02	Peptidyl-prolyl cis–trans isomerase G	SELNEIKENQRpSPVR	−0.23	0.20	395		25.85
Ppig	A2AR02	Peptidyl-prolyl cis–trans isomerase G	ADREQpSPVSK	0.02	0.13	685		44.52
Ppig	A2AR02	Peptidyl-prolyl cis–trans isomerase G	FRRpSEpTPPHWR	0.02	0.02	354, 356		Infinity
Ppig	A2AR02	Peptidyl-prolyl cis–trans isomerase G	KADREQSPVpSK	0.03	0.11		688	33.18
Arid1a	A2BH40	AT-rich interactive domain-containing protein 1A	SHHAPMpSPGSSGGGGQPLAR	0.39	0.06	365		6.92
Rsrc2	A2RTL5	Arginine/serine-rich coiled-coil protein 2	LNpSSENGEDR	0.53	0.07	45		32.40
Pex10	B1AUE5	Peroxisome biogenesis factor 10	RSpSLEDR	0.28	0.14		259	22.85
Tcof1	O08784	Treacle protein	DSApSPIQK	0.07	0.17	1303		33.70
Tcof1	O08784	Treacle protein	EASSGSpTPQKPK	0.36	0.14		1114	9.34
Mrp	O35379	Multidrug resistance-associated protein 1	GpSSQLDVNEEVEALIVK	0.48	0.20		289	6.36
Bok	O35425	Bcl-2-related ovarian killer protein	ApSPAPGGR	0.41	0.16		57	
Api5	O35841	Apoptosis inhibitor 5	TSEDTSpSGSPPK	0.00	0.14		462	21.51
Ncf2	O70145	Neutrophil cytosol factor 2	ATVVASVVHQDNFSGFAPLQPQSAEPPPRPKpTPEIFR	−0.43	0.01		233	16.77
Ncf2	O70145	Neutrophil cytosol factor 2	pTPEIFR	−0.26	0.02		233	Infinity
Ncf2	O70145	Neutrophil cytosol factor 2	IHPQSQPQEDTSPESDIPPPPNSpSPPGR	−0.16	0.09		323	18.30
Ncf2	O70145	Neutrophil cytosol factor 2	LQLpSPGHK	0.19	0.09		332	Infinity
Pip5k1c	O70161	Phosphatidylinositol 4-phosphate 5-kinase type-1 gamma	RTQpSSGQDGRPQEEPHAEDLQK	0.22	0.03		554	
Pip5k1c	O70161	Phosphatidylinositol 4-phosphate 5-kinase type-1 gamma	TQpSSGQDGRPQEEPHAEDLQK	0.49	0.09		554	6.97
Nmt1	O70310	Glycylpeptide N-tetradecanoyltransferase 1	SGLpSPANDTGAK	−0.11	0.15	47		22.01
Dok2	O70469	Docking protein 2	KGpSPGLEEK	−0.12	0.25		124	Infinity
Zfp106	O88466	Zinc finger protein 106	ATHVPENpSDTEQDVFTAKPAR	−0.59	0.00	1381		24.15
Sap30	O88574	Histone deacetylase complex subunit SAP30	KGSDDDGGDpSPVQDIDTPEVDLYQLQVNTLR	0.62	0.19	137		19.32
Pak1	O88643	Serine/threonine-protein kinase PAK 1	DVATSPISPTENNTpTPPDALTR	0.16	0.20	230		21.51
Mbp	P04370	Myelin basic protein	pSVGKLSQTASEDSDVFGEADAIQNNGTSAEDTAVTDSK	−0.51	0.05		31	16.18
Ncl	P09405	Nucleolin	AAVpTPGKK	0.28	0.05		84	Infinity
Ncl	P09405	Nucleolin	VEGSEPpTTPFNLFIGNLNPNK	−0.97	0.53		303	8.08
Spp1	P10923	Osteopontin	LVLDPKpSKEDDR	0.60	0.33		271	Infinity
CDK3	P11440;P97377;Q80YP0		IGEGpTpYGVVYK	0.01	0.05	14		72.25
Lmnb1	P14733	Lamin-B1	VTVpSRASSSR	0.31	0.01		402	10.33
Hist1h1c	P15864	Histone H1.2	KATGAApTPKK	−0.50	0.00		146	23.64
Ptpra	P18052	Receptor-type tyrosine-protein phosphatase alpha	TEDVEPQSVPLLARpSPSTNR	0.81	0.24		202	24.15
Nelfe	P19426	Negative elongation factor E	pSLSEQPVVDTATATEQAK	−0.04	0.13		49	7.71
Nfkb1	P25799	Nuclear factor NF-kappa-B p105 subunit	KLpSFTESLTGDSPLLSLNK	−0.31	0.04	940		13.27
Bmi1	P25916	Polycomb complex protein BMI-1	KSpSLNGSSATSSG	−0.23	0.02		314	7.87
U2af2	P26369	Splicing factor U2AF 65 kDa subunit	GAKEEHGGLIRpSPR	−0.08	0.02	79		Infinity
Apex1	P28352	DNA-(apurinic or apyrimidinic site) lyase	AAADDGEEPKpSEPETK	−0.40	0.15		18	48.99
Apex1	P28352	DNA-(apurinic or apyrimidinic site) lyase	AAADDGEEPKSEPEpTKK	−0.34	0.23		22	12.17
Prkcd	P28867	Protein kinase C delta type	ASTFCGpTPDYIAPEILQGLK	−0.18	0.08		509	8.43

Prkcd	P28867	Protein kinase C delta type	ASTFCGTPDpYIAPEILQGLK	−0.05	0.11		512	8.43
Ptpn6	P29351	Tyrosine-protein phosphatase non-receptor type 6	DLpSGPDAETLLK	−0.51	0.21	10		60.94
Ptpn6	P29351	Tyrosine-protein phosphatase non-receptor type 6	pTSSKHKEEVYENVHSK	−0.32	0.12		555	13.24
Mrs1	P30204	Macrophage scavenger receptor types I and II	LCPHEREDADCSpSESVKFDAR	0.96	0.05		23	13.27
Cdk4	P30285	Cyclin-dependent kinase 4	ALQHSYLHKEEpSDAE	−0.51	0.11		300	35.16
Rpl12	P35979	60S ribosomal protein L12	IGPLGLpSPK	−0.48	0.03	38		Infinity
Lig1	P37913	DNA ligase 1	NQVVPEpSDSPVKR	−0.33	0.12	49		13.15
Htt	P42859	Huntingtin	pSGSIVELLAGGGSSCpSPVLSR	−0.04	0.07	411	396	
Hist1h1e	P43274	Histone H1.4	APKpSPAK	−0.05	0.13	187		Infinity
Hist1h1d	P43277	Histone H1.3	KATGAApTPKK	−0.50	0.00		146	23.64
Sipa1	P46062	Signal-induced proliferation-associated protein 1	SGpSDAGEVRPPTPASPR	−0.46	0.24	53		9.34
Pla2g4a	P47713	Cytosolic phospholipase A2	CSVpSLSNVEAR	0.06	0.15	728		30.70
Lmna	P48678	Prelamin-A/C	KLEpSSESR	0.78	0.35	423		
Brca1	P48754	Breast cancer type 1 susceptibility protein homolog	RApSDAFPEEK	0.18	0.07		686	Infinity
Mcm4	P49717	DNA replication licensing factor MCM4	VpTPTQSLR	−0.12	0.01	19		51.64
Mcm4	P49717	DNA replication licensing factor MCM4	SEESRSpSPNR	−0.25	0.02	32		
Plcb3	P51432	1-Phosphatidylinositol 4,5-bisphosphate phosphodiesterase beta-3	NNpSISEAK	−0.50	0.17		1105	
Aaat	P51912	Neutral amino acid transporter B	MPpSSEPELIQVK	1.18	0.46		505	
Aaat	P51912	Neutral amino acid transporter B	MPSpSEPELIQVK	0.82	0.21		506	
Aaat	P51912	Neutral amino acid transporter B	NEVpSLNPLPLATEEGNPLLK	0.74	0.24		518	94.00
Usp10	P52479	Ubiquitin carboxyl-terminal hydrolase 10	TCDpSPQNPVDFISGPVPDSPFPR	−0.58	0.23	208		
Sh3bp1	P55194	SH3 domain-binding protein 1	ERTEADLPKPTpSPK	−0.27	0.16	456		
Rrp1	P56183	Ribosomal RNA processing protein 1 homolog A	EAGpSEAESSSADPGPGR	−0.03	0.14		434	46.44
Pcbp1	P60335	Poly(rC)-binding protein 1	VMTIPYQPMPApSSPVICAGGQDR	0.12	0.15	190		23.34
Tra2b	P62996	Transformer-2 protein homolog beta	RHpSHpSHSPMSTR	0.49	0.24	95,97		19.59
Pkn1	P70268	Serine/threonine-protein kinase N1	TpSTFCGTPEFLAPEVLTDTSYTR	−0.23	0.05		777	
Tp53bp1	P70399	Tumor suppressor p53-binding protein 1	RSDSPEIPFQAATGpSSDGLDSSSSGNSFVGLR	0.15	0.21	1458		11.53
Tp53bp1	P70399	Tumor suppressor p53-binding protein 1	SEDRPpSSPQVSVAAVETK	0.05	0.24		261	11.51
Tp53bp1	P70399	Tumor suppressor p53-binding protein 1	LHDDEAMETEKPLLPSQPpTVSPQASTPVSR	0.05	0.10		421	7.05
Tp53bp1	P70399	Tumor suppressor p53-binding protein 1	MESLGpSPR	−0.13	0.14		527	35.82
Vasp	P70460	Vasodilator-stimulated phosphoprotein	NSTpTLPR	−0.74	0.35	311		13.24
Wnk1	P83741	Serine/threonine-protein kinase WNK1	KEKPELAEPSHLNGPSpSDLEAAFLSR	0.19	0.23	2007		
Wnk1, Wnk2, Wnk4	P83741; Q3UH66; Q80UE6	Serine/threonine-protein kinase WNK1, WNK2, WNK4	RApSFAK	−0.29	0.17	352		Infinity
Srdf3	P84104	Serine/arginine-rich splicing factor 3	RRpSPPPR	0.18	0.01	108		
Mcm6	P97311	DNA replication licensing factor MCM6	VETPDVNLDQEEEIQMETDEGQGGVNGHADpSPAPVNR	−0.13	0.08		689	13.90
Mcm6	P97311	DNA replication licensing factor MCM6	FNGSSEDApSQETVSKPSLR	0.15	0.20		704	5.92
Etv6	P97360	Transcription factor ETV6	ISYpTPPEpSPVASHR	0.19	0.20	18		16.22
Etv6	P97360	Transcription factor ETV6	RLpSPVEK	−0.21	0.18	215		Infinity
Lig3	P97386	DNA ligase 3	LTTTGQVTpSPVK	−0.16	0.12	211		22.85
Epas1	P97481	Endothelial PAS domain-containing protein 1	RpSSSELR	−0.48	0.32		10	
Smn	P97801	Survival motor neuron protein	GpTGQSDDSDIWDDTALIK	−0.24	0.14	22		21.33
Rbbp6	P97868	E3 ubiquitin-protein ligase RBBP6	VDGDREKpSPR	0.08	0.07		1053	
Hnrnpul2	Q00PI9	Heterogeneous nuclear ribonucleoprotein U-like protein 2	SKpSPPPPEEEAKDEEEDQTLVNLDTYTSDLHFQISK	0.08	0.07	226		24.21
Top1	Q04750	DNA topoisomerase 1	EKENGFpSSPPR	0.21	0.10		113	16.22

(continued on next page)

Table 3 (*continued*)

Protein ID	Swiss accession	Protein name	Peptide sequence [a]	Ratio (log2 H/L)	CV	By similarity [b]	Novel p-site [c]	Max Ascore [d]
Cdk18	Q04899	Cyclin-dependent kinase 18	LGEGTYApTVFK	0.01	0.03	134		
Larp7	Q05CL8	La-related protein 7	pTASEGpSEAETPEAPKQPAK	0.22	0.19	256	251	9.34
Tle3	Q08122	Transducin-like enhancer protein 3	DAPTpSPASVASSSSTPSSK	−0.05	0.20	286		7.93
Ttc21b	Q0HA38	Tetratricopeptide repeat protein 21B	VQpSFLEK	−0.04	0.16		311	
Mcm10	Q0VBD2	Protein MCM10 homolog	LATLFGDVEDLpTDDEVATSK	−0.26	0.17	85		56.02
Gsk3a	Q2NL51	Glycogen synthase kinase-3 alpha	GEPNVSpYICSR	−0.12	0.04	279		
Usp39	Q3TIX9	U4/U6.U5 tri-snRNP-associated protein 2	EADEDpSEPEREVR	0.00	0.04	81		Infinity
Usp39	Q3TIX9	U4/U6.U5 tri-snRNP-associated protein 2	EREADEDpSEPEREVR	0.09	0.11	81		Infinity
Smarca4	Q3TKT4	Transcription activator BRG1Transcription activator BRG1	DSEAGSSTPpTTSTR	0.03	0.07		1392	
Uri1	Q3TLD5	Unconventional prefoldin RPB5 interactor	STSpSEEAVATEAGGSSLDELQENHPK	0.06	0.11		440	13.19
Prrc2c	Q3TLH4	Protein PRRC2C	ATSTpSPNSQSSK	−0.71	0.42		2628	15.06
CI078	Q3TQI7	Uncharacterized protein C9orf78 homolog	VGDpTEKPEPERSPPNR	−0.41	0.07	253		26.37
Pbxip1	Q3TVI8	Pre-B-cell leukemia transcription factor-interacting protein 1	GREPpSSSQPVVPVDVEDQAK	−0.51	0.07		164	11.51
Lbr	Q3U9G9	Lamin-B receptor	KSGpSISpSSPSR	0.04	0.05		67, 70	
D2Wsu81e	Q3UHX9	Uncharacterized protein C9orf114 homolog	TEEAILISLAALQPGLpTQVGSRPApSPLSGPR	0.18	0.04		370, 378	15.32
Arhgap17	Q3UIA2	Rho GTPase-activating protein 17	ADSSSGGGPVFSSTGILEQGLSPGDpSSPPKPK	−0.36	0.01		574	
Edc4	Q3UJB9	Enhancer of mRNA-decapping protein 4	GPGQVSTAASALSLDLQEVEPLGLPQApSPSR	0.20	0.03	727		8.68
Edc4	Q3UJB9	Enhancer of mRNA-decapping protein 4	pTRSPDVISSASTALSQDIPEIASEALSR	−0.12	0.11	731		11.53
Ell2	Q3UKU1	RNA polymerase II elongation factor ELL2	LSNApSPNPNEGVK	0.24	0.18	501		35.40
Ncbp1	Q3UYV9	Nuclear cap-binding protein subunit 1	RKpTSDANETEDHLESLICK	0.65	0.06	21		5.29
Ncbp1	Q3UYV9	Nuclear cap-binding protein subunit 1	RHSpYENDGGQPHKR	0.92	0.19		8	9.25
Lrrfip1	Q3UZ39	Leucine-rich repeat flightless-interacting protein 1	AGpSREPVEDPQSGSSGK	−0.14	0.16	614		42.56
Lrrfip1	Q3UZ39	Leucine-rich repeat flightless-interacting protein 1	SEQQAEALDpSPQKK	−0.24	0.17		547	45.15
Kif22	Q3V300	Kinesin-like protein KIF22	QVEpSFLK	−0.52	0.31		642	
Ckk15	Q3V3A1	Cyclin-dependent kinase 15	pSLPFGAApSSYLNLEK	−0.17	0.04		92,99	
Ccdc88b	Q4QRL3	Coiled-coil domain-containing protein 88B	LGADGAGpSTESLGGPLETELPEGR	−1.07	0.39		1350	16.22
Ccnl1	Q52KE7	Cyclin-L1	AEEKpSPVSINVK	−0.38	0.04	358		18.49
Ccnl1	Q52KE7	Cyclin-L1	GLNLDGTPALSTLGGFpSPApSKPSSPR	−0.36	0.11	341, 344		
Srrm1	Q52KI8	Serine/arginine repetitive matrix protein 1	HRPpSpSPATPPPK	−0.05	0.06	400		7.53
Srrm1	Q52KI8	Serine/arginine repetitive matrix protein 1	HRPpSSPApTPPPK	−0.04	0.05	400		4.35
Srrm1	Q52KI8	Serine/arginine repetitive matrix protein 1	REpSPpSPAPKPR	0.34	0.11	450		Infinity
Srrm1	Q52KI8	Serine/arginine repetitive matrix protein 1	APQTpSSPPPVR	0.04	0.20	713		19.16
Srrm1	Q52KI8	Serine/arginine repetitive matrix protein 1	RRPpSPR	0.08	0.02		320	Infinity
Srrm1	Q52KI8	Serine/arginine repetitive matrix protein 1	HRPpSpSPATPPPK	−0.05	0.06		400, 401	7.53
Srrm1	Q52KI8	Serine/arginine repetitive matrix protein 1	HRPSpSPApTPPPK	0.03	0.06		401, 404	8.58
Srrm1	Q52KI8	Serine/arginine repetitive matrix protein 1	TRHpSPTPQQSNR	0.05	0.11		412	13.79
Srrm1	Q52KI8	Serine/arginine repetitive matrix protein 1	KAQVpSPQS	0.24	0.18		943	32.07
Trap150	Q569Z6	Thyroid hormone receptor-associated protein 3	NKKpSPEIHR	0.73	0.24	669		Infinity
Trap150	Q569Z6	Thyroid hormone receptor-associated protein 3	IDISPpSTFR	0.82	0.23	681		11.95
Mctp2	Q5RJH2	Multiple C2 and transmembrane domain-containing protein 2	VQpYAELK	−0.05	0.14		859	
Synrg	Q5SV85	Synergin gamma	SLpSLGDKEISR	−0.24	0.02	1067		16.99

Lrmp	Q60664	Lymphoid-restricted membrane protein	RSpSTLAWDR	0.15	0.14		450	16.22
Hnrnpd	Q60668	Heterogeneous nuclear ribonucleoprotein D0	NEEDEGHSNpSSPR	0.09	0.15	82		10.28
Prpf4b	Q61136	Serine/threonine-protein kinase PRP4 homolog	ARpSPAEEK	0.23	0.08	258		Infinity
Prpf4b	Q61136	Serine/threonine-protein kinase PRP4 homolog	RLSpSPR	−0.25	0.25	411		8.58
Npm	Q61937	Nucleophosmin	DLKPpSTPR	0.77	0.12		216	7.38
Ctr9	Q62018	RNA polymerase-associated protein CTR9 homolog	RRPPKGEEGpSEEEETENGPKPK	−0.10	0.16		970	22.33
Trim28	Q62318	Transcription intermediary factor 1-beta	RPAASSAAAASAAASpSPAGGGGEAQELLEHCGVCR	0.11	0.17	51		14.88
Trim28	Q62318	Transcription intermediary factor 1-beta	LDLDLTpSDSQPPVFK	−0.16	0.21		499	13.27
Arid3a	Q62431	AT-rich interactive domain-containing protein 3A	AAAAGLGHPpSSPGGSEDGPPISGDEDTAR	−0.13	0.04		77	
Sqstm1	Q64337	Sequestosome-1	EVDPSTGELQSLQMPESEGPSpSLDPSQEGPTGLK	0.12	0.07		54	
Top2b	Q64511	DNA topoisomerase 2-beta	KTSFDQDpSDVDIFPSDFTSEPPALPR	−1.07	0.00	1568		25.73
Rbl1	Q64701	Retinoblastoma-like protein 1	VIAISGDADpSPAKR	−0.90	0.06		1036	39.33
Sbno1	Q689Z5	Protein strawberry notch homolog 1	RPpSFSSAPVISPASNSAPANSNSNSNSSLVTSQDAVER	−0.37	0.09	812		8.68
Git1	Q68FF6	ARF GTPase-activating protein GIT1	ARpSMDSSDLSDGAVTLQEYLELKK	−0.17	0.04	419		18.34
Mars	Q68FL6	Methionine-tRNA ligase, cytoplasmic	GpSPKPAAVEAVTAAGSQHIQTLTDEVTK	−0.23	0.07	827		34.37
Hectd1	Q69ZR2	E3 ubiquitin-protein ligase HECTD1	RLDpSSGER	0.21	0.17		357	
Hectd1	Q69ZR2	E3 ubiquitin-protein ligase HECTD1	RPpSLQR	−0.26	0.19		1716	Infinity
Larp4b	Q6A0A2	La-related protein 4B	SPpSPVHLPEDPKVAEK	−0.52	0.26	603		12.32
Ralgapa1	Q6GYP7	Ral GTPase-activating protein subunit alpha-1	VRHFpSQSEDTGNEVFGALHEEQPLPR	0.29	0.08	772		6.66
Ralgapa1	Q6GYP7	Ral GTPase-activating protein subunit alpha-1	SSpSTSDILEPFTVER	−0.06	0.20	796		
Ralgapa1	Q6GYP7	Ral GTPase-activating protein subunit alpha-1	pSSSTSDILEPFTVER	0.05	0.21		794	
Nipbl	Q6KCD5	Nipped-B-like protein	AITSLLGGGpSPK	0.33	0.03	139		
U2surp	Q6NV83	U2 snRNP-associated SURP motif-containing protein	VKpSPpSPK	0.03	0.04	946, 948		Infinity
U2surp	Q6NV83	U2 snRNP-associated SURP motif-containing protein	EKDECpTPTRK	−0.12	0.04		919	37.74
U2surp	Q6NV83	U2 snRNP-associated SURP motif-containing protein	KEKDECTPpTR	−0.15	0.02		921	
Zc3h11a	Q6NZF1	Zinc finger CCCH domain-containing protein 11A	RLpSSASTGKPPLSVEDDFEK	0.02	0.06	740		6.00
Eif4g1	Q6NZJ6	Eukaryotic translation initiation factor 4 gamma 1	SFpSKEVEER	−0.19	0.19	1189		18.88
Eif4g1	Q6NZJ6	Eukaryotic translation initiation factor 4 gamma 1	RSFpSKEVEER	−0.14	0.07	1189		14.57
Rbm26	Q6NZN0	RNA-binding protein 26	RLNHpSPPQSSSR	0.09	0.12	127		26.94
Apbb1ip	Q6P542	ATP-binding cassette sub-family F member 1	EAEQGpSGEEKEEKEGDLK	−0.18	0.13		225	Infinity
Kif15	Q6P9L6	Kinesin-like protein KIF15	AFAEVSSTETNDKGLQGFpSPK	−0.20	0.05	568		38.29
Fhod1	Q6P9Q4	FH1/FH2 domain-containing protein 1	TPQpSPVSR	−0.17	0.13	502		37.54
Fkbp15	Q6P9Q6	FK506-binding protein 15	pSNSLSEQLTVNSNPDTVK	−0.14	0.13	342		6.36
Txlna	Q6PAM1	Alpha-taxilin	EQGVESPGAQPASpSPR	0.18	0.13	523		22.85
Smarcc2	Q6PDG5	SWI/SNF complex subunit SMARCC2	KRpSPSPpSPTPEAK	0.00	0.09	306		12.65
Chd4	Q6PDQ2	Chromodomain-helicase-DNA-binding protein 4	MSQPGpSPSPK	−0.08	0.10	1528		22.01
Scn10a	Q6QIY3	Sodium channel protein type 10 subunit alpha	WQREEpSPR	−0.61	0.31		1071	
Fmnl3	Q6ZPF4	Formin-like protein 3	pSIEDLQPPNALSAPFTNSLAR	0.40	0.05	174		
Fnbp4	Q6ZQ03	Formin-binding protein 4	ALEEGDGSVSGSpSPR	0.03	0.12	440		9.34
Larp1	Q6ZQ58	La-related protein 1	ETESAPGpSPR	−0.83	0.45		498	23.64
Kdm1a	Q6ZQ88	Lysine-specific histone demethylase 1A	KLPPPPPQAPPEEENEpSEPEEPSGVEGAAFQSR	−0.16	0.14	167		16.54
Znrf2	Q71FD5	E3 ubiquitin-protein ligase ZNRF2	AYSGpSDLPSGTGSGGGGADGAR	−0.05	0.05		20	5.88
Mybbp1a	Q7TPV4	Myb-binding protein 1A	DIPSDpTQSPVSTK	0.58	0.24	1162		10.33
Atxn2l	Q7TQH0	Ataxin-2-like protein	STSTPTpSPGPR	−0.78	0.12	687		
Clasp1	Q80TV8	CLIP-associating protein 1	VLSTpSTDLEAAVADALK	−0.11	0.14	794		13.58
Madd	Q80U28	MAP kinase-activating death domain protein	ATLpSDSEIETNSATSAIFGK	−0.14	0.09		1237	
Pum2	Q80U58	Pumilio homolog 2	pTPGSRQASPpTEVVER	−0.20	0.14	183	174	13.19
Suz12	Q80U70	Polycomb protein Suz12	ASMSEFLEpSEDGEVEQQR	0.12	0.04		548	27.35

(continued on next page)

Table 3 (*continued*)

Protein ID	Swiss accession	Protein name	Peptide sequence [a]	Ratio (log2 H/L)	CV	By similarity [b]	Novel p-site [c]	Max Ascore [d]
Pgrmc2	Q80UU9	Membrane-associated progesterone receptor component 2	LLKPGEEPSEpYTDEEDTKDHSKQD	0.34	0.01	204		15.50
Galnt7	Q80VA0	N-acetylgalactosaminyltransferase 7	HAGGDpSQRDVMQR	0.88	0.06		103	
Lyric	Q80WJ7	Protein LYRIC	RRpSPPR	0.00	0.10		84	
Ubap2l	Q80X50	Ubiquitin-associated protein 2-like	STSAPQMSPGSSDNQSSpSPQPAQQK	0.01	0.17	496		18.99
Fam76b	Q80XP8	Protein FAM76B	VSSLpSPEQEQGLWK	0.24	0.18	193		26.53
Nucks1	Q80XU3	Nuclear ubiquitous casein and cyclin-dependent kinase substrate 1	IRpSSPR	−0.32	0.04		39	
Trim65	Q8BFW4	Tripartite motif-containing protein 65	RDpSATSHSAR	−0.59	0.30		89	28.35
Eif4b	Q8BGD9	Eukaryotic translation initiation factor 4B	pTGSESSQTGASATSGR	0.37	0.11	420		11.53
Eif4b	Q8BGD9	Eukaryotic translation initiation factor 4B	SRTGpSESSQTGASATSGR	0.12	0.03	422		14.23
Snip1	Q8BIZ6	Smad nuclear-interacting protein 1	RPDAPAASLpSPPAAEPGHSGHR	−0.14	0.08	50		11.01
Sgta	Q8BJU0	Small glutamine-rich tetratricopeptide repeat-containing protein alpha	SRpTPSASHEEQQE	0.35	0.17	305		24.21
Smg1	Q8BKX6	Serine/threonine-protein kinase SMG1	pSLRVPEK	−0.34	0.12		2362	
Gtf3c2	Q8BL74	General transcription factor 3C polypeptide 2	VSpSPTKPK	0.07	0.10	219		19.33
Srsf7	Q8BL97	Serine/arginine-rich splicing factor 7	SApSLRR	0.33	0.15	204		
Hirip3	Q8BLH7	HIRA-interacting protein 3	TLDpSEEEQPR	−0.09	0.14		575	42.10
Elmo1	Q8BPU7	Engulfment and cell motility protein 1	IAFDAESEPNNSSGpSMEK	0.12	0.20	344		43.03
Ppp1r18	Q8BQ30	Phostensin	LAGSGDDpSPKRK	0.27	0.07		212	39.78
Clasp2	Q8BRT1	CLIP-associating protein 2	SRpSDIDVNAAAGAK	−0.33	0.13	376		27.69
Srrm2	Q8BTI8	Serine/arginine repetitive matrix protein 2	HSGSTSPpYPK	0.14	0.11	966		18.04
Srrm2	Q8BTI8	Serine/arginine repetitive matrix protein 2	LKSGMpSPEQSK	0.21	0.10	1097		24.64
Srrm2	Q8BTI8	Serine/arginine repetitive matrix protein 2	SGMpSPEQSK	0.22	0.04	1097		27.99
Srrm2	Q8BTI8	Serine/arginine repetitive matrix protein 2	SGSpSPGLR	−0.43	0.14	1400		13.24
Srrm2	Q8BTI8	Serine/arginine repetitive matrix protein 2	CRpSPGMLEPLGSAR	0.46	0.03	2084		85.78
Srrm2	Q8BTI8	Serine/arginine repetitive matrix protein 2	pTSPLMLDR	0.18	0.14	2350		8.58
Srrm2	Q8BTI8	Serine/arginine repetitive matrix protein 2	VKSpSTPPRQpSPSR	0.05	0.02	875, 882		13.24
Srrm2	Q8BTI8	Serine/arginine repetitive matrix protein 2	RKEpTPpSPR	0.18	0.04	2688, 2691		Infinity
Srrm2	Q8BTI8	Serine/arginine repetitive matrix protein 2	pSSTPPRQSPpSR	0.10	0.11	875, 882		
Srrm2	Q8BTI8	Serine/arginine repetitive matrix protein 2	SGTPPRPGpSVTNMQADECTATPQR	−0.05	0.19		829	10.36
Srrm2	Q8BTI8	Serine/arginine repetitive matrix protein 2	SRDpSPTGSSGSFHLCPGVTPSSIVPGESCFSASFVQQK	0.37	0.07		993	10.66
Srrm2	Q8BTI8	Serine/arginine repetitive matrix protein 2	DKFSPpTQDRPESSTVLK	0.25	0.01		1153	12.65
Srrm2	Q8BTI8	Serine/arginine repetitive matrix protein 2	SGAGpSPPGKR	0.32	0.14		1179	41.19
Srrm2	Q8BTI8	Serine/arginine repetitive matrix protein 2	DGLPRpTPSRR	0.10	0.08		1390	31.51
Srrm2	Q8BTI8	Serine/arginine repetitive matrix protein 2	RVPpSPTPVPK	0.00	0.15		2535	13.27
Srrm2	Q8BTI8	Serine/arginine repetitive matrix protein 2	IHTTALTGQSPPLASGHQGEGDAPpSVEPGApTNIQQPSSPAPSTK	0.06	0.22		316, 322	
Srrm2	Q8BTI8	Serine/arginine repetitive matrix protein 2	REIpSpSSPTSK	0.18	0.08		452, 453	8.65
Phka2	Q8BWJ3	Phosphorylase b kinase regulatory subunit alpha, liver isoform	pSLNLVDSPQPLLK	−0.77	0.17	729		88.57
Golim4	Q8BXA1	Golgi integral membrane protein 4	EMEHNVEEpTYGEHPDDKNNDGEEQGVHNR	0.40	0.12		603	
Tbc1d4	Q8BYJ6	TBC1 domain family member 4	EGVPKpSR	−0.14	0.17		931	
Srek1	Q8BZX4	Splicing regulatory glutamine/lysine-rich protein 1	AADEKGpSPR	−0.09	0.25		465	Infinity
Map1s	Q8C052	Microtubule-associated protein 1S	ANpSQDSLASR	−0.12	0.03	462		58.33
Trmt10a	Q8C1Z8	tRNA methyltransferase 10 homolog A	LGpTSDGEEERQEPR	−0.17	0.04		21	

Trmt10a	Q8C1Z8	tRNA methyltransferase 10 homolog A	LGTpSDGEEERQEPR	−0.17	0.11		22	33.68
Dock2	Q8C3J5	Dedicator of cytokinesis protein 2	VEEEPIpSPGSTLPEVK	1.03	0.10	1683		11.56
CX038	Q8C5K5	Uncharacterized protein CXorf38 homolog	DAGRQpTPER	−0.27	0.02	315		
Ppfibp1	Q8C8U0	Liprin-beta-1	TApSAPNLAETEKETAEHLNLAGTSR	−0.44	0.09	500		6.90
Dido1	Q8C9B9	Death-inducer obliterator 1	NTTKPETIPDMEDpSPPVpSDSEEQQESVR	−0.13	0.20	806		
Tceb3	Q8CB77	Transcription elongation factor B polypeptide 3	SYpSPEHR	0.35	0.00	125		21.75
Abi1	Q8CBW3	Abl interactor 1	LGSQHpSPGR	−0.20	0.16	225		29.64
Nup88	Q8CEC0	Nuclear pore complex protein Nup88	NQSPAEAEKPAASTpSPSCPSLPPHLPTR	−0.11	0.23		47	10.36
Clasrp	Q8CFC7	CLK4-associating serine/arginine rich protein	ITFITSFGGpSDEEAAAAAAAAAAASGAAPGKPPAPPQTGGPAPGR	−0.06	0.01	335		19.94
Brf1	Q8CFK2	Transcription factor IIIB 90 kDa subunit	GGGSPPRDDpSQPPER	−0.50	0.03	552		
Mef2c	Q8CFN5	Myocyte-specific enhancer factor 2C	NpSPGLLVSPGNLNK	−1.56	0.65		222	52.41
Lat4	Q8CGA3	Large neutral amino acids transporter small subunit 4	LCLpSTVDLEVK	0.63	0.22		297	24.44
Ep400	Q8CHI8	E1A-binding protein p400	LKGFDpTSPEHSLDLGISGR	0.25	0.01		922	7.48
Copa	Q8CIE6	Coatomer subunit alpha	NLpSPGAVESDVR	0.58	0.22	173		52.62
Eif3b	Q8JZQ9	Eukaryotic translation initiation factor 3 subunit B	GHPpSAGAEEEGGSDGSAAEAEPR	0.55	0.22		111	64.46
Bclaf1	Q8K019	Bcl-2-associated transcription factor 1	KAEGEPQEESPLKpSK	0.80	0.29	181		22.24
Lrrc25	Q8K1T1	Leucine-rich repeat-containing protein 25	APDpSPPSR	0.40	0.13		238	11.56
Mtmr3	Q8K296	Myotubularin-related protein 3	RSSDPSLNEK	−0.32	0.08	633		
Edc3	Q8K2D3	Enhancer of mRNA-decapping protein 3	SQDVAISPQQQQCSK	−0.35	0.05	131		137.23
Slc38a1	Q8K2P7	Sodium-coupled neutral amino acid transporter 1	RSLpTNSHLEK	0.23	0.18	54		28.28
Matr3	Q8K310	Matrin-3	SYpSPDGKEpSPSDKK	−0.02	0.07	606		13.24
Sash3	Q8K352	SAM and SH3 domain-containing protein 3	RKPpSNASDKEPTQK	−1.22	0.11		7	
Nod2	Q8K3Z0	Nucleotide-binding oligomerization domain-containing protein 2	AQpSSVPGSK	−0.07	0.06		570	
Ddx54	Q8K4L0	ATP-dependent RNA helicase DDX54	ALPSFPTSECVpSDVEPDTR	−0.19	0.16	74		22.81
Gtf2f2	Q8R0A0	General transcription factor IIF subunit 2	HYQTEEKpSD	0.13	0.09	248		55.91
Ccdc12	Q8R344	Coiled-coil domain-containing protein 12	LKGQEDSLASAVDATTGQEACDpSD	−0.09	0.18	165		22.31
Ab1ip	Q8R5A3	Amyloid beta A4 precursor protein-binding family B member 1-interacting protein	RSpSDTCGpSPALPSK	−0.71	0.09	532		27.56
Ab1ip	Q8R5A3	Amyloid beta A4 precursor protein-binding family B member 1-interacting protein	RSpSDTCGSPALPSK	−0.64	0.21	532		17.90
Ab1ip	Q8R5A3	Amyloid beta A4 precursor protein-binding family B member 1-interacting protein	pSSDTCGSPALPSK	−0.42	0.16		531	
Gripap1	Q8VD04	GRIP1-associated protein 1	SLSSpSPQAQPPRPAELSDEEVAELFQR	0.11	0.06	657		28.87
Uhrf1	Q8VDF2	E3 ubiquitin-protein ligase UHRF1	RPLIApSPSQPPPALR	−1.09	0.31		289	12.16
Hdlbp	Q8VDJ3	Vigilin	EAKETDPGpSPR	−0.01	0.12	944		29.93
Golm1	Q91XA2	Golgi membrane protein 1	LQEEVPpSEEQMPQEK	0.47	0.27		213	Infinity
Ssf1	Q91YU8	Suppressor of SWI4 1 homolog	ARADGDpSDAEDPGAPPEAVGAGQPEDEEDDAEYFR	−0.38	0.28		362	106.03
Gcp2	Q921G8	Gamma-tubulin complex component 2	VLAIEpTK	0.66	0.34		594	
Cic	Q924A2	Protein capicua homolog	FAELPEFRPEEVLPpSPTLQSLATpSPR	0.11	0.06	2275, 2284		23.64
Myo5a	Q99104	Unconventional myosin-Va	TSpSIADEGTYTLDSILR	0.86	0.22		1650	16.20
Med24	Q99K74	Mediator of RNA polymerase II transcription subunit 24	LLpSSSDDDANILSSPTDR	0.50	0.16	860		24.44
Rbm10	Q99KG3	RNA-binding protein 10	LASDDRPpSPPR	0.00	0.13	723		63.27
Nmd3	Q99L48	60S ribosomal export protein NMD3	DATIPVESDTDDEGAPR	0.06	0.10	468		8.65
Nmd3	Q99L48	60S ribosomal export protein NMD3	DATIPVESDpTDDEGAPR	−0.07	0.11	470		
Nasp	Q99MD9	Nuclear autoantigenic sperm protein	KPEEEpSPRKDDAK	−0.49	0.19	712		Infinity

(continued on next page)

Table 3 (*continued*)

Protein ID	Swiss accession	Protein name	Peptide sequence [a]	Ratio (log2 H/L)	CV	By similarity [b]	Novel p-site [c]	Max Ascore [d]
Ehbp1l1	Q99MS7	EH domain-binding protein 1-like protein 1	RSpSVNGEAGPVPPPR	−0.16	0.05	1444		38.42
Ehbp1l1	Q99MS7	EH domain-binding protein 1-like protein 1	VApSRDTDLSCSSK	−0.50	0.07		1383	30.66
Ehbp1l1	Q99MS7	EH domain-binding protein 1-like protein 1	AHGpSFSHVR	0.09	0.20		1460	21.77
Raf1	Q99N57	RAF proto-oncogene serine/threonine-protein kinase	RApSDDGKLTDSSK	−0.40	0.04	43		13.39
Rtn4	Q99P72	Reticulon-4	RRGSGpSVDETLFALPAASEPVIPSSAEK	0.55	0.14	167		8.91
Nup155	Q99P88	Nuclear pore complex protein Nup155	AAPQpSPSVPK	0.36	0.25	992		10.33
Nckx3	Q99PD7	Sodium/potassium/calcium exchanger 3	GVNGpTRR	−0.01	0.25		397	
Rrbp1	Q99PL5	Ribosome-binding protein 1	KDGpSPSQAK	−0.28	0.21	786		10.33
Rrbp1	Q99PL5	Ribosome-binding protein 1	LASpSPKDR	0.20	0.17		135	20.35
Rrbp1	Q99PL5	Ribosome-binding protein 1	KSEGpSPNQGK	−0.06	0.03		766	17.87
Igf2bp3	Q9CPN8	Insulin-like growth factor 2 mRNA-binding protein 3	QApSPGSVSK	−0.11	0.08		184	11.56
Denr	Q9CQJ6	Density-regulated protein	LTVENSPKQEpTGITEGQGPVGEEEEK	−0.37	0.20	79		14.04
Rpl14	Q9CR57	60S ribosomal protein L14	AAILKApSPK	−0.10	0.04	139		Infinity
Golph3	Q9CRA5	Golgi phosphoprotein 3	AAGGGGGpSGEDEAQSR	0.13	0.16		35	120.04
Ranbp3	Q9CT10	Ran-binding protein 3	VLpSPPKLNEANSDTSR	−0.03	0.17	257		22.39
Ranbp3	Q9CT10	Ran-binding protein 3	ERTSSLpTHSEEK	−0.10	0.06		60	6.59
Ppil4	Q9CXG3	Peptidyl-prolyl cis–trans isomerase-like 4	INHTVILDDPFDDPPDLLIPDRpSPEPTKEQLDSGR	−0.17	0.12	178		16.25
Rbm33	Q9CXK9	RNA-binding protein 33	SIVNTpSPPCR	−0.43	0.28	792		16.22
Ssr1	Q9CY50	Translocon-associated protein subunit alpha	AQKRpSVGSDE	1.30	0.00		281	37.91
Serbp1	Q9CY58	Plasminogen activator inhibitor 1 RNA-binding protein	pSKSEEAHAEDSVMDHHFR	1.86	0.15	327		31.51
Serbp1	Q9CY58	Plasminogen activator inhibitor 1 RNA-binding protein	TDKSpSASAPDVDDPEAFPALA	0.93	0.04	391		13.27
Nde1	Q9CZA6	Nuclear distribution protein nudE homolog 1	TSGPASGRGpTK	0.04	0.14	211		
CX026	Q9D0B6	UPF0368 protein Cxorf26 homolog	GADpSGGEKEEGANR	−0.30	0.07	184		Infinity
CX026	Q9D0B6	UPF0368 protein Cxorf26 homolog	GADpSGGEKEEGANREGEK	−0.21	0.07	184		Infinity
Armc10	Q9D0L7	Armadillo repeat-containing protein 10	LRPSRSAEDLpTDGSYDDILNAEQLKK	0.24	0.11		48	12.77
Chaf1b	Q9D0N7	Chromatin assembly factor 1 subunit B	NQTHQGSpSPGSR	0.13	0.14		417	11.51
Tras	Q9D0R2	Threonine-tRNA ligase, cytoplasmic	ASSPpSGKMDGEKPVDASEEK	−0.49	0.13		10	10.64
Kti12	Q9D1R2	Protein KTI12 homolog	ApTSPVANGGVLAAVSK	−0.03	0.20		156	16.22
Saal1	Q9D2C2	Protein SAAL1	KPENPSEpSDTEEPTICGPTQDDFHMK	0.03	0.06		376	3.04
Polr3c	Q9D483	DNA-directed RNA polymerase III subunit RPC3	RRpSSDEDATGEPK	−0.15	0.11		204	11.36
Wdr20	Q9D5R2	WD repeat-containing protein 20	pSNSLPHSAVSNAASK	−0.05	0.02	430		
Rpap3	Q9D706	RNA polymerase II-associated protein 3	AVDNPPRGpSPK	−0.40	0.08		429	Infinity
Fip1l1	Q9D824	Pre-mRNA 3′-end-processing factor FIP1	RHEpSEEGDSHR	0.54	0.21	541		79.50
Eef1g	Q9D8N0	Elongation factor 1-gamma	pTPEFLR	−0.26	0.02	46		
Nvl	Q9DBY8	Nuclear valosin-containing protein-like	ESLPLDLpSDDQSNSK	−0.64	0.49	190		15.62

Pak1ip1	Q9DCE5	p21-activated protein kinase-interacting protein 1	GNpSPVTAK	0.03	0.17		361	41.33
Dtd1	Q9DD18	D-tyrosyl-tRNA(Tyr) deacylase 1	SASpSGAEGDVSSEREP	−0.04	0.16	197		24.44
Senp3	Q9EP97	Sentrin-specific protease 3	NHLpSPQEGGATPQVPSPCCR	−0.13	0.13	163		7.42
Arfgap1	Q9EPJ9	ADP-ribosylation factor GTPase-activating protein 1	SSDpSWDVWGSGSASNNK	−0.26	0.02		362	
Tlr1	Q9EPQ1	Toll-like receptor 1	TLpSLQKNQLK	−0.03	0.21		381	
Tcf20	Q9EPQ8	Transcription factor 20	AGpSSPTQGAQNEAPR	0.06	0.22		587	22.85
Tsc22d4	Q9EQN3	TSC22 domain family protein 4	SFpTGGLGQLAGPGK	−0.13	0.09	167		14.01
Ranbp2	Q9ERU9	E3 SUMO-protein ligase RanBP2	SHETDGGpSAHGDEEDDGPHFEPVVPLPDKIEVK	−0.59	0.17	1154		13.59
Inpp5d	Q9ES52	Phosphatidylinositol 3,4,5-trisphosphate 5-phosphatase 1	DSSLGPGRGEGPPpTPPSQPPLpSPK	0.06	0.12		964, 972	34.55
Inpp5d	Q9ES52	Phosphatidylinositol 3,4,5-trisphosphate 5-phosphatase 1	KEQEpSPK	−0.32	0.07		1038	Infinity
Ddx24	Q9ESV0	ATP-dependent RNA helicase DDX24	FGATAHLGpSPCKDR	−0.63	0.47	288		11.89
Plek	Q9JHK5	Pleckstrin	pSIRLPETIDLGALYLSMKDPEK	0.48	0.03	117		13.98
Ddx21	Q9JIK5	Nucleolar RNA helicase 2	GKEANGDAGEKpSPK	−0.20	0.11		181	Infinity
Ddx21	Q9JIK5	Nucleolar RNA helicase 2	EANGDAGEKpSPK	0.11	0.18		181	Infinity
Ddx21	Q9JIK5	Nucleolar RNA helicase 2	EASGDAGEKpSPR	0.25	0.19		218	63.29
Acin1	Q9JIX8	Apoptotic chromatin condensation inducer in the nucleus	GVQAGNpSDTEGGQPGRK	0.18	0.19	838		24.75
Mlh1	Q9JK91	DNA mismatch repair protein Mlh1	AAPTSSPGSpSR	−0.33	0.13		473	
Nudt5	Q9JKX6	ADP-sugar pyrophosphatase	EpSTESSPGKHLVTSEELISEGK	−0.28	0.11		6	4.49
Fmnl1	Q9JL26	Formin-like protein 1	EAAADTSGREEPPTPKpSPPK	−0.40	0.19	1021		24.75
Chaf1a	Q9QWF0	Chromatin assembly factor 1 subunit A	ATIKPVPSVVIIDLTENCSDIPDpSPEGHSELSPDT AGVVTTVEGAAK	0.14	0.04		122	6.81
Chaf1a	Q9QWF0	Chromatin assembly factor 1 subunit A	GGRSpSPSTPACR	−0.19	0.09		294	
Rad18	Q9QXK2	E3 ubiquitin-protein ligase RAD18	EVpSPQQTR	0.00	0.05	485		24.15
Cbx8	Q9QXV1	Chromobox protein homolog 8	VDDKPSpSPGDSSK	−0.70	0.17		164	
Myo9b	Q9QY06	Unconventional myosin-Ixb	AQDKPESPSGpSTQIQR	0.59	0.03		1268	7.38
Prkab1	Q9R078	5′-AMP-activated protein kinase subunit beta-1	RDpSSGGAKDGDRPK	−0.31	0.00	24		21.99
Trex2	Q9R1A9	Three prime repair exonuclease 2	pSSLENPER	−3.53	0.09		38	
Prkra	Q9WTX2	Interferon-inducible double stranded RNA-dependent protein kinase activator A	HRAEAPPLQREDSGpTFSLGK	0.23	0.08		20	
Man1	Q9WU40	Inner nuclear membrane protein Man1	VLLGFSSDEpSDVEASPR	0.69	0.07	140		13.38
Chip	Q9WUD1	STIP1 homology and U box-containing protein 1	LGpTGGGGSPDKSPSAQELK	0.41	0.09		15	19.27
Twf2	Q9Z0P5	Twinfilin-2	LIRGPGENGEDpS	−0.56	0.13	349		
Ilf3	Q9Z1X4	Interleukin enhancer-binding factor 3	RPMEEDGEEKpSPSKK	0.04	0.12	382		24.15
Pdpk1	Q9Z2A0	3-Phosphoinositide-dependent protein kinase 1	ANpSFVGTAQYVSPELLTEK	−0.27	0.25	244		24.15

[a] The preceding p indicates phosphorylated amino acid.
[b] Novel phosphorylation sites in mouse.
[c] Novel phosphorylation sites.
[d] Sites with Ascores > 13 have a p-value <0.05 and >95% certainty for correct phosphorylation site localization. Sites with Ascores > 19 have a p-value <0.01 and >99% certainty for correct phosphorylation site localization.

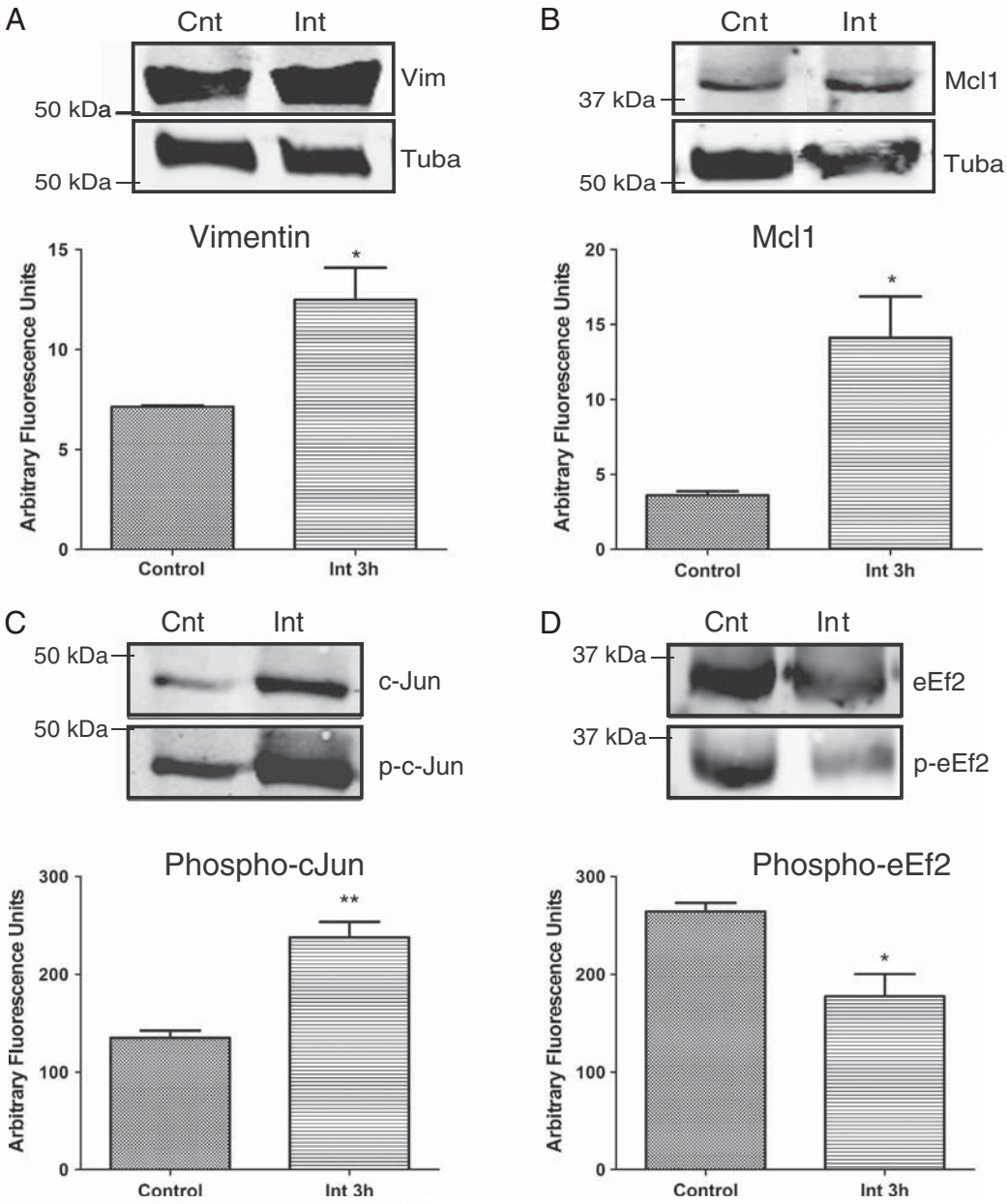

Fig. 2 – Validation of differential expression and phosphorylation levels of selected proteins in RAW 264.7 macrophages. Samples were separated on 10% 1D-SDS-PAGE gels and transferred onto nitrocellulose membranes. Western-blotting for Vimentin, Mcl1, Phospho c-Jun and Phospho eEf2, were performed. Data are expressed as the means ± SD of three independent experiments (*, $p < 0.01$; **, $p < 0.05$).

involved in oxidative stress pathways. These proteins regulate the cellular redox balance and protect the ER against the deleterious effects of the oxidative stress [40]. Proline dehydrogenase was previously shown to be essential for proline protection against hydrogen peroxide-induced cell death [41].

Mitochondria are important organelles that mediate energy metabolism, cell signaling and homeostasis and cell death in eukaryotic cells [42]. The observed increase in the level of mitochondrial ribosome biogenesis suggests an increased macrophage activity in response to *C. albicans*. West et al. proved that, during TLR signaling, mitochondria are recruited to the phagosome where they contribute to bactericidal activity [43]. Mitochondrial metabolism is directly related to the metabolic status of the cell and we find in the current and previous studies that macrophage metabolism is altered after interaction with *Candida* [17,19].

Many of the differentially expressed proteins identified in our study relate to the inflammatory response. The decrease in Fabp4 alters the macrophages lipid composition and enhances peroxisome proliferator-activated receptor (PPAR) activity, leading to increased expression of the scavenger receptor CD36. A tyrosine kinase signaling cascade downstream of CD36 is a key regulator of MAPK pathways, such as ERK1/2 and NF-κB pathways, that induce pro-inflammatory cytokine and

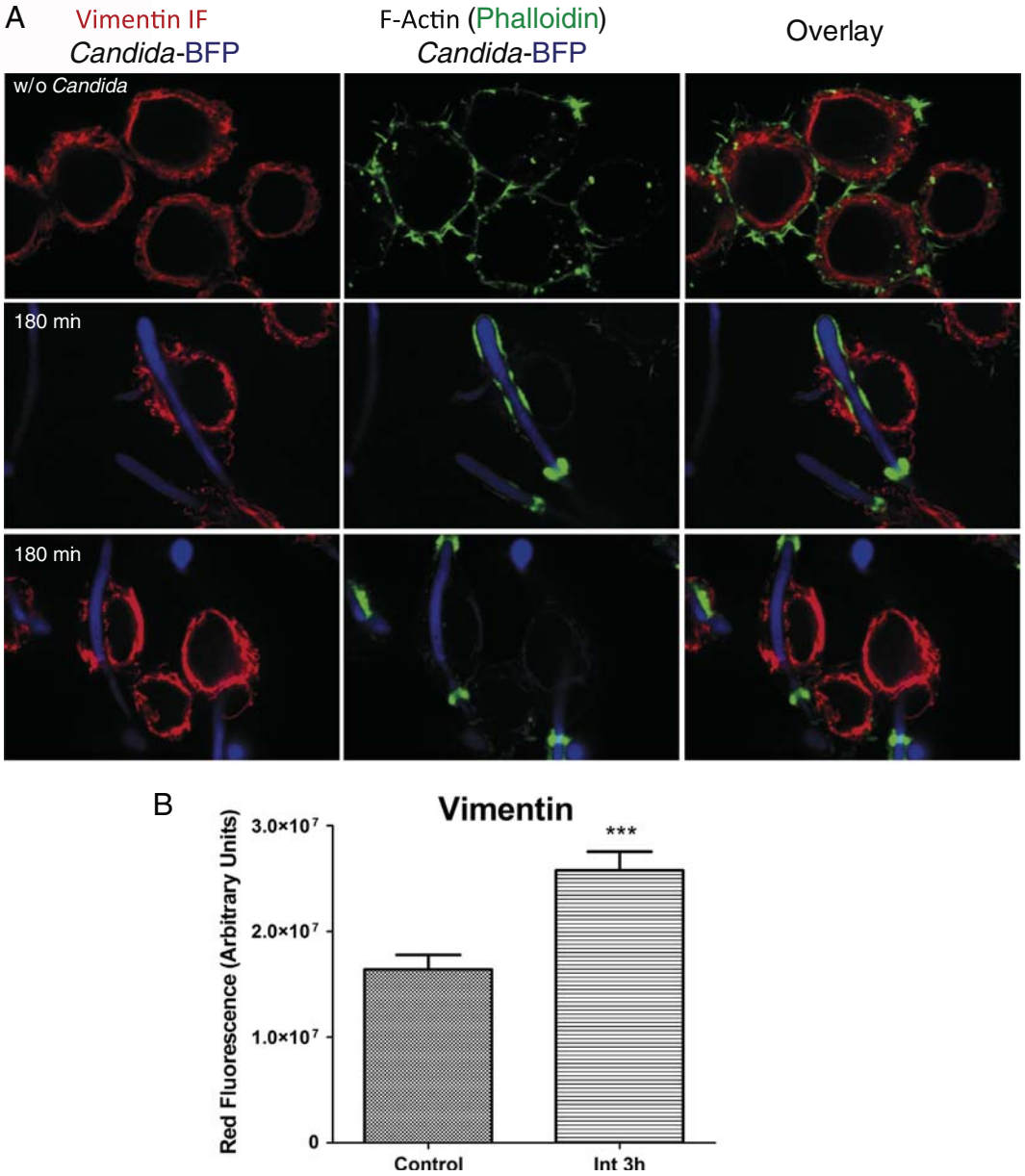

Fig. 3 – Vimentin increasing in macrophages after *C. albicans* interaction. (A) Confocal images showing localization of Vimentin in RAW 264.7 macrophages incubated with *C. albicans*-BFP. Images were taken without or after 3 h of co-incubation with *C. albicans*. (B) Quantitation of Vimentin fluorescence. Representative micrographs are showed and statistical data are represented as mean ± SD of two different experiments (*, $p < 0.001$).**

chemokine production in response to beta amyloid [44–46]. In addition, SelS overexpression [47], Osteopontin (Spp1) phosphorylation and Nfatc2 dephosphorylation [48] play an important role in NF-κB activation. Translocation of NF-κB to the nucleus activates the transcription of pro-inflammatory cytokines genes [40]. The LPS-binding PRR CD14, which displayed increased expression upon interaction with *Candida*, associates with TLR4 for *C. albicans* O-linked mannan recognition [14]. This interaction gives rise to several pro-inflammatory signals, including NF-κB activation, release of nitric oxide (NO), prostaglandin E2 (PGE2), interleukin-6 (IL-6), tumor necrosis factor-alpha (TNF-α) and cyclooxygenase-2 (COX-2) [8,14,49].

Vimentin was previously shown to play a role in inflammation, as it has bactericidal activity that is enhanced by pro-inflammatory cytokines [34]. And finally, we found an increased phosphorylation status for macrophage scavenger receptor class A (SR-A, CD204) that plays a significant role in mediating signals triggered by cytokines, growth factors and stress [50–52].

On the other hand we also detected increased expression of anti-inflammatory signals in the presence of *C. albicans*. One of the up-regulated proteins was Tyrobp also known as DAP12, which associates with the receptor TREM-1. These proteins might be involved in regulating the magnitude of the inflammatory response [53]. Colony-stimulating factor-1 receptor (CSF1R) that recognizes M-CSF was decreased upon interaction with *Candida*. M-CSF is the primary regulator of survival, proliferation, differentiation and function of mononuclear

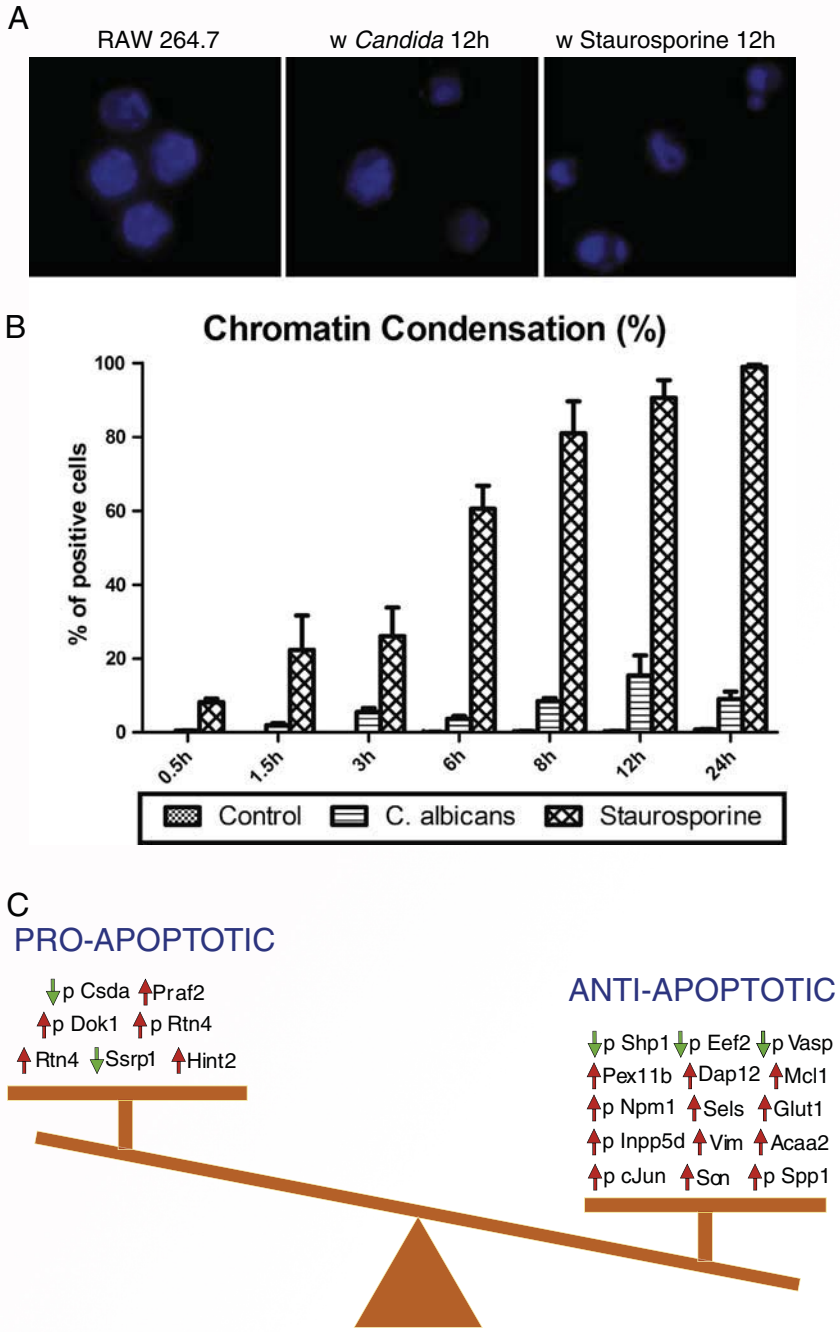

Fig. 4 – Prevalence of anti-apoptotic signals in RAW 264.7 macrophages after interaction with *C. albicans*. Macrophages incubated with *C. albicans* or 5 mM Staurosporine during different time points. Cells were fixed and nuclei were stained with DAPI, and the percentage of the chromatin-condensed cells was counted. In each sample, at least 100 cells were counted. Representative micrographs (A) and the percentages of the cells with condensed chromatin (B) are shown. (C) Diagram of the different pro- and anti-apoptotic signals in macrophages during the response to the yeast.

phagocytes [54] and the downregulation of CSF1R might suggest a reduced sensitivity for this cytokine.

4.2. *Cytoskeletal rearrangement during the macrophage–Candida interaction*

As previously reported, many of the differentially expressed proteins during incubation with *Candida* were involved in cytoskeletal modifications. As shown in Tables 1 and 2, 5 proteins and 19 phosphoproteins were differentially expressed during the interaction. Vimentin is a widely expressed intermediate filament protein involved in structural processes, such as cytoskeletal rearrangement and in supporting and anchoring of organelles (nucleus, ER and mitochondria) in the cytosol [55]. Other proteins identified in our study are related to cytoskeleton polarization, such as Cd2ap [56] Flmn2 [57], Lmna [58],

Stathmin (Stmn1) [59], Twf2 [60], tubulins and myosins. All of these proteins are affecting macrophage function by regulating phagocytosis, ruffling, vesicle rocketing, and cell motility.

4.3. *The interaction with the yeast does not induce the apoptosis in RAW 264.7 macrophages*

Apoptosis of infected cells constitutes part of the host defense, limiting the dissemination of ingested microorganisms by prompting the effective clearance of infected cells by resident and recruited phagocytes [61]. The converse of this strategy is the repression of programmed cell death in invaded host cells, allowing the pathogen to replicate and/or silently persist, whilst remaining invisible to the immune system [62]. Well-known pathogens that employ this strategy include *Legionella pneumophila*, *Chlamydiae* spp., *Rickettsia rickettsii*, *Neisseria gonorrhoeae* and *Mycobacterium tuberculosis* [63,64]. The ability of *C. albicans* to induce apoptosis in J774 macrophages has already

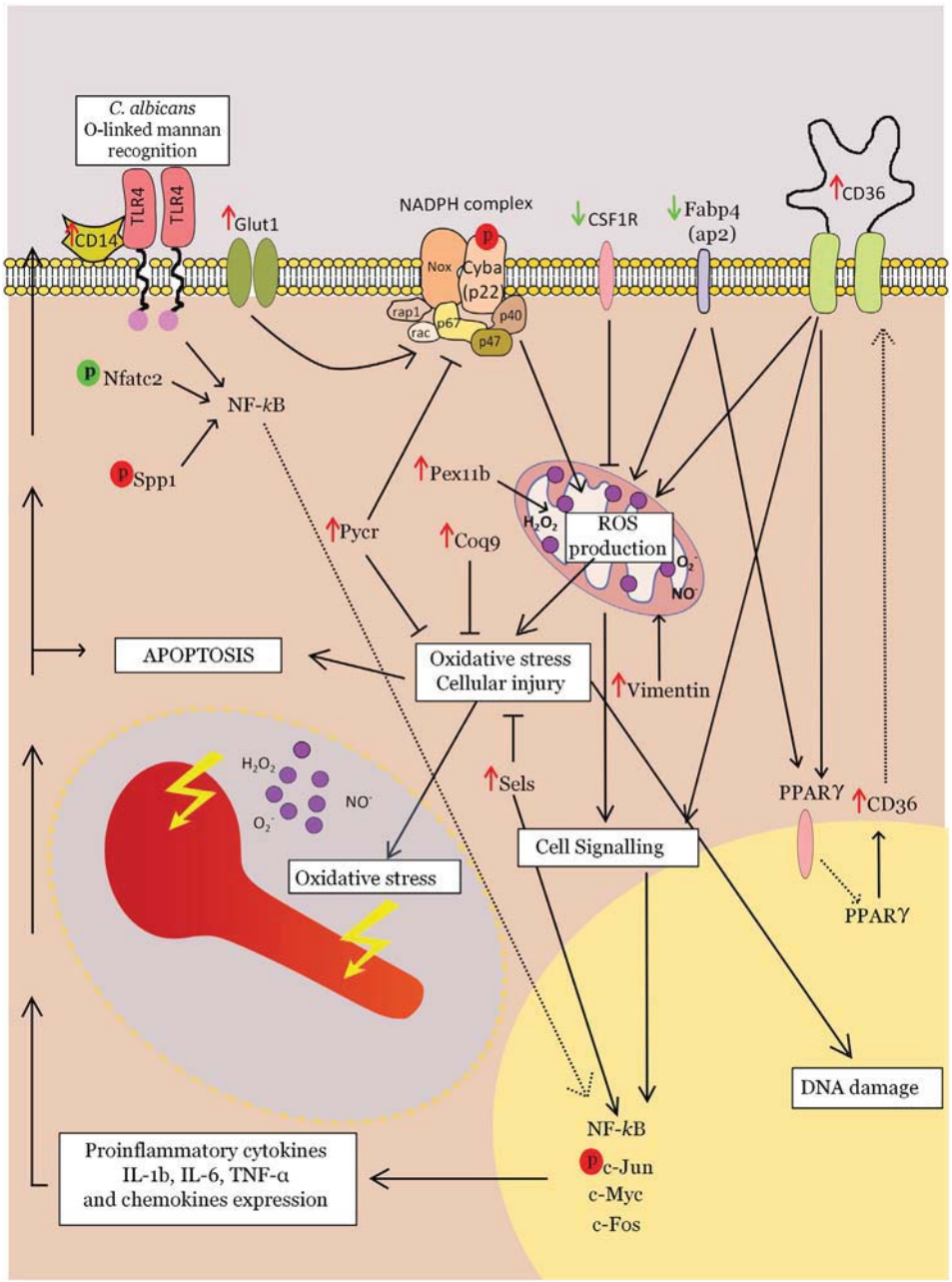

Fig. 5 – Schematic overview of macrophage proteins and phosphoproteins related to immune and stress responses differentially regulated upon *C. albicans* interaction. Changes in the macrophage proteins after the interaction with the yeast and their putative roles in some of the principal pathways are represented in the following way: red arrow, proteins with higher abundance; green arrow, lower abundance; red circle, increased phosphorylation and green circle, decreased phosphorylation.

been described [65]. Previous work of our group described both pro- and anti-apoptotic signals in our RAW 264.7 macrophages [17]. Our current work allows the quantitative comparison of pro- and anti-apoptotic signals in macrophages upon the interaction with *Candida*.

As pro-apoptotic signals, we found the increase in Rtn4 (Nogo-A), Hint2 and Praf2, a decrease in Ssrp1, an increase in phosphorylation of Dok1and Rtn4 and a decrease in phosphorylation of Csda. Rtn4 knockdown in cardiomyocytes markedly attenuated hypoxia/reoxygenation-induced apoptosis [66]; Hint2 [67] and Praf2 [68] overexpression sensitize cells to apoptosis, and Ssrp1 degradation during apoptosis is a two-step process coupling caspase cleavage and ubiquitin-dependent proteolysis [69]. Dok1 phosphorylation can affect several cell signaling processes and plays a role in activin-induced apoptosis [70]. Cold-shock domain protein A (Csda) is a target of Bcr-Abl induced phosphorylation, and Csda phospho-deficient mutant resulted in an increase in apoptosis [71]. The identification of these differentially regulated proteins in the macrophages–*Candida* samples suggests pro-apoptotic signals.

However, we also identify proteins and phosphoproteins related to inhibition of apoptosis. We found increased levels of Glut1, Sels, Pex11b, Tyrobp (Dap12), Mcl1, Vimentin, Acaa2 [72] and Son, increased phosphorylation of nucleophosmin (Npm1), Inpp5d, c-Jun and Osteopontin (Spp1) and decreased phosphorylation of Vasp, Ptpn6 (Shp1) [73] and eEf2. Overexpression of SelS might protect RAW 264.7 macrophages against ER stress-induced cytotoxicity and apoptosis, resulting in promotion of cell survival [74]. Pex11b deficiency enhances neuronal apoptosis [75] and we found this protein to be downregulated in our model.

A major indicator of anti-apoptotic signal in our macrophage–*Candida* sample is the increase in the Bcl2 family member Myeloid cell leukemia 1 (Mcl1). Mcl1 promotes cell viability during phenotypic transitions such as the stimulation of proliferation or differentiation [76]. *M. tuberculosis* induces resistance in infected macrophages by up-regulating Mcl1 expression [77]. Some of the proteins found in our study are functionally related to the increase in Mcl1. Ligation of TREM2 with DAP12 stimulates an increase in the abundance of Mcl1 in osteoclasts [78] and the activation of eEF2 by dephosphorylation in Th^{57}, plays a role in Mcl1 levels [79]. An anti-apoptotic effect of Vimentin has been reported in Jurkat cells [80].

Another anti-apoptotic event is the increased phosphorylation of nucleophosmin (NPM), a nucleolar phosphoprotein that binds the tumor suppressors p53 and p19Arf. NPM is thought to be indispensable for ribogenesis, cell proliferation, and survival after DNA damage [81]. Phosphorylation of Vasp was associated with the induction of apoptosis [82] and our macrophage–*Candida* samples showed decreased phosphorylation of this protein. Anti-apoptotic effects of c-Jun phosphorylation at Ser^{73} were previously described for a Ser^{63}Ala, Ser^{73}Ala mutant that resulted in increased apoptosis [83]. Spp1 is a phosphorylated glycoprotein involved in many physiological and pathological processes, including apoptosis. Ligand binding activates several downstream kinases including focal adhesion kinase (FAK), mitogen-activated protein kinase (MAPK)/extracellular signal-regulated kinase (ERK) kinase (MEK) 1/2 and phosphatidylinositol 3-kinase (PIK3)/Akt. Akt and ERK1/2 phosphorylates caspase-9 at Ser^{196} and Thr^{125}, respectively; and inhibits caspase-3 activation [84]. Together, these responses suggest a strong anti-apoptotic signature of macrophages during the interaction with *C. albicans*.

To determine whether macrophages incubated with *C. albicans* are pro- or anti-apoptotic, we conducted various apoptosis assays. Chromatin condensation, TUNEL assays and caspase-3 and Vimentin cleavage studies convincingly showed the absence of apoptotic macrophages in the presence of *C. albicans* (Fig. 4A, B and Suppl. Fig. 3). Our findings might be surprising as Ibata-Ombetta et al. [65] detect apoptosis in macrophages using a 20:1 yeast:J774 macrophages ratio and Rotstein et al. [85] showed an increase in the percentage of apoptotic neutrophils when increasing the yeast: neutrophil ratio. On the other hand, in human monocytes, Heidenreich et al. showed an inhibition of apoptosis in macrophages using 1:1 and 1:50 ratios [86]. In conclusion, the kind of phagocyte and the multiplicity of infection might be crucial for induction/inhibition of apoptosis by *C. albicans*. An interesting future direction would be to determine if the anti-apoptotic response is regulated by the macrophage or by the pathogen. On the one hand, the inhibition of apoptosis could be a host immune mechanism to reinforce defenses against the invading pathogen. On the other hand, stimulation of anti-apoptotic signals might be a *Candida* virulence factor that favors replication and dissemination inside macrophages.

5. Conclusions

As conclusions, SILAC technology has allowed us to identify new proteins and phosphopeptides involved in the macrophage response to *Candida*, pointing out to the pro-inflammatory and anti-apoptotic effects of *C. albicans* on RAW 264.7 macrophages, suggesting that macrophages are trying to destroy *C. albicans* increasing the inflammation and, in the same direction, the inhibition of apoptosis could be a mechanism of the host immune system to reinforce the defense against the infection by remaining macrophages viable and active against *Candida*. However the infected macrophages can favor the replication and dissemination of the pathogens that remain alive inside them, unraveling another *C. albicans* putative virulence factor.

Supplementary data to this article can be found online at http://dx.doi.org/10.1016/j.jprot.2013.06.026.

Acknowledgments

Proteomics experiments were carried out in the Proteomics Unit UCM-Parque Científico, a member of the National Institute for Proteomics, ProteoRed, funded by Instituto de Salud Carlos III (ISCIII) and in the Protein Research Group Laboratory, University of Southern Denmark. The authors would like to thank Maria Luisa Hernáez and Jimmy Ytterberg for their support in sample analysis. J.A. R.-C. was the recipient of a fellowship from Ministerio de Ciencia e Innovación.

This work was supported by BIO 2009-07654 and BIO 2012-31767 from the Ministerio de Economía y Competitividad, PROMT (S2010/BMD-2414) from the Comunidad Autónoma de Madrid, and REIPI, Spanish Network for the Research in

Infectious Diseases (RD06/0008/1027 and RD12/0015/0004) from the ISCIII; and the Banco Santander Central Hispano-Universidad Complutense Research Group (UCM-920685). Dr. C. Nombela is the director of the Special Chair in Genomics and Proteomics.

REFERENCES

[1] Pfaller MA, Yu WL. Antifungal susceptibility testing. New technology and clinical applications. Infect Dis Clin North Am 2001;15:1227–61.
[2] Eggimann P, Garbino J, Pittet D. Epidemiology of *Candida* species infections in critically ill non-immunosuppressed patients. Lancet Infect Dis 2003;3:685–702.
[3] Pfaller MA, Diekema DJ. Epidemiology of invasive candidiasis: a persistent public health problem. Clin Microbiol Rev 2007;20:133–63.
[4] Ashman RB, Farah CS, Wanasaengsakul S, Hu Y, Pang G, Clancy RL. Innate versus adaptive immunity in *Candida albicans* infection. Immunol Cell Biol 2004;82:196–204.
[5] de Repentigny L. Animal models in the analysis of *Candida* host–pathogen interactions. Curr Opin Microbiol 2004;7: 324–9.
[6] Bistoni F, Vecchiarelli A, Cenci E, Puccetti P, Marconi P, Cassone A. Evidence for macrophage-mediated protection against lethal *Candida albicans* infection. Infect Immun 1986;51:668–74.
[7] Qian Q, Jutila MA, van Rooijen N, Cutler JE. Elimination of mouse splenic macrophages correlates with increased susceptibility to experimental disseminated candidiasis. J Immunol 1994;152:5000–8.
[8] Netea MG, Brown GD, Kullberg BJ, Gow NA. An integrated model of the recognition of *Candida albicans* by the innate immune system. Nat Rev Microbiol 2008;6:67–78.
[9] Netea MG, van der Meer JW, Kullberg BJ. Both TLR2 and TLR4 are involved in the recognition of *Candida albicans*. Microbes Infect 2006;8:2821–2 [author reply 3–4].
[10] McGreal EP, Miller JL, Gordon S. Ligand recognition by antigen-presenting cell C-type lectin receptors. Curr Opin Immunol 2005;17:18–24.
[11] Rogers NC, Slack EC, Edwards AD, Nolte MA, Schulz O, Schweighoffer E, et al. Syk-dependent cytokine induction by Dectin-1 reveals a novel pattern recognition pathway for C type lectins ROGERS2005. Immunity 2005;22: 507–17.
[12] Jongstra-Bilen J, Puig Cano A, Hasija M, Xiao H, Smith CI, Cybulsky MI. Dual functions of Bruton's tyrosine kinase and Tec kinase during Fcgamma receptor-induced signaling and phagocytosis. J Immunol 2008;181:288–98.
[13] Strijbis K, Tafesse FG, Fairn GD, Witte MD, Dougan SK, Watson N, et al. Bruton's Tyrosine Kinase (BTK) and Vav1 Contribute to Dectin1-Dependent Phagocytosis of Candida albicans in Macrophages. PLoS Pathog 2013;9: e1003446.
[14] Netea MG, Van Der Graaf CA, Vonk AG, Verschueren I, van der Meer JW, Kullberg BJ. The role of toll-like receptor (TLR) 2 and TLR4 in the host defense against disseminated candidiasis. J Infect Dis 2002;185:1483–9.
[15] Poulain D, Jouault T. *Candida albicans* cell wall glycans, host receptors and responses: elements for a decisive crosstalk. Curr Opin Microbiol 2004;7:342–9.
[16] Fernández-Arenas E, Cabezón V, Bermejo C, Arroyo J, Nombela C, Diez-Orejas R, et al. Integrated proteomics and genomics strategies bring new insight into *Candida albicans* response upon macrophage interaction. Mol Cell Proteomics 2007;6:460–78.
[17] Reales-Calderon JA, Martinez-Solano L, Martinez-Gomariz M, Nombela C, Molero G, Gil C. Sub-proteomic study on macrophage response to *Candida albicans* unravels new proteins involved in the host defense against the fungus. J Proteomics 2012;75:4734–46.
[18] Martínez-Solano L, Reales-Calderón JA, Nombela C, Molero G, Gil C. Proteomics of RAW 264.7 macrophages upon interaction with heat-inactivated *Candida albicans* cells unravel an anti-inflammatory response. Proteomics 2009;9:2995–3010.
[19] Martínez-Solano L, Nombela C, Molero G, Gil C. Differential protein expression of murine macrophages upon interaction with *Candida albicans*. Proteomics 2006;6(Suppl. 1):S133–44.
[20] Johnson SA, Hunter T. Phosphoproteomics finds its timing. Nat Biotechnol 2004;22:1093–4.
[21] Nuhse TS, Stensballe A, Jensen ON, Peck SC. Large-scale analysis of in vivo phosphorylated membrane proteins by immobilized metal ion affinity chromatography and mass spectrometry. Mol Cell Proteomics 2003;2:1234–43.
[22] Thingholm TE, Jorgensen TJ, Jensen ON, Larsen MR. Highly selective enrichment of phosphorylated peptides using titanium dioxide. Nat Protoc 2006;1:1929–35.
[23] Zhang X, Ye J, Jensen ON, Roepstorff P. Highly efficient phosphopeptide enrichment by calcium phosphate precipitation combined with subsequent IMAC enrichment. Mol Cell Proteomics 2007;6:2032–42.
[24] Thingholm TE, Jensen ON, Robinson PJ, Larsen MR. SIMAC (sequential elution from IMAC), a phosphoproteomics strategy for the rapid separation of monophosphorylated from multiply phosphorylated peptides. Mol Cell Proteomics 2008;7:661–71.
[25] Ong SE, Blagoev B, Kratchmarova I, Kristensen DB, Steen H, Pandey A, et al. Stable isotope labeling by amino acids in cell culture, SILAC, as a simple and accurate approach to expression proteomics. Mol Cell Proteomics 2002;1:376–86.
[26] Ong SE, Mann M. A practical recipe for stable isotope labeling by amino acids in cell culture (SILAC). Nat Protoc 2006;1:2650–60.
[27] Gillum AM, Tsay EYH, Kirsch DR. Isolation of the *Candida albicans* gene for orotidine-5′-phosphate decarboxilase by complementation of *S. cerevisiae* ura3 and *E. coli* pyrF mutations. Mol Gen Genet 1984;198:179–82.
[28] Gobom J, Nordhoff E, Mirgorodskaya E, Ekman R, Roepstorff P. Sample purification and preparation technique based on nano-scale reversed-phase columns for the sensitive analysis of complex peptide mixtures by matrix-assisted laser desorption/ionization mass spectrometry. J Mass Spectrom 1999;34:105–16.
[29] Kokubu M, Ishihama Y, Sato T, Nagasu T, Oda Y. Specificity of immobilized metal affinity-based IMAC/C18 tip enrichment of phosphopeptides for protein phosphorylation analysis. Anal Chem 2005;77:5144–54.
[30] Larsen MR, Thingholm TE, Jensen ON, Roepstorff P, Jorgensen TJ. Highly selective enrichment of phosphorylated peptides from peptide mixtures using titanium dioxide microcolumns. Mol Cell Proteomics 2005;4:873–86.
[31] Beausoleil SA, Villen J, Gerber SA, Rush J, Gygi SP. A probability-based approach for high-throughput protein phosphorylation analysis and site localization. Nat biotechnol 2006;24:1285–92.
[32] Vizcaino JA, Cote R, Reisinger F, Foster JM, Mueller M, Rameseder J, et al. A guide to the Proteomics Identifications Database proteomics data repository. Proteomics 2009;9: 4276–83.
[33] Benes P, Maceckova V, Zdrahal Z, Konecna H, Zahradnickova E, Muzik J, et al. Role of vimentin in regulation of monocyte/macrophage differentiation. Differentiation 2006;74:265–76.
[34] Mor-Vaknin N, Punturieri A, Sitwala K, Markovitz DM. Vimentin is secreted by activated macrophages. Nat Cell Biol 2003;5:59–63.

[35] Perlson E, Michaelevski I, Kowalsman N, Ben-Yaakov K, Shaked M, Seger R, et al. Vimentin binding to phosphorylated Erk sterically hinders enzymatic dephosphorylation of the kinase. J Mol Biol 2006;364:938–44.
[36] Byun Y, Chen F, Chang R, Trivedi M, Green KJ, Cryns VL. Caspase cleavage of vimentin disrupts intermediate filaments and promotes apoptosis. Cell Death Differ 2001;8:443–50.
[37] Nakanishi K, Maruyama M, Shibata T, Morishima N. Identification of a caspase-9 substrate and detection of its cleavage in programmed cell death during mouse development. J Biol Chem 2001;276:41237–44.
[38] Babior BM. NADPH oxidase: an update. Blood 1999;93:1464–76.
[39] Sheppard FR, Kelher MR, Moore EE, McLaughlin NJ, Banerjee A, Silliman CC. Structural organization of the neutrophil NADPH oxidase: phosphorylation and translocation during priming and activation. J Leukoc Biol 2005;78:1025–42.
[40] Pahl HL, Baeuerle PA. The ER-overload response: activation of NF-kappa B. Trends Biochem Sci 1997;22:63–7.
[41] Natarajan SK, Zhu W, Liang X, Zhang L, Demers AJ, Zimmerman MC, et al. Proline dehydrogenase is essential for proline protection against hydrogen peroxide-induced cell death. Free Radic Biol Med 2012;53:1181–91.
[42] Chan DC. Mitochondria: dynamic organelles in disease, aging, and development. Cell 2006;125:1241–52.
[43] West AP, Brodsky IE, Rahner C, Woo DK, Erdjument-Bromage H, Tempst P, et al. TLR signalling augments macrophage bactericidal activity through mitochondrial ROS. Nature 2011;472:476–80.
[44] Moore KJ, El Khoury J, Medeiros LA, Terada K, Geula C, Luster AD, et al. A CD36-initiated signaling cascade mediates inflammatory effects of beta-amyloid. J Biol Chem 2002;277:47373–9.
[45] El Khoury JB, Moore KJ, Means TK, Leung J, Terada K, Toft M, et al. CD36 mediates the innate host response to beta-amyloid. J Exp Med 2003;197:1657–66.
[46] Bamberger ME, Harris ME, McDonald DR, Husemann J, Landreth GE. A cell surface receptor complex for fibrillar beta-amyloid mediates microglial activation. J Neurosci 2003;23:2665–74.
[47] Kryukov GV, Castellano S, Novoselov SV, Lobanov AV, Zehtab O, Guigo R, et al. Characterization of mammalian selenoproteomes. Science 2003;300:1439–43.
[48] Vejda S, Piwocka K, McKenna SL, Cotter TG. Autocrine secretion of osteopontin results in degradation of I kappa B in Bcr-Abl-expressing cells. Br J Haematol 2005;128:711–21.
[49] Netea MG, Marodi L. Innate immune mechanisms for recognition and uptake of *Candida* species. Trends Immunol 2010;31:346–53.
[50] Johnson GL, Lapadat R. Mitogen-activated protein kinase pathways mediated by ERK, JNK, and p38 protein kinases. Science 2002;298:1911–2.
[51] Hollifield M, Bou Ghanem E, de Villiers WJ, Garvy BA. Scavenger receptor A dampens induction of inflammation in response to the fungal pathogen *Pneumocystis carinii*. Infect Immun 2007;75:3999–4005.
[52] Villwock A, Schmitt C, Schielke S, Frosch M, Kurzai O. Recognition via the class A scavenger receptor modulates cytokine secretion by human dendritic cells after contact with *Neisseria meningitidis*. Microbes Infect 2008;10:1158–65.
[53] Ford JW, McVicar DW. TREM and TREM-like receptors in inflammation and disease. Curr Opin Immunol 2009;21:38–46.
[54] Ji XH, Yao T, Qin JC, Wang SK, Wang HJ, Yao K. Interaction between M-CSF and IL-10 on productions of IL-12 and IL-18 and expressions of CD14, CD23, and CD64 by human monocytes. Acta Pharmacol Sin 2004;25:1361–5.
[55] Katsumoto T, Mitsushima A, Kurimura T. The role of the vimentin intermediate filaments in rat 3Y1 cells elucidated by immunoelectron microscopy and computer-graphic reconstruction. Biol Cell 1990;68:139–46.
[56] Dustin ML, Olszowy MW, Holdorf AD, Li J, Bromley S, Desai N, et al. A novel adaptor protein orchestrates receptor patterning and cytoskeletal polarity in T-cell contacts. Cell 1998;94:667–77.
[57] Goode BL, Eck MJ. Mechanism and function of formins in the control of actin assembly. Annu Rev Biochem 2007;76:593–627.
[58] Broers JL, Ramaekers FC, Bonne G, Yaou RB, Hutchison CJ. Nuclear lamins: laminopathies and their role in premature ageing. Physiol Rev 2006;86:967–1008.
[59] Lovric J, Dammeier S, Kieser A, Mischak H, Kolch W. Activated raf induces the hyperphosphorylation of stathmin and the reorganization of the microtubule network. J Biol Chem 1998;273:22848–55.
[60] Palmgren S, Vartiainen M, Lappalainen P. Twinfilin, a molecular mailman for actin monomers. J Cell Sci 2002;115:881–6.
[61] Williams GT. Programmed cell death: a fundamental protective response to pathogens. Trends Microbiol 1994;2:463–4.
[62] Akarid K, Arnoult D, Micic-Polianski J, Sif J, Estaquier J, Ameisen JC. *Leishmania major*-mediated prevention of programmed cell death induction in infected macrophages is associated with the repression of mitochondrial release of cytochrome c. J Leukoc Biol 2004;76:95–103.
[63] Fischer SF, Schwarz C, Vier J, Hacker G. Characterization of antiapoptotic activities of *Chlamydia pneumoniae* in human cells. Infect Immun 2001;69:7121–9.
[64] Toossi Z, Wu M, Rojas R, Kalsdorf B, Aung H, Hirsch CS, et al. Induction of serine protease inhibitor 9 by *Mycobacterium tuberculosis* inhibits apoptosis and promotes survival of infected macrophages. J Infect Dis 2012;205:144–51.
[65] Ibata-Ombetta S, Idziorek T, Trinel PA, Poulain D, Jouault T. *Candida albicans* phospholipomannan promotes survival of phagocytosed yeasts through modulation of bad phosphorylation and macrophage apoptosis. J Biol Chem 2003;278:13086–93.
[66] Sarkey JP, Chu M, McShane M, Bovo E, Mou YA, Zima AV, et al. Nogo-A knockdown inhibits hypoxia/reoxygenation-induced activation of mitochondrial-dependent apoptosis in cardiomyocytes. J Mol Cell Cardiol 2011;50:1044–55.
[67] Martin J, Magnino F, Schmidt K, Piguet AC, Lee JS, Semela D, et al. Hint2, a mitochondrial apoptotic sensitizer down-regulated in hepatocellular carcinoma. Gastroenterology 2006;130:2179–88.
[68] Vento MT, Zazzu V, Loffreda A, Cross JR, Downward J, Stoppelli MP, et al. Praf2 is a novel Bcl-xL/Bcl-2 interacting protein with the ability to modulate survival of cancer cells. PLoS One 2010;5:e15636.
[69] Landais I, Lee H, Lu H. Coupling caspase cleavage and ubiquitin–proteasome-dependent degradation of SSRP1 during apoptosis. Cell Death Differ 2006;13:1866–78.
[70] Yamakawa N, Tsuchida K, Sugino H. The rasGAP-binding protein, Dok-1, mediates activin signaling via serine/threonine kinase receptors. EMBO J 2002;21:1684–94.
[71] Sears D, Luong P, Yuan M, Nteliopoulos G, Man YK, Melo JV, et al. Functional phosphoproteomic analysis reveals cold-shock domain protein A to be a Bcr-Abl effector-regulating proliferation and transformation in chronic myeloid leukemia. Cell Death Dis 2010;1:e93.
[72] Cao W, Liu N, Tang S, Bao L, Shen L, Yuan H, et al. Acetyl-coenzyme A acyltransferase 2 attenuates the apoptotic effects of BNIP3 in two human cell lines. Biochim Biophys Acta 2008;1780:873–80.
[73] Christophi GP, Hudson CA, Panos M, Gruber RC, Massa PT. Modulation of macrophage infiltration and inflammatory activity by the phosphatase SHP-1 in virus-induced demyelinating disease. J Virol 2009;83:522–39.

[74] Kim KH, Gao Y, Walder K, Collier GR, Skelton J, Kissebah AH. SEPS1 protects RAW264.7 cells from pharmacological ER stress agent-induced apoptosis. Biochem Biophys Res Commun 2007;354:127–32.
[75] Li X, Baumgart E, Morrell JC, Jimenez-Sanchez G, Valle D, Gould SJ. PEX11 beta deficiency is lethal and impairs neuronal migration but does not abrogate peroxisome function. Mol Cell Biol 2002;22:4358–65.
[76] Craig RW. MCL1 provides a window on the role of the BCL2 family in cell proliferation, differentiation and tumorigenesis. Leukemia 2002;16:444–54.
[77] Sly LM, Hingley-Wilson SM, Reiner NE, McMaster WR. Survival of *Mycobacterium tuberculosis* in host macrophages involves resistance to apoptosis dependent upon induction of antiapoptotic Bcl-2 family member Mcl-1. J Immunol 2003;170:430–7.
[78] Peng Q, Malhotra S, Torchia JA, Kerr WG, Coggeshall KM, Humphrey MB. TREM2- and DAP12-dependent activation of PI3K requires DAP10 and is inhibited by SHIP1. Sci Signal 2010;3:ra38.
[79] Bewley MA, Pham TK, Marriott HM, Noirel J, Chu HP, Ow SY, et al. Proteomic evaluation and validation of cathepsin D regulated proteins in macrophages exposed to *Streptococcus pneumoniae*. Mol Cell Proteomics 2011;10 [M111 008193].
[80] Lahat G, Zhu QS, Huang KL, Wang S, Bolshakov S, Liu J, et al. Vimentin is a novel anti-cancer therapeutic target; insights from in vitro and in vivo mice xenograft studies. PLoS One 2010;5:e10105.
[81] Colombo E, Bonetti P, Lazzerini Denchi E, Martinelli P, Zamponi R, Marine JC, et al. Nucleophosmin is required for DNA integrity and p19Arf protein stability. Mol Cell Biol 2005;25:8874–86.
[82] Deguchi A, Soh JW, Li H, Pamukcu R, Thompson WJ, Weinstein IB. Vasodilator-stimulated phosphoprotein (VASP) phosphorylation provides a biomarker for the action of exisulind and related agents that activate protein kinase G. Mol Cancer Ther 2002;1:803–9.
[83] Wisdom R, Johnson RS, Moore C. c-Jun regulates cell cycle progression and apoptosis by distinct mechanisms. EMBO J 1999;18:188–97.
[84] Wai PY, Kuo PC. The role of Osteopontin in tumor metastasis. J Surg Res 2004;121:228–41.
[85] Rotstein D, Parodo J, Taneja R, Marshall JC. Phagocytosis of *Candida albicans* induces apoptosis of human neutrophils. Shock 2000;14:278–83.
[86] Heidenreich S, Otte B, Lang D, Schmidt M. Infection by *Candida albicans* inhibits apoptosis of human monocytes and monocytic U937 cells. J Leukoc Biol 1996;60:737–43.

SUPPLEMENTAL MATERIAL

Supplemental Tables: Available in the CD and in http://dx.doi.org/10.1016/j.jprot.2013.06.026

Supplemental Table S1. Macrophage proteins identified after *C. albicans* interaction.

Supplemental Table S2. Macrophage phosphopeptides identified after *C. albicans* interaction.

Supplemental Figure S1:

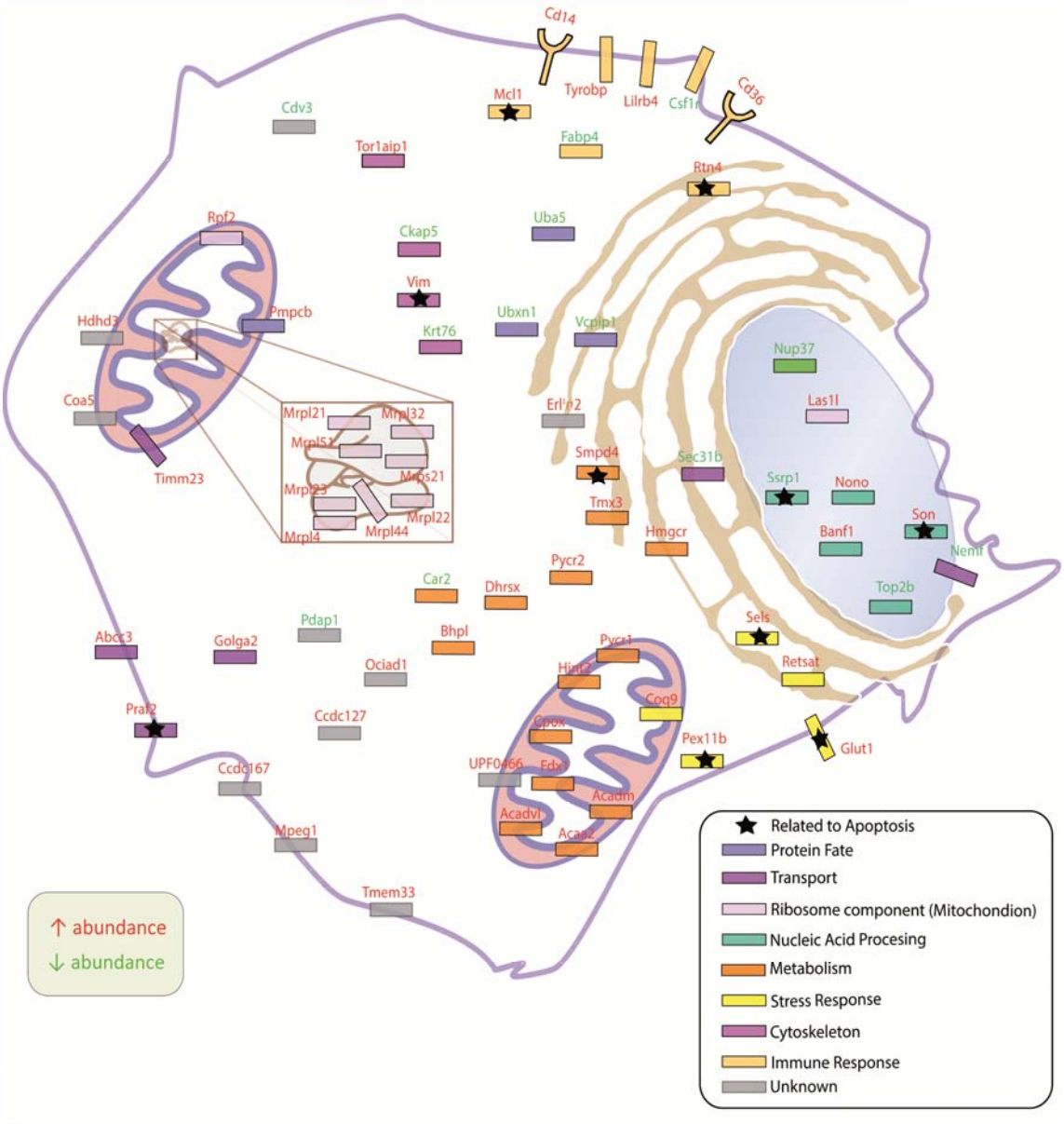

Fig. S.1. Illustration of macrophage proteins over and underexpressed during *C. albicans* interaction. Macrophage proteins with higher (in red) and lower (in green) abundance after the interaction with the yeast are represented and classified according to their biological role (color squares). Proteins related to apoptosis are highlighted with a star.

Supplemental Figure S2:

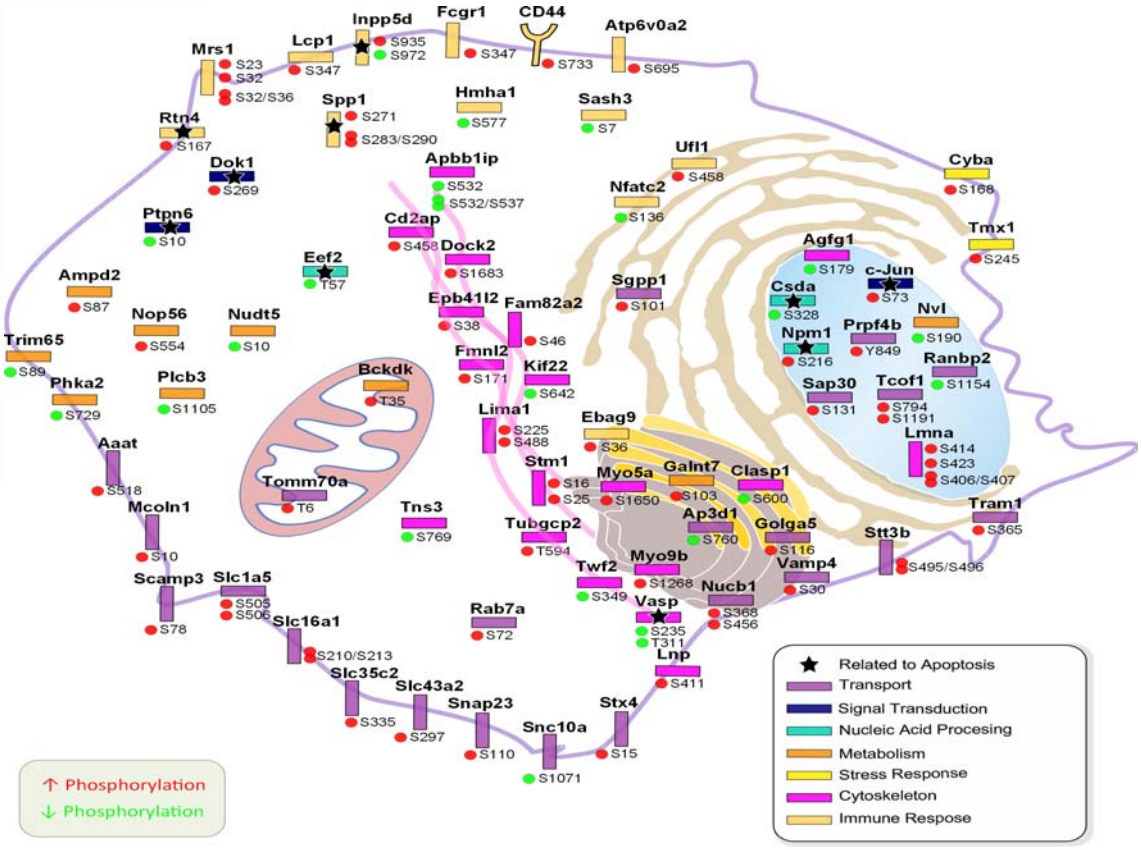

Suppl. Figure S2

Fig. S.2. Overview of interesting phosphopeptides identified in RAW 264.7 macrophages in response to *C. albicans*. Significantly increased (red dot) or decreased (green dot) phosphopeptides are shown. Double dots stand for peptide multiple phosphorylation.

Supplemental Figure S3:

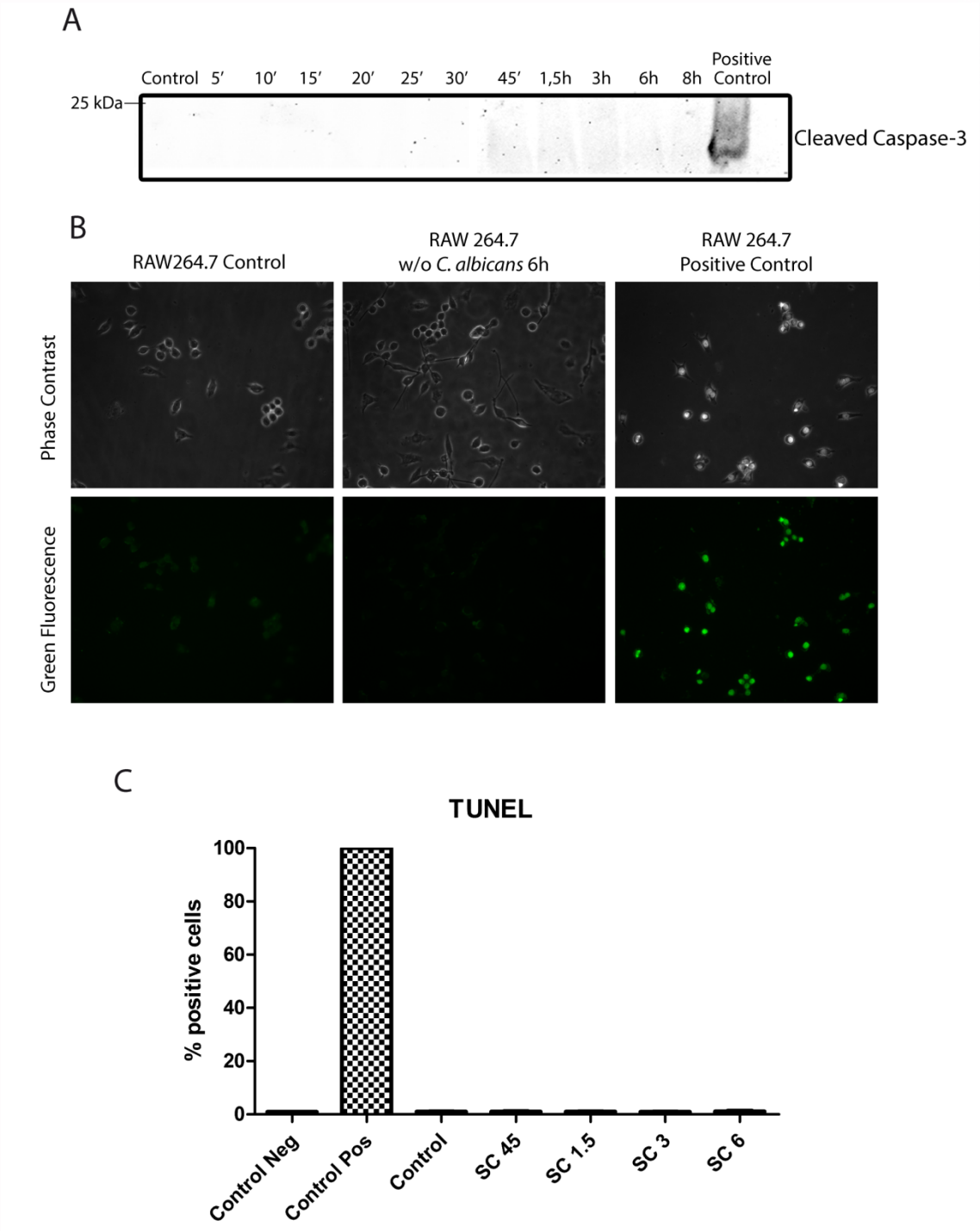

Fig. S.3. Study of additional apoptotic markers in RAW 264.7 macrophages after interaction with *C. albicans*. Determination of Cleaved caspase-3 by Western blotting (A). TUNEL assay on macrophages after interaction. Representative micrographs (B) and the percentages of TUNEL + cells comparing with positive control (100%) (+ DNAse) (C) are shown.

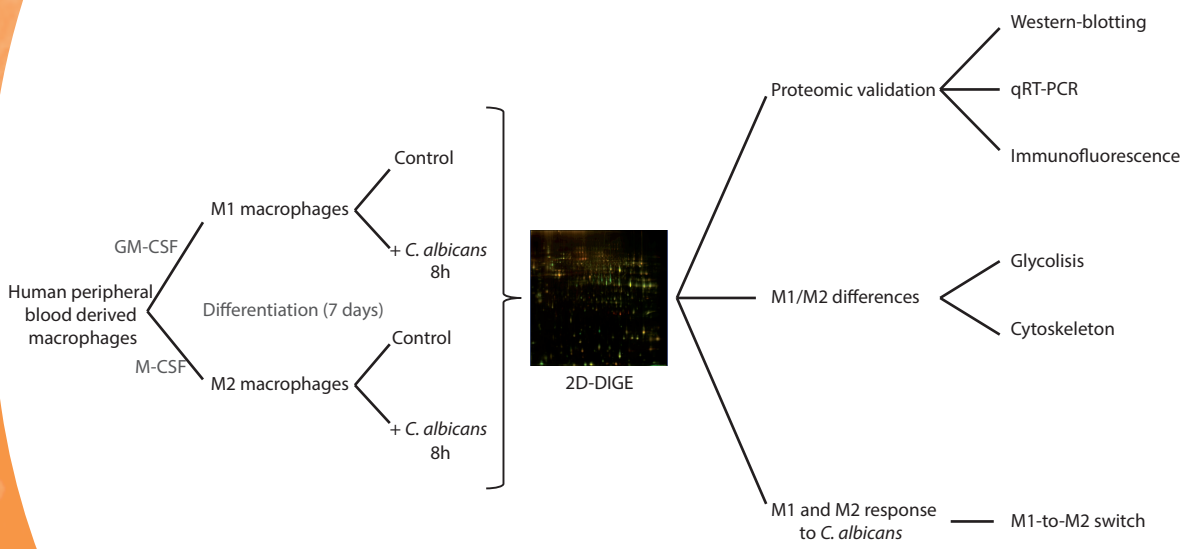

Capítulo III

*** Este capítulo contiene material suplementario que se encuentra disponible después del capítulo**

RESEARCH ARTICLE

Proteomic characterization of human proinflammatory M1 and anti-inflammatory M2 macrophages and their response to *Candida albicans*.

Jose Antonio Reales-Calderón [a,b] , Noemí Aguilera-Montilla[c], Ángel Luis Corbí [c], Gloria Molero [a,b],* and Concha Gil [a,b].

[a] Departamento de Microbiología II, Facultad de Farmacia, Universidad Complutense de Madrid, Madrid, Spain
[b] Instituto Ramón y Cajal de Investigaciones Sanitarias (IRYCIS), Madrid, Spain
[c] Centro de Investigaciones Biológicas, Consejo Superior de Investigaciones Científicas, Madrid, Spain.

In response to different stimuli, macrophages can differentiate into either a pro-inflammatory subtype (M1, classically activated macrophages) or acquire an anti-inflammatory phenotype (M2, alternatively activated macrophages). *Candida albicans* is the most important opportunistic fungus in nosocomial infections, and it is contended by neutrophils and macrophages during the first steps of the invasive infection. Murine macrophages responses to *C. albicans* have been widely studied, whereas the responses of human polarized macrophages remain less characterized. In this study we have characterized the proteomic differences between human M1- and M2-polarized macrophages, both in basal conditions and in response to *C. albicans*, by quantitative proteomics (2-Dimensional In Gel Electrophoresis). This proteomic approach allowed us to identify metabolic routes and cytoskeletal rearrangement components that are the most relevant differences between M1 and M2 macrophages. The analysis has revealed Fructose 1,6-bisphosphatase (Fbp1), a critical enzyme in gluconeogenesis, up-regulated in M1, as a novel protein marker for macrophage polarization. Regarding the response to *C. albicans*, an M1-to-M2 switch in polarization was observed. This M1-to-M2 switch might contribute to *Candida* pathogenicity by decreasing the generation of specific immune responses, thus enhancing fungal survival and colonization, or instead, may be part of the host attempt to reduce the inflammation and limit the damage of the infection.

Article info:
Submmited

Keywords:
Macrophage polarization / Candida albicans/ M1 and M2 macrophages/ Metabolism / Cytoskeleton

1 Introduction

Candida albicans is an opportunistic pathogen causing symptomatic infections especially in patients with compromised immune functions [1-3] . This opportunistic yeast possesses the remarkable ability to survive and proliferate in a changing environment, adapting its growth to physiological extremes of pH, osmolarity, availability of nutrients, and temperature [4]. *C. albicans* is a commensal fungus present in the skin and mucosal flora in the majority of healthy humans. The transition from unicellular yeast to filamentous forms is a crucial *C. albicans* virulence factor, and appears to determine tissue invasion and escape from the host immune response [5].

Phagocytic cells play a key role in innate immunity against *C. albicans*, by capturing, killing and processing the pathogen for presentation to T cells. Furthermore, dendritic cells and macrophages are able to discriminate between *C. albicans* yeast and hyphal-phases, leading to different adaptive T helper responses in each case [5, 6]. Macrophages are phagocytic cells that play an essential role in the primary response to pathogens,

in the maintenance of tissue homeostasis, in the promotion and resolution of inflammation, and in tissue repair processes [7]. Macrophages exhibit a considerable phenotypic diversity and functional plasticity that confer them the ability to efficiently respond to tissue injuries. In general, two main subtypes of polarized macrophages have been defined: M1 and M2 [8, 9]. Macrophages differentiated under the influence of granulocyte macrophage colony-stimulating factor (GM-CSF), IFNɣ or pathogen-associated molecular patterns are termed M1 or classically activated, whereas those exposed to macrophage colony-stimulating factor (M-CSF), IL-4 or IL-13 are termed M2 or alternatively activated. M1 and M2 macrophages differ in their profile of cytokine, chemokine and cell surface receptors, and exert opposite effector functions during infectious and inflammatory responses. Upon stimulation, M1 macrophages are characterized by a proinflammatory cytokine response (IL 12^{high}, IL 23^{high} and IL 10^{low}), generation of reactive oxygen and nitrogen intermediates, promotion of Th1 response, and strong microbicidal and tumoricidal activities. By contrast, M2 macrophages are primarily immunosuppressive and characterized by an IL 12^{low}, IL 23^{low}, IL 10^{high} phenotype, the promotion of Th2/Th regulatory, Treg, responses and potent tissue remodeling and tumor promotion activities, and exhibit an overall less efficient microbicidal capacity [10-12].

The response of murine macrophages to *C. albicans* has been widely studied by our group using proteomic and phosphoproteomic approaches. We have previously shown that *C. albicans* has a proinflammatory effect on RAW 264.7 macrophages, where it also promotes changes in cytoskeleton and activates pathways that prevent macrophage apoptosis [13-15]. In the present work we report for the first time the identification of the profile of differential protein expression in human M1 and M2 macrophages, as well as the determination of their distinctive responses to *C. albicans*. The 2D-DIGE technology has allowed us to identify 51 proteins differentially expressed between M1 and M2 macrophages, as well as the identification of 30 proteins whose expression is altered in either M1 or M2 macrophages exposed to *C. albicans*. Our results contribute to the dissection of the molecular mechanisms by which differentially polarized macrophages cope with pathogens, and can pave the way for the identification of novel antifungal strategies.

2 Materials and methods

2.1 *C. albicans* strains

The *C. albicans* strain was a clinical isolate (SC5314) [16], and was maintained on solid YED medium (1% D-glucose, 1% Difco Yeast Extract and 2% agar) and incubated at 30ºC for at least 2 days before use.

2.2 Isolation and culture of human blood derived macrophages

Human peripheral blood mononuclear cells (PBMC) were isolated from buffy coats of healthy donors over a Lymphoprep (Nycomed Pharma, Oslo, Norway) gradient according to standard procedures [17]. Monocytes were purified from PBMC by magnetic cell sorting using anti-CD14-coated beads (Miltenyi Biotech, Bergisch Gladbach, Germany). To generate M1 (GM-CSF) and M2 (M-CSF) monocyte-derived macrophages, $CD14^+$ cells were cultured onto 12-wells plates at a concentration of $0.5x10^6$ cells/ml for 7 days in complete medium supplemented with 1000 U/ml rhGM-CSF (ImmunoTools) or 10 ng/ml M-CSF (ImmunoTools), respectively, and with cytokine addition every two days. After 7 days, positive control M1 and M2 macrophages were stimulated with 10 ng/ml LPS and cultured for 24h before collecting supernatants for cytokine determination.

2.3 Macrophage cell line

For interaction studies, M1 or M2 macrophages were incubated with *C. albicans* at a MOI (multiplicity of infection; macrophage/yeast ratios) 1:0.1, 1:1 and 1:5. After 3, 6, 12 and 18 h at 37°C, supernatants were collected and cytokines production was measured.

2.4 Determination of cytokine production

Supernatants from M1 and M2 macrophages (untreated, LPS- or *Candida*-treated) were tested for cytokine production by ELISA using matched paired antibodies specific for IL-10, TNF-α and IL6 (Immunotools) and IL-12p40 (BD Biosciences), and according to manufacturer's instructions. Cytokine production was measured in a total of 8 independent macrophage preparations, and protein extracts from 4 of them were further analyzed by 2D-DIGE.

2.5 *C. albicans* phagocytosis assays

C. albicans yeasts were pre-labeled with 1 µM Oregon Green 488 (Molecular Probes) in the dark with gentle shaking (30°C) for 1h. Dye uptake and cell viability were confirmed by visualization of green fluorescence using a FITC filter after 2 washes with PBS and propidium iodide staining. M1 and M2 macrophages were generated onto 18-mm glass sterile coverslips placed in 12-well plates and confronted with 0.1, 1 or 5 labeled yeasts per macrophage at 37ºC and 5% CO_2. Interaction was stopped after 3, 6, 12 or 18h and cells were then washed with ice-cold PBS and fixed in 4% paraformaldehyde for 30 min. To distinguish between internalized and attached/non-ingested yeasts, *C. albicans* cells were counterstained with 2.5 M calcofluor white (Sigma) for 15 min in the dark. After several washes, coverslips were mounted with specific mounting medium (DakoCytomation Denmark A/S). The number of ingested cells (green fluorescence) and/or

adhered/non-ingested (calcofluor white blue fluorescence) were quantified by fluorescence microscopy with FITC (excitation/emission BP 480/30 and BP 535/40, respectively) and UV filters (excitation/ emission BP 365/12 and long pass 397, respectively). Three different replicates with two different slides were prepared for each MOI and time point. At least 500 *C. albicans* cells were scored per slide, and results were expressed as the percentage of yeasts internalized by macrophages.

2.6 Candidacidal activity assay

The Candidacidal activity in vitro was carried out by a growth inhibition assay by CFU measurement as previously reported [18]. In brief, M1 and M2 macrophages were confronted with 0.1, 1 or 5 labeled yeasts per macrophage at 37 ºC in a 5% CO_2 tmosphere. As a control, the same amount of yeasts was grown in complete media. After 3, 6, 12 or 18h of interaction, fungi were diluted 1:200 and 1:2000 and the solutions were plated on YED agar in triplicate. After 24-48h at 30ºC, CFU were counted. Four independent experiments were carried out, and the statistical significance of the differences in CFU numbers was evaluated by using the Student *t* test.

2.7 Cell lysates

M1 and M2 macrophages from 4 different donors and exhibiting an adequate cytokine profile in response to LPS (M1: IL-10^{low}, $IL12^{high}$ and M2: IL-10^{high}, $IL12^{low}$) [19] were infected with *C. albicans* at a 1:1 ratio. After 8h of co-culture, cells were washed 3 times with PBS and protein samples were extracted in 200 µl of RIPA Buffer (150mM NaCl, 50mM Tris, pH 7.5, 1% NP40, 0.25% sodium deoxycolate and 1:1000 protease inhibitor cocktail). Lysates were clarified by centrifugation at 14000 ×g at 4 °C for 20 min and stored at -80 ºC. To clean up samples, proteins were precipitated using the 2D-Clean Up Kit (GE Healthcare) and resuspended in 30mM Tris-HCl, 7M urea, 2M thiourea, 4% CHAPS. Protein concentration was determined using the Bradford assay (Bio-Rad).

2.8 Quantitative proteomics

2.8.1 Sample labeling

Four biological replicates from control and treated M1 and M2 macrophages were fluorescently labeled for DIGE analysis following the protocol of the manufacturer. Briefly, 200 pmol of Cy Dye (N-hydroxysuccinamide esters of cyanine fluorescent dyes from GE Healthcare) in 1µl of anhydrous N, N dimethylformamide (DMF, Sigma) per 25µg of protein were used. After 30 min of incubation on ice in the dark, the reaction was quenched with 10mM L Lysine for 10 min under the same conditions.

2.8.2 Two-dimensional differential in-gel electrophoresis (2D-DIGE)

Control and *C. albicans*-treated M1 and M2 macrophage labeled samples were combined according to the experimental design and four 2-DE gels were performed. Each gel contained a pair of Cy3 and Cy5 labeled samples (25µg of protein of each sample), corresponding to the control and treated M1 and M2 samples (dye-swaps were performed), and a 25µg aliquot of a Cy2 labeled pooled standard made by mixing equal amounts of the four proteomes. The mixtures (75µg) were diluted 1:1 with the loading buffer [7M urea, 2M thiourea, 4% (w/v) CHAPS, 2% DTT and 4% pharmalytes, pH 3-11]. First dimension (IEF) of the 2DE was performed with 18 cm Immobiline IPG-strips (GE Healthcare) providing a non-linear pH 3-11 gradient, passively rehydrated with 350 µl of rehydration buffer [7M urea, 2M thiourea, 4% (w/v) CHAPS, 100mM DeStreak and 2% IPGphor buffer, pH 3-11] during 8h. The mixtures were then applied by cup loading. The IEF was performed at 20ºC using the following sequential steps: 120 V for 1 h; 500 V for 2h; 500-2000 V gradient for 2 h; 2000–5000 V gradient for 6h; 5000 V for 12h. After the IEF, strips were equilibrated for 12 min in reducing solution [100mM Tris-HCl (pH 8.0), 6M urea, 30% (v/v) glycerol, 2% (w/v) SDS, 2% (w/v) DTT], and then for 5 min in alkylating solution [100mM Tris-HCl (pH 6.8), 6M urea, 30% (v/v) glycerol, 2% (w/v) SDS, and 2.5% (w/v) Iodoacetamide and 0.002% bromophenol blue]. The equilibrated strips were transferred onto 12% homogenous polyacrylamide gels (2.6% C) in low fluorescent glass plate using an Ettan-DALT six system (GE Healthcare). Electrophoresis was carried out at 15W/gel for about at 20ºC.

2.8.3. Image visualization and DIGE data analysis

After electrophoresis, the differentially labeled co-resolved proteins within each gel were imaged using a Typhoon 9400 laser scanner (GE Healthcare). For the Cy3, Cy5 and Cy2 image acquisition, the 532-nm/580-nm, 633-nm/670-nm and 488-nm/520-nm excitation/emission wavelengths were used respectively, adjusting the pixel size resolution to 100 microns. The gel images obtained were cropped in the ImageQuant v5.1 software (GE Healthcare). For spot detection, determination of quantity, inter-gel matching and statistics gel images were analyzed using DeCyder v6.5 software (GE Healthcare). The differential in-gel analysis (DIA) module was used to assign spot boundaries and to calculate parameters such as normalized spot volumes. The intergel variability was corrected by matching, and normalized with the internal standard spot maps in the biological variation analysis (BVA) module. Control *versus* treated (M1 and M2 separately) and M1 *versus* M2 (either untreated or exposed to *Candida*) comparisons were subsequently performed. Statistical significance was assessed for each change in abundance using Student's *t*-test and 2-ANOVA analyses. Statistical significance was considered to be at the

95% confidence level when standardized average spot volume ratios exceeded ± 1.3 in at least six of the eight analyzed gels (i.e., 18 of the 24 analyzed images) [20].

2.8.4. Protein identification by Mass Spectrometry

After fluorescence scanning, the total protein profile was detected by staining the DIGE gels with Colloidal Coomassie Blue (CCB). The changes observed by 2D-DIGE analyses were aligned with CCB profiling, and the spots of interest were manually excised from the gels and transferred to microcentrifuge tubes. Samples were in-gel reduced, alkylated and digested with trypsin according to Sechi and Chait [21]. Briefly, spots were washed twice with double-distilled water, dehydrated with 75% acetonitrile (ACN) and dried in a Savant SpeedVac, reduced with 10mM DTT and alkylated with 55mM iodoacetamide. Finally, samples were digested with 12.5ng/l sequencing-grade trypsin (Roche Molecular Biochemicals, IN, USA) in 25 mM ammonium bicarbonate (pH 8.5) overnight at 37ºC. After digestion, the supernatants were collected and 1µl was spotted onto a matrix assisted laser desorption ionization (MALDI) target plate and allowed to air-dry at room temperature. Then, 0.5µl of a 3mg/ml of α-cyano-4-hydroxy-trans-cinnamic acid matrix in 0.1% TFA-50% ACN was added to the dried peptide digest spots and again allowed to air-dry again. MS analyses were performed in a MALDI-TOF/TOF spectrometer 4700 Proteomics Analyzer (PerSeptives Biosystems, Framingham, MA). The instrument was operated in reflector positive ion mode, with an accelerating voltage of 20000 V. All mass spectra were internally calibrated using auto-digested trypsin peptides. MALDI-TOF spectra with a signal-to-noise 20 were collated and represented as a list of monoisotopic molecular weights. Proteins for which peptide mass fingerprints provided an ambiguous identification were subjected to MS/MS sequencing analyses. MALDI TOF/TOF fragmentation spectra with a signal-to-noise 10 were collected by selecting the suitable precursor ions of each MALDI-TOF peptide mass map. Fragmentation was carried out using the acquisition method 1kV ion reflector mode CID on and precursor mass window ±10 Da.

Protein identification was done at the Proteomics Facility of Universidad Complutense de Madrid-Parque Científico de Madrid, Spain (UCM-PCM), a member of ProteoRed Network. For protein identification, the monoisotopic peptide mass fingerprinting data obtained from MS and the amino acid sequence obtained from each peptide fragmentation in MS/MS analyses were used to search for protein *Candida*tes using Mascot version 2.1 from Matrix Science (http://www.matrixscience.com). The searches for peptide mass fingerprints and tandem MS spectra were performed using Swiss-Prot release 53.0 (http://www.expasy.ch/sprot) and TrEMBL release 37.0 (http://www.ebi.ac.uk/trembl) databases without taxonomy restriction, containing 269293 and 4672908 sequence entries respectively for each software version and database release. The Mascot search parameters were (1) species, all; (2) allowed number of missed cleavages, 1; (3) fixed modification, carbamidomethyl cystein; (4) variable modifications, methionine oxidation; (5) peptide tolerance, ± 50 (PMF) -100 (combined search) ppm; (6) MS/MS tolerance, ± 0.3 Da; and (7) peptide charge, + 1. In all identified proteins, the probability score was greater than the one fixed by Mascot as being significant, that is, a p value < 0.05. The parameters for the combined search (peptide mass fingerprint and MS/MS spectra) were the same as described above.

2.9. Quantitative PCR

Total RNA was extracted using the RNeasy® Mini kit or AllPrep® DNA/RNA/Protein Mini kit (Qiagen, Germany) following manufacturer's guidelines. cDNA was synthesized using the Reverse Transcription System kit (Applied Biosystems, USA). Oligonucleotides for selected genes were designed according to the Roche software (Universal Probe Roche library). Quantitative real-time PCR (qRT-PCR) was performed or an iQTM5 (Biorad, USA). Assays were made in triplicate and results normalized according to the expression level of TBP. Results were expressed using the ΔΔCt method for quantitation.

10. Western-blotting

Fifty µg of protein per well were separated onto 10% SDS-polyacrylamide minigels and transferred to Hybond-ECL Nitrocellulose membranes (Amersham Biosciences). The western-blotting was performed with Odyssey system (Infrared Imaging System (LI-COR Biosciences, Nebraska, USA), which allows the measurement of the relative levels of fluorescence of the different bands and simultaneous labeling with 2 different antibodies. After 1h of incubation with primary antibodies: 1/2000 monoclonal anti-Vimentin (SIGMA), 1/2000 monoclonal anti-Moesin (Abcam), 1/2000 monoclonal anti-Actin (ICN Biomedicals), 1/3000 rat polyclonal Anti-Tubulin (Serotec/Bionova), 1/1000 rabbit polyclonal anti-Enolase A (Santa Cruz), membranes were washed 4 times in PBS with 0.1 % Tween-20. After this, membranes were incubated with fluorescently labeled secondary antibodies: 1/4000 IRDye 800CW conjugated Goat (polyclonal) anti-Rabbit IgG, 1/2000 highly cross absorbed (LI-COR Biosciences) and 1/4000 IRDye 680 conjugated Goat (polyclonal) anti-Mouse IgG, highly cross absorbed (LI-COR Biosciences) or IRDye 680 Goat anti-Rat IgG, highly cross absorbed (LI-COR Biosciences) for 60 min at room temperature and protected from light. The membranes were washed again and scanned for fluorescence detection with Odyssey system (LI-COR Biosciences, Nebraska, USA). Data were expressed as mean □ SD. The unpaired Student's t-test was used to compare differences between groups and $p<0.05$ was considered significant.

11. Fluorescence Microscopy

M1 and M2 macrophages were cultured and differentiated onto 18-mm coverslips placed in 12-well plates during 7 days at 37ºC and 5% CO_2. After this, macrophages were confronted with *C. albicans* at 37ºC and 5% CO_2 during 8h, at a ratio 1:1. Coverslips were washed twice with PBS and cells were fixed with 3.7% formaldehyde in PBS for 30 min at 4ºC. The coverslips were then washed twice with PBS and cell membranes were permeabilized for 15 min with PBS containing 0.2% Tween 20 at room temperature. At that point, the coverslips were washed twice 10 min in gentle sacking, and overlaid with 1/500 monoclonal anti-Moesin (Abcam), incubated for 1h, washed with PBS 3 times and overlaid with 1/2000 Alexa Fluor 568 anti-mouse antibody (Invitrogen) and with 1/2000 Phalloidin FITC (Sigma-Aldrich), incubated for 1h, washed with PBS 3 times in the dark and mounted with anti-fading solution with DAPI. Digital images were captured using a confocal fluorescence microscopy Leica TCS SP2.

3 Results

3.1 Effector functions of M1 and M2 macrophages in response to *C. albicans*

In an attempt to understand the response of human macrophages against *C. albicans* infections, the effector functions of M1 and M2 macrophages exposed to live *C. albicans* SC5314 strain were assessed. In addition, and to dissect the molecular mechanisms underlying the macrophage antifungal response, we evaluated the proteomic signature of control and *C. albicans*-treated M1 (GM-CSF) and M2 (M-CSF) macrophages.

Using 4 donors, first, cytokine secretion, *C. albicans* phagocytosis and killing by M1 and M2 macrophages were evaluated at different macrophage:*Candida* MOIs (10:1, 1:1 and 1:5) and at different interaction times (3, 6, 12 and 18h), as a means to determine the experimental condition that produces an adequate balance between macrophage stimulation and pathogen-induced cell death. At a MOI 10:1 the macrophages response to the yeast was moderate, while at 1:5 ratio the interaction with *Candida* was toxic for the macrophages. At a MOI of 1:1, M2 macrophages exhibited a lower, although non statistically significant, yeast uptake than M1 macrophages after 3h and the difference disappeared at later time points (Supplemental Figure S1 A and B). Regarding fungicidal activity, M2 macrophages exhibited a higher killing ability after 3h, but the Candidacidal ability of both macrophage subpopulations was similar at longer co-incubation times (Supplemental Figure S1C). On the other hand, and as expected, the presence of *Candida* yeasts during 12-18h induced the production of higher levels of IL-12p40 in M1 and IL-10 in M2 macrophages (Supplemental Figure S1D). Since a 12h incubation usually led to an unacceptably high level of macrophage death, all subsequent experiments were done using a 1:1 macrophage-yeast ratio and a co-incubation time of 8h.

3.2 Comparative proteomic analysis of M1 and M2 macrophages and their response to *C. albicans* infection

Once the functional response of M1 and M2 macrophages to *C. albicans* had been analyzed and the optimal conditions for the macrophage-yeast co-culture established, fully polarized M1 and M2 macrophages from 4 different donors were exposed to *C. albicans* infection and proteomic analysis was carried out. As shown in Figure 1, whereas LPS yielded the expected cytokine profile in M1 and M2 macrophages, the 8h exposure to *C. albicans* only increased the production of IL-10 by M2 macrophages, not having a significant effect on the expression of the rest of the analyzed cytokines in either M1 or M2 macrophages (Figure 1).

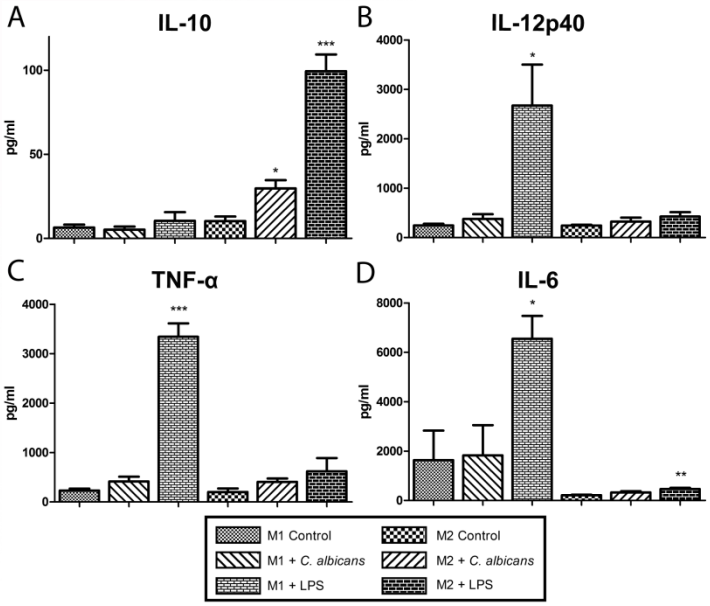

Figure 1. Cytokine profile of *C. albicans*-stimulated M1- and M2-polarized macrophages. IL-10 (A), IL-12p40 (B), TNFα (C) and IL-6 (D) levels in M1 and M2 macrophages exposed to either C. albicans or LPS (as positive control), as determined by ELISA. Macrophages were either untreated or treated with *C. albicans* for 8h or LPS (10ng/ml) for 24h. Data are represented as mean ± SD (n=4), and statistical significance relative to the corresponding non-stimulated macrophage subtype is indicated (*, $p<0.05$; **, $p<0.01$; ***, $p<0.001$).

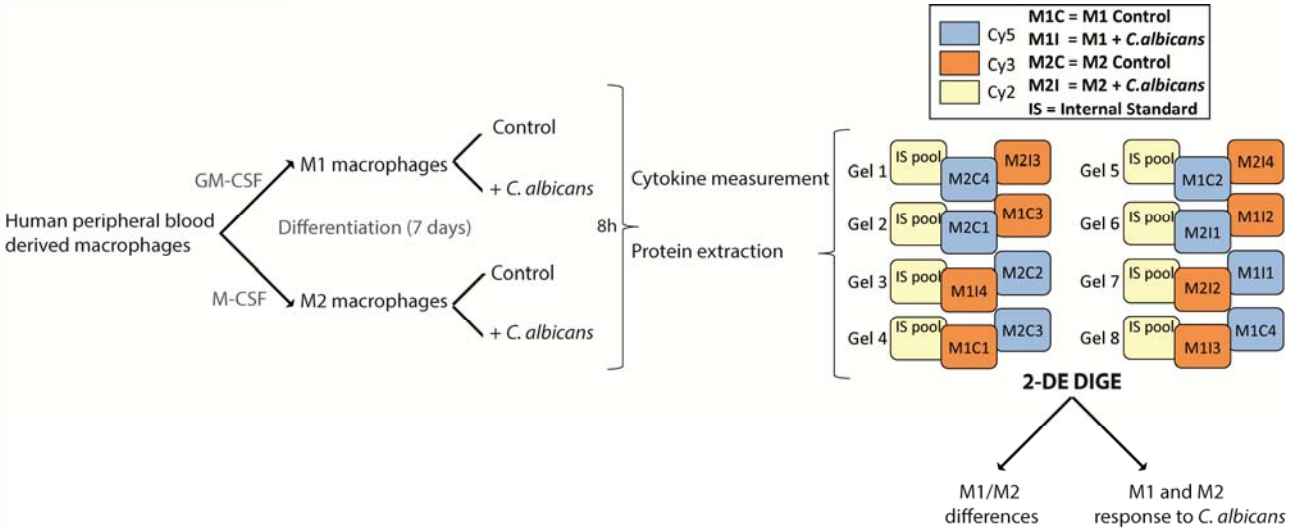

Figure 2. Flow chart for analysis of M1 and M2 macrophages proteome and their response to *C. albicans*. Workflow of the quantitative 2-D DIGE. Four replicates of M1 and M2 macrophages, control and after 8h of interaction with *C. albicans* were obtained and labeled with Cy3 and Cy5. Internal standard consisted of a pool of all the protein samples used in the experiment. Differentially expressed proteins determined by 2-D DIGE were excised from the gel and identified by Mass Spectrometry.

Protein samples of untreated or *Candida*-exposed (8h, MOI 1:1) M1 and M2 macrophages were analyzed using 2D-DIGE methodology according to the scheme shown in Figure 2. After eight-plex 2D-DIGE, 3 individual images were obtained from each gel, corresponding to Cy2-, Cy3- and Cy5-labeled samples. The 24 gel images were analyzed using DeCyder software. Differences in protein expression between M1 and M2 macrophages on the one hand, and the *C. albicans* effect on M1 or M2 protein profile on the other hand, were analyzed. DIA analysis allowed the detection of a total of 1889 protein spots on each image. Then, inter-image spot matching was carried out by BVA analysis. In this step, 1527 spots were matched on the gels, and their average abundances among the 24 images of our study were calculated. Only changes within 95% confidence interval ($p<0.05$) and with standardized average spot volume ratios exceeding 1.3 in at least 6 of the 8 analyzed gels were considered. Regarding untreated macrophages, this analysis identified 83 spots with higher intensity in M1 macrophages, and 61 spots with higher intensity in M2 macrophages (Figure 3)

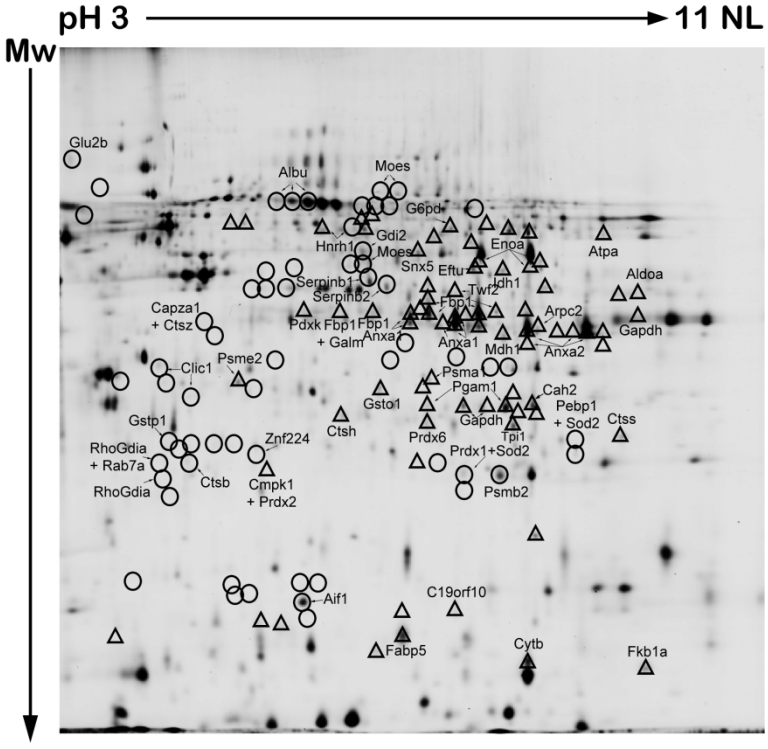

Figure 3. Representative 2-DE of M1 and M2 polarized macrophages. Proteins were resolved in the 3-11 (non linear) pH range on the first dimension, and on 10% polyacrylamide gels on the second dimension. Proteins differentially expressed between M1 and M2 macrophages (Ratio=M1/M2) were identified by mass spectrometry. Spots included into triangles match proteins that are more abundant in M1 macrophages while circled spots correspond to proteins with higher expression in M2 macrophages.

Table 1. Functional classification of M1 and M2 macrophages differentially abundant proteins identified from 2D-DIGE broad range pH gels (pH 3-11 NL IPG Strips)

Master Nº	Protein ID[a]	Swiss Prot[a]	Protein Name	Av, Ratio[c]	T-test[c]	2-ANOVA[c]	M_r[b]	pI[b]	Score[b]	Nº Pept[b]	% Cov[d]	Expect
METABOLISM												
334	G6PD	P11413	Glucose-6-phosphate 1-dehydrogenase	1.8	0.09	0.04	59675	6.39	90	14	22	2.2E-05
342	ATPA	P25705	ATP synthase subunit alpha, mitochondrial	1.69	0.03	0.01	59828	9.16	118	11	25	3.2E-08
471	ENO1	P06733	Alpha-enolase	1.39	0.14	0.02	47481	7.01	172	19	54	1.3E-13
473	ENO1	P06733	Alpha-enolase	2.03	0.01	0.00	47481	7.01	90	13	34	2.20E-05
488	ENO1	P06733	Alpha-enolase	1.71	0.03	0.03	47481	7.01	185	22	53	6.40E-15
520	FBP1	P09467	Fructose-1,6-bisphosphatase 1	1.49	0.11	0.04	37190	6.54	139	20	48	2.6E-10
564	FBP1	P09467	Fructose-1,6-bisphosphatase 1	3.77	0.01	0.00	37190	6.54	141	20	45	1.6E-10
598	ALDOA	P04075	Fructose-bisphosphate aldolase A	1.37	0.15	0.03	39851	8.30	77	12	40	4.00E-04
637	FBP1	P09467	Fructose-1,6-bisphosphatase 1	1.43	0.02	0.01	37190	6.54	181	10	20	1.6E-14
645	FBP1	P09467	Fructose-1,6-bisphosphatase 1	8.68	0.00	0.00	37190	6.54	248	29	60	1.6E-14
654	FBP1	P09467	Fructose-1,6-bisphosphatase 1	7.06	0.00	0.00	37190	6.54	98	15	41	3.10E-06
656*	FBP1	P09467	Fructose-1,6-bisphosphatase 1	1.95	0.02	0.00	37190	6.54	155	20	46	6.4E-12
656*	GALM	Q96C23	Aldose 1-epimerase	1.95	0.02	0.00	37970	6.18	74	10	32	7.20E-04
663	FBP1	P09467	Fructose-1,6-bisphosphatase 1	3.77	0.02	0.00	37190	6.54	156	23	46	5.1E-12
676	PDXK	O00764	Pyridoxal kinase	1.47	0.02	0.05	35308	5.75	103	13	24	1E-06
684	GAPDH	P04406	Glyceraldehyde-3-phosphate dehydrogenase	1.34	0.10	0.01	36201	8.57	176	21	59	5.10E-14
723	CTSZ	Q9UBR2	Cathepsin Z	-1.55	0.02	0.01	34530	6.70	60	7	26	0.018
743	MDHC	P14152	Malate dehydrogenase, cytoplasmic	2.11	0.02	0.02	36631	6.91	92	13	44	1.30E-05
923	CAH2	P00918	Carbonic anhydrase 2	2.74	0.00	0.00	29285	6.87	75	9	32	6.40E-04
924	PGAM1	P18669	Phosphoglycerate mutase 1	2.53	0.02	0.00	28900	6.67	155	17	58	6.4E-12
926	GAPDH	P04406	Glyceraldehyde-3-phosphate dehydrogenase	1.84	0.02	0.00	36201	8.57	75	9	24	7.00E-04
927	GAPDH	P04406	Glyceraldehyde-3-phosphate dehydrogenase	1.35	0.17	0.05	36201	8.57	56	10	34	0.05
947	PGAM1	P18669	Phosphoglycerate mutase 1	1.4	0.02	0.01	28900	6.67	97	12	55	4.2E-06
960	TPI1	TPI1	Triosephosphate isomerase	2	0.09	0.03	26938	5.46	202	19	73	1.3E-16
1349	FABP5	Q01469	Fatty acid-binding protein, epidermal	2.26	0.02	0.00	15497	6.60	93	11	65	9.50E-06
STRESS RESPONSE/OXIDOREDUCTASE ACTIVITY												
493	IDH1	O75874	Isocitrate dehydrogenase [NADP]	1.74	0.01	0.00	46915	6.53	111	16	38	1.6E-07
903	GSTO1	P78417	Glutathione S-transferase omega-1	1.93	0.07	0.03	27833	6.23	92	12	41	1.2E-05
979	PRDX6	P30041	Peroxiredoxin-6	1.36	0.23	0.05	25133	6.00	82	10	52	1.2E-05
1048*	SOD2	P04179	Superoxide dismutase [Mn], mitochondrial	-2.85	0.00	0.00	24878	8.35	78	6	20	3.00E-04
1080*	PRDX1	Q06830	Peroxiredoxin-1	-1.86	0.07	0.01	22324	8.27	93	9	93	1.1E-05
1080*	SOD2	P04179	Superoxide dismutase [Mn], mitochondrial	-1.86	0.07	0.01	24878	8.35	240	10	31	2E-20
1082	PRDX2	P32119	Peroxiredoxin-2	1.41	0.23	0.04	22049	5.66	66	4	14	0.0057

Table 1. Continuation

IMMUNE RESPONSE												
68	PRKCSH	P14314	Glucosidase 2 subunit beta	-3.66	0.05	0.01	60357	4.33	94	18	30	9.1E-06
524	SERPINB1	P30740	Leukocyte elastase inhibitor	-1.39	0.20	0.03	42829	5.90	119	15	42	2.6E-08
535	SERPINB2	P05120	Plasminogen activator inhibitor 2	-1.82	0.05	0.02	46851	5.46	141	22	5	1.6E-10
679	ANXA1	P04083	Annexin A1	1.97	0.02	0.00	38918	6.57	233	24	63	1E-19
681	ANXA1	P04083	Annexin A1	1.3	0.09	0.02	38918	6.57	223	24	71	1E-18
710	ANXA1	P04083	Annexin A1	1.47	0.09	0.03	38918	6.57	62	7	23	0.012
717	ANXA2	P07355	Annexin A2	1.55	0.02	0.00	38808	7.57	243	28	54	1E-20
721	ANXA1	P04083	Annexin A1	2.1	0.02	0.00	38918	6.57	331	32	77	1.60E-29
725	ANXA1	P04083	Annexin A1	1.54	0.03	0.01	38918	6.57	286	28	71	5.1E-25
726	ANXA2	P07355	Annexin A2	1.61	0.03	0.01	38808	7.57	316	33	64	5.10E-28
730	ANXA2	P07355	Annexin A2	1.34	0.07	0.00	38808	7.57	282	30	67	1.30E-24
781	ANXA2	P07355	Annexin A2	1.31	0.04	0.35	38808	7.57	163	19	52	1E-12
871	PSMA1	P25786	Proteasome subunit alpha type-1	1.46	0.07	0.02	29822	6.15	82	15	40	1.40E-04
892	PSME2	Q9UL46	Proteasome activator complex subunit 2	1.43	0.01	0.03	27515	5.44	116	15	45	5.1E-08
1032	GSTP1	P09211	Glutathione S-transferase P	-2.57	0.00	0.00	23569	5.43	105	3	17	6.4E-07
1064	CTSB	P07858	Cathepsin B	-2.35	0.01	0.00	38766	5.88	352	13	20	1.3E-31
1079	PSMB2	P49721	Proteasome subunit beta type-2	-1.57	0.19	0.03	22993	6.51	67	9	31	0.004
1294	AIF1	P55008	Allograft inflammatory factor 1	-2.96	0.01	0.00	16693	5.97	76	14	64	5.00E-04
1301	C19orf10	Q969H8	UPF0556 protein C19orf10	1.42	0.02	0.06	18897	6.20	62	8	35	0.014
1408	FKB1A	P62942	Peptidyl-prolyl cis-trans isomerase FKBP1A	1.66	0.16	0.04	12000	7.88	70	10	62	0.0021
1409	CSTB	P04080	Cystatin-B	2.92	0.06	0.00	11190	6.96	163	7	55	1E-12
1521	CTSS	P25774	Cathepsin S	1.47	0.24	0.02	38099	8.61	103	13	42	1E-06
CYTOSKELETAL COMPONENTS AND ACTIN BINDING PROTEINS												
157	MOES	P26038	Moesin	-1.55	0.01	0.00	67892	6.08	267	36	51	4E-23
159	MOES	P26038	Moesin	-1.74	0.00	0.00	67892	6.08	117	22	33	4E-08
487	MOES	P26038	Moesin	-1.75	0.00	0.00	67892	6.08	67	5	6	0.0041
584	TWF2	Q6IBS0	Twinfilin-2	1.37	0.26	0.03	39751	6.37	126	14	50	5.1E-09
723	CAPZA1	P52907	F-actin-capping protein subunit alpha-1	-1.55	0.02	0.01	33073	5.45	82	8	46	1.3E-04
734	ARPC2	O15144	Actin-related protein 2/3 complex subunit 2	1.34	0.01	0.00	34426	6.84	78	11	37	2.9E-04

Table 1. Continuation

NUCLEIC ACID PROCESSING												
356	HNRH1	P31943	Heterogeneous nuclear ribonucleoprotein H	1.56	0.04	0.02	49484	5.89	80	12	35	1.80E-04
362	HNRH1	P31943	Heterogeneous nuclear ribonucleoprotein H	-1.48	0.02	0.01	49484	5.83	153	20	53	1E-11
500	EFTU	P49411	Elongation factor Tu, mitochondrial	1.42	0.00	0.02	49852	7.26	114	16	30	8.10E-08
1082	CMPK1	P30085	Cytidine monophosphate kinase	1.41	0.23	0.04	22436	5.44	113	7	23	1E-07
TRANSPORT												
423	GDI2	P50395	Rab GDP dissociation inhibitor beta	-1.79	0.00	0.00	51087	6.11	176	25	45	5.1E-14
424	SNX5	Q6P5V6	Sorting nexin-5	1.31	0.02	0.10	47072	6.31	90	7	19	1.9E-05
848	CLIC1	O00299	Chloride intracellular channel protein 1	-1.3	0.06	0.04	27248	5.09	58	7	45	0.035
906	CLIC1	O00299	Chloride intracellular channel protein 1	-1.61	0.02	0.01	27248	5.09	205	17	65	6.40E-17
1052	RAB7A	P51149	Ras-related protein Rab-7a	-2.14	0.01	0.00	23760	6.40	78	7	31	3.40E-04
1055	ZNF224	Q9NZL3	Zinc finger protein 224	-1.83	0.08	0.01	84874	9.01	59	11	22	0.027
PROTEIN FATE												
975	CTSH	P09668	Cathepsin H	1.79	0.06	0.03	38053	8.35	107	6	20	4E-07
OTHER FUNCTIONS												
184	ALB	P02768	Serum albumin	-1.98	0.03	0.08	71317	5.92	42	1	2	0.0012
189	ALB	P02768	Serum albumin	-1.96	0.05	0.06	71317	5.92	66	8	9	0.0053
194	ALB	P02768	Serum albumin	-1.85	0.06	0.04	71317	5.92	80	11	16	2.10E-04
1048*	PEBP1	P30086	Phosphatidylethanolamine-binding protein 1	-2.85	0.00	0.00	21158	7.01	277	17	87	4E-24
1052	GDIA1	P52565	Rho GDP-dissociation inhibitor 1	-2.14	0.01	0.00	23250	5.02	85	5	18	5.8E-05
1077	GDIA1	P52565	Rho GDP-dissociation inhibitor 1	-2.44	0.00	0.04	23250	5.02	65	9	34	0.0063

[a] Protein name and accession number according to Human PSD & GPCR-PD human, mouse and rat database (Mouse Protein Report with PSD Interactions) of Proteome Bioknowledge Library (https://www.proteome.com/control/tools/proteome). These proteins spots are labeled with the same Protein ID in Figure 2. [b] Experimental molecular mass, pI, matched peaks/unmatched peaks peptides and protein score are derived from Mascot result page. [c] Average ratio, student's t-test and 2-ANOVA p-values were calculated using Decyder software v6. [d] The protein coverage corresponds to a percentage in proteins identified by peptide mass fingerprinting. For proteins identified by PMF combined with fragmentation analysis of some peptides, the protein coverage and the protein score data are derived from the Mascot results page of the combined search. * Shown the spots with more than 1 protein identified in it.

When comparing control *C. albicans*-treated macrophages, the analysis yielded 12 spots with higher intensity and 2 spots with lower intensity in *C. albicans*-treated M1 macrophages (Figure 4A). For M2 macrophages, 20 spots showed increase and 26 showed decrease in intensity upon interaction with yeasts (Figure 4B).

The spots with different intensity in the various comparisons were subsequently digested in-gel and analyzed by MALDI-TOF-MS. Mascot database search using the peptide mass fingerprint spectra allowed the identification of the proteins in 71 spots identified from the gels corresponding to the M1-M2 comparison (Figure 3), 11 spots from the gels corresponding to the treated versus control M1 comparison (Figure 4A) and 31 in the untreated versus *Candida* treated macrophage M2 comparison (Figure 4B). Proteins identified as differentially expressed at the distinct experimental conditions are summarized in Table 1 (M1 versus M2 macrophages), Table 2 (untreated versus *Candida*-treated M1 macrophages) and Table 3 (untreated versus *Candida*-treated M2 macrophages), with detailed information regarding accession number, experimental and theoretical pI and MW values, and identification parameters.

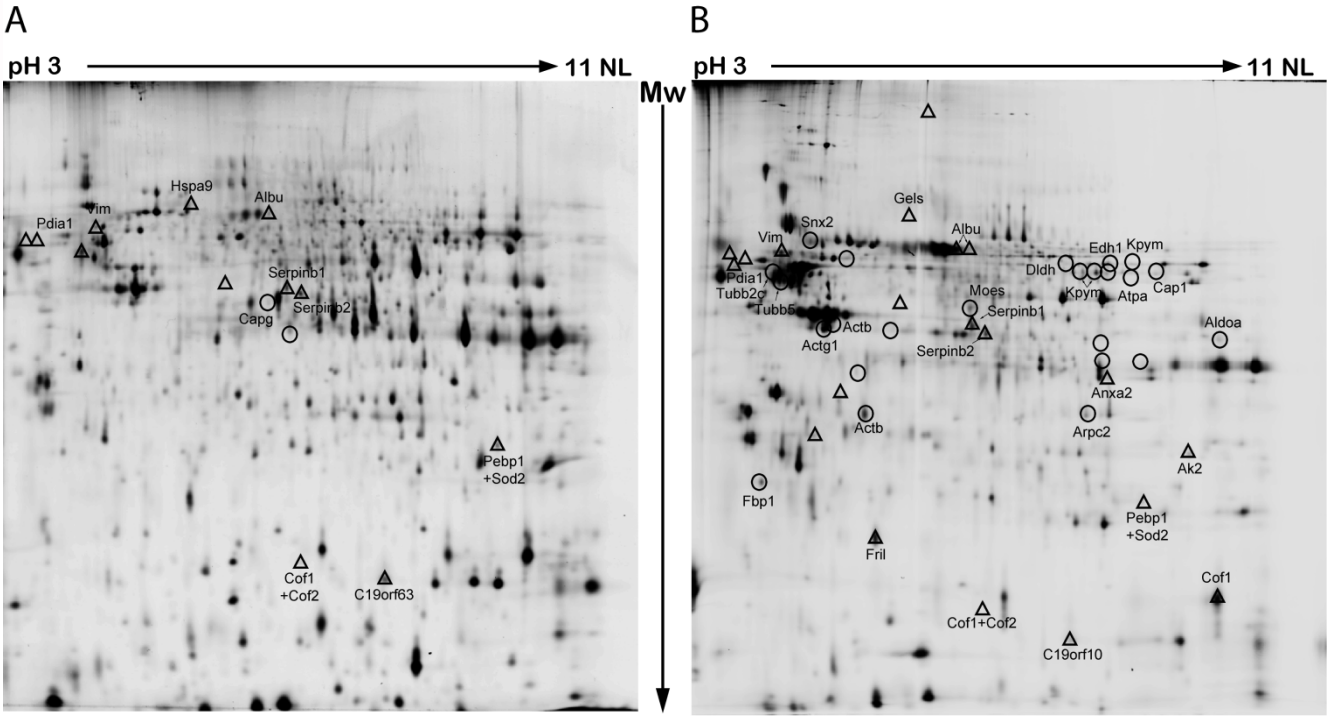

Figure 4. Representative 2-DE of M1 and M2 in response to *C. albicans*. Proteins were resolved in the 3-11 (non linear) pH range on the first dimension, and on 10% polyacrylamide gels on the second dimension. Proteins exhibiting a significantly altered expression in M1 (A) and M2 macrophages (B) after interaction with *C. albicans* were identified by mass spectrometry. Circled spots match with down-expressed proteins in macrophages after the interaction with the yeast and spots included into triangles match with over-expressed proteins.

A database search was carried out to assess the activity of the differentially expressed proteins in order to assign them into distinct functional groups. The analysis of the proteins differentially expressed between M1 and M2 macrophages revealed a significant enrichment in proteins related to metabolism and cytoskeleton rearrangement (Table 1). This result is compatible with the considerable morphological differences existing between monocyte-derived M1 and M2 macrophages 19. On the other hand, most of the proteins regulated in M1 macrophages in response to *Candida* were related to stress response and cytoskeleton (Table 2), whereas those modulated by *Candida* in M2 macrophages were related to stress, cytoskeleton and metabolism (Table 3).

3.3 Validation of the proteomic analysis

As a means to confirm the above proteomic results, protein extracts were generated from 3 independent untreated and *C. albicans*-treated macrophage samples, and the levels of differentially expressed proteins were analyzed by Western blotting. For the M1/M2 comparison, Moesin and Enolase-1 were chosen, while Vimentin was selected to validate the M1 response to *C. albicans*, and Vimentin, Actin, Moesin and Tubulin for the M2 macrophage response to *Candida*. Western blot data confirmed the increase in Moesin and the decrease in Enolase in M2 macrophages (Figure 5A), the increase in Vimentin both in M1 and M2 macrophages after interaction with *Candida* (Figure 5B and C), and the decrease in Moesin, Actin and Tubulin in M2 macrophages (Figure 5C).

Table 2. Functional classification of M1 polarized macrophages differentially abundant proteins in response to *C. albicans* identified from 2D-DIGE broad range pH gels (pH 3-11 NL IPG Strips).

Master Nº	Protein ID[a]	Swiss Prot[a]	Protein Name	Av, Ratio[c]	T-test[c]	2-ANOVA	M_r[b]	pI[b]	Score[b]	Nº Pept[b]	% Cov[d]	Expect
STRESS RESPONSE/OXIDOREDUCTASE ACTIVITY												
136	GRP75	P38646	Stress-70 protein, mitochondrial	1.54	0.04	0.32	73920	5.87	191	31	39	1.6E-15
247	PDIA1	P07237	Protein disulfide-isomerase	1.48	0.23	0.01	57480	4.76	125	17	31	6.4E-09
1048*	SOD2	P04179	Superoxide dismutase [Mn], mitochondrial	1.47	0.08	0.04	24878	8.35	78	6	20	3.00E-04
IMMUNE RESPONSE												
524	SERPINB1	P30740	Leukocyte elastase inhibitor	1.50	0.24	0.02	42829	5.90	119	15	42	2.6E-08
535	SERPINB2	P05120	Plasminogen activator inhibitor 2	2.67	0.03	0.00	46851	5.46	141	22	5	1.6E-10
1263	C19orf10	Q969H8	UPF0556 protein C19orf10	3.24	0.26	0.01	18897	6.20	152	7	32	1.3E-11
CYTOSKELETAL COMPONENTS AND ACTIN BINDING PROTEINS												
218	VIM	P08670	Vimentin	2.33	0.04	0.02	53676	5.06	297	30	65	4E-26
597	CAPG	P40121	Macrophage-capping protein	-1.50	0.05	0.04	38779	5.88	92	13	36	1.20E-05
1215	COF1	P23528	Cofilin-1	1.34	0.44	0.02	18719	8.22	87	4	18	4.40E-05
1215	COF2	Q9Y281	Cofilin-2	1.34	0.44	0.02	18839	7.66	80	3	13	2.20E-04
OTHER FUNCTIONS												
206	ALB	P02768	Serum albumin	1.92	0.31	0.04	71317	5.92	137	8	14	4E-10
1048*	PEBP1	P30086	Phosphatidylethanolamine-binding protein 1	1.47	0.08	0.04	21158	7.01	277	17	87	4E-24

[a] Protein name and accession number according to Human PSD & GPCR-PD human, mouse and rat database (Mouse Protein Report with PSD Interactions) of Proteome Bioknowledge Library (https://www.proteome.com/control/tools/proteome). These proteins spots are labeled with the same Protein ID in Figure 3A. [b] Experimental molecular mass, pI, matched peaks/unmatched peaks peptides and protein score are derived from Mascot result page. [c] Average ratio, student's t-test and 2-ANOVA p-values were calculated using Decyder software v6. [d] The protein coverage corresponds to a percentage in proteins identified by peptide mass fingerprinting. For proteins identified by PMF combined with fragmentation analysis of some peptides, the protein coverage and the protein score data are derived from the Mascot results page of the combined search. * Shown the spots with more than 1 protein identified in it.

Table 3. Functional classification of M2 polarized macrophages differentially abundant proteins in response to *C. albicans* identified from 2D-DIGE Broad Range pH Gels (pH 3-11 NL IPG Strips).

Master Nº	Protein ID[a]	Swiss Prot[a]	Protein Name	Av, Ratio[c]	T-test[c]	2-ANOVA	M_r[b]	pI[b]	Score[b]	Nº Pept[b]	% Cov[d]	Expect
STRESS RESPONSE/OXIDOREDUCTASE ACTIVITY												
247	PDIA1	P07237	Protein disulfide-isomerase	2.31	0.01	0.01	57480	4.76	125	17	31	6.4E-09
299	DLDH	P09622	Dihydrolipoyl dehydrogenase, mitochondrial	-1.38	0.06	0.02	54713	7.95	58	8	12	0.033
1048*	SOD2	P04179	Superoxide dismutase [Mn], mitochondrial	1.31	0.29	0.04	24878	8.35	78	6	20	3.00E-04
IMMUNE RESPONSE												
524	SERPINB1	P30740	Leukocyte elastase inhibitor	1.73	0.04	0.02	42829	5.90	119	15	42	2.6E-08
535	SERPINB2	P05120	Plasminogen activator inhibitor 2	2.57	0.02	0.00	46851	5.46	141	22	5	1.6E-10
781	ANXA2	P07355	Annexin A2	2.61	0.01	0.05	38808	7.57	163	19	52	1E-12
1263	C19orf10	Q969H8	UPF0556 protein C19orf10	8.06	0.01	0.01	18897	6.20	152	7	32	1.3E-11
CYTOSKELETAL COMPONENTS AND ACTIN BINDING PROTEINS												
75	GELS	P06396	Gelsolin	2.03	0.04	0.05	86043	5.90	94	13	21	9.10E-06
218	VIM	P08670	Vimentin	1.49	0.28	0.02	53676	5.06	297	30	65	4E-26
305	CAP1	Q01518	Adenylyl cyclase-associated protein 1	-1.47	0.04	0.44	52222	8.27	72	15	28	0.0014
348	TUBB2C	P68371	Tubulin beta-2C chain	-1.32	0.03	0.35	50255	4.79	150	22	38	2E-11
400	TUBB5	P07437	Tubulin beta chain	-1.56	0.03	0.06	50095	4.78	164	24	38	8.10E-13
487	MOES	P26038	Moesin	-1.30	0.12	0.03	67892	6.08	67	5	6	0.0041
593	ACTB	P60709	Actin, cytoplasmic 1	-1.49	0.04	0.01	42052	5.29	103	13	33	1.00E-06
611	ACTG1	P63261	Actin, cytoplasmic 2	-1.57	0.03	0.01	42108	5.31	157	18	56	4E-12
823	ARPC2	O15144	Actin-related protein 2/3 complex subunit 2	-1.32	0.06	0.01	34426	6.84	202	25	56	1.3E-16
863	ACTB	P60709	Actin, cytoplasmic 1	-1.38	0.01	0.00	42052	5.29	76	13	33	5.30E-04
1186	COF1	P23528	Cofilin-1	1.59	0.01	0.06	18719	8.22	129	14	75	2.60E-09
1215*	COF1	P23528	Cofilin-1	2.01	0.02	0.02	18719	8.22	87	4	18	4.40E-05
1215*	COF2	Q9Y281	Cofilin-2	2.01	0.02	0.02	18839	7.66	80	3	13	2.20E-04
METABOLISM												
258	KPYM	P14618	Pyruvate kinase isozymes M1/M2	-1.59	0.01	0.01	58470	7.96	56	7	13	0.045
310	ATPA	P25705	ATP synthase subunit alpha, mitochondrial	-1.95	0.00	0.00	59828	9.16	86	15	31	5.30E-05
312	KPYM	P14618	Pyruvate kinase isozymes M1/M2	-1.47	0.05	0.03	58470	7.96	81	12	34	1.80E-04
318	KPYM	P14618	Pyruvate kinase isozymes M1/M2	-1.63	0.07	0.04	58470	7.96	179	24	50	2.6E-14
599	ALDOA	P04075	Fructose-bisphosphate aldolase A	-1.71	0.00	0.09	39851	8.30	143	18	45	1E-10
940	AK2	P54819	Adenylate kinase 2, mitochondrial	1.84	0.09	0.04	26689	7.67	78	12	42	3.30E-04
1056	FBP1	P09467	Fructose-1,6-bisphosphatase 1	-1.64	0.04	0.21	37190	6.54	181	10	20	1.6E-14
1520	FRIL	P02792	Ferritin light chain	1.42	0.03	0.06	20064	5.51	96	13	56	4.6e-006

Table 3. Continuation

TRANSPORT												
160	SNX2	O60749	Sorting nexin-2	-1.51	0.01	0.13	58549	5.04	101	16	31	1.60E-06
270	EHD1	Q9H4M9	EH domain-containing protein 1	-1.62	0.00	0.01	60646	6.35	109	20	29	2.6E-07
OTHER FUNCTIONS												
206	ALB	P02768	Serum albumin	1.68	0.01	0.04	71317	5.92	137	8	14	4E-10
212	ALB	P02768	Serum albumin	1.75	0.02	0.17	71317	5.92	192	12	12	1.3E-15
1048*	PEBP1	P30086	Phosphatidylethanolamine-binding protein 1	1.31	0.29	0.04	21158	7.01	277	17	87	4E-24

[a] Protein name and accession number according to Human PSD & GPCR-PD human, mouse and rat database (Mouse Protein Report with PSD Interactions) of Proteome Bioknowledge Library (https://www.proteome.com/control/tools/proteome). These proteins spots are labeled with the same Protein ID in Figure 3B. [b] Experimental molecular mass, pI, matched peaks/unmatched peaks peptides and protein score are derived from Mascot result page. [c] Average ratio, student's t-test and 2-ANOVA p-values were calculated using Decyder software v6. [d] The protein coverage corresponds to a percentage in proteins identified by peptide mass fingerprinting. For proteins identified by PMF combined with fragmentation analysis of some peptides, the protein coverage and the protein score data are derived from the Mascot results page of the combined search. * Shown the spots with more than 1 protein identified in it.

Additionally, qRT-PCR was also used to confirm the proteomic data. In this case, the relative level of SERPINB2 mRNA was determined, since PAI-2 (the SERPINB2 gene-encoded protein) was found to be significantly more expressed in M2-polarized macrophages (Figure 3). Analysis of two independent samples revealed that SERPINB2 levels were higher in M2 than in M1 macrophages in agreement with DIGE results (Figure 5D). Besides, SERPINB2 mRNA increased in both M1 and M2 macrophages after the interaction with *C. albicans* (Figure 5D), also in concordance to the proteomic results.

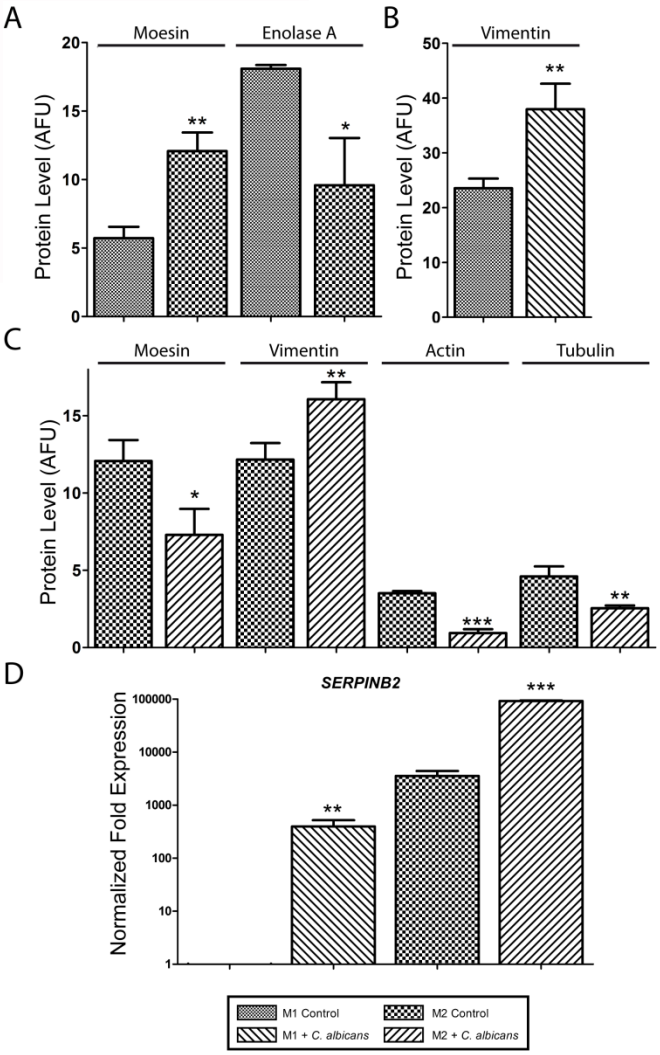

Figure 5. Validation of the differential expression of proteins in M1 and M2 macrophages by western-blotting and qPCR. Western blot quantification (Arbitrary Fluorescence Units:AFU) of the levels of Moesin and Enolase A (A), Vimentin (B), Moesin, Vimentin Actin and Tubulin (C) in macrophages under the experimental conditions indicated. (D) SERPINB2 mRNA expression levels determined by qRT-PCR in M1 and M2 macrophages either treated or untreated with *C. albicans* for 8h or LPS (10ng/ml) for 24h. Means ± SD are shown. Statistically significant differences are indicated (*, $p<0.05$; **, $p<0.01$; ***, $p<0.001$).

Finally, cytoskeleton immunofluorescence (Moesin and Actin) was done in order to illustrate the differences in morphology between M1 and M2 macrophages. M1 macrophages display a more round morphology in vitro (with the typical "fried egg" morphology) compared to M2, which show a more elongated and fibroblastoid shape [22] (Figure 6). Actin showed a decrease in their cytoplasmic concentrations, as it appeared both in the 2D-DIGE results and in the Western blot validations. However, actin cytoskeleton immunofluorescence showed that the decrease in cytoplasmic actin might be caused by the intense polymerization of actin to the phagocytic cups around *C. albicans* (Figure 6). Consequently, the extraction procedure, which is not so efficient for isolation of cytoskeletal proteins, might be causing this apparent contradiction. Nevertheless, these results suggest that the infection with the yeast has a global impact on actin, myosin and intermediate filaments distribution in macrophages.

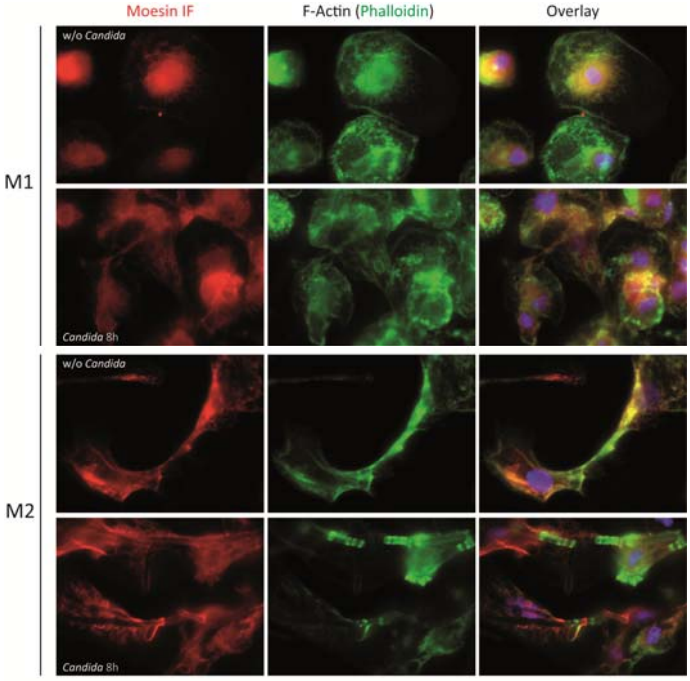

Figure 6. Differential location of Actin and Moesin in M1 and M2 polarized macrophages. Representative images showing Phalloidin staining (Actin) and Moesin inmunofluorescence in M1 and M2 control macrophages and after the incubation with *C. albicans* for 8h.

4 Discussion

Macrophages play a crucial role in innate and adaptive immunity and are key mediators in the inflammatory response, host defense and maintenance of tissue homeostasis. Depending on the surrounding signals, macrophages differentiate into a proinflammatory subtype (M1), also known as classically activated, or an anti-inflammatory and tissue-repairing subtype (M2), known as alternatively activated. Several recent studies have been focused on the phenotypic

and gene expression differences between M1 and M2 macrophages [23-25] and the differences in their response to different microorganisms such as *Trypanosoma brucei* [26], *Mycobacterum tuberculosis* [27], *Salmonella* species, and *Listeria monocytogenes* [28, 29]. Phenotypic markers of murine polarized macrophages have been extensively studied, whereas their human counterparts remain less characterized. In this study we have explored for the first time the differences in the proteome between M1 and M2 polarized human macrophages as well as in the dissimilarities between M1 or M2 responses against *C. albicans*. Due to the relevance of the M1/M2 switch in inflammation, tumorigenesis and wound healing [30, 31], this proteomic approach will contribute to understand the differences in the molecular mechanisms of macrophage polarization and to the identification of novel opportunities for generating more efficient immune and inflammatory responses against *C. albicans*. Besides, new virulence factors of this pathogen can be unraveled.

The 2D-DIGE comparisons between M1 and M2 polarized human macrophages have allowed the identification of 144 spots, 71 of which were subsequently identified and found to correspond to 51 proteins (Figure 3). Functional analysis of the differentially expressed proteins revealed that the most relevant pathways significantly modulated by macrophage polarization were metabolic routes, stress and immune responses, as well as cytoskeleton rearrangement (Table 1). Metabolism related proteins were the most affected functional category between M1/M2 macrophages. These proteins are involved in different metabolic routes, such us glycolysis, gluconeogenesis, tricarboxylic cycle, oxidative phosphorylation and pentose phosphate shunt. These findings are well in agreement with the known intrinsic metabolic differences between M1 and M2 macrophages, as well as with the different response to hypoxia shown by both macrophage subtypes [32]. This latter study revealed that the anaerobic glycolitic pathway prevails in M1 macrophages, whereas the oxidative glucose metabolism and the fatty acid oxidation preponderate in M2 [32]. Accordingly, and in line with this findings, the differentially expressed proteins between M and M2 macrophages include Glucose 6-phosphate dehydrogenase (G6PD), Alpha enolasa (Eno1), Fructose 1,6-bisphosphatase (Fbp1), Fructose bisphosphate aldolase A (AldoA), Aldose 1-epimerase (Galm), Phosphaglycerate mutase 1 (Pgam1) and Triosephosphate isomerase (Tpi1) (Figure 7), all them directly involved in glycolysis and energy production. Altogether, these results further confirm that the status of glucose metabolism and energy production is a central difference between both types of macrophages, and points to several glycolytic enzymes as useful protein markers to distinguish M1 and M2 polarization states. Importantly, one of the most differentially expressed proteins is Fbp1, which was identified in 7 different 2D-DIGE protein species. Fbp1, that catalyzes the hydrolysis of fructose-1,6-biphosphate, is regulated through Pfk-2 (Phosphofructokinase 2) and Fbpase-2 (Fructose 2,6-bisphosphate) activities and plays a critical role in gluconeogenesis. Consequently, Fbp1 constitutes an interesting marker that links macrophage polarization and its metabolic state, and represents a novel potential metabolic target for modulating macrophage polarization. G6PD has also been found as differentially expressed between both macrophage subtypes. Interestingly, G6PD is a major intracellular source of NADPH generation and the first and rate-limiting enzyme of the pentose phosphate pathway (PPP), whose modulation influences macrophage polarization (greater flux through in M1, reduced flow through PPP in M2) [33]. The higher levels of G6PD in M1 macrophages might therefore result in increased NADPH levels, which are required both for the production of ROS and RNS, and for the elimination of these ROS via glutathione peroxidase and catalase in different cell types [34, 35].

The higher expression of superoxide dismutase (SOD2) that we have found in M2 macrophages is in agreement with the reduced production of reactive oxygen species (ROS) and, consequently, with the lower microbicidal ability reported for alternative macrophages [8, 9]. However, in our hands, M2 macrophages were able to kill *C. albicans* as efficiently as M1 macrophages at 8h of co-incubation, suggesting the involvement of oxygen independent mechanisms in this candidacidal activity. Alternatively, the ability of *C. albicans* to degrade and inhibit the production of host-derived ROS [5] may be more efficient against M1 macrophages, thus diminishing their antifungal activity and conferring them a phenotype similar to M2 macrophages.

Regarding the macrophage response to *C. albicans*, 2D-DIGE analyses revealed changes in 14 spots in *C. albicans*-treated M1 macrophages and 40 spots in *C. albicans*-treated M2 macrophages. As previously explained, M1 donors showed important biological variations among them, thus causing less significantly differentially expressed spots.

The infection of macrophages with *C. albicans* causes an extreme remodeling of the host cell cytoskeleton that may affect functions such as phagocytosis, cytokinesis, mitosis, intracellular transport and endo- and exocytosis. In this regard, it is worth to bold that 4 out of the 11 proteins differentially expressed between control and *Candida*-treated M2 macrophages are cytoskeletal components. In particular, cofilin expression is increased in M2 macrophages during the interaction with *C. albicans* while Arp2/3 expression is decreased. Since cofilin promotes the depolymerization of actin filaments and the Arp2/3 complex has a role in actin polymerization [36], it is conceivable that actin is more fragmented in infected M2 macrophages, with the consequent effect on cell migration, adhesion and phagocytosis.

Besides cytoskeletal proteins, the functional analysis of the proteomic alterations induced in macrophages by *C. albicans* exposure also revealed differences in redox and stress related proteins, as well as proteins involved in the immune response and cell recognition. Interestingly, and when globally considered, the variations in protein expression observed seem to suggest that interaction with *C. albicans* skews the proteomic profile of M1 macrophages towards that of M2 macrophages. In agreement with this observation, IL12p40, TNF-α and IL-6,

whose release characterizes M1 macrophages, are not significantly induced in M1 macrophages after 8h of co-incubation with *C. albicans*. Along the same line, the expression of PAI-2 and SOD2, two proteins found to be more abundant in M2 control macrophages, increases in both M1 and M2 macrophages after fungal interaction. PAI-2 is induced during many inflammatory processes and viral, bacterial and parasitic infections [37, 38], and it is often one of the most up-regulated proteins in activated monocytes/macrophages, being up to 0.25% of total protein [37]. Importantly, PAI-2 has been recently reported as a negative regulator of Th1-mediated immune responses [39], further reinforcing the idea of an M1-to-M2 switch in macrophage polarization in the presence of *C. albicans*.

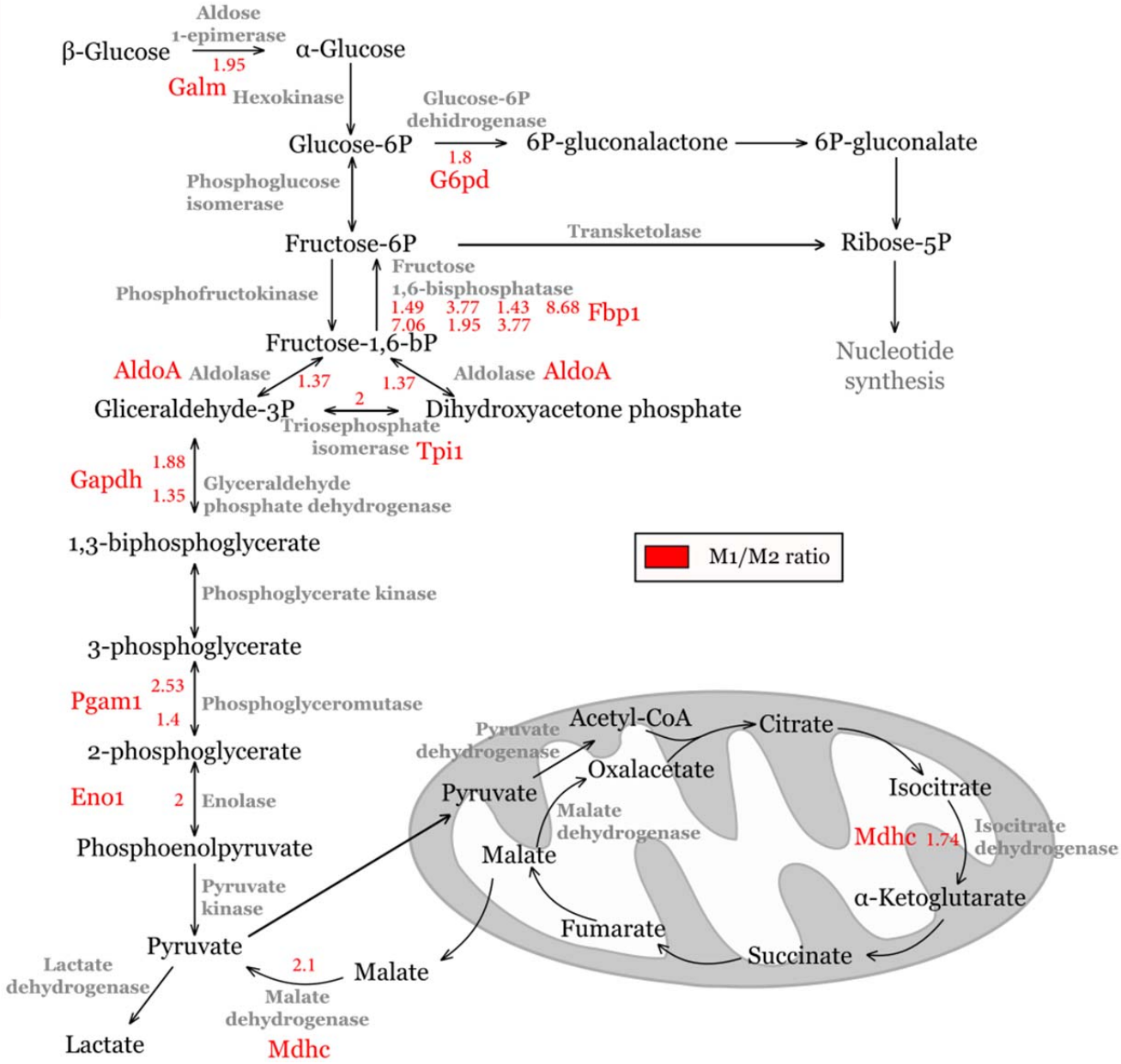

Figure 7. Changes in the glycolytic enzymes in M1 and M2 macrophages. Chart showing that differentially expressed proteins between M1 and M2 macrophages are significantly enriched in enzymes of the gluconeogenic, glycolytic, and pentose phosphate pathways, as determined by Pathway enrichment analysis. Numbers indicate the ratio of the level of each protein in M1 macrophages relative to M2. Different ratios in the same protein designate different protein species located in different spots.

The global proteomic comparison among M1 and M2 polarized macrophages, and their specific responses to the opportunistic pathogen *C. albicans*, has revealed that the most important differences between both types of macrophages are related to metabolic pathways, specifically glycolysis and gluconeogenesis, whereas the interaction with *C. albicans* seems

to promote a M1-to-M2 switch in polarization as well as a limitation in Th1 inflammatory responses during fungal infection. Previous in vivo studies in mice in which the virulence of a wild type *C. albicans* and a mutant strain were compared, showed that the less virulent mutant induced less pro-inflammatory effect, reducing damage in mice, thus increasing survival to infection [40] among other effects. This might be pointing out to macrophage attempt to control inflammatory response in order to reduce host damage. However, previous experiments with RAW 264.7 murine macrophages have shown that the interaction with *C. albicans* induces a clear pro-inflammatory response [14, 15, 41] indicating that the kind of macrophages and the experimental condition (MOI macrophage:*Candida*) used are crucial to determine the response to the pathogen and the final result of the interaction.

Whether the changes that we report here contribute to in vivo *Candida* pathogenicity by enhancing fungal survival and colonization, or by decreasing the generation of specific immune responses, or instead, it is part of the host attempt to reduce the damage of the infection, it is a matter that deserves further investigation

Acknowledgments

Proteomics experiments were carried out in the Proteomics Unit UCM-Parque Científico, a member of the National Institute for Proteomics, ProteoRed, funded by Instituto de Salud Carlos III (ISCIII). The authors would like to thank Montserrat Martínez-Gomariz for their support in sample analysis and to Francisco Sánchez-Madrid for the Moesin antibody. J.A. R.-C. was the recipient of a fellowship from Ministerio de Ciencia e Innovación.

This work was supported by BIO 2009-07654 and BIO 2012-31767 from the Ministerio de Economía y Competitividad, PROMT (S2010/BMD-2414) from the Comunidad Autónoma de Madrid, and REIPI, Spanish Network for the Research in Infectious Diseases (RD06/0008/1027 and RD12/0015/0004) from the ISCIII; and the Banco Santander Central Hispano-Universidad Complutense Research Group (UCM-920685).

5 References

1. Pfaller, M. A.; Yu, W. L., Antifungal susceptibility testing. New technology and clinical applications. Infect Dis Clin North Am 2001, 15, (4), 1227-61.

2. Pfaller, M. A.; Diekema, D. J., Epidemiology of invasive candidiasis: a persistent public health problem. Clin Microbiol Rev 2007, 20, (1), 133-163.

3. Pitarch, A.; Nombela, C.; Gil, C., *Candida albicans* biology and pathogenicity: insights from proteomics. Methods Biochem Anal 2006;49:285-330.

4. Hube, B., From commensal to pathogen: stage- and tissue-specific gene expression of *Candida albicans*. Curr Opin Microbiol 2004, 7, (4), 336-41.

5. Cheng, S. C.; van de Veerdonk, F. L.; Lenardon, M.; Stoffels, M.; Plantinga, T.; Smeekens, S.; Rizzetto, L.; Mukaremera, L.; Preechasuth, K.; Cavalieri, D.; Kanneganti, T. D.; van der Meer, J. W.; Kullberg, B. J.; Joosten, L. A.; Gow, N. A.; Netea, M. G., The dectin-1/inflammasome pathway is responsible for the induction of protective T-helper 17 responses that discriminate between yeasts and hyphae of *Candida albicans*. J Leukoc Biol 2011, 90, (2), 357-66.

6. d'Ostiani, C. F.; Del Sero, G.; Bacci, A.; Montagnoli, C.; Spreca, A.; Mencacci, A.; Ricciardi-Castagnoli, P.; Romani, L., Dendritic cells discriminate between yeasts and hyphae of the fungus *Candida albicans* . Implications for initiation of T helper cell immunity in vitro and in vivo. J Exp Med 2000, 191, (10), 1661-1674.

7. Gordon, S.; Taylor, P. R., Monocyte and macrophage heterogeneity. Nat Rev Immunol 2005, 5, (12), 953-64.

8. Gordon, S., Alternative activation of macrophages. Nat Rev Immunol 2003, 3, (1), 23-35.

9. Martinez, F. O.; Helming, L.; Gordon, S., Alternative activation of macrophages: an immunologic functional perspective. Annu Rev Immunol 2009, 27, 451-83.

10. Stout, R. D.; Suttles, J., Functional plasticity of macrophages: reversible adaptation to changing microenvironments. J Leukoc Biol 2004, 76, (3), 509-13.

11. Vega, M. A.; Corbí, A., Human macrophage activation: Too many functions and phenotypes for a single cell type Inmunología 2006, 25, (4), 1-24.

12. Mantovani, A.; Sica, A.; Sozzani, S.; Allavena, P.; Vecchi, A.; Locati, M., The chemokine system in diverse forms of macrophage activation and polarization. Trends Immunol 2004, 25, (12), 677-86.

13. Martínez-Solano, L.; Nombela, C.; Molero, G.; Gil, C., Differential protein expression of murine macrophages upon interaction with *Candida albicans*. Proteomics. 2006, 6 Suppl 1:S133-44., S133-S144.

14. Martínez-Solano, L.; Reales-Calderón, J. A.; Nombela, C.; Molero, G.; Gil, C., Proteomics of RAW 264.7 macrophages upon interaction with heat-inactivated *Candida albicans* cells unravel an anti-inflammatory response. Proteomics 2009, 9, (11), 2995-3010.

15. Reales-Calderon, J. A.; Sylvester, M.; Strijbis, K.; Jensen, O. N.; Nombela, C.; Molero, G.; Gil, C., *Candida albicans* induces pro-inflammatory and anti-apoptotic signals in macrophages as revealed by quantitative proteomics and phosphoproteomics. J Proteomics 2013.

16. Gillum, A. M.; Tsay, E. Y.; Kirsch, D. R., Isolation of the *Candida albicans* gene for orotidine-5'-phosphate decarboxylase by complementation of S. cerevisiae ura3 and E. coli pyrF mutations. Mol Gen Genet 1984, 198, (1), 179-82.

17. Puig-Kroger, A.; Sierra-Filardi, E.; Dominguez-Soto, A.; Samaniego, R.; Corcuera, M. T.; Gomez-Aguado, F.; Ratnam, M.; Sanchez-Mateos, P.; Corbi, A. L., Folate receptor beta is expressed by tumor-associated macrophages and constitutes a marker for M2 anti-inflammatory/regulatory macrophages.

Cancer Res 2009, 69, (24), 9395-403.
18. Diez-Orejas, R.; Molero, G.; Moro, M. A.; Gil, C.; Nombela, C.; Sanchez-Perez, M., Two different NO-dependent mechanisms account for the low virulence of a non-mycelial morphological mutant of *Candida albicans*. Med Microbiol Immunol 2001, 189, (3), 153-160.
19. Verreck, F. A.; de Boer, T.; Langenberg, D. M.; Hoeve, M. A.; Kramer, M.; Vaisberg, E.; Kastelein, R.; Kolk, A.; de Waal-Malefyt, R.; Ottenhoff, T. H., Human IL-23-producing type 1 macrophages promote but IL-10-producing type 2 macrophages subvert immunity to (myco)bacteria. Proc Natl Acad Sci U S A 2004, 101, (13), 4560-5.
20. Karp, N. A.; McCormick, P. S.; Russell, M. R.; Lilley, K. S., Experimental and statistical considerations to avoid false conclusions in proteomics studies using differential in-gel electrophoresis. Mol Cell Proteomics 2007, 6, (8), 1354-64.
21. Sechi, S.; Chait, B. T., Modification of cysteine residues by alkylation. A tool in peptide mapping and protein identification. Anal Chem 1998 Dec 15 ;70(24):5150-5158.
22. Verreck, F. A.; de Boer, T.; Langenberg, D. M.; van der Zanden, L.; Ottenhoff, T. H., Phenotypic and functional profiling of human proinflammatory type-1 and anti-inflammatory type-2 macrophages in response to microbial antigens and IFN-gamma- and CD40L-mediated costimulation. J Leukoc Biol 2006, 79, (2), 285-93.
23. Martinez, F. O.; Gordon, S.; Locati, M.; Mantovani, A., Transcriptional profiling of the human monocyte-to-macrophage differentiation and polarization: new molecules and patterns of gene expression. J Immunol 2006, 177, (10), 7303-11.
24. Gustafsson, C.; Mjosberg, J.; Matussek, A.; Geffers, R.; Matthiesen, L.; Berg, G.; Sharma, S.; Buer, J.; Ernerudh, J., Gene expression profiling of human decidual macrophages: evidence for immunosuppressive phenotype. PLoS One 2008, 3, (4), e2078.
25. Lacey, D. C.; Achuthan, A.; Fleetwood, A. J.; Dinh, H.; Roiniotis, J.; Scholz, G. M.; Chang, M. W.; Beckman, S. K.; Cook, A. D.; Hamilton, J. A., Defining GM-CSF- and macrophage-CSF-dependent macrophage responses by in vitro models. J Immunol 2012, 188, (11), 5752-65.
26. Bosschaerts, T.; Guilliams, M.; Stijlemans, B.; De Baetselier, P.; Beschin, A., Understanding the role of monocytic cells in liver inflammation using parasite infection as a model. Immunobiology 2009, 214, (9-10), 737-47.
27. Lugo-Villarino, G.; Verollet, C.; Maridonneau-Parini, I.; Neyrolles, O., Macrophage polarization: convergence point targeted by Mycobacterium tuberculosis and HIV. Front Immunol 2011, 2, 43.
28. Benoit, M.; Desnues, B.; Mege, J. L., Macrophage polarization in bacterial infections. J Immunol 2008, 181, (6), 3733-9.
29. Mege, J. L.; Mehraj, V.; Capo, C., Macrophage polarization and bacterial infections. Curr Opin Infect Dis 2011, 24, (3), 230-4.
30. Allavena, P.; Sica, A.; Garlanda, C.; Mantovani, A., The Yin-Yang of tumor-associated macrophages in neoplastic progression and immune surveillance. Immunol Rev 2008, 222, 155-61.
31. Olefsky, J. M.; Glass, C. K., Macrophages, inflammation, and insulin resistance. Annu Rev Physiol 2010, 72, 219-46.
32. Odegaard, J. I.; Chawla, A., Alternative macrophage activation and metabolism. Annu Rev Pathol 2011, 6, 275-97.
33. Haschemi, A.; Kosma, P.; Gille, L.; Evans, C. R.; Burant, C. F.; Starkl, P.; Knapp, B.; Haas, R.; Schmid, J. A.; Jandl, C.; Amir, S.; Lubec, G.; Park, J.; Esterbauer, H.; Bilban, M.; Brizuela, L.; Pospisilik, J. A.; Otterbein, L. E.; Wagner, O., The sedoheptulose kinase CARKL directs macrophage polarization through control of glucose metabolism. Cell Metab 2012, 15, (6), 813-26.
34. Spolarics, Z., Endotoxemia, pentose cycle, and the oxidant/antioxidant balance in the hepatic sinusoid. J Leukoc Biol 1998, 63, (5), 534-41.
35. Spolarics, Z., A carbohydrate-rich diet stimulates glucose-6-phosphate dehydrogenase expression in rat hepatic sinusoidal endothelial cells. J Nutr 1999, 129, (1), 105-8.
36. Wear, M. A.; Schafer, D. A.; Cooper, J. A., Actin dynamics: assembly and disassembly of actin networks. Curr Biol 2000, 10, (24), R891-5.
37. Schroder, W. A.; Major, L.; Suhrbier, A., The role of SerpinB2 in immunity. Crit Rev Immunol 2011, 31, (1), 15-30.
38. Thuong, N. T.; Dunstan, S. J.; Chau, T. T.; Thorsson, V.; Simmons, C. P.; Quyen, N. T.; Thwaites, G. E.; Thi Ngoc Lan, N.; Hibberd, M.; Teo, Y. Y.; Seielstad, M.; Aderem, A.; Farrar, J. J.; Hawn, T. R., Identification of tuberculosis susceptibility genes with human macrophage gene expression profiles. PLoS Pathog 2008, 4, (12), e1000229.
39. Schroder, W. A.; Le, T. T.; Major, L.; Street, S.; Gardner, J.; Lambley, E.; Markey, K.; MacDonald, K. P.; Fish, R. J.; Thomas, R.; Suhrbier, A., A physiological function of inflammation-associated SerpinB2 is regulation of adaptive immunity. J Immunol 2010, 184, (5), 2663-70.
40. Díez-Orejas, R.; Molero, G.; Navarro-García, F.; Pla, J.; Nombela, C.; Sánchez-Pérez, M., Reduced virulence of *Candida albicans* MKC1 mutants: a role for mitogen-activated protein kinase in pathogenesis. Infection and Immunity 1997, 65, (2), 833-837.
41. Reales-Calderon, J. A.; Martinez-Solano, L.; Martinez-Gomariz, M.; Nombela, C.; Molero, G.; Gil, C., Sub-proteomic study on macrophage response to *Candida albicans* unravels new proteins involved in the host defense against the fungus. J Proteomics 2012, 75, (15), 4734-46.

SUPPLEMENTAL MATERIAL

Supplemental Figure S1:

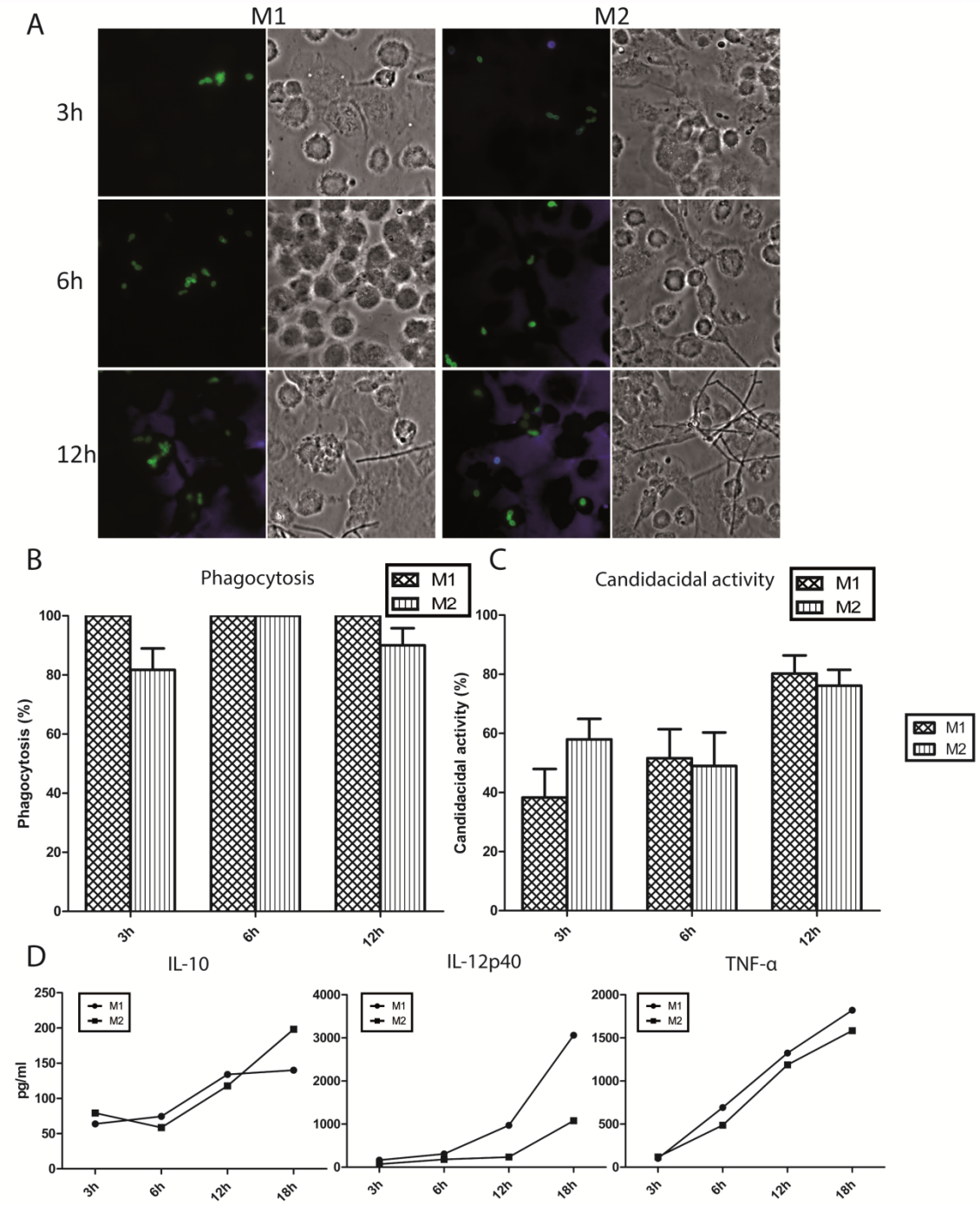

Fig. S.1. M1 and M2 polarized macrophages response to *C. albicans*. (A) Representative images of *C. albicans* SC5314 phagocytosis assays by M1 and M2 macrophages at a MOI 1:1. **(B)** Quantification of phagocytosis of *C. albicans* yeasts. **(C)** Candidacidal activity of M1 and M2 macrophages at different co-incubation times. The values in the y axis represent the percentage of *C. albicans* SC5314 CFU inhibition after the interaction with M1 and M2 macrophages with respect to control yeasts. **(D)** IL-10, IL-12p40 and TNFα levels of *C. albicans*-stimulated M1- and M2-polarized macrophages after 3, 6, 12 and 18h of co-incubation.

Supplemental Figure S2:

A

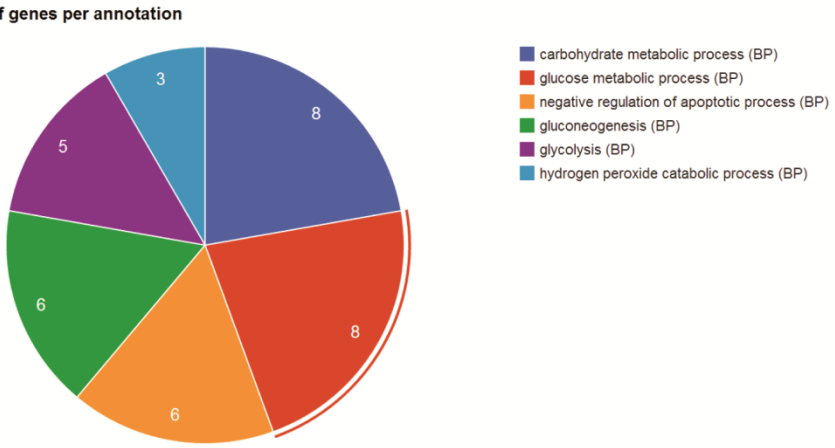

Genes	NGR	TNGR	NG	TNG	Hyp	Hyp*	Annotations
G6PD,GALM,ENO1,ALDOA,TPI1,PGAM1,FBP1,GAPDH	290	34208	8	42	2,2E-09	2,41E-07	GO:0005975: carbohydrate metabolic process (BP)
G6PD,ENO1,FABP5,ALDOA,TPI1,PGAM1,FBP1,GAPDH	98	34208	8	42	3,7E-13	1,2E-10	GO:0006006: glucose metabolic process (BP)
ALB,AIF1,SOD2,CTSH,ANXA1,GSTP1	272	34208	6	42	9,9E-07	6,39E-05	GO:0043066: negative regulation of apoptotic process (BP)
ENO1,ALDOA,TPI1,PGAM1,FBP1,GAPDH	42	34208	6	42	1,2E-11	1,94E-09	GO:0006094: gluconeogenesis (BP)
ENO1,ALDOA,TPI1,PGAM1,GAPDH	45	34208	5	42	2,6E-09	2,08E-07	GO:0006096: glycolysis (BP)
PRDX6,PRDX1,PRDX2	19	34208	3	42	1,6E-06	8,88E-05	GO:0042744: hydrogen peroxide catabolic process (BP)

B

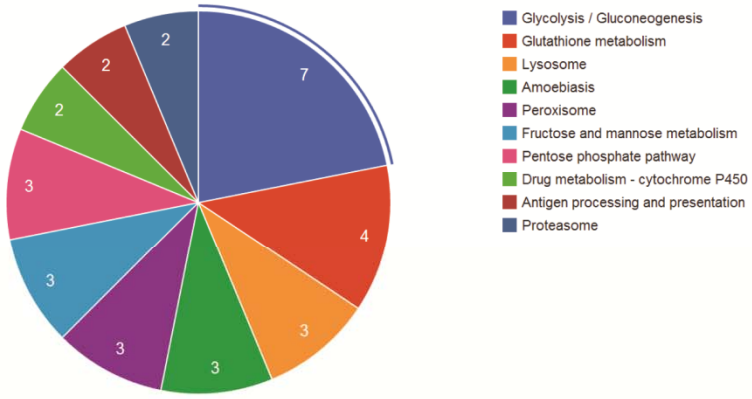

Genes	NGR	TNGR	NG	TNG	Hyp	Hyp*	Annotations
FBP1,GALM,ALDOA,ENO1,GAPDH,TPI1,PGAM1	62	34208	7	42	1,2E-12	3,72E-11	(KEGG) 00010: Glycolysis / Gluconeogenesis
GSTO1,G6PD,IDH1,GSTP1	44	34208	4	42	2,6E-07	4,11E-06	(KEGG) 00480: Glutathione metabolism
CTSS,CTSH,CTSZ	121	34208	3	42	0,00045	0,002048	(KEGG) 04142: Lysosome
RAB7A,SERPINB2,SERPINB1	102	34208	3	42	0,00027	0,001448	(KEGG) 05146: Amoebiasis
PRDX1,IDH1,SOD2	76	34208	3	42	0,00011	0,000727	(KEGG) 04146: Peroxisome
FBP1,ALDOA,TPI1	36	34208	3	42	1,2E-05	9,56E-05	(KEGG) 00051: Fructose and mannose metabolism
FBP1,G6PD,ALDOA	27	34208	3	42	4,9E-06	5,26E-05	(KEGG) 00030: Pentose phosphate pathway
CTSS,PSME2	56	34208	2	42	0,00217	0,007726	(KEGG) 04612: Antigen processing and presentation
GSTO1,GSTP1	70	34208	2	42	0,00337	0,009806	(KEGG) 00982: Drug metabolism - cytochrome P450
PSME2,PSMB2	40	34208	2	42	0,00111	0,004458	(KEGG) 03050: Proteasome

Fig. S.2. Functional classification of proteins differentially expressed between M1 and M2 macrophages. Pie chart representation and tables of the Gene Ontology classification of differentially expressed proteins between M1 and M2, as categorized by Genecodis according to their Biological Process (A) and KEGG Pathways (B).

Discusión

Los macrófagos son unas de las células inmunitarias más importantes en la respuesta frente las infecciones, participan tanto en la respuesta innata como en la adaptativa. Tras la activación por diversos agentes, son capaces de fagocitar al microorganismo, secretar citoquinas proinflamatorias y quimioquinas para tratar de contener y eliminar la infección (Plowden*, et al.*, 2004). Los macrófagos son muy importantes desde la etapa de colonización del organismo hasta la infección diseminada de *C. albicans* y, dada la importancia de estas células en la resolución de las candidiasis invasivas, decidimos abordar el estudio de la respuesta de macrófagos murinos RAW 264.7 y de macrófagos humanos M1 y M2 a *C. albicans* SC5314 (cepa parental virulenta) mediante un análisis proteómico. El estudio de las proteínas que varían su concentración o su activación/inactivación en los macrófagos por fosforilación/defosforilación a lo largo de la interacción nos proporciona información a tiempo real de las respuestas de los macrófagos durante la interacción.

1. RESPUESTA DE LOS MACRÓFAGOS MURINOS FRENTE A *C. albicans*:

Estudios previos de nuestro grupo se han centrado en la interacción *Candida*-macrófago para intentar encontrar tanto nuevos factores de virulencia y mecanismos de defensa activa de la levadura como mecanismos de actuación del macrófago para la destrucción del hongo. Dado a la escasez de estudios proteómicos y genómicos de esta interacción, nuestro grupo de investigación ha estudiado, desde ambos puntos de vista proteómico y genómico, la respuesta de *Candida* a la interacción con el macrófago (Fernández-Arenas*, et al.*, 2007), para ello se utilizó el ratio 1:1 (macrófago: levadura). En este trabajo se describió un cambio rápido en la levadura para adaptarse al ambiente hostil del fagosoma. Además permitió hacer una hipótesis sobre la muerte celular programada o muerte por apoptosis de *C. albicans* tras su interacción con el macrófago, relacionado con la remodelación del citoesqueleto de actina, la mitocondria y la autofagia.

Por otra parte, mediante estudios proteómicos en gel, se ha visto que los macrófagos también responden de manera rápida a la interacción con la levadura (Martínez-Solano*, et al.*, 2006, Martínez-Solano*, et al.*, 2009). Estos estudios, realizados en una fase temprana de la interacción, 45 minutos, han permitido ver las diferencias entre la respuesta frente a las levaduras vivas y las levaduras inactivadas por calor, permitiendo concluir que hay un gran cambio en procesos tan importantes como la reorganización del citoesqueleto, el metabolismo, la síntesis de proteínas y las respuestas pro-inflamatorias y de estrés celular frente a las levaduras vivas mientras que las inactivadas tienen un efecto antiinflamatorio en los macrófagos. Sin embargo, estos estudios del proteoma total no han permitido identificar ciertas proteínas que estaban variando en el macrófago en respuesta a la levadura porque son minoritarias y su identificación es más difícil.

Para obtener una visión más amplia e identificar una mayor cantidad de proteínas se procedió a la obtención secuencial de diferentes extractos subcelulares: citosol, membranas/organelas, núcleo y citoesqueleto aumentando el tiempo de interacción a 3 horas. Estas fracciones enriquecidas en las proteínas correspondientes a cada compartimento se analizaron mediante 2D-DIGE,

trabajo descrito en el capítulo I. Esta tecnología permite detectar y cuantificar los patrones de expresión diferencial de una manera más sensible, eliminándose las variaciones gel a gel (debido a la existencia de un estándar interno) y así las comparaciones entre las distintas condiciones en los diferentes geles pueden hacerse con un mayor grado de confianza.

Todos los cambios que ocurren en el macrófago desde el reconocimiento de la levadura por la célula fagocítica por los PRRs, llevan a la activación de múltiples redes de señalización celular y factores de transcripción específicos que median su respuesta (McGreal*, et al.*, 2005, Netea*, et al.*, 2008). La activación de los distintos receptores, por separado o combinados, dirigen todos los cambios morfológicos y fisiológicos en el macrófago, así como la presentación de antígenos a las células T (McGreal*, et al.*, 2005). Muchas de estas señales son controladas por MAPK, vía cascadas de fosforilación/defosforilación de estas proteínas en residuos de serina, treonina y tirosina, que son blanco de diferentes kinasas y fosfatasas (Johnson*, et al.*, 2004). Por este motivo, se describe en el capítulo II el estudio fosfoproteómico realizado a gran escala, basado en el marcaje metabólico de las proteínas *in vivo* y, el posterior enriquecimiento de los fosfopéptidos mediante cromatografía. Las técnicas proteómicas sin gel ofrecen una mayor sensibilidad que las técnicas en gel. Sin embargo, debido, sobre todo, a que los estudios de caracterización funcional de la fosforilación de la mayoría de proteínas son muy escasos, los datos obtenidos son algo más difíciles de analizar. El marcaje metabólico con aminoácidos en cultivo celular (SILAC) combinado con el enriquecimiento en fosfopéptidos (SIMAC: *Sequential* IMAC: *Immobilized Metal Affinity Chromatography*) (Thingholm*, et al.*, 2008) y la precipitación con fosfato cálcico (CPP, combinado con TiO_2) (Zhang*, et al.*, 2007) permitieron ver los cambios en las proteínas y los fosfopéptidos de los macrófagos en respuesta a *C. albicans* obteniendo datos complementarios a los de la proteómica en gel.

Ambas técnicas nos proporcionan mucha información en la respuesta de los macrófagos frente a las infecciones fúngicas pero, cada técnica tiene sus ventajas e inconvenientes. Uno de los problemas de la proteómica en gel, es la cantidad de proteína presente en cada mancha proteica disponible para su identificación, además de ser muy difícil el estudio de proteínas de alto peso molecular y con elevada hidrofobicidad. Por el contrario, es muy útil para el estudio de diferentes isoformas proteicas y para realizar inmunoproteómica. Por otra parte, la proteómica libre de gel se ha ido mejorando en los últimos años, aumentando su sensibilidad, reproducibilidad y automatización. Sin embargo, son muchos los estudios que indican que la combinación de ambas técnicas proporcionan resultados complementarios (Charro*, et al.*, 2011, Finamore*, et al.*, 2010). Por tanto, la combinación de nuestros estudios de proteómica con gel (2D-DIGE) y libre de gel (SILAC + MS/MS) proporciona una visión global de las funciones afectadas en el macrófago tras la interacción con *C. albicans*. Hemos visto que hay un aumento en la respuesta inflamatoria, un incremento del estrés oxidativo, cambios en el metabolismo y la reorganización del citoesqueleto, así como una prevalencia de las señales anti-apoptóticas frente a las pro-apoptóticas, que van a

ser detalladas teniendo en cuenta el conjunto de los dos estudios.

1.1. Incremento de la respuesta oxidativa y proinflamatoria.

Uno de los mecanismos más importantes para contener y tratar de matar a un patógeno es la producción de una gran variedad de productos tóxicos, como son, óxido nítrico (NO), anión superóxido (O_2^-), y peróxido de hidrógeno (H_2O_2), que tienen actividad candidacida directa (Romani y Bistoni, 2001). Como podemos observar en la Tabla 1 del capítulo I y las Tablas 1 y 2 del capítulo II, son muchas las proteínas que están favoreciendo la **respuesta oxidativa e inflamatoria** en la célula fagocítica y que resumimos en la figura 12.

Tras la interacción con *C. albicans*, la generación del "**estallido respiratorio**" es iniciado por el complejo NADPH oxidasa asociado a la membrana celular (Babior, 1999). Este complejo está compuesto por diferentes subunidades, una de las cuales identificamos en nuestro experimento de SILAC: **Cyba** (C*ytochrome b-light chain subunit*), también conocida como p22-phox. El complejo produce una gran cantidad de ROS y NOS, principales efectores del daño a los agentes patógenos, pero también a las propias proteínas del macrófago. Además, el aumento de **Pex11b** (*Peroxisomal biogenesis factor 11*), de **Glut1** (*Glucose transporter type 1*), del receptor **CD36** y de **Uqcrc1p** (*Ubiquinol-cytochrome c reductase core protein 1*) (Sun*, et al.*, 2008), junto con la disminución de la proteína **Fabp4** (*Fatty acid-binding protein*) y las oxidoreductasas **Prdx1** (*Peroxiredoxin 1*) (Shan*, et al.*, 2005) y **Pdia1** (*Protein disulfure isomerase 1*), están contribuyendo a la producción de O_2^-, H_2O_2 y NO^-. Este incremento en el estrés oxidativo intracelular se validó mediante inmunofluorescencia con dihidrorodamina 123 a diferentes tiempos de interacción, viéndose una **acumulación de estas especies reactivas del oxígeno a los 45 minutos, 1'5h y 3h** (Figura 4, Capítulo I).

Para reducir el daño por el estrés oxidativo, hay una serie de proteínas con función antioxidante que están aumentando en el macrófago, como son, **SelS** (*Selenoprotein S*), **Coq9** (*Ubiquinone biosynthesis protein*) y **Pycr** (*Pyrroline-5-carboxylate reductase 1*); estas proteínas podrían estar regulando el balance redox en la célula y protegiendo así el retículo endoplasmático de los efectos dañinos del estrés oxidativo (Pahl*, et al.*, 1997).

El aumento de la síntesis de ribosomas mitocondriales está muy relacionado con el **estrés oxidativo**, ya que sugiere un aumento en la actividad de la mitocondria cuando el macrófago está interaccionando con la levadura. Las mitocondrias son muy importantes en el metabolismo energético, la señalización celular y la muerte celular en células eucariotas (Chan, 2006), por lo que este incremento en la actividad, estaría sugiriéndonos un aumento de la actividad de los macrófagos para combatir la infección. Estudios previos han descrito un reclutamiento de mitocondrias a los fagosomas tras la señalización mediada por TLRs, además de un aumento en la producción de ROS mitocondrial, contribuyendo a la actividad microbicida de los macrófagos (West*, et al.*, 2011). Estos hechos estarían en concordancia con nuestros resultados y ese cambio metabólico del macrófago sería un mecanismo de obtención de energía extra para la lucha.

Respecto al efecto en **la respuesta inflamatoria**, son muchas las proteínas que están directamente relacionadas con el aumento de las **señales**

proinflamatorias en el macrófago en respuesta a *Candida* (Figura 12). La disminución de **Fabp4** (*Fatty acid-binding protein*) altera la composición lipídica de los macrófagos e induce la actividad de PPAR (*Peroxisome proliferator-activated receptor*), lo que lleva a la expresión de **CD36**. La activación de la ruta de señalización tirosin-kinasa, es un punto clave para la regulación de las rutas de señalización de MAPK, como las rutas de ERK 1/2 y NF-kB, que inducen la producción de citoquinas proinflamatorias y quimiocinas (Bamberger*, et al.*, 2003, El Khoury*, et al.*, 2003, Moore*, et al.*, 2002).

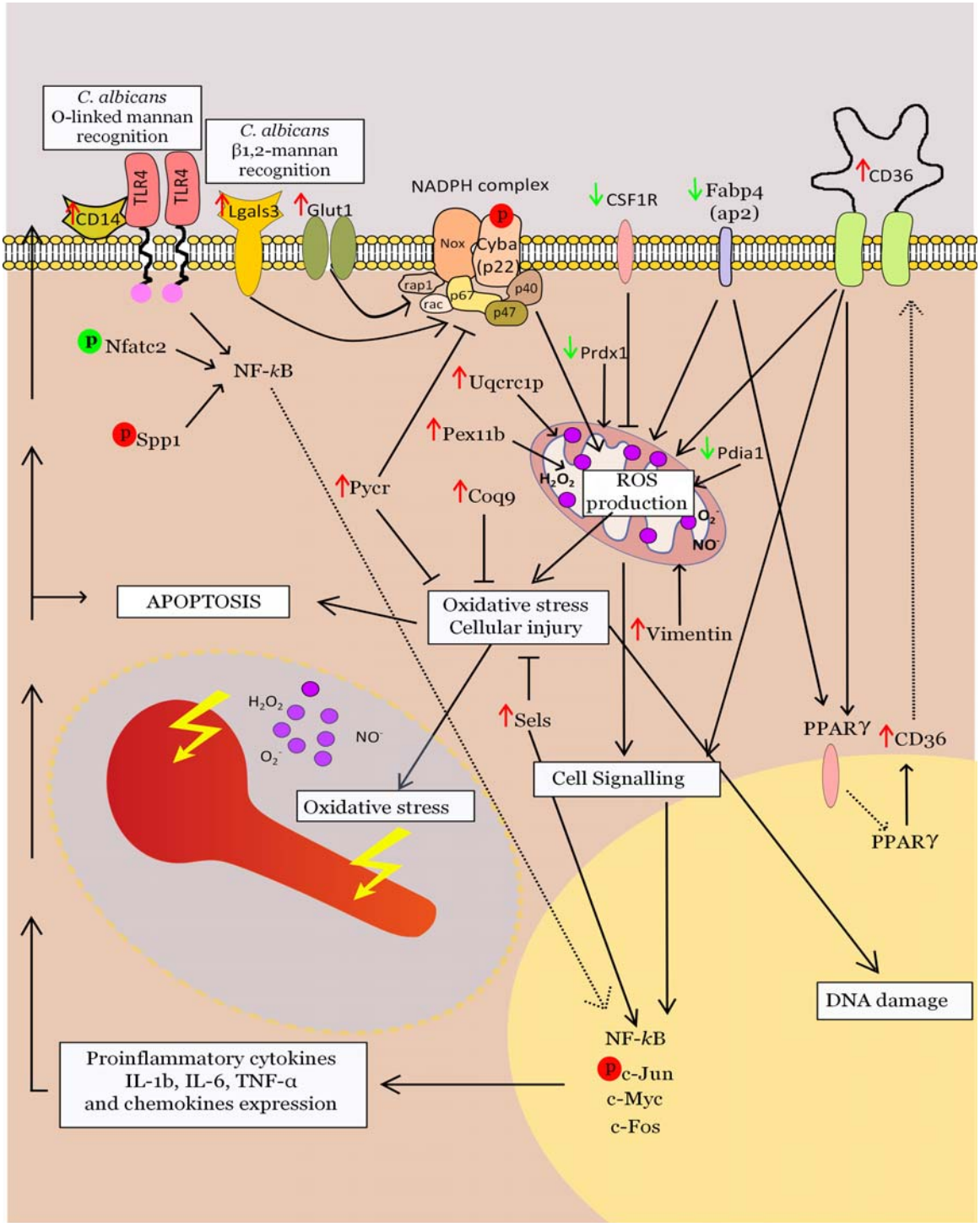

Figura 12: Visión general de las proteínas y fosfoproteínas de expresión diferencial de macrófagos en respuesta a *C. albicans* relacionadas con la respuesta inflamatoria y el estrés oxidativo.

Además, **CD36** aumenta tras la interacción y la **fosforilación de ERK 1 y 2 se ha visto aumentada en nuestro modelo a diferentes tiempos de interacción, desde 45 minutos a las 3 horas** (Martínez-Solano*, et al.*, 2009), lo que indica una activación de la ruta de MAPK por *C. albicans*. Además, se ha descrito que **Prdx1** y **Pdia1** pueden suprimir la ruta de NF-κB y la subsecuente respuesta inflamatoria (Hansen*, et al.*, 2007, Higuchi*, et al.*, 2004, Kisucka*, et al.*, 2008, Rhee*, et al.*, 2005), por esta razón la disminución de estas proteínas podría estar contribuyendo al aumento de la inflamación. El aumento de **SelS** (Kryukov*, et al.*, 2003), la fosforilación de **Spp1** (*Osteopontin*) y la disminución de fosforilación de **Nfatc2** (*Nuclear factor of activated T-cells, cytoplasmic 2*) (Vejda*, et al.*, 2005), tienen un papel muy importante en la activación de esta ruta NF-κB, cuya translocación posterior al núcleo activa la transcripción de genes que codifican citoquinas proinflamatorias (Pahl y Baeuerle, 1997).

También se han identificado una serie de receptores que aumentan con la interacción, como por ejemplo la **Galectina-3** que está relacionada con inflamación, fagocitosis y adhesión a diferentes moléculas (revisado en (Dumic*, et al.*, 2006)). Respecto a la interacción con *C. albicans*, se ha descrito que es un receptor que reconoce β1,2-oligomanosidos (Fradin*, et al.*, 2000b) y es capaz de discriminar entre *C. albicans* y *S. cerevisiae.* Esta proteína está aumentada en macrófagos tras la interacción con *Candida* (Shin*, et al.*, 2006) y es necesaria para el reconocimiento de la levadura en macrófagos tanto humanos (Esteban*, et al.*, 2011) como murinos (Jouault*, et al.*, 2006), contribuyendo al desarrollo de la respuesta proinflamatoria frente a *C. albicans* (Jawhara*, et al.*, 2008) y también en el aumento del estrés oxidativo (Liu*, et al.*, 1995). En este trabajo hemos validado el aumento de esta proteína en la membrana y su disminución en el citosol de los macrófagos tras interaccionar con *C. albicans*, tanto por *western blotting* monodimensional y bidimensional, como por inmunofluorescencia (Figuras 3, 5 y 6, Capítulo I).

Otro receptor que aumenta tras la interacción es **CD14**, que se asocia con TLR4 para el reconocimiento de otro componente de la pared celular de *C. albicans*, el manano (*O-linked mannan)* (Netea*, et al.*, 2002). Este reconocimiento de la levadura lleva a la activación de una serie de rutas de señalización que terminan en la activación de diferentes señales proinflamatorias, como son, la activación de NF-kB, producción de NO, de prostaglandina E2, IL-6, TNF-α y COX-2 (*Ciclooxigenase 2*) (Netea*, et al.*, 2008, Netea*, et al.*, 2010, Netea*, et al.*, 2002).

Finalmente encontramos el receptor SR-A o CD204 (*Macrophage scavenger receptor class A*) que tiene un papel muy importante en la mediación de la producción de citoquinas, factores de crecimiento y estrés celular (Hollifield*, et al.*, 2007, Johnson*, et al.*, 2002, Villwock*, et al.*, 2008), esta proteína la identificamos en nuestro estudio con un aumento en el nivel de fosforilación tras la interacción con la levadura.

Cabe destacar una proteína muy importante, identificada en ambos trabajos, la **Vimentina**. Esta proteína aumenta tanto en la membrana de los macrófagos como en el citoesqueleto (Capítulo I), pero también es la proteína que más cambia en los extractos totales (Capítulo II). La Vimentina es un filamento intermedio que se expone en la superficie de macrófagos activados y también se secreta. Esta proteína juega un papel muy importante durante la inflamación, tiene una

relación directa en la producción de metabolitos oxidativos y en la muerte de microorganismos, viéndose su actividad aumentada por las citoquinas proinflamatorias (Mor-Vaknin*, et al.*, 2003). Estudios de microscopía de fluorescencia han permitido validar este aumento de la proteína en el macrófago, sin embargo, su aumento no lleva a un cambio en su localización, ni a un reclutamiento de la proteína a la copa fagocítica tras el reconocimiento de *Candida* (Figura 3, Capítulo II). Además, Vimentina y Galectina-3 son secretadas por los macrófagos y se ha descrito un efecto microbicida directo de las mismas. En el caso de Galectina-3 se ha descrito un efecto candidacida directo (Kohatsu*, et al.*, 2006) mientras que en el caso de Vimentina se ha descrito que es capaz de matar a *Escherichia coli* (Mor-Vaknin*, et al.*, 2003). Hemos validado un aumento de las mismas en el sobrenadante de los macrófagos que interaccionan con *C. albicans* y comprobado que casi el 50% de la actividad candidacida de los macrófagos podría atribuirse a los componentes de dicho sobrenadante (Figura 6, Capítulo I).

También encontramos señales antiinflamatorias, por ejemplo, el aumento de Ptpn6 (*Protein tyrosine phosphatase, non-receptor type 6*), una proteína tirosín-fosfatasa que se ha visto que actúa como regulador negativo de la señalización de citoquinas tanto en la inmunidad innata como en la adquirida (Christophi*, et al.*, 2009), la disminución del receptor Tyrobp (*TYRO protein tyrosine kinase-binding protein*), también conocido como DAP12, se asocia a TREM-1 e inicia una señalización regulando la magnitud de la respuesta inflamatoria para evitar una exacerbación de la misma (Ford*, et al.*, 2009). El mismo efecto podría tener la disminución del receptor que reconoce M-CSF; CSF1R (*Colony-stimulating factor- 1 receptor*) (Ji*, et al.*, 2004). Además, la disminución de Hspa5 (*Heat shock protein 5*) (Niu*, et al.*, 2007) y el aumento de Ptges3 (*Prostaglandin E synthase 3*) (Nakatani*, et al.*, 2011) estarían incrementando estas señales antiinflamatorias.

1.2. *C. albicans* induce cambios en el citoesqueleto del macrófago.

Otro de los efectos más directos al reconocer y fagocitar *Candida* es una reorganización del citoesqueleto, de ahí que en análisis de subproteomas fuese en la fracción de citoesqueleto en la que se encontraron mayores cambios en los niveles de proteína, pero, al ser la última fracción que se obtiene, tuvimos problemas para identificar proteínas mediante espectrometría de masas. Solo se pudieron identificar 7 de las 77 "manchas proteicas". Para solucionar este problema se puso a punto un protocolo de enriquecimiento en proteínas de citoesqueleto más selectivo, el cual se analizó para comprobar el porcentaje de enriquecimiento en estas proteínas. Se ha visto que la combinación de las dos fracciones obtenidas con los dos tampones de extracción (que difieren en la cantidad de sales que poseen, para obtener distintos componentes del citoesqueleto) es un buen método de análisis para el estudio de los cambios que ocurren en el macrófago tras reconocer y fagocitar a la levadura.

Además, en los experimentos de SILAC se identificaron 5 proteínas y 19 fosfoproteínas que están relacionadas con estas modificaciones del citoesqueleto del macrófago. Por ejemplo Vimentina, de la que ya hemos hablado previamente, Cd2ap (*CD2-associated protein*) (Dustin*, et al.*, 1998), Flmn2 (*Filamin 2*) (Goode*, et*

al., 2007), Lmna (*Prelamin-A/C*) (Broers*, et al.*, 2006), Stmn1 (*Stathmin*) (Lovric*, et al.*, 1998), Twf2 (*Twinfilin 2*) (Palmgren*, et al.*, 2002), tubulinas y miosinas. Todas ellas varían tras la interacción y están afectando a la función del macrófago regulando la fagocitosis, la motilidad celular, la secreción de vesículas y demás funciones.

1.3. *C. albicans* no induce apoptosis en el macrófago tras la interacción.

Hay una gran cantidad de proteínas identificadas en ambos estudios relacionadas con la apoptosis, tanto pro- como anti-apoptóticas (Figura 13).

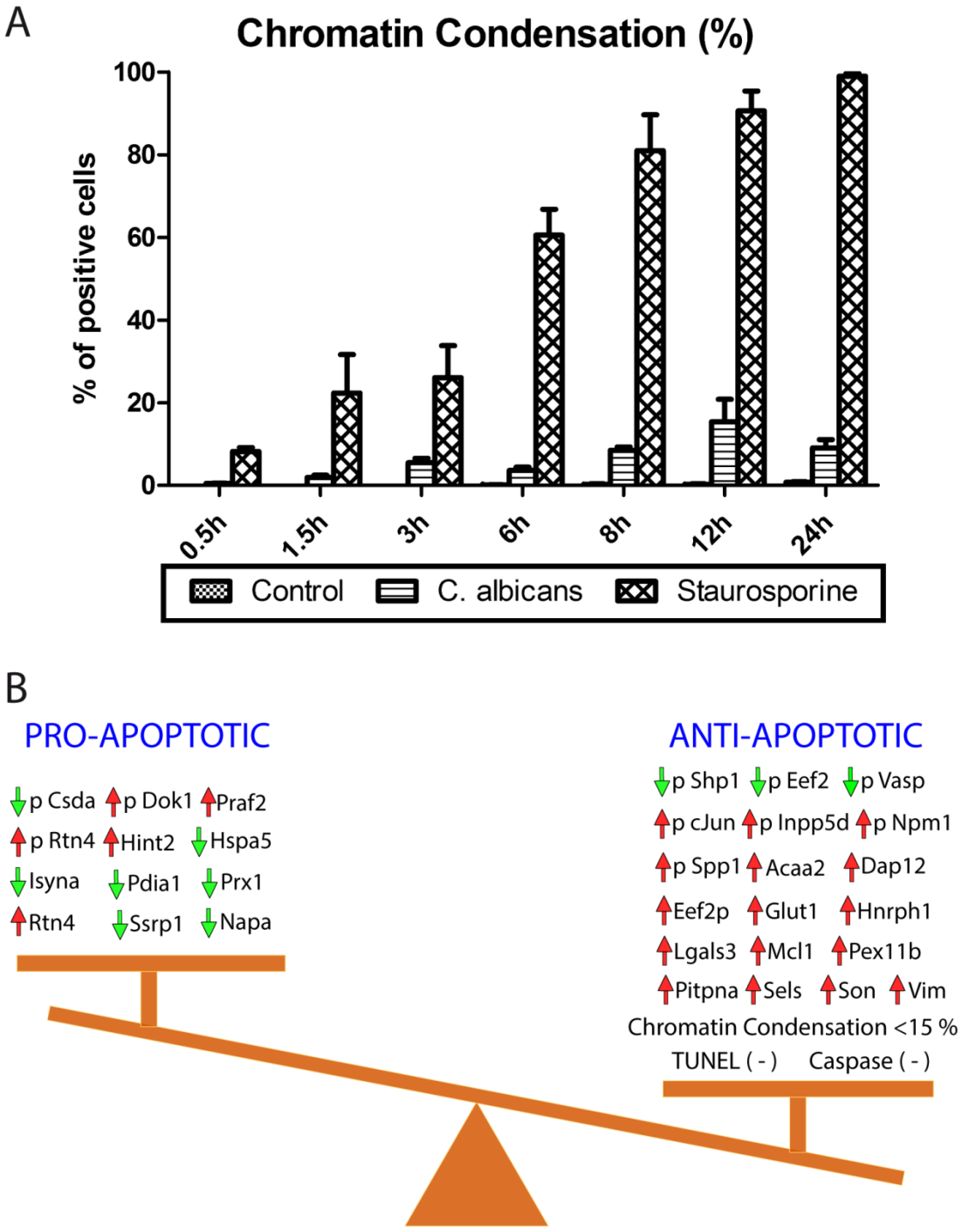

Figura 13. Prevalencia de las señales anti-apoptóticas en los macrófagos RAW 264.7 tras la interacción con *C. albicans*. (A)Gráfica del porcentaje de células con condensación de cromatina en macrófagos control, tras la interacción con la levadura y en el control positivo de apoptosis (5mM Staurosporine) (C) Diagrama de las diferentes señales pro y anti-apoptóticas en los macrófagos en respuesta a la levadura.

La apoptosis es un proceso que forma parte de la defensa del hospedador, es un modelo de muerte celular programada que limita la diseminación de los microorganismos promoviendo la destrucción de las células dañadas por fagocitos reclutados y residentes (Williams, 1994). La represión de la apoptosis por diferentes microorganismos permite al patógeno replicarse y/o persistir dentro célula hospedadora, pasando desapercibido al sistema inmunitario (Akarid*, et al.*, 2004). Son varios los patógenos que emplean esta estrategia, *Legionella pneumophila*, *Chlamydiae* spp., *Rickettsia rickettsii*, *Neisseria gonorrhoeae* y *Mycobacterium tuberculosis* (Fischer*, et al.*, 2001, Toossi*, et al.*, 2012).

Respecto a la activación/represión de la apoptosis en macrófagos por *C. albicans*, son varios los estudios que tratan este tema. Ibata-Ombetta y cols. (Ibata-Ombetta*, et al.*, 2003) y Rotstein y cols. (Rotstein*, et al.*, 2000) detectan apoptosis en macrófagos murinos J774 y neutrófilos, respectivamente, tras la interacción con *C. albicans*. Mientras que, Heidenreich y cols. (Heidenreich*, et al.*, 1996) muestran una inhibición de la apoptosis en macrófagos humanos tras interaccionar con la levadura.

En nuestros estudios encontramos ambas señales, por esta razón se ha realizado ensayos para dilucidar el estado apoptótico del macrófago y cuáles son las señales que van a prevalecer en el tiempo, si van a prevalecer las anti-apoptóticas frente a las pro-apoptóticas o viceversa. Para ello se ha realizado un estudio *in silico* de las proteínas relacionadas con la apoptosis y medición de diferentes marcadores del proceso.

Como **señales pro-apoptóticas**, podemos destacar la disminución de proteínas relacionadas con la protección frente al estrés oxidativo dentro de la célula, aquellas con actividad oxidorreductasa (**Prdx1** y **Pdia1**), las relacionadas con la respuesta de RE (**Napa** y **Hspa5**), también el aumento de **Rtn4** (*Reticulon-4* o Nogo-A), **Hint2** (*Histidine triad nucleotide-binding protein 2*) y **Praf2** (*PRA1 family protein 2*), la fosforilación de **Dok1** (*Docking protein 1*) y **Rtn4** y la disminución de la fosforilación en **Csda** (*Cold-shock domain protein A*). Este hecho hace que la célula sea más susceptible al daño por estos radicales, que las proteínas sufran daño y fragmentación del DNA, todo esto contribuyendo a la apoptosis de diversas maneras. Diversos estudios relacionan estas proteínas con rutas apoptóticas, por ejemplo, la disminución en Prdx1 y Pdia1 está directamente relacionada con la susceptibilidad de la célula a la muerte celular inducida por ROS (Shan*, et al.*, 2005). **Hspa5**, también conocida como Grp78, es miembro de la ruta de respuesta a proteínas desplegadas (UPR) y es un marcador de células apoptóticas (Misra*, et al.*, 2005, Miyake*, et al.*, 2000). Rtn4 es una proteína que delecionada en cardiomiocitos atenúa de forma marcada la apoptosis inducida por la hipoxia/reoxigenación (Sarkey*, et al.*, 2011). Diversos autores señalan una sensibilización a la apoptosis debida al aumento de **Hint2** (Martin*, et al.*, 2006) y **Praf2** (Vento*, et al.*, 2010) y la degradación de **Ssrp1** (*Structure specific recognition protein 1*) durante la apoptosis es un mecanismo debido, de forma conjunta, a la activación de las caspasas y a la proteólisis dependiente de ubiquitina (Landais*, et al.*, 2006). También contribuyen a la inducción de la apoptosis la disminución de **Isyna1** (*Inositol-3-phosphate synthase 1*), requerida para suprimir la apoptosis

en *Arabidopsis thaliana* (Donahue*, et al.*, 2010); y la disminución de **Napa**, siendo las células delecionadas en esta proteína sensibilizadas a los agentes inductores de la apoptosis (Wu*, et al.*, 2010b). Con respecto a las proteínas fosforiladas, la fosforilación de **Dok1** puede afectar a proceso de señalización celular y juega un papel muy importante en la apoptosis inducida por activina (Yamakawa*, et al.*, 2002), mientras que **Csda** es diana de la fosforilación inducida por Bcr-Abl y los mutantes fosfo-deficientes en **Csda** sufren un aumento en apoptosis (Sears*, et al.*, 2010).

Por el contrario, como **señales anti-apoptóticas**, podemos hacer énfasis en la variación de diversas proteínas que comentamos a continuación.

Diversos estudios señalan la variación en la síntesis/sobreexpresión de diversas proteínas con la resistencia a la apoptosis, como el aumento de **Pitpna** (*Phosphatidylinositol transfer protein*), que aumenta significativamente la resistencia a la apoptosis en fibroblastos murinos (Schenning*, et al.*, 2004), de **Hnrph1** (*Heterogeneous nuclear ribonucleoprotein H1*), el cual es necesario para bloquear la ruta de apoptosis MST-2 en células cancerígenas (Veraldi*, et al.*, 2001). También son importantes los aumentos de **Glut1**, **SelS**, **Pex11b**, **Tyrobp** (Dap12), **Mcl1** (***Myeloid cell leukemia 1***), **Vimentin**, **Acaa2** (*3-Ketoacyl-CoA thiolase*) (Cao*, et al.*, 2008), **Son**, **Eef2p** (*Eukaryotic translation elongation factor 2*), **Galectina-3** (Hsu*, et al.*, 2000) y **Vimentina**, y la fosforilación de **Npm1** (*Nucleophosmin*), **Inpp5d** (*Phosphatidylinositol-3,4,5-trisphosphate 5-phosphatase 1*), **c-Jun** y **Spp1** (*Osteopontin*), así como las disminuciones en la fosforilación de **Vasp** (*Vasopresin*) y **eEf2** en RAW 264.7 tras la interacción con *C. albicans*. Se ha descrito que la sobreexpresión de SelS protege a los macrófagos RAW 264.7 frente a la citotoxicidad inducida por estrés de RE y frente a la apoptosis, promoviendo la supervivencia celular (Kim*, et al.*, 2007). La deficiencia en **Pex11b** induce la apoptosis neuronal (Li*, et al.*, 2002), apareciendo esta proteína disminuida en nuestro modelo.

Incuestionablemente, la proteína más importante en la señalización frente a la no activación de las rutas apoptóticas es **Mcl1**, esta proteína es un miembro de la familia de Bcl2 que promueve la viabilidad celular durante transiciones fenotípicas como son la proliferación o la diferenciación (Craig, 2002) y su disminución promueve la apoptosis. En nuestro modelo vemos que hay un aumento de esta proteína en los macrófagos tras la interacción. Lo mismo ocurre en la infección con *M. tuberculosis*, proceso en el que el aumento en **Mcl1 promueve la supervivencia de los macrófagos infectados y reprime la apoptosis en los mismos**, siendo un mecanismo de defensa de *Mycobacterium* para permanecer invisible y sobrevivir dentro de la célula (Sly*, et al.*, 2003). Encontramos algunas proteínas relacionadas directamente con la expression de Mcl1, por ejemplo la unión de TREM2 con DAP12 estimula el aumento de Mcl1 en osteoclastos (Peng*, et al.*, 2010), el aumento de Eef2p y la activación de **Eef2** (por defosforilación en la Th^{57}) (Bewley*, et al.*, 2011) ayudan a mantener los niveles de la proteína y hacen que aumente la síntesis de la misma.

Respecto a los cambios en la fosforilación detectados en el SILAC y relacionados con el posible mecanismo de los mismos en las señales anti-apoptóticas, el aumento en la fosforilación de Npm, una fosfoproteína nucleolar que se une a las proteínas supresoras de tumores p53 y p19Arf, contribuye a la ribogénesis, proliferación celular y promueve la supervivencia tras el daño en el DNA

(Colombo, *et al.*, 2005), mientras que la disminución en la fosforilación de Vasp también contribuye a este efecto, ya que su fosforilación se ha descrito como inductora de la apoptosis (Deguchi, *et al.*, 2002). Además, se ha descrito un efecto anti-apoptótico de la fosforilación de c-Jun en la Ser^{73}. Utilizando mutantes que expresan Ser^{63}Ala, Ser^{73}Ala y no pueden ser fosforilados en estos residuos, se ha observado una ausencia de la protección de estas células frente a la apoptosis (Wisdom, *et al.*, 1999). Spp1 es una glicoproteína fosforilada relacionada con muchos procesos fisiológicos y patológicos, incluidos los procesos apoptóticos. La unión con su ligando conlleva a la activación de diferentes kinasas incluyendo FAK (*focal adhesion kinase*), ERK 1/2 (*extracellular signal-regulated kinase*) y PIK3/AKT (*phosphatidylinositol 3-kinase*). Akt y Erk 1/2 fosforilan caspasa 9 en Ser^{196} y Thr^{125}, respectivamente, e inhiben la activación de caspasa 3 (Wai, *et al.*, 2004), contribuyendo a las señales antiapoptóticas.

El estudio de diferentes marcadores de apoptosis nos sirvió para dilucidar qué señales prevalecían. El estudio de la condensación de cromatina reflejó un **máximo del 15% de células con el DNA condensado a las 12h de interacción con la levadura** (Figura 4, Capítulo III). La **ausencia de activación de Caspasa-3** nos indica que **la ruta de apoptosis mediada por caspasas no está activada**. **Los ensayos de fragmentación de DNA con TUNEL también fueron negativos**. Todos estos datos validan nuestra hipótesis por lo que podríamos concluir que ***C. albicans* no está induciendo apoptosis en los macrófagos** o la está reprimiendo. Respecto a los experimentos previos que comentamos en el inicio del apartado que mostraban la inducción de la apoptosis (Ibata-Ombetta, *et al.*, 2003, Rotstein, *et al.*, 2000) y represión de la misma (Heidenreich, *et al.*, 1996) en fagocitos en respuesta a *C. albicans*, podemos discutir brevemente las causas de los resultados obtenidos por los otros grupos y relacionarlo con lo que ocurre en nuestro modelo. El grupo de Ibata-Ombetta y cols. (2003) describió apoptosis en macrófagos tras la interacción con la levadura utilizando un ratio macrófago/*Candida* de 1:20, además, estos experimentos están realizados la línea celular de macrófagos murinos J774. Por otra parte, Rotstein y cols. (2000) muestran el aumento en el porcentaje de neutrófilos apoptóticos cuando aumentan el ratio neutrófilo/*Candida*. Por el contrario, el grupo de Heidenreich y cols., (1996) utilizando monocitos humanos, muestra una inhibición de la apoptosis en los monocitos utilizando ratios macrófago/*Candida* entre 1:1 y 50:1. Estos datos estarían apoyando los nuestros y el ratio 1:1 es el mismo que utilizamos en nuestro modelo, por lo que es comparable con nuestros resultados. Contrastando todos estos resultados, podemos concluir que el ratio macrófago/levadura es un elemento crucial para la inducción de la apoptosis en macrófagos debido a *C. albicans*, siendo favorable a las señales anti-apoptóticas cuando las células fagocíticas se encuentran en ventaja, ratio 1:1 o menor, lo que podría estar en concordancia con lo que ocurre en condiciones fisiológicas. Mientras que si invertimos la relación macrófago/*Candida*, la célula fagocítica se encuentra en desventaja y entraría en un proceso de muerte celular programada o apoptosis.

Una de las futuras direcciones de este trabajo podría ser determinar si esta respuesta de inhibición de la apoptosis viene determinada por la levadura o por el huésped. Por un lado, la inhibición de la apoptosis podría ser un mecanismo

del sistema inmunitario para contener y destruir *Candida* dentro del macrófago mientras que, por el contrario, la inhibición de la apoptosis por parte de *C. albicans* podría ser un factor de virulencia de la levadura que favorecería su replicación y diseminación dentro de los macrófagos.

2. RESPUESTA DE MACRÓFAGOS HUMANOS M1 Y M2 FRENTE A *C. albicans*:

Los macrófagos son mediadores de la respuesta inflamatoria y, dependiendo de las señales ambientales, pueden diferenciarse principalmente en macrófagos proinflamatorios (M1), también conocidos como activados clásicamente o en macrófagos antiinflamatorios (M2) o conocidos como activados alternativamente. A pesar de ello, se continúa investigando en las activaciones y funciones de los mismos y se siguen clasificando en nuevos subtipos. Por esta razón es de gran interés el estudio de la respuesta de las diferentes subpoblaciones de macrófagos a *C. albicans*.

En el capítulo III se describen las condiciones óptimas puestas a punto para este estudio mediante la medida de citoquinas (IL-10, IL-12p40, IL-6 y TNF-α), de la actividad fagocítica y de la capacidad candidacida de ambos tipos de macrófagos a distintos tiempos de co-incubación (3, 6, 12 y 18 horas) con *C. albicans* y a diferentes ratios macrófago/levadura (1:0.1; 1:1 y 1:5). El análisis de los datos obtenidos nos llevó a la conclusión de que las diferencias en la respuesta entre M1 y M2 a *C. albicans* son mayores entre 6 y 12 h y a un ratio macrófago/levadura de 1:1. Tras 12h, la muerte de los macrófagos es muy alta y se decidió realizar el estudio de proteómica comparativa a las 8h de interacción, momento en el que los macrófagos siguen viables y su respuesta puede ser estudiada con técnicas proteómicas.

Para esta aproximación se realizó un estudio de expresión diferencial con geles bidimensionales (2D-DIGE) utilizando macrófagos diferenciados a M1 y M2 de 4 donantes sanos tras 8h de co-cultivo con *C. albicans*. En este estudio se compararon tanto las diferencias proteómicas entre ambos subtipos de macrófagos como su respuesta a la levadura.

2.1. Diferencias proteómicas entre los macrófagos humanos M1 y M2

En los últimos años se está estudiando las diferencias fenotípicas y genéticas entre los macrófagos M1 y M2 y las diferencias en la respuesta a diferentes microorganismos como *Trypanosoma brucei* (Bosschaerts*, et al.*, 2009), *Mycobacterum tuberculosis* (Lugo-Villarino*, et al.*, 2011), diferentes especies de *Salmonella* y *Listeria monocytogenes* (Benoit*, et al.*, 2008, Mege*, et al.*, 2011).

Debido a la gran importancia de la polarización M1/M2 en la inflamación, tumorogénesis y cicatrización (Allavena*, et al.*, 2008, Olefsky*, et al.*, 2010), en este trabajo se han estudiado por primera vez las diferencias proteómicas de los macrófagos M1 y M2, contribuyendo a la comprensión de las diferencias en los mecanismos moleculares de la polarización de los macrófagos.

La comparación de los macrófagos humanos polarizados M1 y M2 mediante la tecnología 2D-DIGE nos permitido la determinación de 144 "manchas proteicas" de expresión diferencial, 71 de las cuales pudieron ser identificadas, correspondiendo a 51 proteínas diferentes (Figura

3, Capítulo III). El análisis funcional de las proteínas de expresión diferencial mostró que **las rutas más relevantes moduladas por la polarización de macrófagos son las rutas metabólicas, la respuesta inmunitaria y el estrés, además de la reorganización del citoesqueleto**.

El estudio proteómico señala que las diferencias en el metabolismo entre M1 y M2 son muy importantes, las proteínas identificadas **G6PD** (*Glucose 6-phosphate dehydrogenase*), **Eno1** (*Alpha enolasa*), **Fbp1** (*Fructose 1,6-bisphosphatase*), **AldoA** (*Fructose bisphosphate aldolase A*), **Galm** (*Aldose 1-epimerase*), **Pgam1** (*Phosphaglycerate mutase 1*) y **Tpi1** (*Triosephosphate isomerase*)] están relacionadas con la glucolisis/gluconeogénesis, al ciclo de los ácidos tricarboxílicos y con la ruta de las pentosas fosfato entre otras (Figura 14). Este hallazgo está apoyado por ciertos estudios anteriores en los que se detallan las diferencias metabólicas entre diferentes subtipos de macrófagos y entre su respuesta a la hipoxia (Odegaard*, et al.*, 2011). Estos autores indican que en los macrófagos **M1 prevalece la ruta glicolítica anaeróbica**, mientras que en los **M2 hay un predominio del metabolismo oxidativo de la glucosa y de la oxidación de los ácidos grasos**.

Teniendo en cuenta estos resultados, una diferencia central tras la diferenciación de los macrófagos en proinflamatorios y antiinflamatorios sería la forma de obtención de energía y el metabolismo de la glucosa, siendo ciertas enzimas de la glicólisis claves para determinar la orientación de la ruta y posibles marcadores para diferenciar el estado de polarización de los macrófagos. Una de estas proteínas podría ser Fbp1, que ha sido identificada en 7 manchas proteicas en los geles bidimensionales y es más de 8 veces más abundante en los M1. Esta proteína cataliza la hidrólisis de la fructosa-1,6-bifosfato y es un paso clave y crítico entre la glicólisis y la gluconeogénesis, siendo otra enzima la que cataliza la reacción inversa (Pfk-2). **Fbp1 podría ser un marcador que correlacionaría la polarización del macrófago con su estado metabólico**.

Además, G6PD es la mayor fuente de NADPH en la célula y es la enzima limitante de la ruta de las pentosas fosfato. La modulación de esta proteína, diferencialmente expresada en los macrófagos M1, tiene un gran efecto en la polarización de los macrófagos. La ruta de las pentosas fosfato está muy activa en los M1 y poco en los M2 (Haschemi*, et al.*, 2012). Los niveles de G6PD en los M1 podría estar incrementando los niveles de NADPH en la célula, el cual es necesario tanto para la producción de ROS y RNS, como para la eliminación de este ROS vía glutatión peroxidasa y catalasa en diferentes tipos celulares (Spolarics, 1998, 1999).

También se ha visto que SOD2 (*Superoxide dismutase*) es más abundante en los macrófagos M2, reforzando la teoría de que estos macrófagos producen menos ROS y, como consecuencia, poseen una menor actividad microbicida (Gordon, 2003, Martinez*, et al.*, 2009). Sin embargo, en nuestro modelo, los macrófagos M2 fueron capaces de matar *C. albicans* de manera similar a los M1, o incluso mejor, sugiriendo que este mecanismo oxidativo podría ser independiente de la actividad candidacida de los mismos. Podría ser que la habilidad de la levadura de inhibir la producción de ROS (Cheng*, et al.*, 2011) en el huésped fuera más eficiente en los macrófagos M1, disminuyendo así su actividad antifúngica y confiriéndoles un fenotipo similar al de M2.

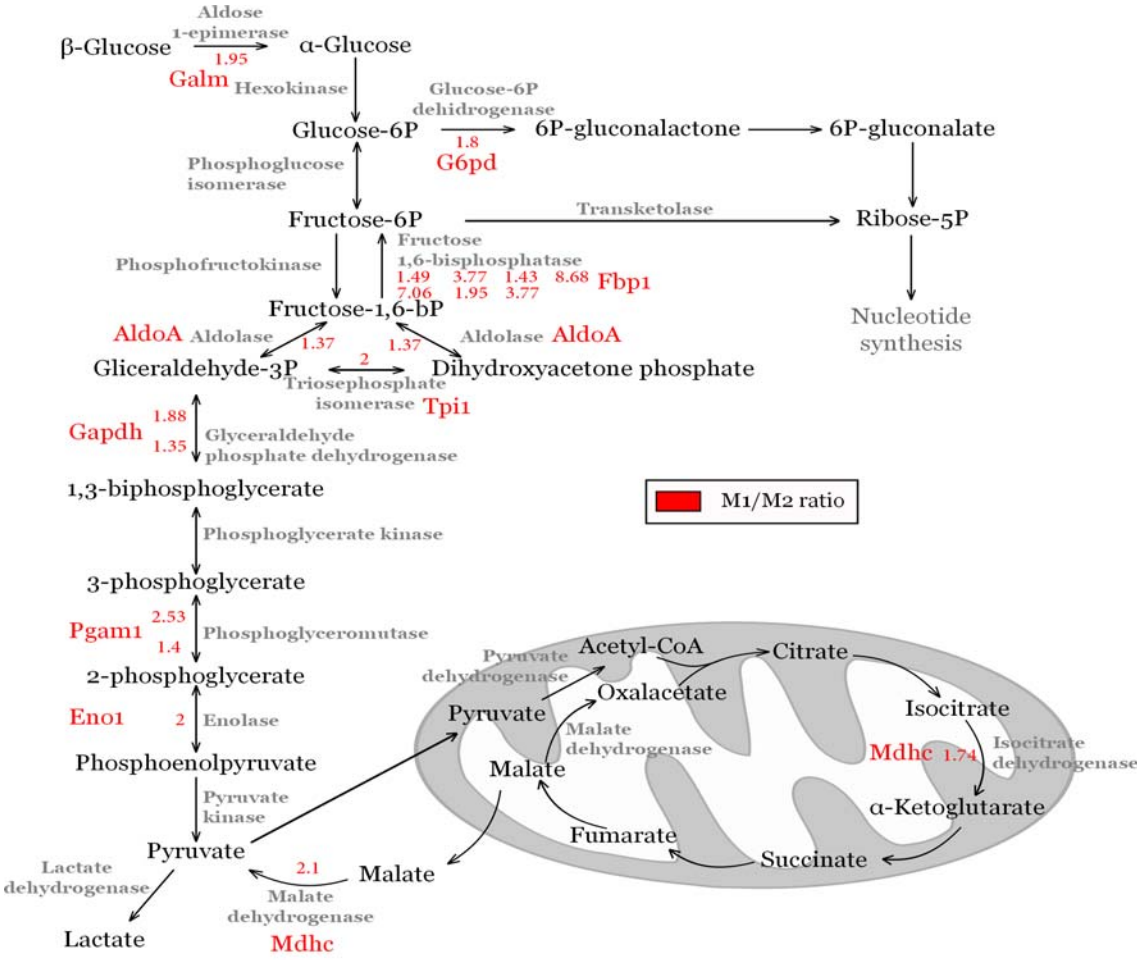

Fig. 7

Figura 14. Cambios en las enzimas glicolíticas en los macrófagos M1 y M2. La gráfica muestra las proteínas de expresión diferencial entre los macrófagos M1 y M2 relacionadas con la ruta de la glicólisis/gluconeogénesis, ruta de las pentosas fosfato y de los ácidos tricarboxílicos.

En resumen, el estudio proteómico de los macrófagos polarizados a M1 y M2 nos ha proporcionado información sobre las enormes diferencias que existen a nivel de metabolismo entre los macrófagos M1 y M2, específicamente en enzimas claves de la ruta de la glicolisis/gluconeogénesis, siendo la Fbp1 más abundante en los M1, un posible marcador de polarización de macrófagos.

2.2. <u>Respuesta de los macrófagos humanos M1 y M2 frente a *C. albicans*</u>:

Además de la comparación entre el proteoma de los macrófagos M1 y M2, en este estudio nos centramos en las diferencias proteómicas tras la interacción de estos macrófagos con *C. albicans*. Los análisis estadísticos mostraron cambios en 14 "manchas proteicas" en los macrófagos M1 tratados con la levadura y 40 "manchas proteicas" en los macrófagos M2 (Figura 4, Capítulo III). El

análisis por espectrometría de masas permitió identificar 11 y 31 proteínas, respectivamente.

Los macrófagos M1 mostraron una gran variabilidad entre los 4 donantes, de ahí que sólo fuera significativo el cambio en 14 "manchas proteicas" y obtuvieramos muy pocos datos significativos de los cambios que están ocurriendo en ellos cuando entran en contacto con la levadura.

La clasificación funcional de las proteínas de expresión diferencial en los macrófagos tras la co-incubación con *C. albicans* muestran que hay una **alteración en el estrés oxidativo, respuesta inmunitaria, y en el reconocimiento y reorganización del citoesqueleto.** Estos datos proteómicos muestran que **los macrófagos M1 responden como macrófagos M2 cuando están interaccionando con *C. albicans***, en nuestro modelo. Apoyando esta deducción, las citoquinas características proinflamatorias IL12p40, TNF-α y la IL-6 no son inducidas significativamente en los macrófagos M1 tras 8 h de incubación con la levadura. Asimismo, la expresión de PAI-2 (*Plasminogen activator inhibitor 2*) y SOD2, dos proteínas más abundantes en los macrófagos M2 control, muestran la misma tendencia, siendo producidas en un ratio similar en ambos tipos de macrófagos en su respuesta frente a *C. albicans*. SERPINB2 es el gen que codifica la proteína PAI-2. Es un marcador relacionado con la polarización de los macrófagos a M2 en humanos (de las Casas-Engel*, et al.*, 2013) y su expresión es inducida tanto en los M1 como en los M2 tras la infección con *C. albicans* (Figura 4, Capítulo III).

Muchas de las proteínas de expresión diferencial en los macrófagos M1 tras su interacción con *C. albicans* también cambian en los M2 con la interacción (Tablas 2 y 3, Capítulo III). De estas proteínas podemos destacar el aumento de Vimentina, que ya describimos su aumento en los macrófagos murinos RAW 264.7 tras su interacción con la levadura (Reales-Calderon*, et al.*, 2012, Reales-Calderon*, et al.*, 2013). Como ya se comentó anteriormente, esta proteína de citoesqueleto está relacionada con la generación de metabolitos oxidativos y la producción de citoquinas proinflamatorias (Mor-Vaknin*, et al.*, 2003).

Centrándonos en la respuesta de los macrófagos M2 a la infección por *C. albicans*, que parece ser más acusada que en los M1, hay un aumento significativo de la secreción de IL-10 tras la exposición a la levadura, aumentando las propiedades antiinflamatorias de los macrófagos alternativos (M2). Lo mismo ocurre con la mayoría de los efectos que vemos en proteínas. Por ejemplo, las diferencias de expresión que existen en enzimas metabólicas entre los macrófagos M1 y M2 se intensifican tras la interacción, dirigiendo la ruta aún más hacia la glicólisis en los M2. Estas observaciones nos confirman que en la activación alternativa, la polarización de los M2 se mantiene tras la interacción con *C. albicans*.

Asimismo, la infección de los macrófagos humanos con *Candida* conlleva una remodelación del citoesqueleto del huésped que puede afectar a su función regulando la fagocitosis, citoquinesis, mortalidad celular, mitosis, transporte intracelular y endo- y exocitosis. En este estudio se han identificado 11 proteínas directamente relacionadas con la reorganización del citoesqueleto. Por ejemplo, la cofilina aumenta en los macrófagos M2 tras la interacción con *C. albicans*, mientras que Arp 2/3 disminuye. En

relación con el citoesqueleto, cofilina promueve la despolimerización de actina y el complejo Arp 2/3 tiene un efecto en la polimerización de actina (Wear*, et al.*, 2000). Sus variaciones de expresión están sugiriendo una fragmentación o despolarización de la actina en los macrófagos infectados con la levadura con su consecuente efecto en la migración y adhesión de los mismos y en la fagocitosis. Sin embargo, los resultados obtenidos en el DIGE y en la validación por *western blotting* e inmunofluorescencia del citoesqueleto de actina muestran una disminución de la actina citoplasmática debido, seguramente, a la intensa polimerización de la actina en la copa fagocítica alrededor de *C. albicans* (Figura 6, capítulo III), lo que podría estar provocando que se haga más insoluble en nuestro tampón de extracción de proteínas utilizado. De ahí esta contradicción entre nuestros datos proteómicos y los obtenidos en la inmunofluorescencia. A pesar de esto, podríamos concluir que la infección de los macrófagos M2 con *C. albicans* tiene un impacto en la reorganización del citoesqueleto de actina, miosina y en los filamentos intermedios.

Como resumen, el estudio de la respuesta de los macrófagos humanos M1 y M2 a la infección con *C. albicans* sugiere que **la interacción con la levadura induce un cambio en la polarización de los M1 hacia M2**, aumentando la respuesta antiinflamatoria de los macrófagos M2. Este efecto podría contribuir, en parte, a la supervivencia y colonización de *C. albicans* durante la infección.

Conclusiones

1. Los estudios proteómicos en gel (electroforesis bidimensional con marcaje con fluorocromos, DIGE) y sin gel (marcaje metabólico, SILAC), aplicados a fracciones sub-celulares y extractos totales, respectivamente, han permitido obtener una visión global de la respuesta de los macrófagos murinos a *C. albicans*.

2. Las funciones principales de las proteínas y fosfoproteínas de expresión diferencial de macrófagos murinos en respuesta a *C. albicans* son: respuesta proinflamatória, estrés oxidativo, reorganización de citoesqueleto, apoptosis y metabolismo.

3. El estudio de las funciones de las proteínas y fosfoproteínas pro- y anti-apoptóticas de expresión diferencial y el posterior análisis de diversos marcadores de apoptosis en los macrófagos, pusieron de manifiesto que *C. albicans* tiene un efecto de inhibición de la apoptosis en macrófagos murinos.

4. El estudio fosfoproteómico con marcaje metabólico SILAC ha permitido la identificación de 922 sitios de fosforilación, de los cuales 327 son nuevos en las proteínas de ratón, útiles para futuros estudios.

5. Se ha puesto a punto un modelo de interacción *C. albicans*-macrófagos humanos proinflamatorios (M1) y antiinflamatorios (M2), comprobándose que ambos tipos de macrófagos son igualmente eficientes fagocitando y destruyendo a *C. albicans* en todas las condiciones estudiadas.

6. El análisis proteómico diferencial de macrófagos M1 y M2 ha demostrado que las principales diferencias entre ambos se deben a proteínas metabólicas y de reorganización del citoesqueleto, siendo la Fructosa 1,6-bifosfatasa (Fbp1) un posible nuevo marcador de macrófagos M1.

7. Basándonos en la producción de citoquinas y en las proteínas de expresión diferencial, la interacción con *C. albicans* de los macrófagos M1 lleva a un cambio de polarización de estos macrófagos proinflamatorios hacia antiinflamatorios.

1. Proteomic studies in gel (DIGE) and off-gel (SILAC), applied to sub-cellular fractions and total extracts, respectively, allowed us to have a global vision of the murine macrophages response against *C. albicans.*

2. In response to *C. albicans,* macrophages showed a pro-inflammatory response, oxidative stress, and changes in cytoskeletal rearrangement, apoptosis and metabolism.

3. Functional studies of differentially expressed pro- and anti-apoptotic proteins and phosphoproteins and the study of different apoptotic markers revealed that *C. albicans* has an inhibitory effect in apoptosis in murine macrophages.

4. The SILAC study allowed the identification of 922 phosphorylation sites, of those, 327 were new murine protein phosphorylation sites. This phosphosites will be useful for future proteomic studies.

5. A model of interaction between *C. albicans* and human pro-inflammatory (M1) and anti-inflammatory (M2) macrophages has been set up, showing that both types of macrophages are equally efficient in phagocytosis and destroying *C. albicans* in the studied conditions.

6. Differential proteomic analysis of human M1 and M2 macrophages revealed that proteins related to metabolism and cytoskeleton rearrangement are the principal differences between both types of macrophages. Fructose 1,6-bisphosphatase (Fbp1) could be a new marker of M1 polarized macrophages.

7. Cytokine measurement and differentially expressed proteins revealed that *C. albicans* induce a switch in polarization of M1 macrophages from pro-inflammatory to anti-inflammatory.

Bibliografía

1. Acosta-Rodriguez, E. V., *et al.*, Surface phenotype and antigenic specificity of human interleukin 17-producing T helper memory cells. *Nature immunol* **2007,** *8* (6), 639-46.
2. Aderem, A.; Underhill, D. M., Mechanisms of phagocytosis in macrophages. *Annu Rev Immunol* **1999a,** *17:593-623.*, 593-623.
3. Aderem, A.; Underhill, D. M., Mechanisms of phagocytosis in macrophages. *Annu Rev Immunol* **1999b,** *17*, 593-623.
4. Aebersold, R.; Mann, M., Mass spectrometry-based proteomics. *Nature* **2003,** *422* (6928), 198-207.
5. Akarid, K., *et al.*, Leishmania major-mediated prevention of programmed cell death induction in infected macrophages is associated with the repression of mitochondrial release of cytochrome c. *J leuk biol* **2004,** *76* (1), 95-103.
6. Akira, S., TLR signaling. *Curr topic microbiol immunol* **2006,** *311*, 1-16.
7. Akira, S.; Hemmi, H., Recognition of pathogen-associated molecular patterns by TLR family. *Immunol Lett* **2003,** *85* (2), 85-95.
8. Allavena, P., *et al.*, The Yin-Yang of tumor-associated macrophages in neoplastic progression and immune surveillance. *Immunol Rev* **2008,** *222*, 155-61.
9. Alonso-Monge, R., *et al.*, Role of the mitogen-activated protein kinase Hog1p in morphogenesis and virulence of *Candida albicans*. *J Bacteriol* **1999,** *181* (10), 3058-68.
10. Anderson, J., *et al.*, Ultrastructure and antigenicity of the unique cell wall pimple of the *Candida* opaque phenotype. *J Bacteriol* **1990,** *172* (1), 224-35.
11. Anderson, J. M.; Soll, D. R., Unique phenotype of opaque cells in the white-opaque transition of *Candida albicans*. *J Bacteriol* **1987,** *169* (12), 5579-88.
12. Babior, B. M., NADPH oxidase: an update. *Blood* **1999,** *93* (5), 1464-76.
13. Bamberger, M. E., *et al.*, A cell surface receptor complex for fibrillar beta-amyloid mediates microglial activation. *The Journal of neuroscience* **2003,** *23* (7), 2665-74.
14. Barnett, J. A., *et al.*, *Yeast: Characteristics and Identification*. 2000; Vol. 3, p 21.
15. Bellocchio, S., *et al.*, The contribution of the Toll-like/IL-1 receptor superfamily to innate and adaptive immunity to fungal pathogens in vivo. *J Immunol* **2004,** *172* (5), 3059-69.
16. Benoit, M., *et al.*, Macrophage polarization in bacterial infections. *J Immunol* **2008,** *181* (6), 3733-9.
17. Bewley, M. A., *et al.*, Proteomic evaluation and validation of cathepsin D regulated proteins in macrophages exposed to *Streptococcus pneumoniae*. *Mol Cell Proteomics* **2011,** *10* (6), M111 008193.
18. Bjellqvist, B., *et al.*, The focusing positions of polypeptides in immobilized pH gradients can be predicted from their amino acid sequences. *Electrophoresis* **1993,** *14* (10), 1023-1031.
19. Blackstock, W. P.; Weir, M. P., Proteomics: quantitative and physical mapping of cellular proteins. *Trends Biotechnol* **1999,** *17* (3), 121-127.
20. Bonnotte, B., *et al.*, Identification of tumor-infiltrating macrophages as the killers of tumor cells after immunization in a rat model system. *J Immunol* **2001,** *167* (9), 5077-83.
21. Bosschaerts, T., *et al.*, Understanding the role of monocytic cells in liver inflammation using parasite infection as a model. *Immunobiology* **2009,** *214* (9-10), 737-47.
22. Braun, B. R.; Johnson, A. D., Control of filament formation in *Candida albicans* by the transcriptional repressor TUP1. *Science* **1997,** *277* (5322), 105-9.
23. Broers, J. L., *et al.*, Nuclear lamins: laminopathies and their role in premature ageing. *Physiol rev* **2006,** *86* (3), 967-1008.
24. Brown, G. C., Nitric oxide and mitochondrial respiration. *Biochim Biophys Acta* **1999,** *1411* (2-3), 351-369.
25. Brys, L., *et al.*, Reactive oxygen species and 12/15-lipoxygenase contribute to the antiproliferative capacity of alternatively activated myeloid cells elicited during helminth infection. *J Immunol* **2005,** *174* (10), 6095-104.
26. Bynoe, M. S., *et al.*, T cells from epicutaneously immunized mice are prone to T cell receptor revision. *Proc Natl Acad Sci U S A* **2005,** *102* (8), 2898-903.
27. Calderone, R. A.; Fonzi, W. A., Virulence factors of *Candida albicans. Trends Microbiol* **2001,** *9* (7), 327-335.
28. Calderone, R. A.; Gow, N. A. R., Host Recognition by *Candida* Species. In *Candida* and Candidiasis. ASM Press, 2002; pp 67-86.
29. Cao, W., *et al.*, Acetyl-Coenzyme A acyltransferase 2 attenuates the apoptotic effects of BNIP3 in two human cell lines. *Biochim Biophys Acta* **2008,** *1780* (6), 873-80.
30. Casadevall, A.; Pirofski, L., Host-pathogen interactions: the attributes of virulence. *J Infect Dis* **2001,** *184* (3), 337-44.
31. Casanova, M., *et al.*, Fab fragments from a monoclonal antibody against a germ tube mannoprotein block the yeast-to-mycelium transition in *Candida albicans. Infect Immun* **1990,** *58* (11), 3810-3812.
32. Cassone, A., *et al.*, Rats clearing a vaginal infection by *Candida albicans* acquire specific,

antibody-mediated resistance to vaginal reinfection. *Infect Immun* **1995,** *63* (7), 2619-2624.
33. Celada, A.; Maki, R. A., Transforming growth factor-beta enhances the M-CSF and GM-CSF-stimulated proliferation of macrophages. *J.Immunol.* **1992,** *148* (4), 1102-1105.
34. Celada, A.; Nathan, C., Macrophage activation revisited. *Immunology today* **1994,** *15* (3), 100-2.
35. Chan, D. C., Mitochondria: dynamic organelles in disease, aging, and development. *Cell* **2006,** *125* (7), 1241-52.
36. Charro, N.*, et al.*, Serum proteomics signature of cystic fibrosis patients: a complementary 2-DE and LC-MS/MS approach. *J Proteomics* **2011,** *74* (1), 110-26.
37. Cheng, S. C.*, et al.*, The dectin-1/inflammasome pathway is responsible for the induction of protective T-helper 17 responses that discriminate between yeasts and hyphae of *Candida albicans*. *Journal of leukocyte biology* **2011,** *90* (2), 357-66.
38. Chilgren, R. A.*, et al.*, Human serum interactions with *Candida albicans J Immunol.* **1968,** *101* (1), 128-132.
39. Christophi, G. P.*, et al.*, Modulation of macrophage infiltration and inflammatory activity by the phosphatase SHP-1 in virus-induced demyelinating disease. *J Virol* **2009,** *83* (2), 522-39.
40. Clauser, K. R.*, et al.*, Rapid mass spectrometric peptide sequencing and mass matching for characterization of human melanoma proteins isolated by two-dimensional PAGE. *Proc Natl Acad Sci U S A* **1995,** *92* (11), 5072-6.
41. Cole, G. T.*, et al.*, Gastrointestinal and systemic candidosis in immunocompromised mice. *J Med Veterin Mycology* **1989,** *27*, 363-380.
42. Colombo, E.*, et al.*, Nucleophosmin is required for DNA integrity and p19Arf protein stability. *Mol Cell Biol* **2005,** *25* (20), 8874-86.
43. Compston, J. E., Bone marrow and bone: a functional unit. *J endocrinology* **2002,** *173* (3), 387-94.
44. Coste, A.*, et al.*, PPARgamma promotes mannose receptor gene expression in murine macrophages and contributes to the induction of this receptor by IL-13. *Immunity* **2003,** *19* (3), 329-39.
45. Craig, R. W., MCL1 provides a window on the role of the BCL2 family in cell proliferation, differentiation and tumorigenesis. *Leukemia* **2002,** *16* (4), 444-54.
46. Cunningham, E. L.; Agard, D. A., Disabling the folding catalyst is the last critical step in alpha-lytic protease folding. *Protein science* **2004,** *13* (2), 325-31.
47. d'Ostiani, C. F.*, et al.*, Dendritic cells discriminate between yeasts and hyphae of the fungus *Candida albicans*. Implications for initiation of T helper cell immunity in vitro and in vivo. *J Exp Med* **2000,** *191* (10), 1661-1674.
48. de las Casas-Engel, M.*, et al.*, Serotonin skews human macrophage polarization through HTR2B and HTR7. *J Immunol* **2013,** *190* (5), 2301-10.
49. Deguchi, A.*, et al.*, Vasodilator-stimulated phosphoprotein (VASP) phosphorylation provides a biomarker for the action of exisulind and related agents that activate protein kinase G. *Mol cancer therap* **2002,** *1* (10), 803-9.
50. Diez-Orejas, R.*, et al.*, Low virulence of a morphological *Candida albicans* mutant. *FEMS Microbiol Lett* **1999,** *176* (2), 311-9.
51. Dixon, D. M.*, et al.*, Fungal infections: a growing threat. *Public Health Rep.* **1996,** *111* (3), 226-235.
52. Donahue, J. L.*, et al.*, The Arabidopsis thaliana Myo-inositol 1-phosphate synthase1 gene is required for Myo-inositol synthesis and suppression of cell death. *Plant Cell* **2010,** *22* (3), 888-903.
53. Douglas, L. J., *Candida* biofilms and their role in infection. *Trends Microbiol* **2003,** *11* (1), 30-6.
54. Dumic, J.*, et al.*, Galectin-3: an open-ended story. *Biochim Biophys Acta* **2006,** *1760* (4), 616-35.
55. Dustin, M. L.*, et al.*, A novel adaptor protein orchestrates receptor patterning and cytoskeletal polarity in T-cell contacts. *Cell* **1998,** *94* (5), 667-77.
56. El Khoury, J. B.*, et al.*, CD36 mediates the innate host response to beta-amyloid. *J Exp Med* **2003,** *197* (12), 1657-66.
57. Enoch, D. A.*, et al.*, Invasive fungal infections: a review of epidemiology and management options. *J Med Microbiol* **2006,** *55* (Pt 7), 809-18.
58. Esteban, A.*, et al.*, Fungal recognition is mediated by the association of dectin-1 and galectin-3 in macrophages. *Proc Natl Acad Sci U S A* **2011,** *108* (34), 14270-5.
59. Eyerich, K.*, et al.*, Patients with chronic mucocutaneous candidiasis exhibit reduced production of Th17-associated cytokines IL-17 and IL-22. *J invest dermatol* **2008,** *128* (11), 2640-5.
60. Farmer, T. B.; Caprioli, R. M., Determination of protein-protein interactions by matrix-assisted laser desorption/ionization mass spectrometry. *J mass spect* **1998,** *33* (8), 697-704.
61. Fenn, J. B.*, et al.*, Electrospray ionization for mass spectrometry of large biomolecules. *Science* **1989,** *246* (4926), 64-71.

62. Fernández-Arenas, E., *et al.*, Integrated proteomics and genomics strategies bring new insight into *Candida albicans* response upon macrophage interaction. *Mol Cell Proteomics.* **2007,** *6* (3), 460-478.
63. Finamore, F., *et al.*, Proteomics investigation of human platelets by shotgun nUPLC-MSE and 2DE experimental strategies: a comparative study. *Blood transfusion* **2010,** *8 Suppl 3*, s140-8.
64. Fischer, A., *et al.*, Specific inhibition of in vitro *Candida* -induced lymphocyte proliferation by polysaccharidic antigens present in the serum of patients with chronic mucocutaneous candidiasis. *J Clin Invest* **1978,** *62* (5), 1005-1013.
65. Fischer, S. F., *et al.*, Characterization of antiapoptotic activities of *Chlamydia pneumoniae* in human cells. *Infect Immun* **2001,** *69* (11), 7121-9.
66. Ford, J. W.; McVicar, D. W., TREM and TREM-like receptors in inflammation and disease. *Curr Opin Immunol* **2009,** *21* (1), 38-46.
67. Fradin, C., *et al.*, Beta-1,2-linked oligomannosides inhibit *Candida albicans* binding to murine macrophage. *J Leukoc Biol* **1996,** *60* (1), 81-87.
68. Fradin, C., *et al.*, beta-1,2-linked oligomannosides from *Candida albicans* bind to a 32-kilodalton macrophage membrane protein homologous to the mammalian lectin galectin-3. *Infect Immun* **2000a,** *68* (8), 4391-4398.
69. Fradin, C., *et al.*, beta-1,2-linked oligomannosides from *Candida albicans* bind to a 32-kilodalton macrophage membrane protein homologous to the mammalian lectin galectin-3. *Infect Immun* **2000b,** *68* (8), 4391-8.
70. Furman, R. M.; Ahearn, D. G., *Candida ciferrii* and *Candida chiropterorum* isolated from clinical specimens. *J Clin Microbiol* **1983,** *18* (5), 1252-5.
71. Garrels, J. I., *et al.*, Protein identifications for a *Saccharomyces cerevisiae* protein database *Electrophoresis* **1994,** *15* (11), 1466-1486.
72. Goerdt, S., *et al.*, Alternative versus classical activation of macrophages. *Pathobiology* **1999,** *67* (5-6), 222-6.
73. Goode, B. L.; Eck, M. J., Mechanism and function of formins in the control of actin assembly. *Annu Rev Biochem* **2007,** *76*, 593-627.
74. Gordon, S., Alternative activation of macrophages. *Nature rev Immunol* **2003,** *3* (1), 23-35.
75. Gordon, S.; Taylor, P. R., Monocyte and macrophage heterogeneity. *Nature rev Immunol* **2005,** *5* (12), 953-64.
76. Gough, M. J., *et al.*, Macrophages orchestrate the immune response to tumor cell death. *Cancer Res* **2001,** *61* (19), 7240-7.
77. Graham, L. M.; Brown, G. D., The Dectin-2 family of C-type lectins in immunity and homeostasis. *Cytokine* **2009,** *48* (1-2), 148-55.
78. Griffin, T. J., *et al.*, Toward a high-throughput approach to quantitative proteomic analysis: expression-dependent protein identification by mass spectrometry. *J Am Soc Mass Specty* **2001,** *12* (12), 1238-46.
79. Gutierrez, J., *et al.*, *Candida dubliniensis*, a new fungal pathogen. *J Basic Microbiol* **2002,** *42* (3), 207-27.
80. Gygi, S. P.; Aebersold, R., Mass spectrometry and proteomics. *Curr op chem biol* **2000,** *4* (5), 489-94.
81. Han, Y.; Cutler, J. E., Antibody response that protects against disseminated candidiasis. *Infect Immun* **1995,** *63* (7), 2714-2719.
82. Hansen, J. M., *et al.*, Nuclear and cytoplasmic peroxiredoxin-1 differentially regulate NF-kappaB activities. *Free radical biol med* **2007,** *43* (2), 282-8.
83. Haschemi, A., *et al.*, The sedoheptulose kinase CARKL directs macrophage polarization through control of glucose metabolism. *Cell metabolism* **2012,** *15* (6), 813-26.
84. Heidenreich, S., *et al.*, Infection by *Candida albicans* inhibits apoptosis of human monocytes and monocytic U937 cells. *J Leukoc Biol* **1996,** *60* (6), 737-743.
85. Heinsbroek, S. E., *et al.*, Dectin-1 escape by fungal dimorphism. *Trends Immunol* **2005,** *26* (7), 352-4.
86. Herre, J., *et al.*, Dectin-1 and its role in the recognition of beta-glucans by macrophages. *Mol Immunol* **2004,** *40* (12), 869-76.
87. Higuchi, T., *et al.*, Protein disulfide isomerase suppresses the transcriptional activity of NF-kappaB. *Biochem Biophys Res Commun.* **2004,** *318* (1), 46-52.
88. Hollifield, M., *et al.*, Scavenger receptor A dampens induction of inflammation in response to the fungal pathogen *Pneumocystis carinii*. *Infect Immun* **2007,** *75* (8), 3999-4005.
89. Houde, M., *et al.*, Phagosomes are competent organelles for antigen cross-presentation. *Nature* **2003,** *425* (6956), 402-6.
90. Hoyer, L. L., The ALS gene family of *Candida albicans*. *Trends Microbiol* **2001,** *9* (4), 176-80.
91. Hsu, D. K., *et al.*, Targeted disruption of the galectin-3 gene results in attenuated peritoneal inflammatory responses. *Am j pathol* **2000,** *156* (3), 1073-83.
92. Huang, J. S., *et al.*, Diverse cellular transformation capability of overexpressed genes in human hepatocellular carcinoma. *Biochemi Biophys Res Comm* **2004,** *%19;315* (4), 950-958.

93. Hube, B., and Naglik, J., Extracellular hydrolases. In *Candida* and Candidiasis. R. A. Calderone (ed.). ASM Press, p. 107-122

2002.

94. Huffnagle, G. B.; Deepe, G. S., Innate and adaptive determinants of host susceptibility to medically important fungi. *Curr Opin Microbiol* **2003,** *6* (4), 344-50.

95. Humphery-Smith, I.*, et al.*, Proteome research: complementarity and limitations with respect to the RNA and DNA worlds. *Electrophoresis* **1997,** *18* (8), 1217-1242.

96. Ibata-Ombetta, S.*, et al.*, *Candida albicans* phospholipomannan promotes survival of phagocytosed yeasts through modulation of bad phosphorylation and macrophage apoptosis. *J Biol Chem* **2003,** *278* (15), 13086-13093.

97. Iobst, S. T.; Drickamer, K., Binding of sugar ligands to Ca(2+)-dependent animal lectins. II. Generation of high-affinity galactose binding by site-directed mutagenesis. *J Biol Chem* **1994,** *269* (22), 15512-9.

98. Issaq, H. J.*, et al.*, Multidimensional high performance liquid chromatography--capillary electrophoresis separation of a protein digest: an update. *Electrophoresis* **2001,** *22* (6), 1133-5.

99. Janeway, C. A., Jr., The immune system evolved to discriminate infectious nonself from noninfectious self. *Immunol Tod* **1992,** *13* (1), 11-16.

100. Janeway, C. A.*, et al.*, Innate Immunity. *Immunobiology* **2005**; Vol. 6, pp 37-102.

101. Jawhara, S.*, et al.*, Colonization of mice by *Candida albicans* is promoted by chemically induced colitis and augments inflammatory responses through galectin-3. *J Infect Dis* **2008,** *197* (7), 972-80.

102. Ji, X. H.*, et al.*, Interaction between M-CSF and IL-10 on productions of IL-12 and IL-18 and expressions of CD14, CD23, and CD64 by human monocytes. *Acta pharmacol Sinica* **2004,** *25* (10), 1361-5.

103. Johnson, G. L.; Lapadat, R., Mitogen-activated protein kinase pathways mediated by ERK, JNK, and p38 protein kinases. *Science* **2002,** *298* (5600), 1911-2.

104. Johnson, S. A.; Hunter, T., Phosphoproteomics finds its timing. *Nature biotechnol* **2004,** *22* (9), 1093-4.

105. Jouault, T.*, et al.*, Specific recognition of *Candida albicans* by macrophages requires galectin-3 to discriminate *Saccharomyces cerevisiae* and needs association with TLR2 for signaling. *J Immunol* **2006,** *177* (7), 4679-87.

106. Jouault, T.*, et al.*, *Candida albicans* phospholipomannan is sensed through toll-like receptors. *J Infect Dis* **2003,** *188* (1), 165-72.

107. Karas, M.; Hillenkamp, F., Laser desorption ionization of proteins with molecular masses exceeding 10,000 daltons. *Anal chem* **1988,** *60* (20), 2299-301.

108. Katakura, T.*, et al.*, CCL17 and IL-10 as effectors that enable alternatively activated macrophages to inhibit the generation of classically activated macrophages. *J Immunol* **2004,** *172* (3), 1407-13.

109. Kicman, A. T.*, et al.*, An introduction to mass spectrometry based proteomics-detection and characterization of gonadotropins and related molecules. *Mol cell endocrinol* **2007,** *260-262*, 212-27.

110. Kim, K. H.*, et al.*, SEPS1 protects RAW264.7 cells from pharmacological ER stress agent-induced apoptosis. *Biochem Biophys Res Commun* **2007,** *354* (1), 127-32.

111. Kisucka, J.*, et al.*, Peroxiredoxin1 prevents excessive endothelial activation and early atherosclerosis. *Circulation res* **2008,** *103* (6), 598-605.

112. Kohatsu, L.*, et al.*, Galectin-3 induces death of *Candida* species expressing specific beta-1,2-linked mannans. *J Immunol* **2006,** *177* (7), 4718-26.

113. Kontoyiannis, D. P.*, et al.*, Breakthrough candidemia in patients with cancer differs from de novo candidemia in host factors and Candida species but not intensity. *Infect Control Hosp Epidemiol* **2002,** *23* (9), 542-545.

114. Koppel, E. A.*, et al.*, Distinct functions of DC-SIGN and its homologues L-SIGN (DC-SIGNR) and mSIGNR1 in pathogen recognition and immune regulation. *Cellular microbiol* **2005,** *7* (2), 157-65.

115. Kryukov, G. V.*, et al.*, Characterization of mammalian selenoproteomes. *Science* **2003,** *300* (5624), 1439-43.

116. Kuhn, D. M.; Ghannoum, M. A., Candida biofilms: antifungal resistance and emerging therapeutic options. *Curr Opin Investig Drugs* **2004,** *5* (2), 186-97.

117. Kullberg, B. J.; Filler, S. G., Candidemia. In *Candida and Candidiasis*, Calderone, R. A., Ed. ASM Press: Washington D.C., 2002; pp 327-340.

118. Kvaal, C.*, et al.*, Misexpression of the opaque-phase-specific gene PEP1 (SAP1) in the white phase of *Candida albicans* confers increased virulence in a mouse model of cutaneous infection KVAAL1999. *Infect Immun* **1999,** *67* (12), 6652-6662.

119. Laemmli, U. K., Cleavage of structural proteins during the assembly of the head of

bacteriophage T4. *Nature* **1970,** *227* (259), 680-685.
120. Lan, C. Y.*, et al.*, Metabolic specialization associated with phenotypic switching in *Candida albicans Proc Natl Acad Sci* **2002,** *99* (23), 14907-14912.
121. Landais, I.*, et al.*, Coupling caspase cleavage and ubiquitin-proteasome-dependent degradation of SSRP1 during apoptosis. *Cell death different* **2006,** *13* (11), 1866-78.
122. Laprade, L.*, et al.*, Spt3 plays opposite roles in filamentous growth in *Saccharomyces cerevisiae* and *Candida albicans* and is required for *C. albicans* virulence. *Genetics* **2002,** *161* (2), 509-19.
123. Lee, K. L.*, et al.*, An amino acid liquid synthetic medium for the development of mycelial and yeast forms of *Candida albicans. Sabouraudia.* **1975,** *13* (2), 148-153.
124. Lehner, P. J.; Cresswell, P., Recent developments in MHC-class-I-mediated antigen presentation. *Curr Opin Immunol* **2004,** *16* (1), 82-9.
125. LeibundGut-Landmann, S.*, et al.*, Syk- and CARD9-dependent coupling of innate immunity to the induction of T helper cells that produce interleukin 17. *Nature immunol* **2007,** *8* (6), 630-8.
126. Lesley, S. A., High-throughput proteomics: protein expression and purification in the postgenomic world. *Protein expres purific* **2001,** *22* (2), 159-64.
127. Li, X.*, et al.*, PEX11 beta deficiency is lethal and impairs neuronal migration but does not abrogate peroxisome function. *Mol Cell Biol* **2002,** *22* (12), 4358-65.
128. Liu, F. T.*, et al.*, Expression and function of galectin-3, a beta-galactoside-binding lectin, in human monocytes and macrophages. *Am j pathol* **1995,** *147* (4), 1016-28.
129. Liu, H.*, et al.*, A model for random sampling and estimation of relative protein abundance in shotgun proteomics. *Anal chem* **2004,** *76* (14), 4193-201.
130. Liu, S.*, et al.*, Electrospray ionization mass spectrometry as a critical tool for revealing new properties of snake venom phospholipase A2. *Rapid com mass spect* **2009,** *23* (8), 1158-66.
131. Lo, H. J.*, et al.*, Nonfilamentous *C. albicans* mutants are avirulent. *Cell* **1997,** *90* (5), 939-49.
132. Louria, D. B., *Candida* infection in experimental animals. In *Candidiasis*. **1985**; 29-51.
133. Lovric, J.*, et al.*, Activated raf induces the hyperphosphorylation of stathmin and the reorganization of the microtubule network. *J Biol Chem* **1998,** *273* (35), 22848-55.
134. Lugo-Villarino, G.*, et al.*, Macrophage polarization: convergence point targeted by *Mycobacterium tuberculosis* and HIV. *Front immunol* **2011,** *2*, 43.
135. Mansour, M. K.; Levitz, S. M., Interactions of fungi with phagocytes. *Curr Opin Microbiol* **2002,** *5* (4), 359-65.
136. Mantovani, A.*, et al.*, Tumour-associated macrophages as a prototypic type II polarised phagocyte population: role in tumour progression. *Eur J Cancer* **2004,** *40* (11), 1660-7.
137. Mantovani, A.*, et al.*, New vistas on macrophage differentiation and activation. *Eur J Immunol* **2007,** *37* (1), 14-6.
138. Mantovani, A.*, et al.*, Macrophage polarization: tumor-associated macrophages as a paradigm for polarized M2 mononuclear phagocytes. *Trends Immunol* **2002,** *23* (11), 549-55.
139. Marr, K. A.*, et al.*, Differential role of MyD88 in macrophage-mediated responses to opportunistic fungal pathogens. *Infect Immun* **2003,** *71* (9), 5280-6.
140. Martin, J.*, et al.*, Hint2, a mitochondrial apoptotic sensitizer down-regulated in hepatocellular carcinoma. *Gastroenterology* **2006,** *130* (7), 2179-88.
141. Martínez-Solano, L.*, et al.*, Differential protein expression of murine macrophages upon interaction with *Candida albicans. Proteomics.* **2006,** *6 Suppl 1:S133-44.*, S133-S144.
142. Martínez-Solano, L.*, et al.*, Proteomics of RAW 264.7 macrophages upon interaction with heat-inactivated *Candida albicans* cells unravel an anti-inflammatory response. *Proteomics* **2009,** *9* (11), 2995-3010.
143. Martinez, F. O.*, et al.*, Alternative activation of macrophages: an immunologic functional perspective. *Annual rev immunol* **2009,** *27*, 451-83.
144. Matsumoto, M.*, et al.*, A novel LPS-inducible C-type lectin is a transcriptional target of NF-IL6 in macrophages. *J Immunol* **1999,** *163* (9), 5039-48.
145. Mayer, F. L.*, et al.*, *Candida albicans* pathogenicity mechanisms. *Virulence* **2013,** *4* (2), 119-28.
146. McGreal, E. P.*, et al.*, Ligand recognition by antigen-presenting cell C-type lectin receptors. *Curr Op Immunol* **2005,** *17* (1), 18-24.
147. McGreal, E. P.*, et al.*, The carbohydrate-recognition domain of Dectin-2 is a C-type lectin with specificity for high mannose. *Glycobiology* **2006,** *16* (5), 422-30.
148. Mege, J. L.*, et al.*, Macrophage polarization and bacterial infections. *Curr Opin Infect Dis* **2011,** *24* (3), 230-4.
149. Meyer, J. E.*, et al.*, Human beta-defensin-2 in oral cancer with opportunistic *Candida* infection. *Anticancer Res* **2004,** *24* (2B), 1025-30.

150. Miller, M. G.; Johnson, A. D., White-opaque switching in *Candida albicans* is controlled by mating-type locus homeodomain proteins and allows efficient mating. *Cell* **2002,** *110* (3), 293-302.
151. Mirgorodskaya, O. A.*, et al.*, Quantitation of peptides and proteins by matrix-assisted laser desorption/ionization mass spectrometry using (18)O-labeled internal standards. *Rapid comm mass spect* **2000,** *14* (14), 1226-32.
152. Misra, U. K.; Pizzo, S. V., Up-regulation of GRP78 and antiapoptotic signaling in murine peritoneal macrophages exposed to insulin. *J Leukoc Biol* **2005,** *78* (1), 187-194.
153. Miyake, H.*, et al.*, Stress protein GRP78 prevents apoptosis induced by calcium ionophore, ionomycin, but not by glycosylation inhibitor, tunicamycin, in human prostate cancer cells. *J Cell biochem* **2000,** *77* (3), 396-408.
154. Moncada, S.*, et al.*, Nitric Oxide: Physiology, Pathophysiology, and Pharmacology. *Pharmacol Rev* **1991,** *43*, 109-142.
155. Montagnoli, C.*, et al.*, B7/CD28-dependent CD4+CD25+ regulatory T cells are essential components of the memory-protective immunity to *Candida albicans J Immunol* **2002,** *169* (11), 6298-6308.
156. Monteoliva, L.; Albar, J. P., Differential proteomics: an overview of gel and non-gel based approaches. *Brief Funct Genomic Proteomic* **2004,** *3* (3), 220-239.
157. Moore, K. J.*, et al.*, A CD36-initiated signaling cascade mediates inflammatory effects of beta-amyloid. *J Biol Chem* **2002,** *277* (49), 47373-9.
158. Mor-Vaknin, N.*, et al.*, Vimentin is secreted by activated macrophages. *Nature cell biology* **2003,** *5* (1), 59-63.
159. Moran, G.*, et al.*, The *Candida dubliniensis* CdCDR1 gene is not essential for fluconazole resistance. *Antimicrob Agents Chemother* **2002,** *46* (9), 2829-41.
160. Mytar, B.*, et al.*, Induction of reactive oxygen intermediates in human monocytes by tumour cells and their role in spontaneous monocyte cytotoxicity. *British J cancer* **1999,** *79* (5-6), 737-43.
161. Nakatani, Y.*, et al.*, Involvement of the constitutive prostaglandin E synthase cPGES/p23 in expression of an initial prostaglandin E2 inactivating enzyme, 15-PGDH. *Prostagl lipid mediators* **2011,** *94* (3-4), 112-7.
162. Nathan, C. F., Secretory products of macrophages NATHAN1987. *J Clin Invest* **1987,** *79* (2), 319-326.
163. Netea, M. G.*, et al.*, An integrated model of the recognition of *Candida albicans* by the innate immune system. *Nature rev Microbiol* **2008,** *6* (1), 67-78.
164. Netea, M. G.; Marodi, L., Innate immune mechanisms for recognition and uptake of *Candida* species. *Trends Immunol* **2010,** *31* (9), 346-53.
165. Netea, M. G.*, et al.*, Toll-like receptor 2 suppresses immunity against *Candida albicans* through induction of IL-10 and regulatory T cells. *J Immunol* **2004,** *172* (6), 3712-3718.
166. Netea, M. G.*, et al.*, The role of toll-like receptor (TLR) 2 and TLR4 in the host defense against disseminated candidiasis. *J Infect Dis* **2002,** *185* (10), 1483-1489.
167. Netea, M. G.*, et al.*, Both TLR2 and TLR4 are involved in the recognition of *Candida albicans*. *Microb infect* **2006,** *8* (12-13), 2821-2.
168. Nett, J.; Andes, D., *Candida albicans* biofilm development, modeling a host-pathogen interaction. *Curr Opin Microbiol* **2006,** *9* (4), 340-5.
169. Nitz, M.*, et al.*, The unique solution structure and immunochemistry of the *Candida albicans* beta -1,2-mannopyranan cell wall antigens. *J Biol Chem* **2002,** *277* (5), 3440-6.
170. Niu, J.*, et al.*, Cardioprotective effects of cerium oxide nanoparticles in a transgenic murine model of cardiomyopathy. *Cardiovasc Res* **2007,** *73* (3), 549-559.
171. O'Farrell, P. H., High resolution two-dimensional electrophoresis of proteins. *The J Biol Chem* **1975,** *250* (10), 4007-4021.
172. Oda, Y.*, et al.*, Accurate quantitation of protein expression and site-specific phosphorylation. *Proc Natl Acad Sci U S A* **1999,** *96* (12), 6591-6.
173. Odds, F. C., *Candida* and candidosis. Baillihre Tindall (ed.) London, 1988a.
174. Odds, F. C., In *Candida* and Candidosis. Baillihre Tindall (ed.) London. 1988b.
175. Odds, F. C., Candida species and virulence. ASM News 60, p. 313-318 **1994**.
176. Odds, F. C., et al., Antifungal agents: mechanisms of action. Trends Microbiol **2003**, 11 (6), 272-9.
177. Odds, F. C.*, et al.*, Fungal virulence studies come of age. *Genome biology* **2001,** *2* (3).
178. Odegaard, J. I.; Chawla, A., Alternative macrophage activation and metabolism. *Ann Rev Pathol* **2011,** *6*, 275-97.
179. Ogawa, M., Differentiation and proliferation of hematopoietic stem cells. *Blood* **1993,** *81* (11), 2844-53.
180. Olefsky, J. M.; Glass, C. K., Macrophages, inflammation, and insulin resistance. *Ann Rev Physiol* **2010,** *72*, 219-46.
181. Ong, S. E.*, et al.*, Stable isotope labeling by amino acids in cell culture, SILAC, as a simple and accurate approach to expression proteomics. *Mol Cell Proteomics* **2002,** *1* (5), 376-86.

182. Pahl, H. L.; Baeuerle, P. A., The ER-overload response: activation of NF-kappa B. *Trends Biochem Sci* **1997,** *22* (2), 63-7.
183. Palm, N. W.; Medzhitov, R., Antifungal defense turns 17. *Nature Immunol* **2007,** *8* (6), 549-51.
184. Palmgren, S*., et al.*, Twinfilin, a molecular mailman for actin monomers. *J Cell Sci* **2002,** *115* (Pt 5), 881-6.
185. Papadimitriou, J. M.; Ashman, R. B., The pathogenesis of acute systemic candidiasis in a susceptible inbred mouse strain. *J Pathol* **1986,** *150*, 257-265.
186. Patterson, S. D., Protein identification and characterization by mass spectrometry. C*urr prot Mol Biol*, **1998**.
187. Patterson, S. D.; Aebersold, R., Mass spectrometric approaches for the identification of gel-separated proteins. *Electrophoresis* **1995,** *16* (10), 1791-1814.
188. Paul, G*., et al.*, Accurate mass measurement at enhanced mass-resolution on a triple quadrupole mass-spectrometer for the identification of a reaction impurity and collisionally-induced fragment ions of cabergoline. *Rapid comm mass spect* **2003,** *17* (6), 561-8.
189. Peman, J*., et al.*, Epidemiology and antifungal susceptibility of **Candida** species isolated from blood: results of a 2-year multicentre study in Spain. *Europ J Clin Microbiol Infect Dis* **2005,** *24* (1), 23-30.
190. Pendrak, M. L.; Klotz, S. A., Adherence of *Candida albicans* to host cells. *FEMS Microbiol Lett* **1995,** *129* (2-3), 103-13.
191. Peng, Q*., et al.*, TREM2- and DAP12-dependent activation of PI3K requires DAP10 and is inhibited by SHIP1. *Science signal* **2010,** *3* (122), ra38.
192. Pfaller, M. A.; Diekema, D. J., Epidemiology of invasive candidiasis: a persistent public health problem. *Clin Microbiol Rev* **2007,** *20* (1), 133-163.
193. Pfaller, M. A*., et al.*, Candida guilliermondii, an opportunistic fungal pathogen with decreased susceptibility to fluconazole: geographic and temporal trends from the ARTEMIS DISK antifungal surveillance program. *J Clin Microbiol* **2006,** *44* (10), 3551-6.
194. Pinzi, S*., et al.*, Flow injection analysis-based methodology for automatic on-line monitoring and quality control for biodiesel production. *Biores technol* **2009,** *100* (1), 421-7.
195. Pitarch, A*., et al.*, *Candida albicans* biology and pathogenicity: insights from proteomics. 2006a.
196. Pitarch, A*., et al.*, Contributions of proteomics to diagnosis, treatment and prevention of candidiasis. 2006b.
197. Plowden, J*., et al.*, Innate immunity in aging: impact on macrophage function. *Aging Cell.* **2004,** *3* (4), 161-167.
198. Polonelli, L*., et al.*, Heat-shock mannoproteins as targets of secretory IgA in *Candida albicans. J Infect Dis* **1994,** *169* (6), 1401-1405.
199. Pomes, R*., et al.*, Genetic analysis of *Candida albicans* morphological mutants. *J Gen Microbiol* **1985,** *131* (8), 2107-13.
200. Puccetti, P*., et al.*, Cure of murine candidiasis by recombinant soluble interleukin-4 receptor. *J Infect Dis* **1994,** *169* (6), 1325-31.
201. Puig-Kroger, A*., et al.*, Folate receptor beta is expressed by tumor-associated macrophages and constitutes a marker for M2 anti-inflammatory/regulatory macrophages. *Cancer Res* **2009,** *69* (24), 9395-403.
202. Qian, W. J*., et al.*, Advances and challenges in liquid chromatography-mass spectrometry-based proteomics profiling for clinical applications. *Mol Cel Proteomics* **2006,** *5* (10), 1727-44.
203. Ralph, P.; Nakoinz, I., Antibody-dependent killing of erythrocyte and tumor targets by macrophage-related cell lines: enhancement by PPD and LPS RALPH1977. *J Immunol* **1977,** *119* (3), 950-954.
204. Ramachandra, L*., et al.*, Phagosomes are fully competent antigen-processing organelles that mediate the formation of peptide:class II MHC complexes. *J Immunol* **1999,** *162* (6), 3263-72.
205. Ramage, G*., et al.*, *Candida* biofilms: an update. *Eukaryot.Cell.* **2005,** *4* (4), 633-638.
206. Re, F.; Strominger, J. L., Toll-like receptor 2 (TLR2) and TLR4 differentially activate human dendritic cells. *J Biol Chem* **2001,** *276* (40), 37692-9.
207. Reales-Calderon, J. A*., et al.*, Sub-proteomic study on macrophage response to *Candida albicans* unravels new proteins involved in the host defense against the fungus. *J Proteomics* **2012,** *75* (15), 4734-46.
208. Reales-Calderon, J. A*., et al.*, *Candida albicans* induces pro-inflammatory and anti-apoptotic signals in macrophages as revealed by quantitative proteomics and phosphoproteomics. *J Proteomics* **2013**.
209. Reeves, E. P*., et al.*, Killing activity of neutrophils is mediated through activation of proteases by K+ flux. *Nature* **2002,** *416* (6878), 291-7.
210. Rhee, S. G*., et al.*, Intracellular messenger function of hydrogen peroxide and its regulation by

peroxiredoxins. *Curr Opin Cell Biol* **2005,** *17* (2), 183-9.
211. Richardson, M. D., Changing patterns and trends in systemic fungal infections. J *antimicrob chem* **2005,** *56 Suppl 1*, i5-i11.
212. Rocha, C. R*., et al.*, Signaling through adenylyl cyclase is essential for hyphal growth and virulence in the pathogenic fungus *Candida albicans*. *Mol Biol Cell* **2001,** *12* (11), 3631-43.
213. Rodriguez, D*., et al.*, Candidemia in neonatal intensive care units: Barcelona, Spain. *Pediatr Infect Dis J* **2006,** *25* (3), 224-9.
214. Roepstorff, P.; Fohlman, J., Proposal for a common nomenclature for sequence ions in mass spectra of peptides. *Biomed mass spect* **1984,** *11* (11), 601.
215. Romani, L., Immunity to fungal infections. *Nature rev Immunology* **2004,** *4* (1), 1-23.
216. Romani, L., Immunity to fungal infections. *Nature rev Immunology* **2011,** *11* (4), 275-88.
217. Romani, L.; Bistoni, F., Systemic immunity in candidiasis. *Fungal Pathog* Eds. New York, 2001; pp 483-514.
218. Romani, L*., et al.*, Gamma interferon modifies CD4+ subset expression in murine candidiasis. *Infect Immun* **1992a,** *60* (11), 4950-2.
219. Romani, L.; Kaufmann, S. H., Immunity to fungi: editorial overview. *Res Immunol* **1998,** *149* (4-5), 277-281.
220. Romani, L*., et al.*, CD4+ subset expression in murine candidiasis. Th responses correlate directly with genetically determined susceptibility or vaccine-induced resistance. *J Immunol* **1993,** *150* (3), 925-31.
221. Romani, L*., et al.*, Neutralizing antibody to interleukin 4 induces systemic protection and T helper type 1-associated immunity in murine candidiasis. *J Exp Med* **1992b,** *176* (1), 19-25.
222. Romani, L.; Puccetti, P., Protective tolerance to fungi: the role of IL-10 and tryptophan catabolism. *Trends Microbiol* **2006,** *14* (4), 183-9.
223. Romani, L.; Puccetti, P., Controlling pathogenic inflammation to fungi. *Exp rev anti-infective therapy* **2007,** *5* (6), 1007-17.
224. Romani, L*., et al.*, Neutralization of IL-10 up-regulates nitric oxide production and protects susceptible mice from challenge with *Candida albicans*. *J Immunol* **1994,** *152* (7), 3514-21.
225. Ross, P. L*., et al.*, Multiplexed protein quantitation in *Saccharomyces cerevisiae* using amine-reactive isobaric tagging reagents. *Mol Cel Proteomics* **2004,** *3* (12), 1154-69.
226. Rotstein, D*., et al.*, Phagocytosis of *Candida albicans* induces apoptosis of human neutrophils. *Shock* **2000,** *14* (3), 278-83.
227. Sagliocco, F*., et al.*, Identification of proteins of the yeast protein map using genetically manipulated strains and peptide-mass fingerprinting. *Yeast* **1996,** *12* (15), 1519-1533.
228. San Millan, R*., et al.*, Effect of monoclonal antibodies directed against *Candida albicans* cell wall antigens on the adhesion of the fungus to polystyrene. *Microbiology.* **1996,** *142* (Pt 8), 2271-2277.
229. Sano, H*., et al.*, Critical role of galectin-3 in phagocytosis by macrophages. *J Clin Invest* **2003,** *112* (3), 389-97.
230. Saporito-Irwin, S. M*., et al.*, *PHR1*. a pH-regulated gene of *Candida albicans*, is required for morphogenesis. *Mol Cellr Biol* **1995,** *15* (2), 601-613.
231. Sarkey, J. P*., et al.*, Nogo-A knockdown inhibits hypoxia/reoxygenation-induced activation of mitochondrial-dependent apoptosis in cardiomyocytes. *J Mol Cell Cardiol* **2011,** *50* (6), 1044-55.
232. Sato, K*., et al.*, Dectin-2 is a pattern recognition receptor for fungi that couples with the Fc receptor gamma chain to induce innate immune responses. *J Biol Chem* **2006,** *281* (50), 38854-66.
233. Scheld, W. M*., et al.*, Influence of preformed antibody on the pathogenesis of experimental *Candida albicans* endocarditis. *Infect Immun* **1983,** *40* (3), 950-955.
234. Schenning, M*., et al.*, Phosphatidylinositol transfer protein alpha regulates growth and apoptosis of NIH3T3 cells: involvement of a cannabinoid 1-like receptor. *J Lipid Res* **2004,** *45* (8), 1555-64.
235. Schneider, J. J*., et al.*, Human defensins. *J Mol Med* **2005,** *83* (8), 587-95.
236. Schofield, D. A*., et al.*, beta-defensin expression in immunocompetent and immunodeficient germ-free and *Candida albicans*-monoassociated mice. *J Infect Dis* **2004,** *190* (7), 1327-34.
237. Sears, D*., et al.*, Functional phosphoproteomic analysis reveals cold-shock domain protein A to be a Bcr-Abl effector-regulating proliferation and transformation in chronic myeloid leukemia. *Cell death dis* **2010,** *1*, e93.
238. Shan, S. W*., et al.*, Comparative proteomic analysis identifies protein disulfide isomerase and peroxiredoxin 1 as new players involved in embryonic interdigital cell death. *Develop dynamics* **2005,** *233* (2), 266-81.
239. Shepherd, M. G*., et al.*, Germ tube induction in *Candida albicans. Can J Microbiol* **1980,** *26* (1), 21-26.
240. Shevchenko, A*., et al.*, Mass spectrometric sequencing of proteins silver-stained

polyacrylamide gels. *Anal.Chem.* **1996,** *68* (5), 850-858.
241. Shin, Y. K*., et al.*, Proteomic analysis of mammalian basic proteins by liquid-based two-dimensional column chromatography. *Proteomics* **2006,** *6* (4), 1143-50.
242. Slutsky, B*., et al.*, High frecuency switching of colony morphology in *Candida albicans. Science* **1985,** *230*, 666-669.
243. Sly, L. M*., et al.*, Survival of Mycobacterium tuberculosis in host macrophages involves resistance to apoptosis dependent upon induction of antiapoptotic Bcl-2 family member Mcl-1. *J Immunol* **2003,** *170* (1), 430-7.
244. Smith, R. D*., et al.*, New developments in biochemical mass spectrometry: electrospray ionization. *Anal chem* **1990,** *62* (9), 882-99.
245. Soares, R. M*., et al.*, Identification of sialic acids on the cell surface of *Candida albicans*. *Biochim Biophys Acta* **2000,** *1474* (2), 262-8.
246. Soll, D. R., Phenotypic switching. In *Candida* and Candidiasis. ASM Press, p. 123-42. . **2002**.
247. Spaccapelo, R*., et al.*, TGF-beta is important in determining the in vivo patterns of susceptibility or resistance in mice infected with *Candida albicans*. *J Immunol* **1995,** *155* (3), 1349-60.
248. Spolarics, Z., Endotoxemia, pentose cycle, and the oxidant/antioxidant balance in the hepatic sinusoid. *J leukoc biol* **1998,** *63* (5), 534-41.
249. Spolarics, Z., A carbohydrate-rich diet stimulates glucose-6-phosphate dehydrogenase expression in rat hepatic sinusoidal endothelial cells. *J nutrition* **1999,** *129* (1), 105-8.
250. Staab, J. F*., et al.*, Adhesive and mammalian transglutaminase substrate properties of *Candida albicans Hwp1*. *Science.* **1999,** *283* (5407), 1535-1538.
251. Stuehr, D. J.; Nathan, C. F., Nitric oxide. A macrophage product responsible for cytostasis and respiratory inhibition in tumor target cells. *J Exp Med* **1989,** *169* (5), 1543-1555.
252. Sun, G*., et al.*, *Mycoplasma pneumoniae* infection induces reactive oxygen species and DNA damage in A549 human lung carcinoma cells. *Infect Immun* **2008,** *76* (10), 4405-13.
253. Sundstrom, P., Adhesins in *Candida albicans*. *Curr Opin Microbiol* **1999,** *2* (4), 353-7.
254. Sundstrom, P., Adhesion in *Candida* spp. *Cell Microbiol* **2002,** *4* (8), 461-469.
255. Tada, H*., et al.*, *Saccharomyces cerevisiae*- and *Candida albicans*-derived mannan induced production of tumor necrosis factor alpha by human monocytes in a CD14- and Toll-like receptor 4-dependent manner. *Microbiol Immunol* **2002,** *46* (7), 503-12.
256. Takeda, K.; Akira, S., TLR signaling pathways. *Seminars Immunol* **2004,** *16* (1), 3-9.
257. Thingholm, T. E*., et al.*, SIMAC (sequential elution from IMAC), a phosphoproteomics strategy for the rapid separation of monophosphorylated from multiply phosphorylated peptides. *Mol Cel Proteomics* **2008,** *7* (4), 661-71.
258. Tonge, R*., et al.*, Validation and development of fluorescence two-dimensional differential gel electrophoresis proteomics technology. *Proteomics* **2001,** *1* (3), 377-396.
259. Toossi, Z*., et al.*, Induction of serine protease inhibitor 9 by *Mycobacterium tuberculosis* inhibits apoptosis and promotes survival of infected macrophages. *J Infect Dis* **2012,** *205* (1), 144-51.
260. Tortorano, A. M*., et al.*, Epidemiology of candidaemia in Europe: results of 28-month European Confederation of Medical Mycology (ECMM) hospital-based surveillance study. *Eur J Clin Microbiol Infect Dis* **2004,** *23* (4), 317-22.
261. Umazume, M*., et al.*, Reduced inhibition of *Candida albicans* adhesion by saliva from patients receiving oral cancer therapy. *J Clin Microbiol* **1995,** *33* (2), 432-439.
262. Underhill, D. M., Macrophage recognition of zymosan particles. *J endotoxin res* **2003,** *9* (3), 176-80.
263. Underhill, D. M.; Gantner, B., Integration of Toll-like receptor and phagocytic signaling for tailored immunity. *Microbes infection* **2004,** *6* (15), 1368-73.
264. Valledor, A. F*., et al.*, Transcription factors that regulate monocyte/macrophage differentiation *J Leukoc Biol.* **1998,** *63* (4), 405-417.
265. Van Der Graaf, C. A*., et al.*, Differential cytokine production and Toll-like receptor signaling pathways by *Candida albicans* blastoconidia and hyphae *Infect Immun* **2005,** *73* (11), 7458-7464.
266. Vazquez-Torres, A.; Balish, E., Macrophages in resistance to candidiasis. *Microbiol Mol Biol Rev* **1997,** *61* (2), 170-92.
267. Vázquez-Torres, A.; Balish, E., Macrophagues in resistance to candidiasis. *Microbiol Mol Biol Rev* **1997,** *61* (2), 170-192.
268. Vázquez-Torres, A*., et al.*, Nitric oxide production does not directly increase macrophage candidacidal activity. *Infect Immun* **1995,** *63*, 1142-1144.
269. Vejda, S*., et al.*, Autocrine secretion of osteopontin results in degradation of I kappa B in Bcr-Abl-expressing cells. *Br J Haematol* **2005,** *128* (5), 711-21.
270. Vento, M. T*., et al.*, Praf2 is a novel Bcl-xL/Bcl-2 interacting protein with the ability to

modulate survival of cancer cells. *PloS one* **2010,** *5* (12), e15636.
271. Veraldi, K. L*., et al.*, hnRNP F influences binding of a 64-kilodalton subunit of cleavage stimulation factor to mRNA precursors in mouse B cells. *Mol Cell Biol* **2001,** *21* (4), 1228-38.
272. Verreck, F. A*., et al.*, Human IL-23-producing type 1 macrophages promote but IL-10-producing type 2 macrophages subvert immunity to (myco)bacteria. *Proc Natl Acad Sci U S A* **2004,** *101* (13), 4560-5.
273. Villwock, A*., et al.*, Recognition via the class A scavenger receptor modulates cytokine secretion by human dendritic cells after contact with *Neisseria meningitidis*. *Microbes infection* **2008,** *10* (10-11), 1158-65.
274. Vonk, A. G*., et al.*, Host defence against disseminated *Candida albicans* infection and implications for antifungal immunotherapy. *Expert Opin Biol Ther* **2006,** *6* (9), 891-903.
275. Vudhichamnong, K*., et al.*, The effect of secretory immunoglobulin A on the in-vitro adherence of the yeast *Candida albicans* to human oral epithelial cells. *Arch Oral Biol* **1982,** *27* (8), 617-621.
276. Vylkova, S*., et al.*, Human beta-defensins kill *Candida albicans* in an energy-dependent and salt-sensitive manner without causing membrane disruption. *Antimicrob Agents Chemother* **2007,** *51* (1), 154-61.
277. Wai, P. Y.; Kuo, P. C., The role of Osteopontin in tumor metastasis. *J surgical res* **2004,** *121* (2), 228-41.
278. Wear, M. A*., et al.*, Actin dynamics: assembly and disassembly of actin networks. *Curr biol* **2000,** *10* (24), R891-5.
279. Weindl, G*., et al.*, Human epithelial cells establish direct antifungal defense through TLR4-mediated signaling. *J clin invest* **2007,** *117* (12), 3664-72.
280. Weis, W. I*., et al.*, The C-type lectin superfamily in the immune system. *Immunol Rev* **1998,** *163*, 19-34.
281. Wells, C. A*., et al.*, The macrophage-inducible C-type lectin, mincle, is an essential component of the innate immune response to *Candida albicans*. *J Immunol* **2008,** *180* (11), 7404-13.
282. West, A. P*., et al.*, TLR signalling augments macrophage bactericidal activity through mitochondrial ROS. *Nature* **2011,** *472* (7344), 476-80.
283. Whitehouse, C. M*., et al.*, Electrospray interface for liquid chromatographs and mass spectrometers. *Analytical chemistry* **1985,** *57* (3), 675-9.
284. Wilkins, A. S., Variation in the human genome. 12-15 June, 1995. CIBA Foundation symposium 197, London, UK. *Bioessays* **1995,** *17* (10), 905-6.
285. Wilkins, M. R*., et al.*, Proteome research: new frontiers in functional genomics. *Springer-Verlag, Berlin.* **1997**.
286. Williams, G. T., Programmed cell death: a fundamental protective response to pathogens. *Trends Microbiol* **1994,** *2* (12), 463-4.
287. Wisdom, R*., et al.*, c-Jun regulates cell cycle progression and apoptosis by distinct mechanisms. *EMBO J* **1999,** *18* (1), 188-97.
288. Wu, Z. Z.; Chao, C. C., Knockdown of NAPA using short-hairpin RNA sensitizes cancer cells to cisplatin: implications to overcome chemoresistance. *Biochem pharmacol* **2010**.
289. Yamakawa, N*., et al.*, The rasGAP-binding protein, Dok-1, mediates activin signaling via serine/threonine kinase receptors. *EMBO J* **2002,** *21* (7), 1684-94.
290. Zelante, T*., et al.*, IL-23 and the Th17 pathway promote inflammation and impair antifungal immune resistance. *Eur J Immunol* **2007,** *37* (10), 2695-706.
291. Zhang, X*., et al.*, Highly Efficient Phosphopeptide Enrichment by Calcium Phosphate Precipitation Combined with Subsequent IMAC Enrichment. *Mol Cel Proteomics* **2007,** *6* (11), 2032-42.
292. Zhu, W*., et al.*, Mass spectrometry-based label-free quantitative proteomics. *J Biomed biotechnol* **2010,** *2010*, 840518.

Anexo

RESEARCH ARTICLE

Proteomics of RAW 264.7 macrophages upon interaction with heat-inactivated *Candida albicans* cells unravel an anti-inflammatory response

Laura Martínez-Solano, Jose Antonio Reales-Calderón, César Nombela, Gloria Molero and Concha Gil

Departamento de Microbiología II, Facultad de Farmacia, Universidad Complutense de Madrid, Madrid, Spain

Murine macrophages (RAW 264.7) were allowed to interact with heat-inactivated cells of *Candida albicans* SC5314 during 45 min. The proteomic response of the macrophages was then analyzed using 2-D gel electrophoresis. Many proteins having differential expression with respect to control macrophages were identified, and their functions were related to important processes, such as cytoskeletal organization, signal transduction, metabolism, protein biosynthesis, stress response and protein fate. Several of these proteins have been described as being involved in the process of inflammation, such as Erp29, Hspa9a, AnxaI, Ran GTPase, P4hb, Clic1 and Psma1. The analysis of the consequences of their variation unravels an overall anti-inflammatory response of macrophages during the interaction with heat-inactivated cells. This result was corroborated by the measurement of TNF-α and of ERK1/2 phosphorylation levels. This anti-inflammatory effect was contrary to the one observed with live *C. albicans* cells, which induced higher TNF-α secretion and higher ERK1/2 phosphorylation levels with respect to control macrophages.

Received: January 8, 2008
Revised: February 6, 2009
Accepted: February 18, 2009

Keywords:
Candida / 2-D PAGE / Differential expression / Inflammation / Macrophages

1 Introduction

Candida albicans still remains an important causal agent of infection in immunodepressed patients [1], and the therapeutic arsenal is reduced and sometimes toxic [2, 3]. Thus, the study of host response to infections can be a useful tool to discover new therapeutic strategies. Among the players taking part in the fight against pathogens, macrophages are crucial elements of the innate and adaptive immunity to systemic candidiasis [4, 5]. The recognition of *C. albicans* by macrophages causes phagocytosis and the production of inflammatory mediators, toxic compounds such as ROS and reactive nitrogen species. Macrophages also capture and process foreign antigens for presentation to T cells, enabling host defence and immunological memory [6]. While macrophages display a wide variety of mechanisms to destroy the fungus, *C. albicans* attempts to survive the action of phagocytes by inhibiting the production of toxic compounds [7] or by preventing phagolysosome fusion [8–10] or modulating the pH of this compartment [10].

Differences in the macrophages response to either live, heat-inactivated (HI) cells or components from C. *albicans* [7, 11, 12] and from other pathogens [13] have been described. Comparison of the macrophage responses against live and inactivated cells of *C. albicans* can give us information about the effect of the pathogen on the host defences and, thus, about virulence factors. Therefore, in the present work, the response of RAW 264.7 cells to HI *C. albicans* SC5314 cells after 45 min of interaction has been studied, showing variations in many proteins whose functions are related to many important processes, such as: cytoskeletal organization, signal transduction, metabolism, protein

Correspondence: Dr. Gloria Molero, Departamento de Microbiología II, Facultad de Farmacia, Universidad Complutense de Madrid, Plaza de Ramón y Cajal s/n, 28040-Madrid, Spain
E-mail: gloros@farm.ucm.es
Fax: +34-1-3941745

Abbreviations: HI, heat-inactivated; **PDI,** protein disulfide isomerase; **PEM,** PIPES, EGTA, $MgCl_2$

biosynthesis, stress response, cellular fate, *etc.* The differences in protein expression have been compared with previous results obtained against live yeasts [14], unravelling contrary effects on the inflammatory response; HI cells induce an anti-inflammatory response while live cells induce a pro-inflammatory one. The proteomic results have been corroborated with TNF-α and ERK1/2 phosphorylation measurements.

2 Materials and methods

2.1 *C. albicans* strains

The *C. albicans* strain used in this study was SC5314 from a clinical isolate [15]. This strain was maintained on solid YED medium (1% D-glucose, 1% Difco yeast extract and 2% agar) and incubated at 30°C for at least 2 days.

To prepare HI yeasts, the cells were collected and resuspended in PBS and heated at 65°C for 2 h. Cells were then washed twice with PBS and resuspended in the same buffer. Inactivation was checked by the absence of growth when 200 μL of the yeast suspension was spread over YED agar plates and incubated at 37°C for 48 h.

For the measurement of TNF-α levels, *C. albicans* cells were inactivated in PBS at 100°C for 10 min or by treatment with 3.7% formaldehyde for 30 min on ice. Cells were then washed twice with PBS and resuspended in the same buffer. Inactivation was checked by the absence of growth when 200 μL of the yeast suspension were spread over YED agar plates and incubated at 37°C for 48 h.

2.2 Cell-line macrophages

2.2.1 Culture medium and reagents

RPMI 1640 medium, FBS, L-glutamine and antibiotics (penicillin–streptomycin) were obtained from GIBCO BRL (Grand Island, NY). Cell-line macrophages were resuspended in RPMI supplemented with glutamine (2 mM), antibiotics (penicillin 100 U/mL–streptomycin 100 μg/mL) and 10% HI FBS (complete medium). Murine TNF-α ELISA kit (Diaclone) for the determination of TNF-α was provided by Bioscience (San Diego, CA).

2.2.2 Macrophage cell line

The RAW 264.7 gamma NO(−) cell line was obtained from the American Type Culture Collection (Rockville, MD). Cells were grown in complete medium in a 5% CO_2 incubator at 37°C and maintained at low densities (75% confluence) and passaged until they reached the confluent state, usually every 3–4 days on sterile culture plates.

2.2.3 Preparation of cytosolic extracts

Cytosolic extracts were prepared as previously described [14]. Three different cytoplasmic extracts were used: murine macrophages (cell line RAW 264.7), macrophages after 45 min of interaction with live *C. albicans* SC5314 (1:1) [14] and macrophages after 45 min of interaction with HI *C. albicans* SC5314 (1:100). After this time, macrophages (20×10^6) were washed with ice-cold PBS to remove yeasts, scraped off the dishes and collected by centrifugation. The cell pellets were homogenized in 1 mL of buffer A (10 mM HEPES, pH 7.9, 1 mM EDTA, 1 mM EGTA, 100 mM KCl, 1 mM DTT, 0.5 mM PMSF, 2 μg/mL aprotinin, 10 μg/mL leupeptin, 2 μg/mL TLCK, 5 mM NaF, 1 mM $NaVO_4$ and 10 mM Na_2MoO_4). After 15 min at 4°C, Nonidet P-40 was added (0.5% v/v), and the tubes were vortexed (15 s) and centrifuged at $8000 \times g$ for 20 min. The supernatants were stored at −80°C. The protein concentration was determined using the 2D-Quant Kit™ (GE Healthcare).

2.3 *C. albicans* – macrophages interaction assays

2.3.1 Phagocytosis quantification

For the quantification of internalized yeasts, 5×10^5 RAW 264.7 macrophages were plated onto 18-mm coverslips placed in 24-well multiwell plates for 24 h at 37°C in a 5% atmosphere. HI and live *C. albicans* were stained with Oregon green at 30°C and shaken for 1 h, washed with PBS-100 mM glycine and resuspended in PBS at a cell density of 5×10^8 cells/mL (HI) or 5×10^6 cells/mL (live). Macrophages were then allowed to interact with 5×10^5 live yeasts or 5×10^7 HI yeasts for 45 min at 37°C in a 5% CO_2 atmosphere. After the interaction, the wells were washed once with PBS at 4°C. The cells were fixed with 4% paraformaldehyde in PBS for 1 h and yeasts were stained with 2.5 μM calcofluor white for 15 min. Then, cells were washed twice with PBS 100 mM glycine and 40 mM glycine and the coverslips were mounted in glass slides using mounting medium. Digital images were captured using an Axioplan Imaging Microscope (Carl Zeiss AG, Germany) [16].

2.3.2 Immunofluorescence assay

2×10^5 RAW 264.7 macrophages were plated onto 18-mm coverslips placed in 24-well multiwell plates for 24 h at 37°C in a 5% atmosphere, washed twice with culture medium without serum, and then treated with 2×10^5 live yeasts or 2×10^7 HI yeasts for 45 min. The coverslips were washed with PEM (100 mM PIPES, 1 mM EGTA and 1 mM $MgCl_2$, pH 6.8) containing 4% PEG 8000 (Sigma), permeabilized for 90 s with PEM containing 0.5% Triton X-100, washed again with PEM–polyethylene glycol, and the coverslip-attached cytoskeletons were fixed with 3.7% formaldehyde

in PEM–PEG–l% DMSO for 30 min at 4°C. The coverslips were placed into a humidified container at 37°C, overlaid with 2 μg/mL affinity-purified anti-tubulin antibody in PBS containing 10 mg/mL BSA and incubated for 1 h. After two washes with PBS and gentle agitation (10 min), the coverslips were overlaid with fluoresceinated anti-rat antibody together with phalloidine–rhodamine (Molecular Probes, diluted 1:20), incubated for 45 min, washed with PBS in the dark and mounted in an anti-fading solution with 4′,6-diamidino-2-phenylindole. Digital images were captured using an Axioplan Imaging Microscope (Carl Zeiss AG) [17].

2.3.3 TNF-α measurement

RAW 264.7 cells (1×10^6 cells/mL *per* well) were exposed to 1×10^6 viable cells or to 1×10^8 HI, formalin inactivated or heated at 100°C cells of *C. albicans* SC5314. Supernatants were collected at 45 min and 3 h to determine TNF-α levels. The amount of TNF-α was determined with the mouse TNF-α ELISA kit, according to the manufacturer's instructions. Diaclone ELISA kits used for the determination of TNF-α were provided by Bioscience.

Data were expressed as mean ± SD. The unpaired Student's *t*-test was used to compare differences between groups and $p < 0.05$ was considered significant.

2.3.4 ERK1/2 phosphorylation detection

RAW 264.7 cells (1×10^6 cells/mL *per* well) were exposed to 1×10^6 viable cells or to 1×10^8 HI cells of *C. albicans* SC5314. Murine macrophages were washed with ice-cold PBS to remove yeasts. Then, macrophages were scraped off the dishes and collected by centrifugation (1000 rpm, 10 min). Cell pellets were homogenized in buffer A (7 M urea, 2 M thiourea, 2% CHAPS, 5 mM $Na_2H_2P_2O_7$, 50 mM NaF, 10 mM $C_3H_7Na_2OP$, 1 mM Na_3VO_4 and protease inhibitor cocktail (Complete Mini, EDTA-free; Roche)). After 15 min at 4°C, they were centrifuged at 8000*g* for 20 min. The supernatants were stored at −80°C. Protein was determined using the RC and DC assay (Reducing agent Compatible and Detergent Compatible Protein assay; Bio-Rad). 50μg of protein *per* well were separated onto 10% SDS-polyacrylamide minigels and transferred to Hybond-ECL Nitrocellulose membranes (Amersham Biosciences). The Western blot was performed with Odyssey system (LI-COR Biosciences, NE), which allows the measurement of the relative levels of fluorescence of the different bands and simultaneous labelling with two different antibodies. After 1 h of incubation with primary antibodies: 1/2000 p44/42 MAP Kinase (3A7) mouse mAb (Cell Signalling Technology) and 1/2000 phospho-p44/42 MAP Kinase (Thr 202/Tyr 204) Ab (Cell Signalling Technology), the membranes were washed four times in PBS+0.1% Tween-20. Then, the membranes were incubated with fluorescently labelled secondary antibodies: 1/4000 IRDye 800CW conjugated goat (polyclonal) anti-rabbit IgG, highly cross absorbed (LI-COR Biosciences) and 1/4000 IRDye 680 conjugated goat (polyclonal) anti-mouse IgG, highly cross absorbed (LI-COR Biosciences) for 30–60 min at room temperature and protected from light. The membranes were washed again and scanned for fluorescence detection with Odyssey system (LI-COR Biosciences). In our case, phospho-ERK1/2 and ERK1/2 were detected and measured in the same membrane.

Data were expressed as mean ± SD. The unpaired Student's *t*-test was used to compare differences between groups and $p < 0.05$ was considered significant.

2.4 Analytical and micropreparative 2-D PAGE

2-DE was performed as previously reported, with some modifications [18]. Cytoplasmic extracts (200 μg of protein) were loaded for analytical gels and 1 mg for micropreparative gels. A modification in the sample preparation [19] was made to improve resolution of the 2-DE map of acquired proteins. Thus, supernatants obtained after the lysis were washed twice with ice-cold water and concentrated by ultrafiltration using a pore size of 10 000 Da (Amicon®, Ultra, Millipore) at 4°C prior to separation by 2-D PAGE. Following extraction, interfering components were removed by using the 2D-Clean Kit™ (GE Healthcare). The protein were resuspended in 100 mM Tris, 8 M urea, 2 M thiourea and 4% CHAPS. The first dimension was carried out on the Ettan-IPGphor® Isoelectric focusing unit (GE Healthcare) at 15°C using the following programs: 500 V for 1 h, 500–2000 V for 1 h and 8000 V for 6.5 h and 30 V for 7 h, 60 V for 7 h, 500 V for 1 h, 1000 V for 1 h, 2000 V for 1 h, 2000–5000 V for 3 h and 8000 V for 11 h, for analytical and micro preparative gels, respectively. IPG strips providing a non-linear pH 3–10 gradient (18 cm long, GE Healthcare) were used [20]. After equilibration of strips, the second dimension separation by molecular weight was carried out on homogeneous 10% T polyacrylamide gels using piperazine diacrylamide as a cross-linker. Electrophoresis was conducted at 17 W/gel constant current for 6 h in an Ettan-Dalt Six (GE Healthcare). Analytical gels were SYPRO Ruby stained according to the manufacturer's procedure and preparative gels were silver-stained as described by Shevchenko [21].

2.5 Image acquisition and data analysis

SYPRO Ruby-stained gels were digitalized using a Typhoon 9400 and analyzed with the ImageMaster 2D-Platinum computer software (GE Healthcare).

Using ImageMaster 2D-Platinum tools, protein spots were enumerated, quantified and characterized with respect to their molecular mass and isoelectric point using bilinear

interpolation between landmark features on each image previously calibrated with respect to internal 2-DE standards (GE Healthcare).

2.6 MS analysis of protein spots

The gel spots of interest were manually excised from micro preparative gels using biopsy punches. The proteins selected for the analysis were in-gel reduced, alkylated and digested with trypsin, according to Sechi and Chait [22]. Briefly, spots were washed twice with water, shrunk for 15 min with 100% ACN and dried in a Savant SpeedVac for 30 min. Then, the samples were reduced with 10 mM dithioerytritol in 25 mM ammonium bicarbonate for 30 min at 56°C and subsequently alkylated with 55 mM iodoacetamide in 25 mM ammonium bicarbonate for 20 min in the dark. Finally, samples were digested with 12.5 ng/μL sequencing grade trypsin (Roche Molecular Biochemicals) in 25 mM ammonium bicarbonate (pH 8.5) for at least 6 h at 37°C.

After digestion, the supernatant was collected and 1 μL was spotted onto a MALDI target plate (96 × 2 spot teflon®-coated plates) and allowed to air-dry for 10 min at room temperature. Then, 0.4 μL of a 3 mg/mL of CHCA matrix (Sigma) in 50% ACN was added to the dried peptide digest spots and allowed to air-dry again for another 10 min at room temperature. MALDI-TOF MS analyses were performed in a Voyager-DETM STR instrument (PerSeptives Biosystems), a model fitted with a 337 nm nitrogen laser and operated in reflector mode (it accumulates 150 spectra of single laser shots under threshold irradiance) with an accelerating voltage of 20 000 V. All mass spectra were calibrated externally using a standard peptide mixture: angiotensin I (1296.7), adenocorticotropic hormone fragment 18–39 (2465.2) and 1–17 (2093.1) (Sigma). Peptides from the auto digestion of trypsin were used for the internal calibration. The analysis by MALDI-TOF MS produces peptide mass fingerprints and the peptides observed can be collated and represented as a list of monoisotopic molecular weights.

MS/MS sequencing analyses were carried out using the MALDI-tandem time-of-flight mass spectrometer 4700 Proteomics Analyser (Applied Biosystems, Framingham, MA).

2.7 Database searches

Database searches for the identification of protein spots were carried out submitting the monoisotopic peptide masses assigned to the followed software available on-line: MS-Fit (http://prospector.ucsf.edu), ProFound (http://129.85.19.192/prowl-cgi/ProFound.exe) and Mascot (http://www.matrixscience.com). Databases Swiss-Prot, TrEMBL and Human PSD GPCR-PD were consulted.

The parameters used for the search were as follows: modifications were considered (Cys as an *S*-carboamidomethyl derivative and Met as oxidized methionine), allowing for one missed cleavage site; a restriction was placed on its p*I* (3–10) and a protein mass range from 10 to 100 kDa was accepted. Positive identifications were accepted when at least five matching peptides massed, and at least 20% of the peptide coverage of the theoretical sequences matched within a mass accuracy of 50 or 25 ppm with internal calibration. Peptides were excluded if their masses corresponded to those for trypsin, human keratins or other irrelevant proteins.

3 Results

3.1 Macrophages – *C. albicans* interaction

HI *C. albicans* SC5314 cells, previously stained with Oregon green, were allowed to interact with RAW 264.7 cells for 45 min. Then, the cells were fixed and yeasts outside the macrophages were stained with calcofluor white. The percentage of yeasts inside macrophages (yeasts only stained with Oregon green) was determined by counting at least 25 fields of vision *per* sample. After 45 min of interaction, the percentage of HI *C. albicans* cells phagocytosed by macrophages was about 41% (data not shown), while for viable *C. albicans* cells it was 32% [14].

RAW 264.7 cells exposed either to live or HI C. *albicans* cells for 45 min were stained to visualize α-tubulin and F-actin. As can be observed in Fig. 1, F-actin is polarized at the surface of the macrophages, engulfing the live *C. albicans* cells, but this

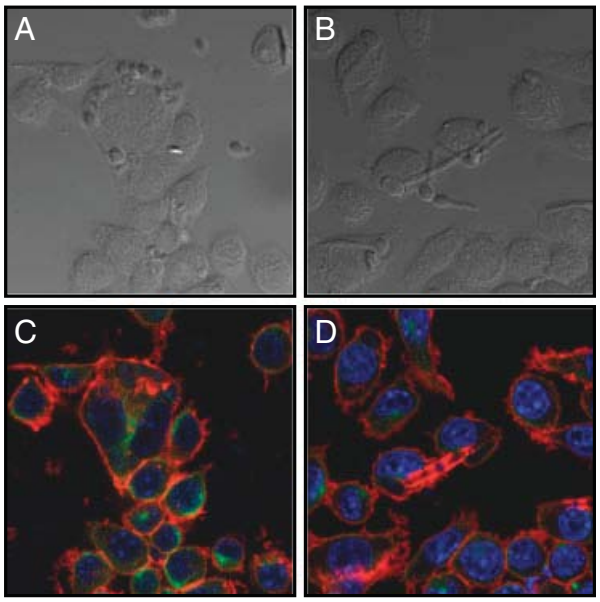

Figure 1. RAW 264.7 cells after 45 min of interaction with HI (A and C) and live *C. albicans* SC5314 cells (B and D). (A and B) Phase contrast micrographs, magnification × 66. (C and D) Immunofluorescence microscopy of the same field. Macrophage microtubules appear in green, actin filaments in red and nuclei in blue.

was not observed around the engulfed ones. In the case of the HI cells, the F-actin was polarized at the surface and around the engulfed cells.

3.2 Study of the macrophage differential protein expression upon interaction with HI *C. albicans*

The protein extracts from RAW 264.7 cells and RAW 264.7 cells+HI *C. albicans* SC5314 were subjected to a comparative analysis using ImageMaster 2D-Platinum computer software (Fig. 2). Cytoplasmic extracts were prepared in triplicate and three different 2-D gels from each single preparation were analyzed. After automated spot detection, spots were manually checked to eliminate any possible artifacts such as background noise or streaks. The patterns of each sample were overlapped and matched, using the selection of 30 common spots present in both images as landmarks, to detect potential differential or identify specific proteins. Spot normalization, as a kind of internal calibration that makes the

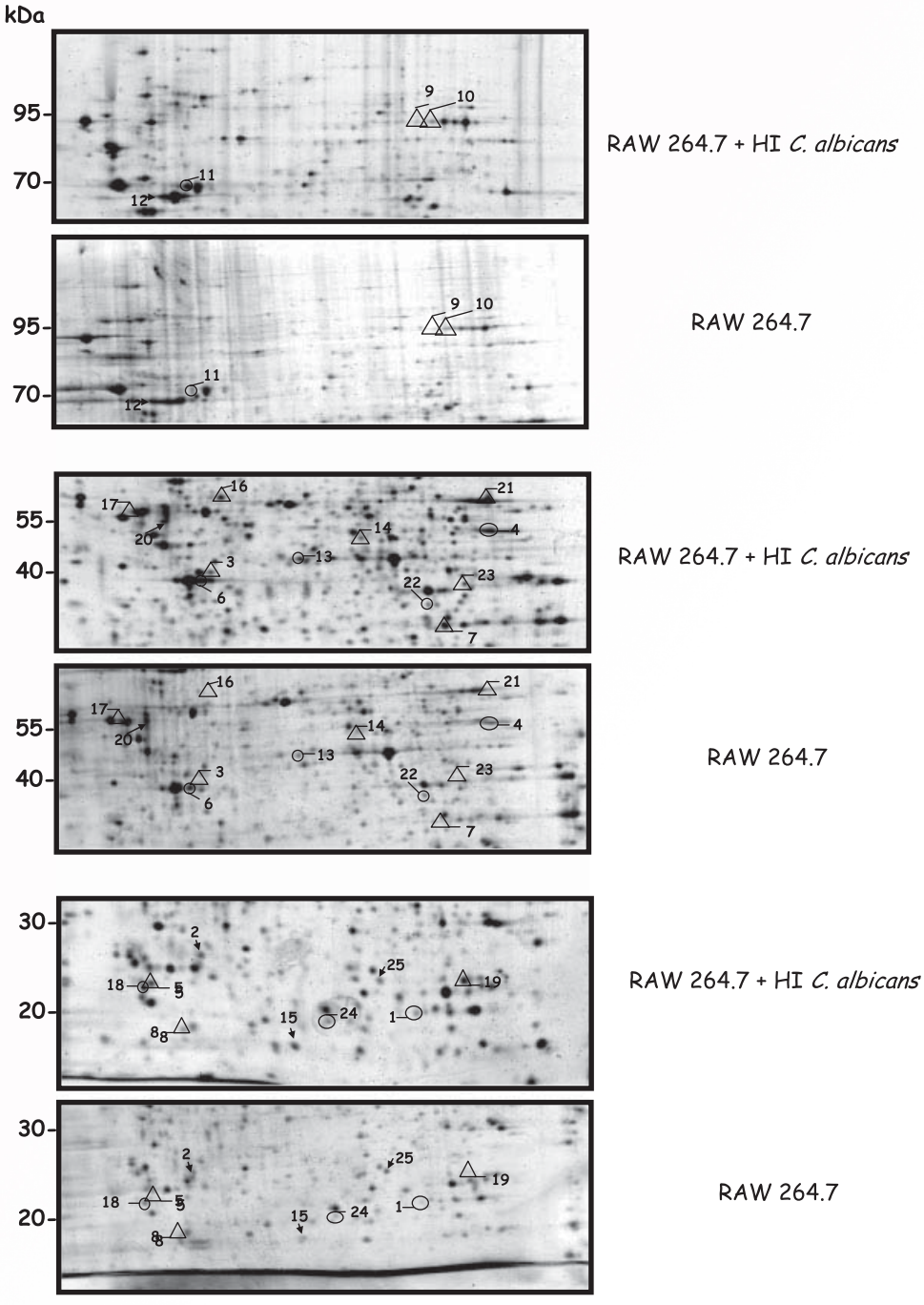

Figure 2. 2-DE gels of cytoplasmic extracts from RAW 264.7 after 45 min of interaction with HI *C. albicans* SC5314 and control RAW 264.7 cells. Only gel areas where differences were found are shown. Numbers indicate the proteins identified and are shown in Table 1.

Table 1. List of proteins identified from cytoplasmic extracts of RAW 264.7 cells that varied their expression level after 45 min of interaction with HI *C. albicans* cells

Name[a]	Function	M_r (kDa)[b]	pI[b]	No. of peptide matched[c]	% of coverage[d]	Accession number[a]	Ratio (%volume)[f]
Morphogenesis							
Tropomyosin γ (Tpm5) (5)[g]	Binding to actin filaments. Cell motility	29.2	4.75	7	25	P21107	*(0.30)
β-Actin (Actb) (6)[g]	Organization and biogenesis of actin cytoskeleton	39.4	5.78	23	65	P60710	+1.52
Vimentin, fragment (Vim) (20)[g]	Class-III intermediate filament. Structural component of cytoskeleton	53.5	5.06	11	28	P48670	−2.10
Capping protein (Capg) (22)	Binding to actin filaments. Cell motility	39	6.47	10	34	Q99LB4	+1.59
Signal transduction							
Annexin A1 (Anxa1) (7)[g]	Calcium/phospholipid-binding protein. Putative inhibitor of phospholipase A2	38.8	7.15	12	36	P10107	*(0.45)
Rho GDP-dissociation inhibitor 2 (Ly-GDI)(Gdid4)[e] (8)	GDP dissociation inhibition. Superoxide metabolism. Immune response	22.9	4.97	CS[h]		Q61599	*(0.23)
Ran GTPase (Ran) (19)[g]	GTPase. GTP-binding protein involved in nucleocyto-plasmic transport	24.4	7.32	8	30	P62827	*(0.23)
Protein kinase C inhibitor protein 1 (KCIP-1, 14-3-3Z) (18)[g]	Signal transduction upon GTPase activity. Antiapoptosis	27.7	4.59	16	57	P63101	+1.60
Metabolism							
Glycolysis and gluconeogenesis							
Triosephosphate isomerase (Tpi) (1)[g]	Triosephosphate isomerase	26.9	7.19	9	30	P17751	+1.74
α-Enolase (Eno1) (13)[g]	2-Phospho-D-glycerate hydrolyase	47.3	6.36	5	22	P17182	+1.63
Pyruvate kinase isozyme M2 (Pkm2) (21)[g]	Pyruvate kinase	57.8	7.42	22	50	P52480	*(0.92)
Fatty acid metabolism							
3-Oxoacid CoA transferase (Oxct1)[e] (4)[g]	CoA transferase activity	56	8.82	MS/MS		Q9DOK2	+1.62
Nucleotide metabolism							
Adenylosuccinate synthetase2 (Adss2) (14)[g]	Nucleotide biosynthesis	50	6.17	6	21	P46664	*(0.13)
Tricarboxylic acid cycle							
Isocitrate dehydrogenase (Idh1)[e] (23)[g]	NADP biosynthesis. Isocitrate metabolism	46.7	6.99	MS/MS		O88844	(0.13)
Electron transport							
Prolyl 4-hydroxylase subunit beta (P4hb) (17)[g]	Electron transport. Procollagen-prolyl 4-hydroxylase. PDI	57.4	4.77	18	33	P09103	*(0.52)
Protein biosynthesis							
Eukaryotic initiation factor 4A-I (Eif4a1) (3)[g]	ATP-dependent RNA helicase. mRNA binding to ribosome. Translation initiation	46.1	5.36	6	21	P60843	*(0.16)
Elongation factor 2 (Eef-2) (9 and 10)[g]	Protein biosynthesis	96	6.42	20	23	P58252	*(0.13)
							*(0.10)
Protein fate							
Protein folding							
Heat shock 70 kDa protein 9B (Hspa9a) (11)[g]	Chaperone involved in the control of cell proliferation and cellular aging	73.7	5.81	29	41	P38647	+1.70

Table 1. Continued

Name[a]	Function	M_r (kDa)[b]	p*I* [b]	No. of peptide matched[c]	% of coverage[d]	Accession number[a]	Ratio (%volume)[f]
Heat shock cognate 71 kDa protein (Hsc70) (12)[g]	Chaperone. Translocates rapidly from the cytoplasm to the nucleus upon stress	71	5.28	30	39	P63017	−1.66
T-complex protein 1 subunit theta (Cctq) (16)[g]	Molecular chaperone; assist the folding of proteins upon ATP hydrolysis. Binds to transcription factors	59.5	5.63	8	14	P42932	*(0.19)
Endoplasmic reticulum protein Erp29, precursor (Erp29)[e] (24)[g]	Processing of secretory proteins within the endoplasmic reticulum (ER). Folding of proteins in the ER	28.8	5.90	MS/MS		P57759	+1.33
Protein degradation							
Proteasome subunit α type-1 (Psma1)[e] (25)[g]	Proteolysis and peptidolysis	29.8	6.22	MS/MS		Q9R1P4	−1.30
Iron homeostasis							
Ferritin light chain 1 (Ftl1) (15)[g]	Iron intracellular storage	20.7	5.78	14	64	P29391	−1.62
Others							
Chloride intracellular channel1 (Clic1) (2)[g]	Chloride channel. Chloride transport	27	4.98	7	48	Q9Z1Q5	−1.59

a) Protein name and accession number according to Human PSD & GPCR-PD human, mouse and rat database (Mouse Protein Report with PSD Interactions) of Proteome Bioknowledge Library (https://www.proteome.com/control/tools/proteome).
b) Experimental molecular mass and p*I*.
c) Number of peptide masses matching the top hit from MASCOT peptide mass fingerprinting.
d) Amino acid sequence coverage for the identified proteins.
e) Proteins analyzed by tandem mass spectrometry using an MALDI-TOF/TOF mass spectrometer.
f) Ratios indicate differentially expressed proteins. The ratio of up-regulated proteins is positive and the one from down-regulated proteins is negative. ∗ Proteins that appear. In brackets, the percentage of volume assigned by ImageMaster 2D Platinum to the proteins that appear after the interaction.
g) The number in brackets refers to the number of the spot in Fig. 2.
h) Proteins analyzed by combined search (peptide mass fingerprinting+ion fragmentation).

data independent of experimental variations between gels, was carried out by using a relative volume (%Vol) to quantify and compare the gel spots; relative volume corresponding to the volume of each spot divided by the total volume of all the spots in the gel. Reproducibility of the gels in each condition was confirmed by statistical analysis (Supporting Information). The analysis was done on a representative number of spots from each condition, for which median and standard deviation of the relative volume (%Vol) have been calculated. The normalized volume of each protein spot in one sample was compared with its counterpart in another sample to determine whether the ratio indicated a statistically significant difference occurring during the macrophages–HI *C. albicans* interaction. Protein spots from the macrophages+*C. albicans* samples with a ratio greater than +1.3 or lower than −1.3 were considered to be up- or down-regulated, respectively, in comparison with control macrophages (Table 1). Nineteen protein spots were up-regulated, whereas 37 were down-regulated. Interestingly, over 100 spots appeared and 70 disappeared after this interaction. The condition of appearing or disappearing indicates a variation in the spot intensity, which was greater than the sensitivity level of the SYPRO Ruby staining.

We have identified 24 of these differentially expressed proteins by MS or by MS/MS using a MALDI-TOF/TOF work station. These proteins are indicated in Table 1 together with their corresponding ratio of increase or decrease.

3.3 TNF-α measurement

RAW 264.7 cells were allowed to interact with live or HI *C. albicans* SC5314 cells for 45 min and 3 h. Then, TNF-α released by macrophages was measured in the supernatants. The macrophages without interaction were used as the control group.

The amount of TNF-α released by macrophages interacting with viable cells was greater than the control, increasing throughout the incubation time (Fig. 3). On the contrary, the interaction with HI cells induced levels of TNF-α similar to or even lower than the control.

The cytokine levels were also measured upon interaction with *C. albicans* cells inactivated either with formaldehyde or by heating at 100°C for 10 min, showing similar levels to the case of live cells.

3.4 ERK activation measurement

Figure 4 shows the relative intensity levels of phospho-ERK1/2 with respect to ERK1/2 from RAW 264.7 cells after the interaction with live or HI *C. albicans* SC5314 cells for 45 min and 3 h. The macrophages without interaction were used as the control group. As can be observed, the relative intensity of the bands is similar for the three conditions: control macrophages, exposed to either live or HI cells at 45 min of interaction. But, when the interaction time was

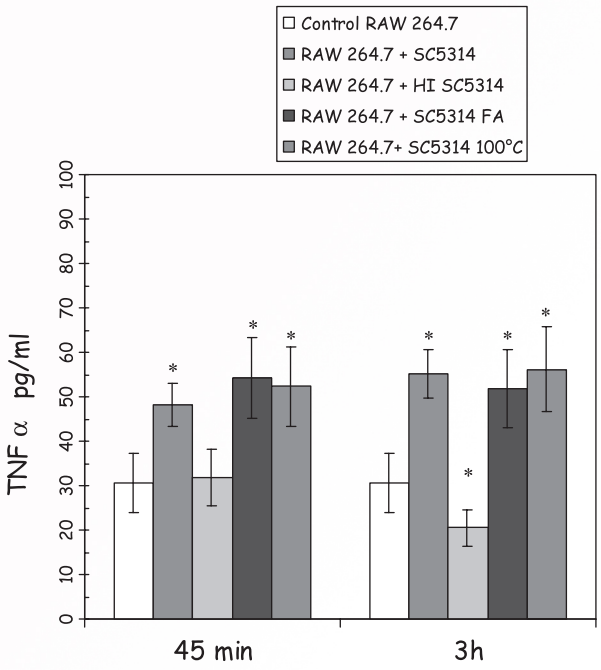

Figure 3. TNF-α levels secreted by RAW 264.7 cells upon interaction for 45 min and for 3 h with live or inactivated *C. albicans* SC5314 cells with respect to control RAW 264.7 cells. Bars show the means ± SD of TNF-α levels from four biological replicates and three different measurements. Statistically significant differences ($p < 0.05$) are marked with an asterisk. HI: *C. albicans* cells inactivated at 65°C for 2 h; FA: *C. albicans* cells inactivated with 3.7% formaldehyde for 30 min on ice; 100°C: *C. albicans* cells inactivated at 100°C for 10 min.

increased to 3 h, *C. albicans* live cells induced higher levels of phosphorylation, in line with TNF-α levels. Western blot experiments were performed with four different biological replicates.

4 Discussion

RAW 264.7 cells were allowed to interact with HI *C. albicans* SC5314 cells for 45 min. At this interaction time, 41% of the cells had been internalized by macrophages (Fig. 1A and C). As can be observed, there is a mixture of stimuli: cells inside and outside macrophages, as in the case of live cells (32% of phagocytosis) (Fig. 1B and D) [14]. When the differential protein expression of macrophages interacting with HI cells was analyzed, a large number of spots (Fig. 2) varied in intensity. The proteins identified (Table 1) are involved in cytoskeletal organization, signal transduction, metabolism, protein biosynthesis, stress response and protein fate. Some of the differences in protein expression were common to those detected during interaction with *C. albicans* live cells [14] and others were exclusive to each condition. Several of the proteins identified have been described by other authors as being involved in processes such as inflammation, morphogenesis, oxidative burst,

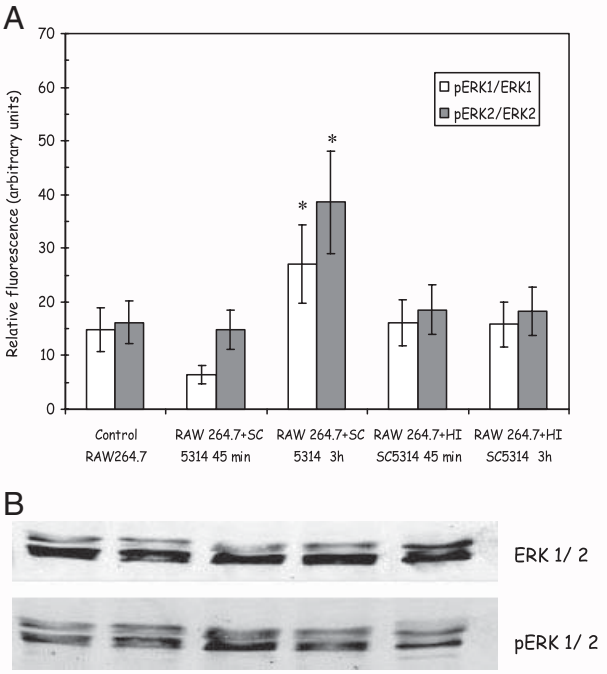

Figure 4. ERK1/2 phosphorylation in RAW 264.7 macrophages upon interaction for 45 min and for 3 h with live or HI *C. albicans* SC5314 cells with respect to control macrophages. (A) Bars show the means ± SD of the relative fluorescence intensity levels from the phosphorylated band with respect to the non-phosphorylated ones from four different biological replicates. Statistically significant differences ($p < 0.05$) are marked with an asterisk. (B) Representative Western blotting of the phosphorylated ERK1/2 bands and the corresponding non-phosphorylated ones at the different conditions assayed.

apoptosis and metabolism. In Table 2 we have summarized the proteins from macrophages that showed differential expression either with live or HI cells, classifying them according both to the already published effects of these proteins on mammalian cells and our hypothesis of their possible effect during their interaction with the *C. albicans*.

4.1 Inflammatory response

Mammalian cells respond to different types of stresses such as chemical, environmental and physiological, with the synthesis of HSPs [23, 24]. Several research groups [25–31] have shown that HS response inhibits the expression of iNOS, COX-2 and TNF-α through inhibition of IκB/NFκB degradation: it inhibits IL-12 production and increases the secretion of IL-10 by peritoneal macrophages, suggesting that not only does it inhibit pro-inflammatory genes, but it also promotes anti-inflammatory ones [32]. In our experimental model, Erp29 and Hspa9a showed increased expression with HI *C. albicans* cells, while Hspa9a and Hspd1 decreased with live *C. albicans* cells. This differential expression might point to an anti-inflammatory response upon interaction with HI cells while it may indicate a pro-inflammatory one with live cells. Only one HSP increased in response to live *C. albicans* cells, Grp78 (Hspa5) [14], whose expression is suppressed when attenuating the myocardial oxidative stress and inflammatory process [33], thus, its increased expression in response to live yeasts could be part of the candidacidal response of macrophages.

Other proteins besides the HSPs whose increase might contribute to the anti-inflammatory effect are AnnexinI (LCP) (both), Ran GTPase and P4hb (HI only). Ran is a GTPase involved in the response to LPS [34], and, subsequently, in the production of inflammatory cytokines. A high level of over expression of Ran in both macrophages and B cells down-regulates LPS signal transduction [35]. P4hb functions as a protein disulfide isomerase (PDI) [36], in the same way as Erp29 [37]. The transcriptional activity of NF-κB is negatively regulated by PDI (Table 2).

Proteins whose decrease during the interaction with HI cells might be contributing to the anti-inflammatory effect are Psma1p, a proteasome protein, and Clic1p, which exhibits both nuclear and plasma membrane chloride channel activity in a human myelomonocytic cell line (U937) [38]. In both cases, its decreased expression has induced anti-inflammatory response (Table 2).

On analyzing the proteins involved in metabolism, the differences seem to point to higher metabolic activity against HI cells, while this was not induced against live *C. albicans* cells (Table 2). This subject requires further investigation concerning the macrophage requirements under the phagocytic process.

Studies on macrophages polarization to the classical or the alternative activation have revealed that the alternative phenotype is accompanied by an up-regulation of genes related to lipid metabolism, specially those involved in fatty acid uptake and oxidation, whose increase is associated with an enhanced supply and use of fatty acids for energy homeostasis by alternatively activated macrophages (reviewed in [39]). Vats *et al.* [40] have revealed an induction of metabolic pathways for fatty acid uptake and oxidation, and this oxidative metabolism attenuates macrophage-mediated inflammation.

As can be deduced, many of the RAW 264.7 proteins that varied their expression when interacting with HI *C. albicans* cells have a possible anti-inflammatory effect, and a mixture of effects was observed upon interaction with live cells. To verify if our hypothesis based on the variations in protein levels was actually taking place, the levels of TNF-α were measured after 45 min and 3 h of interaction with live or HI *C. albicans* cells. TNF-α levels increased in the presence of *C. albicans* live cells while in the presence of HI cells this was not observed (Fig. 3). Thus, the variations in protein expression detected in RAW 264.7 induced, at 45 min of incubation, an overall pro-inflammatory response with live cells and a general anti-inflammatory response with HI *Candida* cells. The inflammatory effect induced by live *C. albicans* cells can be a virulence factor, which is responsible

Table 2. Summary of RAW 264.7 differentially expressed proteins and their putative effect during the interaction with live or HI *C. albicans* cells

Protein[a)]	Accession number[a)]	Ratio Mϕ+ live/control Mϕ[b)] [14]	Ratio Mϕ+HI/ control Mϕ[b)]	Described effects	Hypothetic effect during the interaction with *C. albicans*
Inflammation					
Endoplasmic reticulum protein Erp29, precursor (Erp29)	P57759	1	+1.33	Chaperone and PDI functions [37]	Anti-inflammatory effect with HI
Heat shock 70 kDa protein 9B (Hspa9a)	P38647	−1.59	+1.70	Is one of the HSPs that decrease in cells from gastric mucose during *Helicobacter pylori* infection. Its restoration (together with Hsp70 and others) decreases the inflammatory reaction and inhibits iNOS expression [30]	Decrease with live (pro-inflammatory) and increase with HI cells (anti-inflammatory)
Heat shock 60 kDa protein (Hspd1)	P19226	−1.64	1	It has been described as an essential protein in macrophage protection against *Plasmodium yoelii* [51] and *Toxoplasma gondii* [52] infections.	
				Its decrease has also been described in a proteomic study of ulcerative colitis (a chronic inflammatory disorder) [53]	Inflammatory effect with live cells
Heat shock 70 kDa protein 5 (Hspa5) (Grp78, BiP)	P20029	*	1	Its expression is suppressed by CeO_2 nanoparticles when attenuating the myocardial oxidative stress and inflammatory process [33]	
Annexin A1 (Anxa1)	P10107	*	*	Target for glucocorticoid anti-inflammatory drugs, inhibiting the effect of enzymes like iNOS synthase [54, 55] and critical to control experimental endotoxemia [56, 57]	Anti-inflammatory effect
GTP-binding nuclear protein (Ran)	P62827	+1.54	*	High level of over expression of Ran in both macrophages and B cells down-regulates LPS signal transduction [35]	
Prolyl 4-hydroxylase subunit β (P4hb) PDI	P09103	1	*	Over expression of PDI in RAW 264.7 cells strongly suppressed the LPS-induced production of inflammatory cytokines as well as NF-κB dependent luciferase activity [58]	
Chloride intracellular channel 1 (Clic1)	Q9Z1Q5	1	−1.59	Its inactivation inhibits the production of proinflammatory (TNF-α) and neurotoxic products elaborated by Aβ-stimulated microglial cells [59]	Anti-inflammatory effect with HI cells
Proteasome type 1 subunit alpha (Psma1)	Q9R1P4	1	−1.30	Inhibition of the proteasome in LPS treated macrophages results in a completely blocked LPS-induced expression of multiple inflammatory mediator genes [60]	Anti-inflammatory effect with HI cells
3-Oxoacid CoA transferase (Oxct1)	Q9DOK2	1	+1.62	Increases in the fatty acids metabolism attenuate macrophage-mediated inflammation [40]	

ANEXO

Table 2. Continued

Protein[a)]	Accession number[a)]	Ratio Mϕ+ live/control Mϕ[b)] [14]	Ratio Mϕ+HI/ control Mϕ[b)]	Described effects	Hypothetic effect during the interaction with *C. albicans*
Morphogenesis					
Tropomyosin γ (Tpm5)	P21107	*	*	Binds to actin filaments and prevents them from being depolymerized or severed by cofilin [61, 62]	Increase in the stability of actin filaments
Capping protein (Capg)	Q99LB4	1	+1.59	Barbed-end actin capping protein [63, 64]. Regulation of phagocytosis, ruffling, vesicle rocketing and cell motility, reducing its deletion by 50% the phagocytic capacity of macrophages [65] High-level transient overexpression in NIH3T3 cells [66] decreased actin filament staining in the center of the cells but not in the cell periphery	Decrease in actin filament staining in the centre of the cells but not in the cell periphery (Fig. 1C and D)
β-Actin (Actb)	P60710	1	+1.52	Increases in RAW 264.7 cells infected with *Mycobacterium avium* subsp. *paratuberculosis* [67]	Increase during the interaction with HI cells. Response to infection by intracellular microorganisms
T-complex protein 1 subunit theta (Cctq)	P42932	1	*	One of the eight subunits of the eukaryotic type II chaperonin containing TCP-1 (CCT), which has been involved in the production of native tubulins and actins [68]. Necessary for the response against arsenite [69]	Increase in native actin and tubulin in response to HI cells
L-Plastin (Lcp1)	Q61233	+1.62	1	Cytoskeletal protein signalling to NADPH oxidase [70]	
Oxidative burst					
Rho GDP-dissociation inhibitor 2 (Gdid4)(Ly-GDI)	Q61599	*	*	Rho GDP dissociation inhibitor preferentially expressed in hematopoietic cells [71]. Targeted disruption of Ly-GDI has rendered macrophages able to phagocytose yeasts but with a consistent reduction in their capacity to generate superoxide [72]	Increase of oxidative response with live [14] and HI cells
Ferritin light chain 1 (Ftl1)	P29391	1	−1.62	Ferritin light (19 kDa, L) chain, forming a hollow shell with heavy chain in which iron ions can be sequestered in a non-toxic form, thus preventing the formation of highly toxic ROS [73]. Induced in response to several stresses in macrophages (arsenite, heat stress) and in response to Prostaglandin A [74] together with Hsp70 and Heme oxygenase	Enhancement of the macrophages oxidative response
L-Plastin (Lcp1)	Q61233	+1.62	1	Cytoskeletal protein signalling to NADPH oxidase [70]	Increase of oxidative response with live cells [14]
Vimentin, fragment (Vim)	P48670	1	−2.10	Silencing of vimentin gene expression markedly suppressed the ability of BM2 cells to form macrophage polykaryons active in phagocytosis and producing ROS[75]	Control of the oxidative response
Isocitrate dehydrogenase (Idh1)	O88844	1	*	Supplies NADPH required for GSH production against cellular oxidative damage. Its increase	Protection from oxidative response with HI cells

Table 2. Continued

Protein[a)]	Accession number[a)]	Ratio Mϕ+ live/control Mϕ[b)] [14]	Ratio Mϕ+HI/ control Mϕ[b)]	Described effects	Hypothetic effect during the interaction with *C. albicans*
				enhanced resistance against UVB-induced oxidative injury to cells [76]	
Apoptosis					
Protein kinase C inhibitor protein 1 (KCIP-1) (14-3-3Z)	P63101	*	1.6	Critical antiapoptotic factor by inhibiting p38 MAPK activation in fibroblasts [77] and in lung carcinoma cells [78]	Protection from apoptosis
Heat shock 70 kDa protein 5 (Hspa5) (Grp78, BiP)	P20029	*	1	Protection from apoptosis [79]	
Elongation factor 2 (Eef-2)	P58252	*/+1.52/−1.54	*	Blocks HIV-1 protein R-induced cell death both in fission yeast and human cells, suggesting that EF2 possesses a highly conserved anti-apoptotic activity [80]	
Pyruvate kinase isozyme M2 (Pkm2)	P52480	1	*	Human homologue induces apoptosis upon nuclear translocation [50]	Induction of apoptosis with HI cells
Metabolism					
Triosephosphate isomerase (Tpi)	P17751	1	+1.74	Superexpressed in senescence [81] and hypoxia[82]	
α-Enolase (Eno1)	P17182	1	+1.63	Superexpressed in hypoxia [83] and in cancer cell lines [84]	Supply of the macrophages metabolic requirements during interaction with HI
Pyruvate kinase isozyme M2 (Pkm2)	P52480	1	*	Human homologue shows increased expression in some cancers [85] and rheumatic diseases [86]	
3-Oxoacid CoA transferase (Oxct1)	Q9DOK2	1	+1.62	Catalyzes the conversion of succinyl-CoA to succinate	

a) Protein name and accession number according to Human PSD and GPCR-PD human, mouse and rat database (Mouse Protein Report with PSD Interactions) of Proteome Bioknowledge Library (https://www.proteome.com/control/tools/proteome).
b) 1, proteins that do not vary their expression level; +, proteins that augment; −, proteins that diminish and ∗ proteins that appear after the interaction.

for the tissular damage that this yeast produces in animals with disseminated infection. Mutant *C. albicans* strains that induce a reduced inflammatory damage are less virulent [41], and it is well known that many microorganisms cause disease mainly due to the inflammatory response that they induce in the host.

Other authors, on the contrary, observed higher levels of TNF-α secretion when macrophages (BMDM from C57-B mice) were treated with HI *C. albicans* cells with respect to live cells [12]. The differences between both results are probably due to several facts, such as the temperature of inactivation of yeast cells (boiling *versus* 65°C) a fact that might result in a more intensive exposure of β-glucans, as also suggested by other authors [12]. In fact, *S. cerevisiae* mutants displaying more β-glucans than other strains in their cell surface increase the levels of TNF-α secretion in murine macrophages [42]. Thus, we have inactivated *C. albicans* cells at 100°C and with formaldehyde and we have measured TNF-α levels in the same conditions, showing that these protocols induced higher TNF-α levels (Fig. 3). On the other hand, experiments from another group [43] detected an increase in TNF-α production by murine macrophages infected either with live or inactivated *C. albicans* cells, independently of the method used to inactivate them (heat killed, formalin fixed, *etc.*). Thus, the conditions of the experiment and the cell line used to measure this cytokine must be influencing the results of the experiment to a great extent.

Various intracellular signalling pathways are involved in the modulation of NF-κB activity and in the inflammatory

cytokine expression. Activation of mitogen-activated protein kinase has been demonstrated to be important in the regulation of iNOS and COX-2 expression through control of the activation of NF-κB [44, 45]. As shown in Fig. 4, ERK1/2 phosphorylation levels were similar after 45 min of interaction either with HI and live cells, but, at longer times of incubation (3 h), the levels of phosphorylation were much higher with live cells, thus indicating that the pro-inflammatory signals prevailed over the anti-inflammatory ones. The profile of phosphorylation of ERK1/2 throughout the experiment agrees with the profiles obtained when anti-inflammatory drugs are assayed for this effect [46].

4.2 Other effects

It is not surprising that many differentially expressed proteins were involved in cytoskeletal modifications. The ones identified increased when macrophages were exposed either to live or HI cells and they have been analyzed in the previous work [14]. In summary, the proteins increased in response to both stimuli are enhancing the formation of actin filaments. Some of the proteins related to morphogenesis are also involved in signal transduction in processes such as oxidative burst. This is the case of L-plastin, Ly-GDI and vimentin. On the other hand, unrelated to the cytoskeleton, but involved in the response to oxidative stress, is the reduction observed in Ftl1p (ferritin light chain), which is shown in macrophages exposed to HI cells. As can be observed in Table 2, there is a mixture of enhancing and controlling effects against both kinds of stimuli that requires further investigation to elucidate which effect actually takes place.

HSPs play several roles in cell and tissue physiology. They protect the proteome through their molecular function as chaperones. They may, also, play a more generic role in cell survival and have been involved as inhibitors of a remarkable number of steps in apoptosis (reviewed in [47]). As described by other authors, *C. albicans* does not induce apoptosis in RAW264.7 [48, 49]. Our proteomic results seem to reinforce this observation (Table 2), except for Pkm2, whose human homologue has been related to induction of apoptosis when translocated into the nucleus [50].

In conclusion, our experiments with the RAW 264.7 murine cell line reveal a different proteomic response from macrophages depending on the *C. albicans* status. Some of the effects induced by both stimuli are common, such is the case in cytoskeletal rearrangement and in the anti-apoptotic response, but others are very different, namely in the response to stress and in the inflammatory response. These results point to an important role of inflammation in the progress of disease. Further proteomic experiments with longer interaction times (3 h) will be performed in an in-depth study of the interaction of macrophages with *C. albicans*.

We thank M. L. Hernáez, M.D. Gutierrez, Dr. M. Martínez-Gomariz and Dr. P. Ximénez de Embún (from Proteomics Facility, Complutense University and Scientific Park of Madrid (UCM-PCM), a member of the National Institute for Proteomics, ProteoRed, Spain) for their technical assistance. This work was supported by BIO 01989-2006 from the Comision Interministerial de Ciencia y Tecnología (CYCIT, Spain), S-SAL-0246-2006 DEREMICROBIANA-CM from the Comunidad Autónoma de Madrid, and by the Miniterio de Sanidad y Consumo, Instituto de Salud Carlos III – FEDER, Spanish Network for the Research in Infectious Diseases (REIPI RD06/0008). L. Martínez-Solano and J.A. Reales-Calderón were recipients of fellowships from the Ministerio de Educación. Professor C. Nombela is the director of the Merck Sharp & Dohme (MSD) special chair in Genomics and Proteomics.

The authors have declared no conflict of interest.

5 References

[1] Pfaller, M. A., Diekema, D. J., Epidemiology of invasive candidiasis: a persistent public health problem. *Clin. Microbiol Rev.* 2007, *20*, 133–163.

[2] Bates, D. W., Su, L., Yu, D. T., Chertow, G. M. *et al.*, Mortality and costs of acute renal failure associated with amphotericin B therapy. *Clin. Infect. Dis.* 2001, *32*, 686–693.

[3] Vermes, A., Guchelaar, H. J., Dankert, J., Flucytosine: a review of its pharmacology, clinical indications, pharmacokinetics, toxicity and drug interactions. *J. Antimicrob. Chemother.* 2000, *46*, 171–179.

[4] Bistoni, F., Vecchiarelli, A., Cenci, E., Puccetti, P. *et al.*, Evidence for macrophage-mediated protection against lethal *Candida albicans* infection. *Infect. Immun.* 1986, *51*, 668–674.

[5] Qian, Q., Jutila, M. A., van Rooijen, N., Cutler, J. E., Elimination of mouse splenic macrophages correlates with increased susceptibility to experimental disseminated candidiasis. *J. Immunol.* 1994, *152*, 5000–5008.

[6] McGreal, E. P., Miller, J. L., Gordon, S., Ligand recognition by antigen-presenting cell C-type lectin receptors. *Curr. Opin. Immunol.* 2005, *17*, 18–24.

[7] Chinen, T., Qureshi, M. H., Koguchi, Y., Kawakami, K., *Candida albicans* suppresses nitric oxide (NO) production by interferon-gamma (IFN-gamma) and lipopolysaccharide (LPS)-stimulated murine peritoneal macrophages. *Clin. Exp. Immunol.* 1999, *115*, 491–497.

[8] Marodi, L., Korchak, H. M., Johnston, R. B., Jr., Mechanisms of host defense against *Candida* species. I. Phagocytosis by monocytes and monocyte-derived macrophages. *J. Immunol.* 1991, *146*, 2783–2789.

[9] Marodi, L., Forehand, J. R., Johnston, R. B., Jr., Mechanisms of host defense against *Candida* species. II. Biochemical basis for the killing of Candida by mononuclear phagocytes. *J. Immunol.* 1991, *146*, 2790–2794.

[10] Newman, S. L., Bhugra, B., Holly, A., Morris, R. E., Enhanced killing of *Candida albicans* by human macrophages adherent to type 1 collagen matrices via induction of phagolysosomal fusion. *Infect. Immun.* 2005, *73*, 770–777.

[11] Heinsbroek, S. E., Brown, G. D., Gordon, S., Dectin-1 escape by fungal dimorphism. *Trends Immunol.* 2005, *26*, 352–354.

[12] Wheeler, R. T., Fink, G. R., A drug-sensitive genetic network masks fungi from the immune system. *PLoS Pathog.* 2006, *2*, e35.

[13] Saba, J. A., McComb, M. E., Potts, D. L., Costello, C. E., Amar, S., Proteomic mapping of stimulus-specific signaling pathways involved in THP-1 cells exposed to *Porphyromonas gingivalis* or its purified components. *J. Proteome Res.* 2007, *6*, 2211–2221.

[14] Martínez-Solano, L., Nombela, C., Molero, G., Gil, C., Differential protein expression of murine macrophages upon interaction with *Candida albicans*. *Proteomics* 2006, *6*, S133–S144.

[15] Gillum, A. M., Tsay, E. Y. H., Kirsch, D. R., Isolation of the *Candida albicans* gene for orotidine-5′-phosphate decarboxylase by complementation of *S. cerevisiae ura3* and *E. coli pyrF* mutations. *Mol. Gen. Genet.* 1984, *198*, 179–182.

[16] Fernández-Arenas, E., Cabezón, V., Bermejo, C., Arroyo, J. *et al.*, Integrated proteomics and genomics strategies bring new insight into *Candida albicans* response upon macrophage interaction. *Mol. Cell Proteomics* 2007, *6*, 460–478.

[17] Peyrot, V., Leynadier, D., Sarrazin, M., Briand, C. *et al.*, Interaction of tubulin and cellular microtubules with the new antitumor drug MDL 27048. A powerful and reversible microtubule inhibitor. *J. Biol. Chem.* 1989, *264*, 21296–21301.

[18] Pitarch, A., Pardo, M., Jiménez, A., Pla, J. *et al.*, Two-dimensional gel electrophoresis as analytical tool for identifying *Candida albicans* immunogenic proteins. *Electrophoresis* 1999, *20*, 1001–1010.

[19] Pardo, M., Ward, M., Pitarch, A., Sánchez, M. *et al.*, Cross-species identification of novel *Candida albicans* immunogenic proteins by combination of two-dimensional polyacrylamide gel electrophoresis and mass spectrometry. *Electrophoresis* 2000, *21*, 2651–2659.

[20] Bjellqvist, B., Pasquali, C., Ravier, F., Sanchez, J. C., Hochstrasser, D., A nonlinear wide-range immobilized pH gradient for two-dimensional electrophoresis and its definition in a relevant pH scale. *Electrophoresis* 1993, *14*, 1357–1365.

[21] Shevchenko, A., Wilm, M., Vorm, O., Mann, M., Mass spectrometric sequencing of proteins silver-stained polyacrylamide gels. *Anal. Chem.* 1996, *68*, 850–858.

[22] Sechi, S., Chait, B. T., Modification of cysteine residues by alkylation. A tool in peptide mapping and protein identification. *Anal. Chem.* 1998, *70*, 5150–5158.

[23] Lindquist, S., The heat-shock response. *Annu. Rev. Biochem.* 1986, *55*, 1151–1191.

[24] Morimoto, R. I., Tissieres, A., Georgopoulos, C. (Eds.), *The Stress Response, Function of the Proteins, and Perspectives in Stress Proteins and Biology and Medicine*, Cold Spring Harbor Laboratory Press, New York 1990, pp. 1–36.

[25] Wong, H. R., Finder, J. D., Wasserloos, K., Pitt, B. R., Expression of iNOS in cultured rat pulmonary artery smooth muscle cells is inhibited by the heat shock response. *Am. J. Physiol.* 1995, *269*, L843–L848.

[26] Wong, H. R., Ryan, M., Wispe, J. R., The heat shock response inhibits inducible nitric oxide synthase gene expression by blocking I kappa-B degradation and NF-kappa B nuclear translocation. *Biochem. Biophys. Res. Comm.* 1997, *231*, 257–263.

[27] Yoo, C. G., Lee, S., Lee, C. T., Kim, Y. W. *et al.*, Anti-inflammatory effect of heat shock protein induction is related to stabilization of I kappa B alpha through preventing I kappa B kinase activation in respiratory epithelial cells. *J. Immunol.* 2000, *164*, 5416–5423.

[28] Kim, H. D., Kang, H. S., Rimbach, G., Park, Y. C., Heat shock and 5-azacytidine inhibit nitric oxide synthesis and tumor necrosis factor-alpha secretion in activated macrophages. *Antioxid. Redox. Signal.* 1999, *1*, 297–304.

[29] Shanley, T. P., Ryan, M. A., Eaves-Pyles, T., Wong, H. R., Heat shock inhibits phosphorylation of I-kappaBalpha. *Shock* 2000, *14*, 447–450.

[30] Yeo, M., Park, H. K., Lee, K. M., Lee, K. J. *et al.*, Blockage of HSP 90 modulates *Helicobacter pylori*-induced IL-8 productions through the inactivation of transcriptional factors of AP-1 and NF-kappaB. *Biochem. Biophys. Res Commun.* 2004, *320*, 816–824.

[31] Calderwood, S. K., Theriault, J. R., Gong, J., How is the immune response affected by hyperthermia and heat shock proteins? *Int. J. Hyperthermia* 2005, *21*, 713–716.

[32] Wang, X., Zou, Y., Wang, Y., Li, C., Chang, Z., Differential regulation of interleukin-12 and interleukin-10 by heat shock response in murine peritoneal macrophages. *Biochem. Biophys. Res. Comm.*2001, *287*, 1041–1044.

[33] Niu, J., Azfer, A., Rogers, L. M., Wang, X., Kolattukudy, P. E., Cardioprotective effects of cerium oxide nanoparticles in a transgenic murine model of cardiomyopathy. *Cardiovasc. Res.* 2007, *73*, 549–559.

[34] Kang, A. D., Wong, P. M., Chen, H., Castagna, R. *et al.*, Restoration of lipopolysaccharide-mediated B-cell response after expression of a cDNA encoding a GTP-binding protein. *Infect. Immun.* 1996, *64*, 4612–4617.

[35] Zhao, M., Brunk, U. T., Eaton, J. W., Delayed oxidant-induced cell death involves activation of phospholipase A2. *FEBS Lett.* 2001, *509*, 399–404.

[36] Gong, Q. H., Fukuda, T., Parkison, C., Cheng, S. Y., Nucleotide sequence of a full-length cDNA clone encoding a mouse cellular thyroid hormone binding protein (p55) that is homologous to protein disulfide isomerase and the beta-subunit of prolyl-4-hydroxylase. *Nucleic Acids Res.* 1988, *16*, 1203.

[37] Mkrtchian, S., Baryshev, M., Matvijenko, O., Sharipo, A. *et al.*, Oligomerization properties of ERp29, an endoplasmic reticulum stress protein. *FEBS Lett.* 1998, *431*, 322–326.

[38] Valenzuela, S. M., Martin, D. K., Por, S. B., Robbins, J. M. *et al.*, Molecular cloning and expression of a chloride ion channel of cell nuclei. *J. Biol. Chem.* 1997, *272*, 12575–12582.

[39] Vega, M. A., Corbí, A., Human macrophage activation: too many functions and phenotypes for a single cell type. *Inmunología* 2006, *1-26*.

[40] Vats, D., Mukundan, L., Odegaard, J. I., Zhang, L. *et al.*, Oxidative metabolism and PGC-1beta attenuate macrophage-mediated inflammation. *Cell Metab.* 2006, *4*, 13–24.

[41] Diez-Orejas, R., Molero, G., Navarro-García, F., Pla, J. *et al.*, Reduced virulence of *Candida albicans MKC1* mutants: a role for mitogen-activated protein kinase in pathogenesis. *Infect. Immun.* 1997, *65*, 833–837.

[42] Sakai, Y., Azuma, M., Takada, Y., Umeyama, T. *et al.*, *Saccharomyces cerevisiae* mutant displaying beta-glucans on cell surface. *J. Biosci. Bioeng.* 2007, *103*, 161–166.

[43] Murciano, C., Yanez, A., Gil, M. L., Gozalbo, D., Both viable and killed *Candida albicans* cells induce *in vitro* production of TNF-alpha and IFN-gamma in murine cells through a TLR2-dependent signalling. *Eur. Cytokine Netw.* 2007, *18*, 38–43.

[44] Suh, S. J., Chung, T. W., Son, M. J., Kim, S. H., Moon, T. C. *et al.*, The naturally occurring biflavonoid, ochnaflavone, inhibits LPS-induced iNOS expression, which is mediated by ERK1/2 via NF-kappaB regulation, in RAW264.7 cells. *Arch. Biochem. Biophys.* 2006, *447*, 136–146.

[45] Pergola, C., Rossi, A., Dugo, P., Cuzzocrea, S., Sautebin, L., Inhibition of nitric oxide biosynthesis by anthocyanin fraction of blackberry extract. *Nitric. Oxide* 2006, *15*, 30–39.

[46] Jung, W. K., Lee, D. Y., Choi, Y. H., Yea, S. S. *et al.*, Caffeic acid phenethyl ester attenuates allergic airway inflammation and hyperresponsiveness in murine model of ovalbumin-induced asthma. *Life Sci.* 2008, *82*, 797–805.

[47] Nollen, E. A., Morimoto, R. I., Chaperoning signaling pathways: molecular chaperones as stress-sensing 'heat shock' proteins. *J. Cell Sci.* 2002, *115*, 2809–2816.

[48] Marcil, A., Harcus, D., Thomas, D. Y., Whiteway, M., *Candida albicans* killing by RAW 264.7 mouse macrophage cells: effects of *Candida* genotype, infection ratios, and gamma interferon treatment. *Infect. Immun.* 2002, *70*, 6319–6329.

[49] Panagio, L. A., Felipe, I., Vidotto, M. C., Gaziri, L. C., Early membrane exposure of phosphatidylserine followed by late necrosis in murine macrophages induced by *Candida albicans* from an HIV-infected individual. *J. Med. Microbiol.* 2002, *51*, 929–936.

[50] Stetak, A., Veress, R., Ovadi, J., Csermely, P. *et al.*, Nuclear translocation of the tumor marker pyruvate kinase M2 induces programmed cell death. *Cancer Res.* 2007, *67*, 1602–1608.

[51] Zhang, M., Hisaeda, H., Sakai, T., Ishikawa, H. *et al.*, Macrophages expressing heat-shock protein 65 play an essential role in protection of mice infected with *Plasmodium yoelii*. *Immunology* 1999, *97*, 611–615.

[52] Nakano, Y., Hisaeda, H., Sakai, T., Ishikawa, H. *et al.*, Roles of NKT cells in resistance against infection with *Toxoplasma gondii* and in expression of heat shock protein 65 in the host macrophages. *Microbes. Infect.* 2002, *4*, 1–11.

[53] Hsieh, S. Y., Shih, T. C., Yeh, C. Y., Lin, C. J. *et al.*, Comparative proteomic studies on the pathogenesis of human ulcerative colitis. *Proteomics* 2006, *6*, 5322–5331.

[54] Ferlazzo, V., D'Agostino, P., Milano, S., Caruso, R. *et al.*, Anti-inflammatory effects of annexin-1: stimulation of IL-10 release and inhibition of nitric oxide synthesis. *Int. Immunopharmacol.* 2003, *3*, 1363–1369.

[55] Parente, L., Solito, E., Annexin 1: more than an anti-phospholipase protein. *Inflamm. Res.* 2004, *53*, 125–132.

[56] de Coupade, C., Ajuebor, M. N., Russo-Marie, F., Perretti, M., Solito, E., Cytokine modulation of liver annexin 1 expression during experimental endotoxemia. *Am. J. Pathol.* 2001, *159*, 1435–1443.

[57] Damazo, A. S., Yona, S., D'Acquisto, F., Flower, R. J. *et al.*, Critical protective role for annexin 1 gene expression in the endotoxemic murine microcirculation. *Am. J. Pathol.* 2005, *166*, 1607–1617.

[58] Higuchi, T., Watanabe, Y., Waga, I., Protein disulfide isomerase suppresses the transcriptional activity of NF-kappaB. *Biochem. Biophys. Res Commun.* 2004, *318*, 46–52.

[59] Novarino, G., Fabrizi, C., Tonini, R., Denti, M. A., Malchiodi-Albedi, F. *et al.*, Involvement of the intracellular ion channel CLIC1 in microglia-mediated beta-amyloid-induced neurotoxicity. *J. Neurosci.* 2004, *24*, 5322–5330.

[60] Qureshi, N., Perera, P. Y., Shen, J., Zhang, G. *et al.*, The proteasome as a lipopolysaccharide-binding protein in macrophages: differential effects of proteasome inhibition on lipopolysaccharide-induced signaling events. *J. Immunol.* 2003, *171*, 1515–1525.

[61] Bernstein, B. W., Bamburg, J. R., Tropomyosin binding to F-actin protects the F-actin from disassembly by brain actin-depolymerizing factor (ADF). *Cell Motil.* 1982, *2*, 1–8.

[62] DesMarais, V., Ichetovkin, I., Condeelis, J., Hitchcock-DeGregori, S. E., Spatial regulation of actin dynamics: a tropomyosin-free, actin-rich compartment at the leading edge. *J. Cell Sci.* 2002, *115*, 4649–4660.

[63] Au-Young, J., Robbins, P. W., Isolation of a chitin synthase gene (*CHS1)* from *Candida albicans* by expression in *Saccharomyces cerevisiae*. *Mol. Microbiol.* 1990, *4*, 197–207.

[64] Yu, F. X., Johnston, P. A., Sudhof, T. C., Yin, H. L., gCap39, a calcium ion- and polyphosphoinositide-regulated actin capping protein. *Science* 1990, *250*, 1413–1415.

[65] Witke, W., Li, W., Kwiatkowski, D. J., Southwick, F. S., Comparisons of CapG and gelsolin-null macrophages: demonstration of a unique role for CapG in receptor-mediated ruffling, phagocytosis, and vesicle rocketing. *J. Cell Biol.* 2001, *154*, 775–784.

[66] Sun, H. Q., Kwiatkowska, K., Wooten, D. C., Yin, H. L., Effects of CapG overexpression on agonist-induced motility and second messenger generation. *J. Cell Biol.* 1995, *129*, 147–156.

[67] Taylor, D. L., Thomson, P. C., de Silva, K., Whittington, R. J., Validation of endogenous reference genes for expression

profiling of RAW264.7 cells infected with *Mycobacterium avium* subsp. *paratuberculosis* by quantitative PCR. *Vet. Immunol. Immunopathol.* 2007, *115*, 43–55.

[68] Roobol, A., Sahyoun, Z. P., Carden, M. J., Selected subunits of the cytosolic chaperonin associate with microtubules assembled *in vitro*. *J. Biol. Chem.* 1999, *274*, 2408–2415.

[69] Yokota, S. I., Yanagi, H., Yura, T., Kubota, H., Upregulation of cytosolic chaperonin CCT subunits during recovery from chemical stress that causes accumulation of unfolded proteins. *Eur. J. Biochem.* 2000, *267*, 1658–1664.

[70] Chen, H., Hewison, M., Hu, B., Adams, J. S., Heterogeneous nuclear ribonucleoprotein (hnRNP) binding to hormone response elements: a cause of vitamin D resistance. *Proc. Natl. Acad. Sci. USA* 2003, *100*, 6109–6114.

[71] Adra, C. N., Ko, J., Leonard, D., Wirth, L. J. *et al.*, Identification of a novel protein with GDP dissociation inhibitor activity for the ras-like proteins CDC42Hs and rac I. *Genes Chrom. Cancer* 1993, *8*, 253–261.

[72] Guillemot, J. C., Kruskal, B. A., Adra, C. N., Zhu, S. *et al.*, Targeted disruption of guanosine diphosphate-dissociation inhibitor for Rho-related proteins, GDID4: normal hematopoietic differentiation but subtle defect in superoxide production by macrophages derived from *in vitro* embryonal stem cell differentiation. *Blood* 1996, *88*, 2722–2731.

[73] Balla, G., Jacob, H. S., Balla, J., Rosenberg, M. *et al.*, Ferritin: a cytoprotective antioxidant strategem of endothelium. *J. Biol. Chem.*1992, *267*, 18148–18153.

[74] Elia, G., Polla, B., Rossi, A., Santoro, M. G., Induction of ferritin and heat shock proteins by prostaglandin A1 in human monocytes. Evidence for transcriptional and post-transcriptional regulation. *Eur. J. Biochem.* 1999, *264*, 736–745.

[75] Benes, P., Maceckova, V., Zdrahal, Z., Konecna, H. *et al.*, Role of vimentin in regulation of monocyte/macrophage differentiation. *Differentiation* 2006, *74*, 265–276.

[76] Jo, S. H., Lee, S. H., Chun, H. S., Lee, S. M. *et al.*, Cellular defense against UVB-induced phototoxicity by cytosolic NADP(+)-dependent isocitrate dehydrogenase. *Biochem. Biophys. Res Commun.* 2002, *292*, 542–549.

[77] Xing, H., Zhang, S., Weinheimer, C., Kovacs, A., Muslin, A. J., 14-3-3 proteins block apoptosis and differentially regulate MAPK cascades. *EMBO J.* 2000, *19*, 349–358.

[78] Li, R., Wang, H., Bekele, B. N., Yin, Z. *et al.*, Identification of putative oncogenes in lung adenocarcinoma by a comprehensive functional genomic approach. *Oncogene* 2006, *25*, 2628–2635.

[79] McCormick, T. S., McColl, K. S., Distelhorst, C. W., Mouse lymphoma cells destined to undergo apoptosis in response to thapsigargin treatment fail to generate a calcium-mediated grp78/grp94 stress response. *J. Biol. Chem.* 1997, *272*, 6087–6092.

[80] Zelivianski, S., Liang, D., Chen, M., Mirkin, B. L., Zhao, R. Y., Suppressive effect of elongation factor 2 on apoptosis induced by HIV-1 viral protein R. *Apoptosis* 2006, *11*, 377–388.

[81] Poon, H. F., Castegna, A., Farr, S. A., Thongboonkerd, V. *et al.*, Quantitative proteomics analysis of specific protein expression and oxidative modification in aged senescence-accelerated-prone 8 mice brain. *Neuroscience* 2004, *126*, 915–926.

[82] Yamaji, R., Fujita, K., Nakanishi, I., Nagao, K. *et al.*, Hypoxic up-regulation of triosephosphate isomerase expression in mouse brain capillary endothelial cells. *Arch. Biochem. Biophys.* 2004, *423*, 332–342.

[83] Niklinski, J., Furman, M., Clinical tumour markers in lung cancer. *Eur. J. Cancer Prev.* 1995, *4*, 129–138.

[84] Takashima, M., Kuramitsu, Y., Yokoyama, Y., Iizuka, N. *et al.*, Overexpression of alpha enolase in hepatitis C virus-related hepatocellular carcinoma: association with tumor progression as determined by proteomic analysis. *Proteomics* 2005, *5*, 1686–1692.

[85] Koss, K., Harrison, R. F., Gregory, J., Darnton, S. J., The metabolic marker tumour pyruvate kinase type M2 (tumour M2-PK) shows increased expression along the metaplasia–dysplasia–adenocarcinoma sequence in Barrett's oesophagus. *J. Clin. Pathol.* 2004, *57*, 1156–1159.

[86] Oremek, G. M., Muller, R., Sapoutzis, N., Wigand, R., Pyruvate kinase type tumor M2 plasma levels in patients afflicted with rheumatic diseases. *Anticancer Res.* 2003, *23*, 1131–1134.

ANEXO

